Biostratigraphy and Paleoenvironment in the Neogene of the High Northern Latitudes

Insights from the palynomorph record of ODP Hole 907A in the Iceland Sea

Kumulative Dissertation
Zur Erlangung des akademischen Grades
eines Doktors der Naturwissenschaften

Dr. rer. nat.

am Fachbereich Geowissenschaften
der Universität Bremen

vorgelegt von

Michael Schreck
Bremerhaven, 2012

Gutachter der Dissertation:
Prof. Dr. Ruediger Stein
PD Dr. Karin Zonneveld

Tag des Promotionskolloquiums: 11.07.2012

Name: Michael Schreck Datum: 16.05.2012

Anschrift: Bürgermeister-Smidt-Str. 171, 27568 Bremerhaven

Erklärung

Hiermit versichere ich, dass ich

1. die Arbeit ohne unerlaubte fremde Hilfe angefertigt habe
2. keine anderen als die von mir angegebenen Quellen und Hilfsmittel benutzt habe und
3. die den benutzte Werken wörtlich oder inhaltlich entnommenen Stellen als solche kenntlich gemacht habe.

Bremerhaven, den 16.05.2012

.....

“BUGS DON’T LIE.“

Thomas Cronin (Urbino, Italy, 2009)

Abstract

The Neogene is of crucial importance for our understanding of Earth's climate evolution as it was finally pushed into the cold Quaternary climate with its major glaciations in the high northern latitudes. Notwithstanding, the response of the high northern latitudes to this Cenozoic transition from the Greenhouse into the Icehouse world yet remains poorly constrained due to the virtual absence of calcareous microfossils in high latitude Neogene sediments.

This thesis examines the influence of the long-term climate deterioration on Miocene to Pliocene marine palynomorph assemblages (dinoflagellate cysts, prasinophyte algae, acritarchs) of ODP Hole 907A in the Iceland Sea, a sensitive area physically close to the growing Greenland ice-sheet, which experienced the effects of migrating ocean currents and sea-ice cover. Based on the pristine paleomagnetic record of Site 907, the principal aim of this thesis is to enhance the biostratigraphic application of organic-walled microfossils for (supra)regional correlations in these largely biogenic carbonate free sediments, and to utilize them for paleoenvironmental reconstruction in order to provide new insights into the Neogene history of the Iceland Sea.

This thesis provides absolute age control on a suite of twenty-four dinoflagellate cyst and two acritarch bioevents for the first time in the Neogene of the high northern latitudes. These magnetostratigraphically-calibrated events have been compared across the North Atlantic and adjacent seas to critically evaluate their potential for biostratigraphic correlations within the high latitudes, but also with the mid- and low latitudes. Results show that seven species are useful for supraregional biostratigraphic correlations within the Nordic Seas, and four allow integrating the latter with the mid-latitude North Atlantic. Furthermore, this study highlights four species potentially useful for correlating mid-latitude sequences to the Central Arctic Ocean. Although an additional number of species appears to be valuable on a broader (million year) timescale, most events are clearly asynchronous indicating a strong latitudinal control even in the warmer Miocene.

In a second study, the global paleobiogeographic distribution of the extinct *Batiacasphaera micropapillata* complex has been analysed in order to utilize it for future paleoenvironmental reconstructions. This major component of Neogene palynomorph assemblages in the high northern latitudes is a warm to cool-temperate species complex that may sustain seasonal sea-ice cover. It has an outer-neritic to oceanic affinity, a tolerance for somewhat higher salinities, and is apparently well adapted to enhanced

nutrient availability and the prevailing light regime in the high latitudes. Its Late Miocene decline and its stratigraphically important highest occurrence in the Early Pliocene are closely related to climate deterioration towards the intensification of Northern Hemisphere glaciation.

Based on distinctive changes in palynomorph assemblage composition, which are supplemented by alkenone sea surface temperature estimates, the paleoenvironmental evolution of the Iceland Sea has been reconstructed for the *c.* 15–2.5 Ma interval. Results indicate a close coupling of marine palynomorphs and sea surface temperatures not only to the long-term Neogene climate cooling that occurred after the Middle Miocene Climate Optimum, but also to local changes in ocean circulation due to the Fram Strait opening, sill depth variations of the Greenland-Scotland Ridge, and the shoaling and subsequent closure of the Panama Isthmus. Moreover, a distinct variability in the palynomorph assemblages reflects short-term climate variations that partly coincide with the short-lived Miocene glaciation events (Mi-3 to Mi-6), and the progressive strengthening and freshening of a proto-East Greenland Current towards modern conditions in the Late Miocene and Early Pliocene. The impoverished Pliocene assemblages suggest that major adjustments, with conditions seriously effecting marine productivity have already been established in the Iceland Sea well before the marked expansion of the Greenland ice-sheet at 3.3 Ma and the subsequent intensification of Northern Hemisphere glaciations.

In conclusion, this thesis provides an improved, magnetostratigraphically-calibrated temporal framework for future analyses of high and mid-latitude Miocene to Pliocene sequences, first estimates on the paleoecology of an important Neogene species complex, and ultimately new insights into the paleoenvironmental evolution of an area sensitive for global climate change.

Zusammenfassung

Das Neogen ist von entscheidender Bedeutung für unser Verständnis der Erdklimaentwicklung, da es während dieser Epoche endgültig in das kalte Klima des Quartärs, mit ausgedehnten Vereisungen in der nördlichen Hemisphäre, überging. Trotz dieser Bedeutung sind die Veränderungen innerhalb der hohen nördlichen Breiten während dieses Übergangs von der „Greenhouse-" in die „Icehouse-Welt" nur unzulänglich bekannt, da die neogenen Sedimente der hohen Breiten weitestgehend frei von kalkigen Mikrofossilien sind.

Die vorliegende Arbeit untersucht den Einfluss dieser langfristigen Klimaveränderung auf miozäne und pliozäne Vergesellschaftungen organischwandiger Mikrofossilien (Dinoflagellatenzysten, Prasinophyten, Acritarchen) in der ODP Bohrung 907A aus der Islandsee in unmittelbarer Nähe zum Grönlandeisschild – einer Region, welche durch wechselnde Meeresströmungen und variable Meereisbedeckung beeinflusst wurde. Das Hauptziel dieser Arbeit ist es, den Nutzen von organischwandigen, marinen Mikrofossilen für (über)regionale biostratigrafische Korrelationen in den weitestgehend karbonatfreien Sedimenten der hohen nördlichen Breiten zu verbessern und neue Erkenntnisse über die neogene Klimaentwicklung in der Islandsee zu erhalten.

Die vorliegende Arbeit bietet erstmalig eine absolute Alterskontrolle für 24 Dinoflagellatenzysten und 2 Acritarchen Bioevents aus dem Neogen der hohen nördlichen Breiten. Diese magnetostratigrafisch kalibrierten Bioevents wurden über den Nordatlantik und die angrenzenden Randmeere verglichen um ihr Potential für biostratigrafische Korrelationen innerhalb der hohen nördlichen Breiten, aber auch mit den mittleren und niederen Breiten, zu evaluieren. Die Resultate dieser Untersuchung zeigen, dass sieben Arten überregionale stratigrafische Bedeutung innerhalb des Nordpolarmeeres haben, während vier dieser Arten darüber hinaus auch eine Korrelation mit den mittleren Breiten des Nordatlantiks ermöglichen. Des Weiteren wurden vier Arten identifiziert, die das Potential besitzen den zentralen Arktischen Ozean mit den mittleren Breiten zu korrelieren. Obwohl verschiedene andere Arten auf längeren (Millionen von Jahren) Zeitskalen nützlich erscheinen, sind viele Bioevents asynchron und zeigen damit eine starke Breitenkreisabhängigkeit selbst im wärmeren Miozän.

In einer zweiten Studie wurde die globale, paläobiogeografische Verbreitung des *Batiacasphaera micropapillata* Artenkomplex untersucht, um ihn für zukünftige Paläoumweltrekonstruktionen nutzbar zu machen. Dieser im Neogen der hohen nördlichen Breiten vorherrschende Komplex ist offenbar warm bis kühl-gemäßigt und

übersteht eine saisonale Meerbedeckung. Er bevorzugt den äußeren Schelfbereich und ozeanisches Milieu, toleriert höhere Salzgehalte und ist offenbar sehr gut an eine erhöhte Nährstoffverfügbarkeit sowie die vorherrschenden Lichtbedingungen in den hohen Breiten angepasst. Der Rückgang dieses Artenkomplexes im Obermiozän und sein stratigrafisch wichtiges Verschwinden im Unterpliozän sind eng mit der globalen Klimaabkühlung, welche zur Intensivierung der Nordhemisphären-Vereisung führte, verbunden.

Ausgehend von Veränderungen in der Artenvergesellschaftung, ergänzt durch Meersoberflächentemperaturen, wurde die Entwicklung der Paläoumwelt in der Islandsee für den Zeitraum von *c.* 15–2.5 Ma rekonstruiert. Die Resultate dieser Untersuchung deuten nicht nur auf einen Zusammenhang der Palynomorphen und der Meeresoberflächentemperaturen mit der langfristigen Abkühlung nach dem miozänen Klimaoptimum hin, sondern auch auf Veränderungen in der lokalen Ozeanzirkulation, welche durch die Öffnung der Framstraße, den Schwankungen in der Schwellentiefe des Grönland-Schottland-Rückens sowie der Verflachung und der nachfolgenden Schließung des Isthmus von Panama bedingt sind. Deutliche Variationen in der Artenzusammensetzung reflektieren darüber hinaus kurzfristige Klimaschwankungen, wahrscheinlich im Zusammenhang mit den miozänen Vereisungsereignissen (Mi-3 bis Mi-6) und der sukzessiven Entwicklung des proto-Ostgrönlandstroms zu modernen Bedingungen während des Obermiozän und Unterpliozän. Die verarmten pliozänen Artenvergesellschaftungen in der Islandsee zeigen, dass sich Bedingungen, welche die marine Produktivität beeinträchtigten, bereits deutlich vor der markanten Ausdehnung des grönländischen Eisschildes und der Intensivierung der Nordhemisphären Vereisung in dieser Region eingestellt haben.

Zusammenfassend bietet die vorliegende Arbeit ein verbessertes, magnetostratigrafisch kalibriertes Rahmenwerk für zukünftige Untersuchungen an miozänen und pliozänen Sedimenten in den hohen nördlichen Breiten, erste Angaben zur Paläoökologie eines wichtigen neogenen Artenkomplexes, sowie letztendlich neue Erkenntnisse über die Entwicklung der Paläoumwelt in einer für globale Klimaveränderungen sehr sensiblen Region.

Danksagung

An erster Stelle danke ich Dr. Jens Matthiessen für die intensive und umfassende Einführung in die Welt der Dinoflagellatenzysten, mit der er mir den Einstieg in ein unbekanntes jedoch reizvolles Universum ermöglicht hat. Seine intensive Betreuung, die Möglichkeit zu ständigem Austausch und Diskussion, ob vor dem Mikroskop oder über den Daten, seine Begeisterungsfähigkeit und seine Motivationskünste haben mir, vor allem in der Endphase dieser Arbeit, sehr geholfen.

Des Weiteren gilt mein besonderer Dank Prof. Dr. Ruediger Stein für die vielen bereichernden Erfahrungen die er mir während dieser Zeit ermöglicht hat.

PD Dr. Karin Zonneveld danke ich herzlichst für die Übernahme des Zweitgutachtens.

Bei Dr. Stijn De Schepper möchte mich für die regelmäßigen, gemeinsamen Blicke durchs Mikroskop bedanken, die mir gerade in der Anfangszeit sehr geholfen haben. Weiterhin sei ihm, und vor allem Prof. Dr. Martin J. Head, für die vielen interessanten Diskussionen über die Taxonomie und Ökologie der Dinoflagellatenzysten gedankt, die mein Verständnis entscheidend weiterentwickelt and geprägt haben.

Susi, Rita und Ute gebührt großer Dank für die Unterstützung in den diversen Labors.

Gedankt sei Kirsten Fahl, die mir mit Witz und Humor oft den Start in den Tag erleichtert hat. Und was wäre ein Frühstück auf dem Dach ohne Kirsten?

An dieser Stelle möchte ich natürlich auch allen (ehemaligen) Doktoranden der Geowissenschaften (und anderer Sektionen) für die entspannten Mittagspausen, aber auch die vielen schönen Abende im alten Gästehaus, in der Gilde, am Deich oder auf der „Bürger“ danken. Ohne euch wäre das Leben hier ziemlich langweilig gewesen! Vor allem danke ich David für die kompetenten Diskussionen über König Fußball während zahlloser Champions League Abende. Ich danke natürlich auch den „young sexy palynologists“ für die schönen Erlebnisse während diverser Dino-Tagungen und Workshops, von denen ich stets motiviert zurückgekommen bin.

Mein ganz besonderer Dank gilt Jule „Sonnenschein“ Müller, die mir als Bürokollegin und Feierabendbier-Partnerin durch gute und weniger gute Zeiten geholfen hat und immer mit Rat and Tat für mich da war. Zusammen mit Michelle Zarrieß, Normen Lochthofen, Lars Möller, Nicki Händel, Corinna Kanzog und Corinna Borchard hat sie die Zeit in Bremerhaven zu einem unvergesslichen Lebensabschnitt gemacht. Danke dafür!

Allen meinen Freunden in der „Heimat“ sei für ihre mentale Unterstützung aus der Ferne, aber auch für die benötigte Ablenkung während der oftmals viel zu kurzen Besuche in Berlin gedankt. Besonders dankbar bin ich Ani und Wudi für das Asyl in der Grünberger Straße!

Zum Schluss danke ich natürlich meinen Eltern und meinem Bruder für ihre Liebe und Unterstützung bei allem was hinter mir liegt, aber vor allem dafür, mich nie in meinen Entscheidungen beeinflusst zu haben. Ich widme diese Arbeit meinem viel zu früh verstorbenen Großvater Eberhardt Schreck, der mein großes Interesse an den Geowissenschaften teilte.

List of figures, tables and photo plates

TABLE OF CONTENT

TAXONOMIC DISCLAIMER:

This dissertation is not intended for valid publication of the new taxa proposed herein.

1. Introduction

The history of climate change dates back to the 19th century when the French physicist Joseph Fourier first described the greenhouse effect in 1824. Since then generations of scientists have embarked on studies to investigate changes in the past, the recent, and the future of Earth's climate system. However, it was not before 1990, when the Intergovernmental Panel on Climate Change (IPCC) published its first assessment report, that global climate has become a widely discussed topic in both public and politics. Brought to forefront of public attention by the media, climate change and its effects and consequences are debated controversially, in particular with respect to the impact of mankind.

The Earth climate system is characterised by complex interactions and a natural variability, and underwent significant changes over the 4 billion years before human existence. These changes occurred at various time scales (10^1–10^6 years) driven by mechanisms related to ocean-continent configuration and tectonic activity, orbital configurations, chemistry and physics of the oceans and atmosphere, and biological processes. Therefore it is imperative to study past climate changes in order to decipher causes and consequences, temporal and spatial extent, and frequency of these changes to be able to differentiate the anthropogenic impact from the natural climate variability.

One of the most dramatic effects observed recently with respect to the ongoing changes in world's climate is the decrease in sea-ice cover within the northern high latitudes (Lemke et al., 2007). It gained massive medial attention due to its vigorous impact on global climate but also because of its (socio)economic consequences such as access to formerly inaccessible resources, the opening of new merchant shipping passages, and the destruction of unique habitats for both animals and humans. The Arctic and subarctic seas are very sensitive environments with respect to climate change as they are influenced by a suite of positive feedback mechanisms (e.g. ice/snow albedo, vegetation, permafrost, freshwater balance) that amplify the surface air temperature response to climate forcing (such as insolation), a pervasive feature of climate models known as the Arctic amplification (Manabe and Stouffer, 1980). In turn, these feedback mechanisms influence the Thermohaline Circulation, which is partly responsible for global heat redistribution and regulating atmospheric CO_2 concentrations, and thus a key player within the complexity of Earth's climate system (Rahmstorf, 2006).

Highlighting the importance and sensitivity of the high northern latitudes, this region is ideally suited for studies that aim to monitor past natural climate variability on a variety of timescales. Ultimately, the examination of past climate records helps to evaluate climate-modelling efforts with the unifying goal to improve our understanding of recent climate change, and to enhance our ability to reliably predict their future local, regional, and global consequences — an issue of utmost importance to society.

1.1 Objectives and motivation

A completely new and unique opportunity to gain insights into the long-term climate evolution of the high northern latitudes became available in 2004, when the IODP Exp. 302 (Arctic Coring Expedition, ACEX) recovered deposits from the Lomonosov Ridge in the poorly accessible Central Arctic Ocean (CAO) documenting at least the past 55 Ma. Although a hiatus spans the Late Eocene to Early Miocene (*c.* 44.4–18.2 Ma, Backman et al., 2008), these sediments contain the first continuous record of the environmental and climatic evolution of the central Arctic region during the Neogene (Frank et al., 2008, Fig. 1).

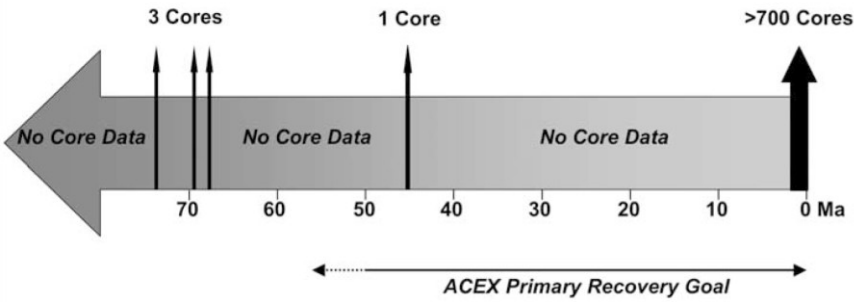

Figure 1: Stratigraphic coverage of existing cores in the Central Arctic Ocean prior to ACEX, and the recovery target for the ACEX drilling expedition (from Backman et al., 2008).

The almost exclusively detrital composition of recovered sediments and the scarcity of traditionally used calcareous biostratigraphic markers severely complicated the establishment of a reliable chronostratigraphic framework and hampered the extraction of paleoceanographic and paleoclimatic information (Backman et al., 2008; O´Regan et al., 2008). However, during post-cruise studies it soon became evident that organic-walled marine palynomorphs are more abundant in Neogene sediments than initially thought after examination of a few core catcher samples during the expedition (Backman et al., 2006; Sangiorgi et al., 2008; Matthiessen et al., 2009b; Matthiessen, unpubl. data). Therefore, marine palynomorphs may provide the independent biostratigraphic control necessary to groundtruth both the Neogene chronostratigraphy (so far primarily based on a few ^{10}Be, and Re-Os isotope data, Frank et al., 2008; Poirier and Hillaire-Marcel, 2011) and paleoclimatic interpretations. Indeed, the stratigraphic range of the acritarch *Decahedrella martinheadii* partly questioned the radiogenic isotope-based age models (Matthiessen et al., 2009b), while the common occurrence of open-marine dinoflagellate cysts challenge previous interpretations of a perennial sea-ice cover since at least middle

Miocene times (Darby, 2008; Krylov et al., 2008; see chapter 2.3 for details). However, to further utilise this unique Central Arctic Ocean Neogene archive for paleoclimatic reconstructions it is of utmost importance to improve the application of marine palynomorphs for biostratigraphic correlations as well as for paleoenvironmental interpretations in the high northern latitudes.

This thesis was embedded in the PACES research program "Lessons from the Past – Tectonic, climate and biosphere development from Greenhouse to Icehouse" at the Alfred Wegener Institute for Polar and Marine Research. In the framework of the project "Neogene Palynomorphs in the Northern High Latitude Cold Water Domain: A Neogene Stratigraphic and Paleoenvironmental Transect across Fram Strait", which was designed to shed light onto the response of the Arctic Ocean and adjacent seas to the global climate deterioration across the Neogene period, the overall goal of this thesis is to enhance the utility of organic-walled microfossils (dinoflagellate cysts, prasinophyte algae, acritarchs) in the largely biogenic carbonate free sediments of an area critical for Late Cenozoic climate evolution. The primary objectives of this thesis are (1) to establish a palynostratigraphic framework for the high northern latitudes calibrated to an independent chronostratigraphy, (2) to critically evaluate the taxonomy and paleoecology of selected Neogene dinoflagellate cyst species, and (3) to reconstruct paleo-environmental conditions in the Iceland Sea across the 15–3 Ma time interval.

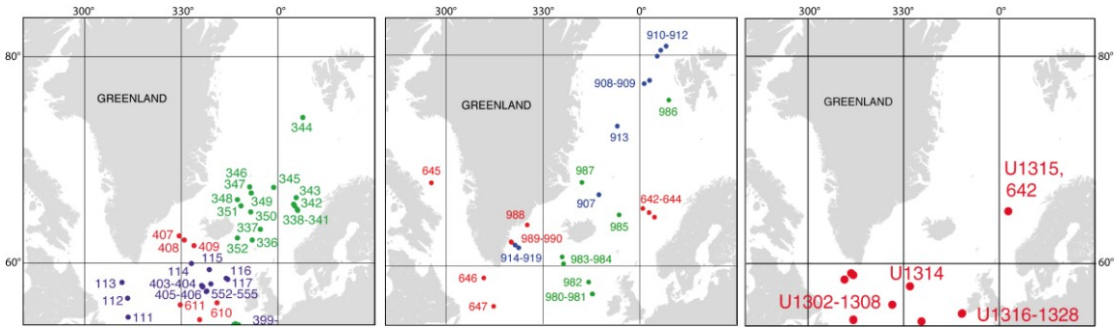

Figure 2: Overview on DSDP (left), ODP (middle), and IODP (right) Expeditions conducted within the high latitudes (Source: http://www-odp.tamu.edu/sitemap).

1) Palynostratigraphy

In contrast to calcareous and biosiliceous microfossils, organic-walled dinoflagellate cysts are the only microfossil group that is present in most (hemi)pelagic Neogene sequences of the high northern latitudes, predisposing them for detailed and reliable biostratigraphic correlations (Mudie et al., 1990). Despite this fact, and although Neogene sequences have been successfully drilled in the subpolar/polar North Atlantic and Arctic

Ocean during various DSDP, ODP, and IODP expeditions in the past 40 years (Fig. 2) a consistent palynostratigraphy is still not available for the region due to the partly inconsistent chronostratigraphic framework of many of these sites. In order to significantly enhance the utility of dinoflagellate cysts in polar environments it is indispensable to study those sites with excellent chronostratigraphy as a means of independently calibrating the dinoflagellate cyst bioevents to an absolute timescale. It is moreover necessary to thoroughly evaluate high latitude bioevents by regional and supraregional comparisons to help identify species promising for future biostratigraphic correlations within the high latitudes but also with the mid- and low latitudes. Therefore, ODP Hole 907A in the Iceland Sea (Fig. 2), which provides a continuous Miocene to Pliocene sedimentary sequence and the most consistent chronostratigraphy of all DSDP/ODP/IODP holes drilled north of the Greenland-Scotland Ridge, has been selected as the reference section for a detailed palynostratigraphic analysis.

Question: *Can we establish a consistent palynostratigraphic framework for the high northern latitude cold-water domain? How does defined bioevents compare on a regional and supraregional scale across the North Atlantic Ocean, and which are the species suitable for biostratigraphic correlations in the Nordic Seas and Arctic Ocean?*

This thesis provides the first magnetostratigraphic calibration of dinoflagellate cyst and acritarch events in the Nordic Seas and thus independent age control on a succession of Neogene high latitude palynomorph events for the first time.

2) Paleoecology

Profound knowledge on the paleoecological affinities of extinct species is crucial for paleoenvironmental reconstructions in pre-Quaternary sediments. However, the assessment of species preferences in the Neogene is strongly hampered by the limited co-occurrence of extinct and extant taxa. Statistical analyses (such as principal component and correspondence analyses) is restricted as Neogene paleoenvironmental variables in the high northern latitudes are virtually unknown, and the application of previously defined paleoenvironmental indices is questionable in the Iceland Sea because they have been established in regions with broadly different environmental conditions and index species are usually not (or only in considerably low numbers) present in the samples. Thus their applicability is seriously hampered, as the majority of taxa could not be assigned a certain preference.

Question: *Can we unravel paleoecological preferences of extinct species in the Iceland Sea in order to utilise them for paleoclimate reconstructions?*

This study provides new quantitative data on species of the extinct genus *Batiacasphaera* from the Iceland Sea and the Central Arctic Ocean, which in combination with published literature, may help to decipher the paleoecology of this important Neogene genus, which dominates Miocene dinoflagellate cyst assemblages in the high northern latitudes.

3) Neogene paleoenvironmental reconstruction

The northern high latitude oceans influence Earth climate on various timescales due to the production of deep-water that effects global ocean circulation, and the feedback mechanism related to the storage of water in continental ice sheets and/or sea-ice (Serreze and Barry, 2011). It is generally believed that they are of eminent relevance to decipher causes and consequences for the major climate transition in the Neogene (Thiede et al. 1998), when Earth's climate was finally pushed into the "icehouse world" with extensive bipolar glaciations (Zachos et al., 2008). Despite being a climatically sensitive region, the response of the Nordic Seas, in particular the cold-water domain of the Iceland Sea, to the Neogene climate cooling is virtually unknown because of 1) the scarcity of calcareous microfossils, and 2) the paucity of continuous records with an unequivocal age model. By contrast, organic-walled palynomorphs exhibit high abundance and diversity in the Neogene of the high latitudes and may help to reconstruct paleoenvironmental changes in order to provide complementary information on the yet poorly known Miocene to Pliocene evolution of the Iceland Sea.

Question: What is the response of the Nordic Seas cold-water domain to the long-term global cooling during the Neogene? Does marine palynomorphs reflect both the long-term trend, and short-term climate variability?

The investigation of the marine palynomorph record may allow semi-quantitative estimates on surface water properties such as temperature, salinity, nutrient availability, and sea-ice cover and thus provide new insights into to the Neogene paleoclimatic history of the Iceland Sea.

1.2 Structure of the thesis

The results of this thesis are discussed in three manuscripts (chapters 3–5, shortly introduced below), which have been submitted to peer-reviewed international scientific journals. Each chapter is intended to be a distinct piece of research that relates to the objectives stated above.

The necessary background information for this thesis is provided in chapter 2. This chapter gives an overview on the present day ocean circulation in the Nordic Seas (2.1), a summary of the tectonic development and the Neogene paleoceanographic evolution of the research area (2.2), a short introduction to dinoflagellates and their cysts; the main object of this thesis (2.3), and presents the material and methods (2.4) used within the framework of this study. The thesis ends with final remarks (chapter 6) including a summary of the main conclusions and a outlook on future perspectives with regard to high northern latitude research in general, and organic-walled marine palynomorphs in particular.

Chapter 3:

Schreck, M., Matthiessen, J. and Head, M. J. (accepted for publication). *A magneto-stratigraphic calibration of Middle Miocene through Pliocene dinoflagellate cyst and acritarch events in the Iceland Sea (Ocean Drilling Program Hole 907A).* Review of Palaeobotany and Palynology.

This study was designed to improve the stratigraphic utility of dinoflagellate cysts and acritarchs within the Neogene of the high northern latitudes in order to tighten biostratigraphic age control within this realm, and to identify those species promising for stratigraphic correlations with the mid- and low latitudes. For this purpose, 20 morphologically distinctive dinoflagellate cyst and one acritarch species have been selected to define 26 bioevents based on their highest/lowest and/or highest common occurrence. These bioevents have been calibrated to the well-constrained magneto-stratigraphy of ODP Hole 907A to provide first order absolute age determinations. Furthermore, these events have been placed into a regional framework by comparison with data from sites across the North Atlantic region and adjacent basins. The discussion focuses on a) the critical evaluation of their biostratigraphic application on a regional and supraregional scale, b) their potential for correlations with lower latitudes of the Northern Hemisphere, and c) possible ecologically or climatically induced asynchronities across the different North Atlantic basins.

Chapter 4:

Schreck, M. and Matthiessen, J. (accepted for publication). *Batiacasphaera micropapillata – Paleobiogeographic distribution and paleoecological implications of a critical Neogene species complex.* The Geological Society London, Special Publications.

The second study aims to decipher the (paleo)ecological affinity of the stratigraphically important extinct dinoflagellate cyst species complex *Batiacasphaera micropapillata*, in order to utilise it for future paleoenvironmental reconstructions. New data from ODP Hole 907A (Iceland Sea) and IODP Hole M0002A (Central Arctic Ocean) have been supplemented by data from literature to derive a comprehensive picture of the spatial and temporal distribution of the *B. micropapillata* complex. Paleobiogeographic distribution maps have been constructed for the Middle and Late Miocene, and the Pliocene and are discussed with regards to the major environmental parameters that may have controlled the distribution of this important Neogene species complex.

Chapter 5:

Schreck, M., Meheust, M., Stein, R. and Matthiessen, J. (submitted). *Response of marine palynomorphs to the Neogene cooling in the Iceland Sea (ODP Hole 907A).* Marine Micropaleontology.

This study addresses the paleoenvironmental evolution of the Iceland Sea during the Neogene. The detailed analysis of marine palynomorphs is supplemented by the first continuous high northern latitude Middle Miocene through Pliocene sea surface temperature record, which provides new constrains on the thermal evolution of this ocean basin. The identified changes in species diversity and concentration, abundance pattern, and assemblage composition depict distinctive paleoceanographic and paleoclimatic signals reflecting both globally recognizable trends and more local events. These events are discussed in the context of the general long-term Cenozoic cooling and its superimposed (short-term) climate variability, and finally utilised to reconstruct the response of the Iceland Sea to climate deterioration that occurred between *c.* 14.5 and 2.5 Ma.

2. Background Information

The following chapter provide introductory information on the research area, its oceanography, tectonics and Neogene paleoenvironment, but also on the material and methodology used to obtain the results, and to derive the conclusions presented in chapters 3 to 5.

2.1 Present-day ocean circulation in the Nordic Seas

The Norwegian-Greenland Sea, also referred to as the Nordic Seas (Johannessen, 1986), is the northernmost part of the North Atlantic. In literature, it is often subdivided into the Norwegian Sea (Norwegian Basin, Lofoten Basin, Vøring Plateau), the Greenland Sea (Greenland Basin, Boreas Basin) and the Iceland Sea (Fig. 3, e.g. Blindheim and Østerhus, 2005) based on topographic constrains – a physiography that reflects the plate tectonic evolution (see chapter 2.2). The Nordic Seas stretches between approximately 63°N and 82°N, and are bracketed by two of the major Arctic gateways, the Greenland-Scotland Ridge in the south, and Fram Strait in the north. The latter constitutes the only deep-water connection between the Arctic Ocean and the World's Ocean. However, both gateways effectively modulate the exchange of surface and deep-water masses between the Arctic Ocean and the North Atlantic and thus determine the present-day circulation pattern in this region. Moreover, the modulation of water mass exchange between the different ocean basins via these gateways plays an important role within the Thermohaline Circulation (Fig. 4), which in turn is suggested to influence climate on a global scale (see Rahmstorf, 2006 for review).

True oceanographic study of the Arctic and subarctic seas began with the exploratory voyages of Carl Coldewey, who investigated the nature of the ice-margin along East Greenland and in Fram Strait in 1868, followed by Fridtjof Nansen's famous expedition into the eastern Arctic Ocean (1893–1896). Since then, massive progress has been made in unravelling the oceanography of these harsh and poorly accessible environments (see Drange et al., 2005 for review).

The present-day surface circulation in the Nordic Seas is characterised by an opposing system of two main longitudinally orientated currents (Fig. 3). Relatively warm and saline surface water originating from the North Atlantic Drift (NAD), the northern continuation of the Gulf Stream system, enters the Nordic Seas from the south across

the Greenland-Scotland Ridge. It continues further north through the Norwegian Sea as the Norwegian Atlantic Current (NAC; Aagard et al., 1987; Rudels et al., 2005). Near Jan Mayen, a fraction flows into the Iceland Sea, and another substantial part of these waters branches off into the Barents Sea (North Cape Current, NCC; Blindheim and Østerhus, 2005). The reminder follows the continental slope northward as the West Spitzbergen Current (WSC). It mixes with Arctic surface water and propagates as a dense and saline subsurface current into the Arctic Ocean (Rudels et al., 1999; Schauer et al., 2002), while parts of this mixed subsurface water reflux back into the Greenland Sea (Johannessen, 1986). A minor portion of the original NAD water has already branched off towards Iceland south of the Greenland-Scotland Ridge at ± 50°N, and rounds the western part of the island clockwise as the Irminger Current (IC).

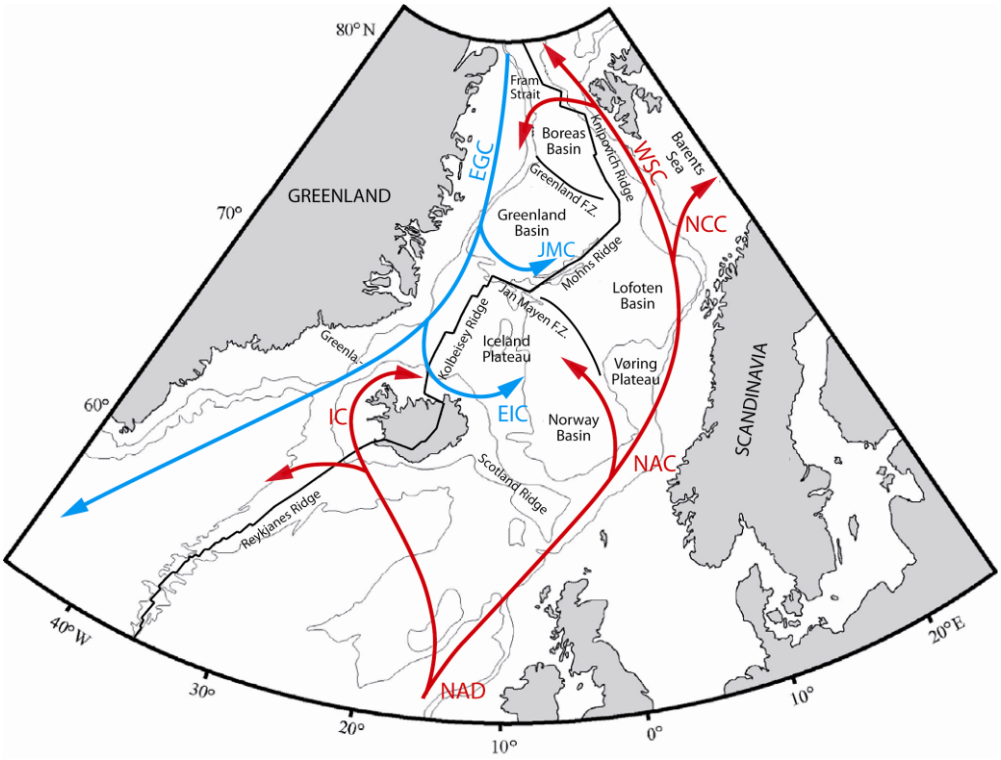

Figure 3: Present day ocean circulation in the Nordic Seas. Blue arrows refer to Arctic Ocean derived cold surface waters: EGC = East Greenland Current, JMC = Jan Mayen Current, EIC = East Iceland Current. Red arrows indicate Atlantic Ocean derived warm surface water: NAD = North Atlantic Drift, NAC = Norwegian Atlantic Current, WSC = West Spitzbergen Current, NCC = North Cape Current, IC = Irminger Current (modified after Johannessen, 1986; Rudels et al., 2005). Also shown is the differentiation of the Nordic Seas into basins and plateaus, and the major tectonic features (redrawn from Thiede and Myhre, 1996).

The advection of Atlantic water into the Nordic Seas and Arctic Ocean is encountered by the East Greenland Current (EGC) transporting cold and less saline polar waters (and sea-ice) southwards (Rudels et al., 2002). This cold water pathway is

paralleled by the North Atlantic waters of the Norwegian Sea, which forms the Arctic Front (Blindheim and Østerhus, 2005). On topographic constrains (Jan Mayen Fracture Zone), some of these waters divert into the Greenland Basin as the Jan Mayen Current (JMC), and form the southern limb of the cyclonic Greenland Gyre (Blindheim and Østerhus, 2005). Before the EGC leaves the Nordic Seas through Denmark Strait, a branch deflects eastwards and mixes with the IC. The resulting East Iceland Current (EIC) flows along the northern coast of Iceland, recirculating these mixed waters in a counter clockwise gyre (Rudels et al., 2005). Due to the configuration of the main currents both a distinct S-N and a strong E-W gradient in sea surface temperatures (and salinity) presently exist, separating the Nordic Seas into a comparatively temperate eastern and polar western domain (Rudels et al., 2005).

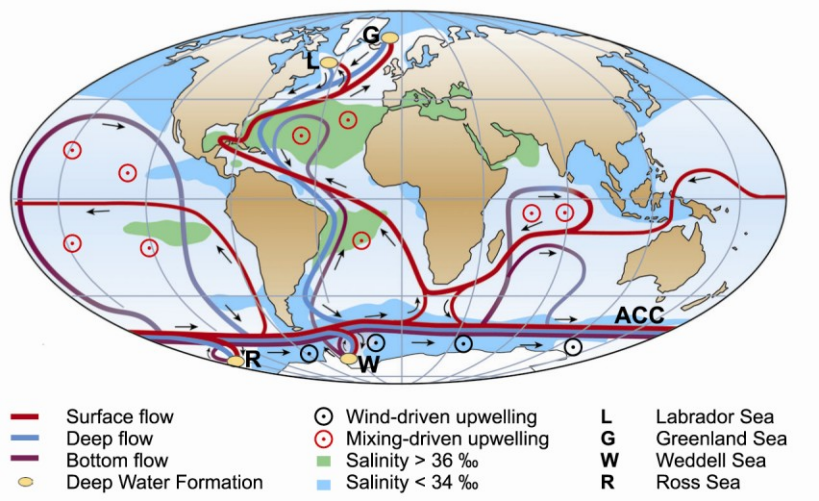

Figure 4: Schematic representation of the global Thermohaline Circulation illustrating the northward transport of warm and salty surface waters in the North Atlantic and the return flow of cold deep waters. Highlighted are the major regions of deep-water formation (from Rahmstorf, 2006).

As the Atlantic water heads north through the Nordic Seas, cooling and mixing with polar water lead to densification and hence vertical convection of this water mass into the deep basins (Rudels and Quadfasel, 1991). Presently, about three-fourths of the Atlantic water entering the Nordic Seas and the Arctic Ocean is transformed into dense overflow waters (Hansen and Østerhus, 2000), particularly in the central gyres of the Greenland and Iceland seas where it forms Norwegian-Greenland Sea Deep-Water (Fig. 4; e.g Aagard, 1985). It is subsequently modified by Arctic deep-water exported through Fram Strait (Rudels and Quadfasel, 1991; Schauer et al., 2002), and finally exported south into the North Atlantic (as Denmark Strait overflow) via Denmark Strait (Rudels et al., 2002) where it contributes to the renewal of North Atlantic Deep-Water (Swift, 1984).

The remaining part of these dense overflow waters is exported south via the Iceland-Faeroe Ridge and Faeroe-Shetland Channel (Fig. 8), whereby the volume transport on either side of Iceland is approximately equal (Blindheim, 2004).

Continuous formation and outflow of this cold and dense deep-water is largely responsible for triggering and sustaining both the Atlantic Meridional Overturning Circulation and the global Thermohaline Circulation (Fig. 4), through which the equatorial warmth is distributed polewards (e.g. Rahmstorf, 2006). Changes within this system on various (geological) time scales are assumed to have played a crucial role in earth climate history (e.g. Broecker, 1985; Flower and Kenneth, 1994; Clark et al., 2002), and are likely of critical importance for future climate change (Rahmstorf, 2006), underlining the relevance of the Nordic Seas for paleoclimate studies.

2.2 Tectonic development and Neogene paleoceanography of the Nordic Seas – A summary

The circulation system in the Nordic Seas (see chapter 2.1) is strongly controlled by its topography, which generally reflects the plate tectonic and volcanic history of this area (Vogt, 1986). Below, the major steps in the tectonic development of this region are presented (Fig. 5) with particular emphasis on the two probably most distinctive features of the "North Atlantic–Arctic Gateway" region, Fram Strait and the Greenland-Scotland Ridge. Build-upon, the Neogene paleoceanographic and paleoenvironmental evolution of the Nordic Seas is briefly summarized.

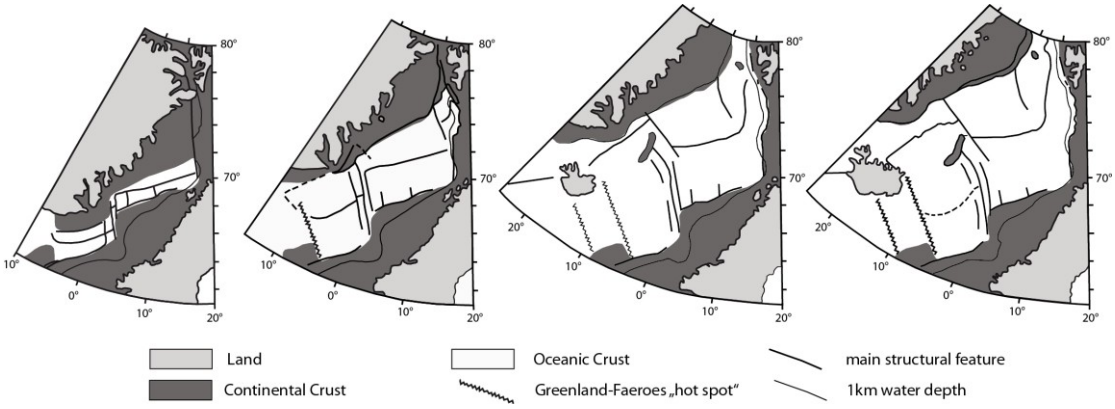

Figure 5: Simplified tectonic evolution of the Nordic Seas (redrawn from Eldholm et al., 1990). From left to right plate tectonic reconstructions for anomaly 23, anomaly 13, anomaly 5, and the present.

The passive continental margins surrounding the Nordic Seas lie within the North Atlantic Volcanic Province (NAVP) that extends from the Charlie Gibbs Fracture Zone at 55°N to the Spitzbergen margin at 75°N (Eldholm et al., 1990). The mid-ocean ridge system (Kolbeinsey-, Mohns-, and Knipovich Ridge), offset by major transforms, defines the plate boundary between the North American and Eurasian plates (Fig. 3). Before complete continental separation in the earliest Eocene (see Vogt, 1986 for review), the Norwegian and Greenland passive margins experienced several post-Caledonian extensional episodes in the Paleozoic and Mesozoic (four major rift phases, e.g. Eldholm et al., 1990; Doré et al., 1991), and a depositional area has been present since the Carboniferous between both margins. Large positive areas and shallow basins developed during this time, which have been subsequently eroded and subsided below sea level after seafloor spreading commenced (Myhre and Thiede, 1995).

The oldest seafloor spreading magnetic anomaly identified is of anomaly 24B age (Talwani and Eldholm, 1977), and it is commonly accepted that seafloor spreading started between anomaly 25 and 24 time (~ 55–50 Ma, Fig. 6). A similar anomaly 24 age has been suggested for the onset of seafloor spreading in the Arctic-Eurasian Basin (Vogt et al., 1979). The subsequent tectonic evolution is roughly divided into two phases and the Lofoten, Greenland and Norway basins developed to deep basins through the Eocene (Thiede and Myhre, 1996), probably isolated throughout this time (Eldholm et al., 1990). With respect to the Iceland Sea, a suite of magnetic anomalies on the Iceland Plateau implies origin of seafloor spreading around anomaly 7 time (~ 24–22 Ma; Talwani and Eldholm, 1977). However, this has been doubted by Vogt et al. (1980) who gave a crustal age between 15–14 Ma (anomaly 5) for the Iceland Plateau (see also discussion in chapter 3). The present distribution of oceanic ridges and fracture zones (Fig. 3), however, reflects a rather complex history of development.

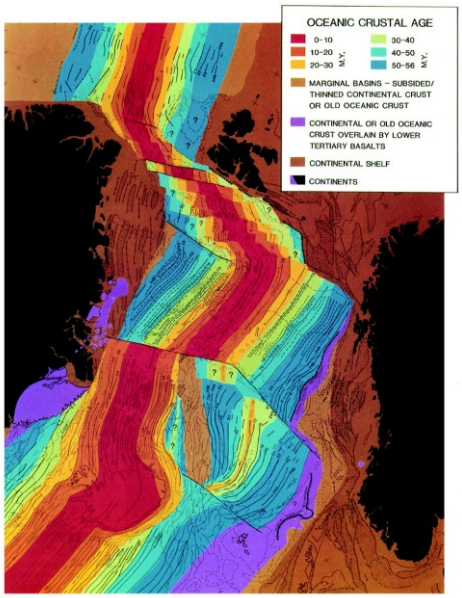

Figure 6: Magnetic lineations, and the type and age of crust in the Nordic Seas (from Vogt, 1986).

Fram Strait is the northernmost Atlantic-Arctic Gateway representing the only deep-water connection between the Arctic Ocean and the rest of the world's ocean. Despite its importance for the global circulation system, the gateway opening and the initiation of a deep-water connection are still under debate (Engen et al., 2008), and the various models span from the early Oligocene to the late Miocene (e.g. Crane et al., 1982; Eldholm et al., 1990; Kristoffersen, 1990; Lawver et al., 1990). This divergence was partly attributed to the weakly developed magnetic anomalies caused by ultra-slow spreading in the Fram Strait region that hampers accurate plate tectonic reconstructions (Thiede and Myhre, 1996; Ehlers and Jokat, 2009). Engen et al. (2008) recently used bathymetry and gravity data to generate a regional Bouguer map, which integrated with seismic data, provides a structural framework for reinterpretation, and the authors proposed an early Miocene gateway initiation. However, gateway initiation strongly depends on the judgment of when the passage became wide enough to facilitate deep-water exchange, and if the gateway required only a narrow Lena Trough, the early Miocene date (20–15 Ma) probably applies

to its formation (Engen et al., 2008). Instead, Kristoffersen (1990) and Lawver et al. (1990) argued that oceanic subsidence and further seafloor spreading was required to become effective, placing the gateway origin near the formation of well-developed seafloor spreading anomalies in Chron 5 (~ 10 Ma) (Fig. 7, Engen et al., 2008). Validation of plate tectonic reconstructions by paleoceanographic records is inherently difficult, as the GSR has also governed deep-water exchange between the North Atlantic and Arctic Ocean. However, based on a simple analytic two-layer model Jakobsson et al. (2007) assumed that Fram Strait reached sufficient width (40–50km; present-day width 400km) to efficiently ventilate the deep Arctic Ocean at ~ 17.5 Ma, suggesting an early Miocene gateway initiation. According to their age-width estimation, Fram Strait began to open at greater depth by ~ 14 Ma, a crucial timing with respect to Earth's climate evolution (see discussion chapter 5). This timing is supported by benthic foraminiferal evidence from the Lomonosov Ridge and Fram Strait (Kaminski et al., 2006; Kaminski, 2007).

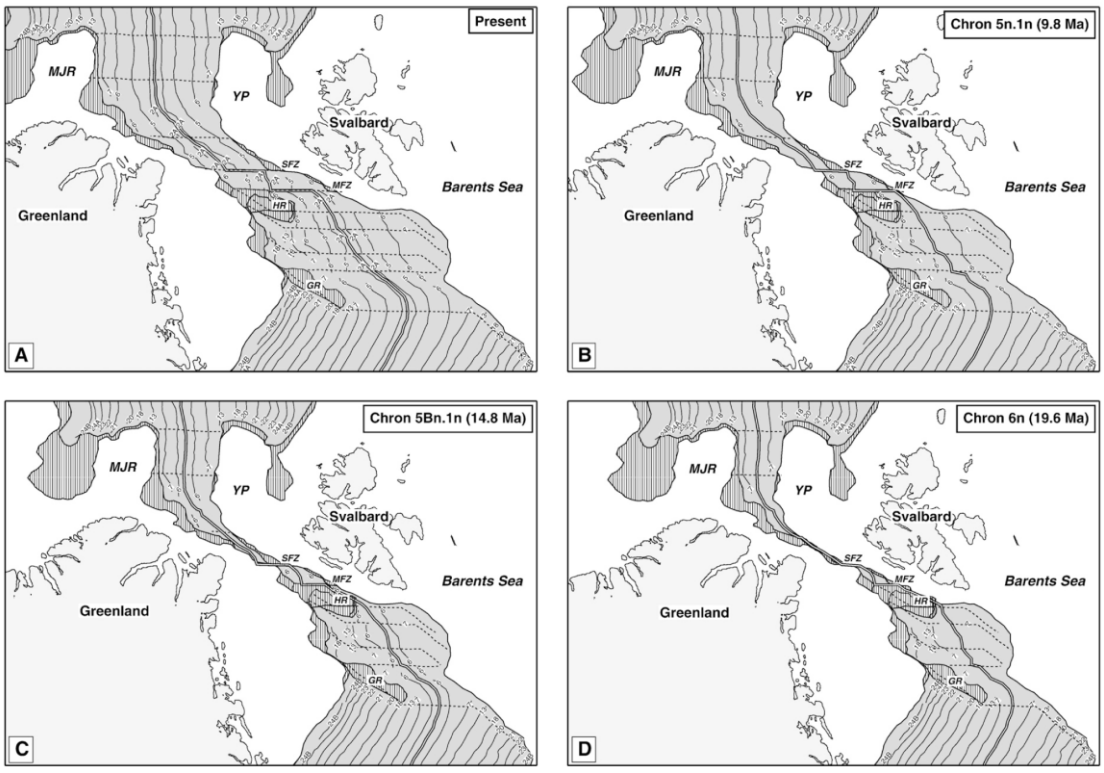

Figure 7: Plate tectonic reconstruction of the Fram Strait gateway (from Engen et al., 2008). Oceanic crust is shaded and magnetic anomalies shown as annotated bold lines. Reconstructions indicate: A) present day Lena Trough; B) development of first well developed seafloor spreading anomalies during late Miocene times (~ 10 Ma); C) formation of an initial, narrow oceanic corridor during early Miocene times (20–15 Ma); D) closure between Svalbard and NE-Greenland prior to early Miocene times (~ 20 Ma).

The southern gateway, the Greenland-Scotland Ridge, is an anomalous shallow aseismic bathymetric feature, which has been formed by excessive production (probably above sea-level) of volcanic material (Iceland plume) between 50–35 Ma, and is underlain by anomalous (up to 30km) thick crust (Thiede and Eldholm, 1983; Bott, 1983). This plume is a major convective upwelling within the mantle beneath Iceland, which has had an important effect upon the structural development of the North Atlantic Ocean over the last 60 Ma (Thiede and Eldholm, 1983). Morphologically, the ridge can be subdivided into three parts (Fig. 8): (1) the Greenland-Iceland Ridge, or Denmark Strait (sill depth ~ 600m), (2) the Iceland-Faeroe Ridge (sill depth 400–600m), and (3) the Faeroe-Shetland Channel with sill depth between 900–1000m (Thiede and Myhre, 1996). These shallow sills, with the deepest passage being not more than 1000m, making overflow water sensitive to even small changes in ridge height.

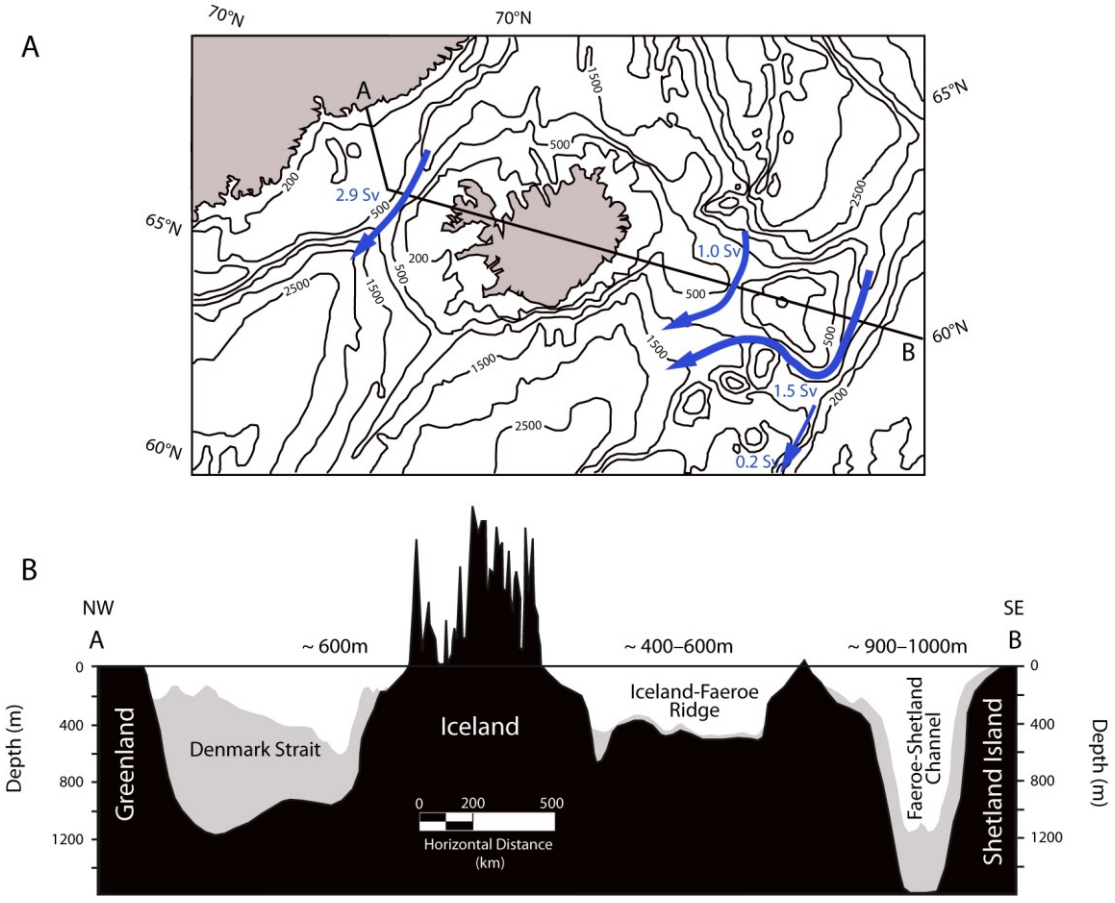

Figure 8: A) Bathymetric map of the Greenland-Scotland Ridge region. Blue arrows indicate the volume (in Sverdrup) of overflow water exported into the North Atlantic via the different pathways (after Blindheim, 2004). GSR overflow is roughly equal east and west of Iceland. B) A–B cross section along the Greenland-Scotland Ridge. Sediment coverage is shaded grey (redrawn from Wright and Miller, 1996).

These vertical motions are known to occur with at least two timescales; i) long-term subsidence (timescale of tens of million years) controlled by cooling of the lithospheric plate as it drifts away from the mid-ocean ridge, and ii) short-term subsidence (timescale of 1–10 Ma) controlled by rapid buoyancy fluctuations within the Iceland plume (Poore et al., 2006).

The GSR acted as a barrier for water mass (and marine biota) exchange, but vice versa also as a land bridge (Thulean Bridge, McKenna, 1983) between the Eurasian and North American continents during large parts of its geological history. Therefore, the GSR has been subject to many studies including tectonics, sedimentology, paleoceanography, (micro)paleontology, and modeling (e.g. Bohrmann et al., 1990; Wold, 1994; Wright and Miller, 1996; Poore et al., 2006, 2009; Butzin et al., 2011; Denk et al., 2011; Robinson et al., 2011; for pre-1983 studies see Bott et al., 1983 and references therein), but in particular its short-term subsidence history remains only poorly constrained yet.

The Neogene paleoceanography is rather complex as one has to take into account the properties of surface, intermediate, and bottom waters of the different ocean basins, the variability of sea-ice cover and iceberg input, the history of ice sheets on the surrounding continents, and the mode of water mass exchange between the North Atlantic and Nordic Seas as well as between the Nordic Seas and the Arctic Ocean. As the paleoenvironmental evolution of the Nordic Seas will be discussed in detail in chapter 5 only the major steps are summarized here (see also Fig. 26).

The Eocene to Early Miocene Nordic Seas were likely filled with nutrient rich surface waters as indicated by rich siliceous microfossil assemblages (Martini and Müller, 1976; Hull et al., 1996; Scherer and Koç, 1996; Suto, 2006) and high concentrations of dinoflagellate cysts (Manum et al., 1989; Firth, 1996). This high fertility has been created in an isolated poorly ventilated ocean with limited surface and deep-water exchange as also suggested by laminated or stratified sediments (Thiede and Myhre, 1996), agglutinated benthic foraminifera (Osterman and Spiegler, 1996), organic geochemistry (Ikehara et al., 1999), and the long-term subsidence history of the GSR (Wright and Miller, 1996; Poore et al., 2006). The modern Thermohaline Circulation (with cold EGC and warm NAC) was absent (including decreased meridionality), which presumably created a more zonal circulation within the Nordic Seas probably dominated by a large cyclonic gyre (Henrich et al., 1989; Bohrman et al., 1990). A recently published modeling study (Herold et al., 2012) suggests considerably fresher conditions, and the absence of

deep-water formation during the Early Miocene. Although the Nordic Seas have been assumed ice-free throughout this time interval (Thiede and Myhre, 1996), first local glaciations might have appeared on Greenland in the Middle Eocene as suggested by Eldrett et al. (2007) and Tripati et al. (2008). A similar age has been suggested for the initiation of Central Arctic Ocean sea-ice (St. John, 2008; Stickley et al., 2009).

Major paleoceanographic changes occurred in the Middle Miocene and were strongly coupled to the onset of overflow across the GSR, which caused major hiatuses on the Vøring Plateau (Thiede et al., 1989; Bohrmann et al., 1990; Bruns et al., 1998), and onset or increase of drift sedimentation (Shor and Poore, 1979; Wold, 1994) and widespread erosion (Mountain and Tucholke, 1985) in the North Atlantic. The advection of Atlantic waters into the Nordic Seas shifted the predominant biosiliceous sedimentation pattern towards carbonate accumulation (Bohrman et al., 1990; Cortese et al., 2004), and consequently resulted in initiation of deep water formation as recorded by foraminiferal faunas (Schnitker, 1986) and benthic $\delta^{13}C$ values (Wright and Miller, 1996; Poore et al., 2006; Butzin et al., 2011). Around the same time the transition from a poorly to well-ventilated Arctic Ocean furthermore suggests the initiation of a deep-water connection to the Arctic Ocean (Jacobsson et al., 2007), and the establishment of modern like ice drift pattern via Fram Strait has been proposed (Knies and Gaina, 2008). However, the onset of small-scale glaciations on the circum-Arctic continents is still under debate but most Nordic Seas records suggest an early Late Miocene age for the occurrence of first significant ice-rafted debris (IRD; see Thiede et al., 2011 for review). Although the prevalence of a Middle Miocene perennial sea-ice cover in the Central Arctic Ocean (Darby, 2008; Krylov et al., 2008) has been challenged (Matthiessen et al., 2009b), it is likely that at least a seasonal sea-ice cover existed. This uncertainty is also reflected in modeling studies. According to DeConto et al. (2008), the CO_2 threshold for bipolar glaciations was crossed ~ 25 Ma, indicating a potential contribution of northern hemisphere ice to Miocene sea-level variations, which is in conflict with de Boer et al. (2010) who suggest that the threshold for northern hemisphere glaciations was not passed before the end of the Miocene. Notwithstanding, the inflow of warm North Atlantic derived waters from the south and of cold Arctic derived waters from the north points towards the establishment of a proto-Thermohaline Circulation in the Nordic Seas in the Middle Miocene (Knies and Gaina, 2008).

The Late Miocene is characterized by alternations in carbonate and biogenic opal deposition that reflect periodic re-arrangements in surface and deep-water circulation

(Bohrman et al., 1990; Cortese et al., 2004) coupled to variations in GSR sill depth (Poore et al., 2006). Progressive climate deterioration is not only revealed by different microfossil groups (Locker and Martini, 1989; Manum et l., 1989; Mudie, 1989; Stabell and Koç, 1996; Poulsen et al., 1996), but also in the $\delta^{18}O$ of benthic and planktonic foraminifera (Fronval and Jansen, 1996). Moreover, the shifts in the biogenic sedimentation patterns broadly correspond to repetitive IRD pulses recorded at several sites in the Nordic Seas (Henrich et al., 1989; Jansen and Sjoholm, 1991; Wolf and Thiede, 1991; Fronval and Jansen, 1996; Wolf-Welling et al., 1996; Butt et al., 2001; Winkler et al., 2002) suggesting the existence of continental glaciations large enough to reach sea level. The early Late Miocene initiation of an East Greenland Current precursor (Wolf-Welling et al., 1996) is in contrast to the findings of Knies and Gaina (2008), but the subsequent onset of Denmark Strait overflow in the middle Late Miocene (Aksu and Hillaire-Marcel, 1989; Kaminski et al., 1989; Bohrmann et al., 1990; Wold, 1994) indicates the establishment of a circulation pattern that closely resembled the modern one. As a consequence, increased meridionality presumably favored the growth of continental ice.

Following a relatively warm period at the Miocene/Pliocene boundary (Locker and Martini, 1989; Henrich et al., 1989) probably associated with a strengthening of the NAC due to shoaling of the Panama Isthmus (Haug and Tiedemann, 1998), a stepwise cooling occurred in the Nordic Seas region. It has been recently assumed that shoaling of the Panama Isthmus not only led to an enhanced NAC but also to Arctic throughflow of Pacific water via Bering Strait, and thus to the establishment of a modern-type (fresh) East Greenland Current, which overcompensated the inflow of warmer North Atlantic water and finally led to the thermal isolation of Greenland (Sarntheim et al., 2009). Starting with a marked expansion of the Greenland ice sheet at 3.3 Ma (Jansen et al., 2000), the intensification of Northern Hemisphere glaciations between 3.5–2.4 Ma led to extensive regional scale glaciations formed on the circum-Arctic continents (Jansen et al., 2000; Kleiven et al., 2002; Mudelsee and Raymo, 2005; Knies et al., 2009), interrupted by a brief excursion to warmer climates during the Mid-Pliocene Climate Optimum (see Salzmann et al., 2011 for review). Probably characterized by unusually high temperatures in the Nordic Seas (Knies et al., 2002; Robinson, 2009), this interval might have been associated with a submerged GSR as suggested by modeling studies (Robinson et al., 2011). Further climate cooling seems to be related to reduced North Atlantic Deep-Water production after 3 Ma (Raymo et al., 1992), and even more pronounced after 2 Ma (Poore et al., 2006). The Middle Pleistocene transition between 1.2 and 0.7 Ma, which

progressively replaced the low-amplitude 41 kyr periodicity by high-amplitude 100 kyr cycles in global ice volume (Lisiecki and Raymo, 2005), is also reflected in the deep-sea sediments of the Nordic Seas (e.g. Baumann et al., 1996; Fronval and Jansen, 1996; Jansen et al., 2000; Henrich et al., 2002; Knies et al., 2009), and the thereby induced pronounced glacial/interglacial variability in sedimentation and biogenic production is the most prominent paleoceanographic pattern of the past 1 Ma (for review on Late Pleistocene to Holocene climate and sea-ice history see Wanner et al., 2008; Miller et al., 2010a; Polyak et al., 2010).

However, it must be acknowledged that most information presented above is derived from sites along the pathways of warm Atlantic water inflow (i.e. Norwegian Sea) or even south of the GSR, whereas the history of the cold-water domain (including the Iceland Sa as the study area for this thesis) is often inferred indirectly from other data and the detailed paleoenvironmental evolution still remains virtually unknown.

2.3 Dinoflagellates and their cysts – An overview

The application of microfossils such as dinoflagellate cysts in paleoenvironmental studies requires a profound knowledge on their biology (e.g. Mudie et al, 2001). On that account, the following chapter provides the necessary background information on the biology, morphology, and taxonomy of dinoflagellates and their cysts. However, as the focus of this thesis is on Neogene dinoflagellate cysts only a brief overview is given whilst detailed and specific aspects on the biology of dinoflagellates and their cysts are discussed in Taylor (1987), and a comprehensive overview on morphology and taxonomy is provided by Fensome et al. (1993), Williams et al. (2000), and Fensome and Williams (2004). Subsequently, the potential bias within a fossil assemblage is discussed, and this chapter ends with an overview on the history of high latitude Neogene dinoflagellate cyst research.

2.3.1 Biology, morphology and taxonomy

Dinoflagellates are eukaryotic, unicellular organisms that were recently assigned to the super-group Chromalveolata (Adl et al., 2005). They are one of the most important primary producers in marine environments (together with diatoms and coccolithophorids) but also occur in freshwater habitats or even sea-ice (Matthiessen et al., 2005). To date, about 1600 living marine and 230 freshwater species are known (Taylor, 1987), whereas ~ 4070 fossil species have been catalogued (Fensome and Williams, 2004). Many dinoflagellate species are phototrophic and thus restricted to the photic zone of the particular habitat but according to Larsen and Sournia (1991) about one-half of the living species are heterotrophic or mixotrophic (a combination of both trophic strategies), making this group highly complex in terms of feeding behaviour (Schnepf and Elbrächter, 1992; Smayda and Reynolds, 2003). Besides light and nutrient availability other factors such as sea surface temperature, sea-ice cover, salinity, structure of the water column (vertical stability, turbulence, tidal mixing), and competition with other plankton groups control the spatial and temporal distribution of dinoflagellates and their cysts (see Matthiessen et al, 2005 for a recent review).

The assignment of an organism to the division Dinoflagellata is based on several features, including the possession of an amphiesma (complex outer region of cell membrane), two dissimilar flagella (a longitudinal and a traverse), presence of specific biomarkers (dinosterol and amphisterols) and the unique type of nucleus (dinokaryon) with constantly condensed chromosomes (see Fensome et al., 1993 for discussion). The

life cycle of a dinoflagellate (Fig. 9) is complex but all species are known or at least believed to have a haplontic life cycle (Fensome et al., 1993). Asexual (vegetative) reproduction is brought about in different ways (binary fission, desmoschisis, eleutheroschisis, sporogenesis) depending on species (Taylor, 1987); whereas sexual reproduction usually involves the fusion of two haploid gametes produced by the vegetative cells. Fusion produces a planozygote (motile diploid stage) and in some dinoflagellate species, a non-motile hypnozygote (i.e. resting cyst) is formed within the theca of the motile stage (encystment), which may results in a reflection of morphological features of the motile form on the cyst (e.g. paratabulation). After a variable length of dormancy period (up to more than a century) (Lewis et al., 1999; Ribeiro et al., 2011), excystment occur and the cyst behaves as a passive particle in the water column (Anderson et al., 1985). The cyst wall consists of a highly resistant, macromolecular organic compound termed dinosporin (e.g. Versteegh and Blokker, 2004; de Leeuw et al., 2006), and it is this resting cyst that is preserved in the geological record. However, only about 15–20% (ca. 200 species) of all living dinoflagellate species produce fossilisable cysts (Head, 1996). Although cysts with calcareous walls are known to occur in both the modern ocean and the geological record (e.g. Zonneveld et al., 2005; Heinrich et al., 2011) they are not discussed in this chapter.

The morphological terminology of both dinoflagellates and cysts has been extensively described and illustrated in numerous publications (e.g. Williams et al., 2000). With respect to dinoflagellate cysts, the most important identification criterion is the presence of a tabulation pattern (manifestation of the dinoflagellates amphiesmal structure on the cyst; Fensome et al., 1993), which is the determining feature assigning a dinoflagellate affinity, and thus separating dinoflagellate cysts from other palynomorphs such as prasinophytes and chlorophytes. Tabulation can be expressed in various ways through different types of ornamentation (e.g. ridges along plate boundaries, position of spines or processes) or the shape of the archeopyle (Evitt, 1985); which is an opening in the cyst wall, formed along a preformed structure (principle archeopyle suture) during excystment of the protoblast. Its shape and position is genus-specific and remarkably stable over geological times (Fensome et al., 1993). On species level, taxonomic descriptions are based on criteria usually visible under light microscope and include overall body shape and size, the ornamentation on the cyst surface, internal wall structure and their differentiation, position and shape of processes or appendages, and also tabulation (Dale and Dale 2002).

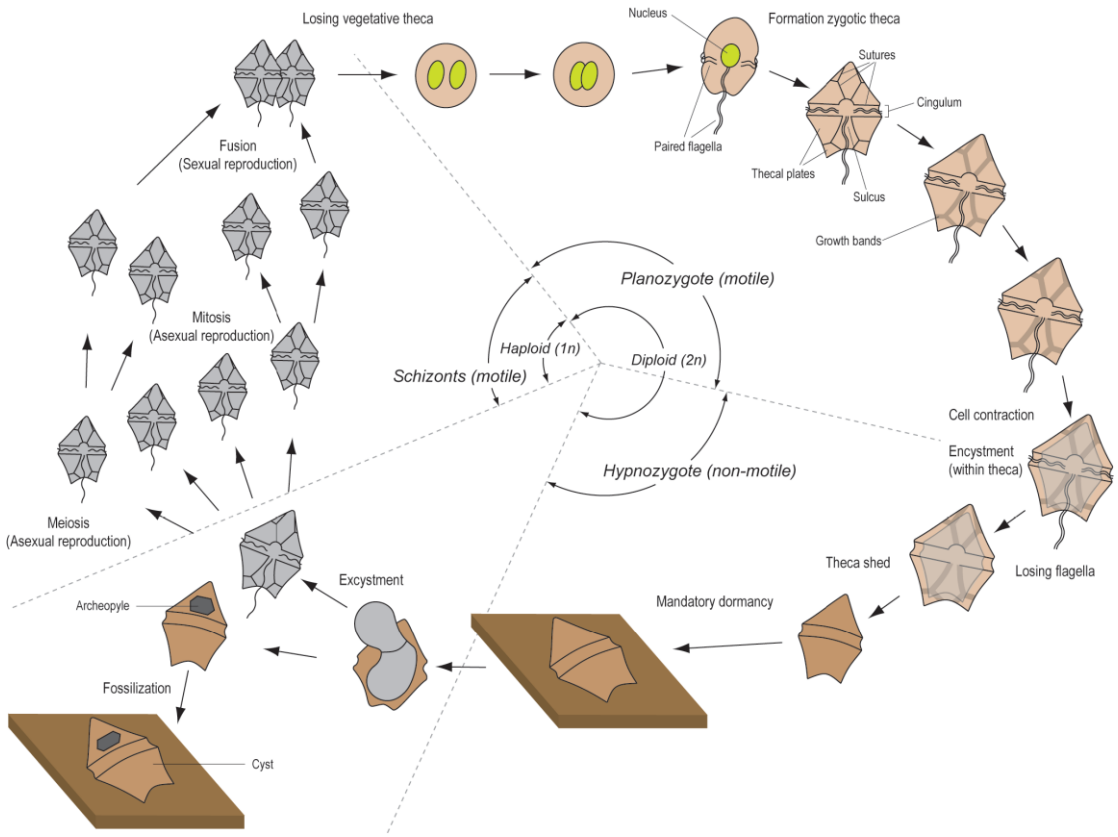

Figure 9: Idealized life cycle involving sexual reproduction and cyst formation. Also shown is terminology of different life stages and characteristic morphological features (from Verleye, 2011).

2.3.2 Taphonomic bias of the fossil assemblage

While sinking through the water column, plankton communities do not remain unchanged (Matthiessen et al., 2005), and biotic and abiotic processes bias the transformation of a living dinoflagellate community into the fossil cyst assemblage (Fig. 10).

a) As previously mentioned, only about 15–20% of the living dinoflagellates produce fossilisable cysts at all (e.g. Dale, 1976; Head, 1996), generating only a fragmentary image of the living community, and a selected record in the sediments. If the same is assumed for the geological past, then a fossil assemblage can inevitably only provide an estimate for the diversity of the living assemblage from which it originated.

b) Dinoflagellate cysts are composed of macromolecular organic compounds (Kokinos et al., 1998; Versteegh and Blokker, 2004; de Leeuw et al., 2006) and have been previously considered extremely resistant against degradation processes (e.g. Dale, 1996). However, recent studies have shown a species/genera dependent selective preservation (Zonneveld et al., 1997, 2007, 2010a; Versteegh et al., 2010) with oxygen generally being

the most destructive agent. Therefore, well-oxygenated bottom water can cause species selective aerobic degradation and it has been shown that cysts of phototrophic gonyaulacoids are less sensitive to oxidation than cysts of heterotrophic peridinioid species (see Zonneveld et al., 2008 for review). This aerobic degradation may be a rapid process that considerably changes dinoflagellate cyst concentration and assemblage composition (Kodrans-Nsiah et al., 2008).

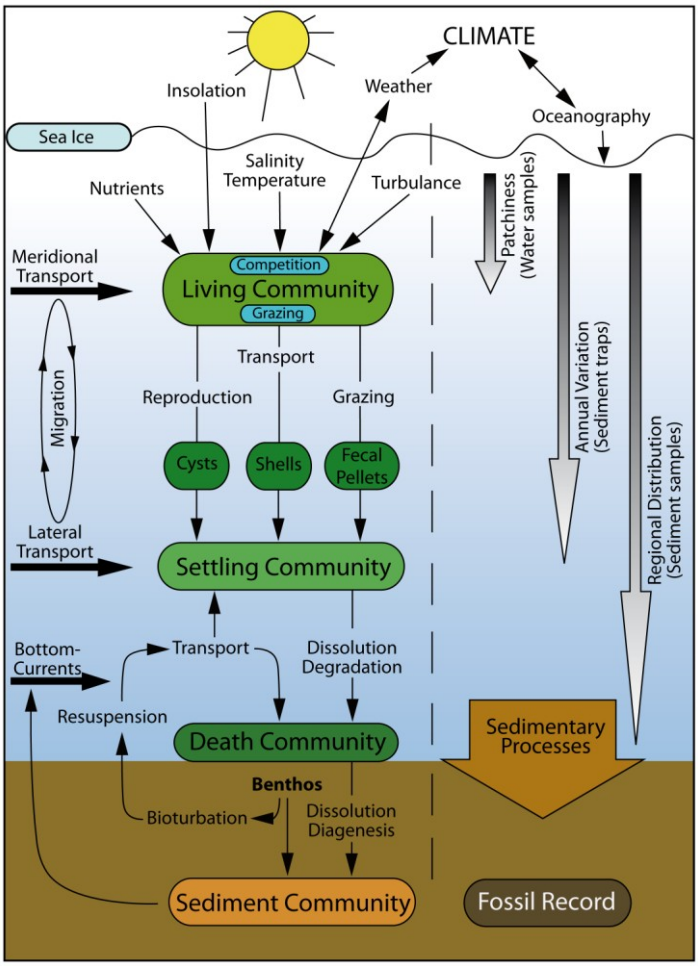

Figure 10: Successive stages in the formation of fossil sediment assemblages and their spatio-temporal information content (modified from Samtleben et al., 1995; Matthiessen et al., 2005).

c) In the water column, dinoflagellate cysts behave comparable to passive particles or silt (Anderson et al, 1985; Mudie and Harland, 1996), and sinking velocities of cysts are usually higher than those of the respective vegetative cell (Anderson et al., 1985). Although Anderson et al. (1985) observed generally low sinking rates (6–11 m d^{-1}), a more recent study suggests much faster velocities (~ 274 m d^{-1}, Zonneveld et al, 2010b) that may be even accelerated due to incorporation into fecal pellets (Dale, 1992; Honjo, 1996; Mudie, 1996). However, cysts might be subject to transport by ocean currents

(surface and bottom currents) as they descent to the sea floor, but little evidence is available to what magnitude this factor influences the final cyst recovery (Dale and Dale, 1992). On one hand for example, plankton and sediment samples suggest an influence of the North Atlantic Drift on the distribution of *Operculodinium centrocarpum* sensu Wall and Dale (e.g. Harland, 1983; Okolodkov, 1999; Matthiessen et al., 2001), whereas on the other hand, sediment trap studies show no detectable influence on cyst association during settlement through the water column (e.g. Zonneveld and Brummer, 2000; Zonneveld et al., 2010b). Moreover, the global distribution of dinoflagellate cysts in recent sediments demonstrates that distinct associations can be related to biogeographical zones and that long-distance transport may be negligible (Marret and Zonneveld, 2003). Therefore, its impact on distribution pattern of cysts still remains controversially discussed (Matthiessen et al., 2005). However, even if not completely in-situ, the dinoflagellate cyst association can at least give information on the prevailing currents and their physical characteristics that might have brought the cysts into the depositional area.

Lateral transport from the adjacent continental shelf into the deep sea might be a second important mechanism as species numbers of oceanic cysts are relatively low and most cysts found in open marine settings may be derived from neritic environments (Dale, 1992; Dale and Dale, 1992). However, there is again only little evidence from sediment trap studies (Harland and Pudsey, 1999; Zonneveld and Brummer, 2000; Susek et al., 2005; Zonneveld et al., 2010b), but it is likely that vulnerability of cysts for lateral transport varies in different seasons or different environments (Zonneveld and Brummer, 2000).

d) Grazing is another factor controlling both dinoflagellate growth in the surface water layer, cyst descent to the sea floor, and accumulation in the sediment. Dinoflagellates and sinking cysts may be subject to grazing by ciliates including tintinids, copepods, foraminifera, radiolarians and dinoflagellates themselves (Matthiessen et al., 2005). For the common fossil cysts, however, these processes appear to be of minor importance as the benthic grazers seems to prefer athecate, non-fossilisable and thus easily degradable cysts (Persson and Rosenberg, 2003).

2.3.3 Biogeographic distribution of recent dinoflagellate cysts

As mentioned previously, dinoflagellate cysts are distributed in a broad range of environments in dependency of their ecological affinities. The first systematic studies on the biogeographic distribution of cysts initiated more than forty years ago, when

individual taxa have been related visually or by means of statistical analyses to environmental gradients (e.g. Wall and Dale, 1976; Wall et al., 1977; Harland, 1983; see Marret and Zonneveld, 2003 for review). Subsequently, species abundances have been related to oceanographic and environmental parameters, and transfer functions (using Modern Analogue Technique [MAT]; see Guiot and de Vernal, 2007 for review) have been widely used to quantitatively reconstruct sea surface temperature and salinity (both on a seasonal or annual scale), and sea-ice cover in Quaternary sediments (e.g. Matthiessen et al., 2001; de Vernal et al., 2005; Esper and Zonneveld, 2007; Radi and de Vernal, 2008; Holzwarth et al., 2010). Notwithstanding it should be noted, that some methodological aspects of the MAT (i.e. spatial autocorrelation within training sets) are questioned (Telford, 2006; Telford and Birks, 2005).

The distribution of modern dinoflagellate cysts in the Arctic and subarctic seas was first studied on regionally restricted data sets (e.g. Harland et al., 1980; Harland, 1982; Mudie and Short, 1985; Mudie, 1992; Matthiessen, 1995), which were subsequently expanded by collaborative efforts (e.g. de Vernal et al., 1997; Rochon et al., 1999; de Vernal et al., 2001; de Vernal et al., 2005) and combined in a Northern Hemisphere database that meanwhile comprises 1491 sites and 67 taxa (Bonnet et al., 2012). A similar database has recently been established for the Southern Ocean (Esper and Zonneveld, 2007) comprising 350 sites to date (Verleye and Louwye, 2010).

The most comprehensive compilation of the geographical distribution and ecological affinities of modern organic-walled dinoflagellate cysts on a global scale is based on 61 individual species from 835 sites (Marret and Zonneveld, 2003), and includes samples from the Atlantic Ocean and adjacent seas, the Southern Ocean, Arabian Sea and the northwestern Pacific.

Besides the alignment of cyst distribution to environmental variables, recent studies also try to assess the potential of linking morphological variability (such as species process length) to environmental parameters (Mertens et al., 2010, 2012; Verleye et al., 2012).

2.3.4 Neogene dinoflagellate cysts in high northern latitudes

Mesozoic and Cenozoic dinoflagellate cysts have been widely used as a stratigraphic tool in hydrocarbon exploration and academic research since the middle of the 20th century (e.g. Stover et al., 1996). The application of dinoflagellate cyst assemblages in reconstructing high latitude Neogene paleoenvironments, however, is a relatively new field in marine micropaleontology as the high latitudes only received little attention due

to its hostile and poorly accessible environment. There was accordingly little understanding of knowledge on Neogene dinoflagellate cysts and it was not before the 1970s when Williams (1975) published the first Neogene dinoflagellate cyst biozonation on drill holes from offshore eastern Canada. Subsequently, assemblages of Miocene to Pliocene age have been reported frequently from the Northern Hemisphere (Manum, 1976; Williams and Bujak, 1977; Harland, 1979; Matsuoka, 1983; Bujak, 1984; Brown and Downie, 1984; Edwards, 1984, 1986; Bujak and Matsuoka, 1986; Wrenn and Kokinos, 1986; Powell, 1986; Mudie, 1987; Matsuoka et al., 1987), and also the Arctic Ocean (Bujak and Davis, 1981; Mudie, 1985).

Notwithstanding, knowledge on Neogene high latitude dinoflagellate cyst assemblages first increased significantly through successfully drilling Miocene to Pliocene sequences in subarctic environments such as the Norwegian Sea, Baffin Bay, and the Labrador Sea during Deep Sea Drilling Project (DSDP) Leg 38 and Ocean Drilling Program (ODP) Legs 104 and 105. Shipboard studies and detailed onshore work revealed that dinoflagellate cysts are continuously present in these sediments (Manum, 1976; Manum et al., 1989; Mudie, 1989; de Vernal and Mudie, 1989a,b; Head et al., 1989b,c) even from possibly ice-covered regions, and thus provide a suitable tool for stratigraphic purposes. Accordingly, a number of local and/or regional subarctic zonations have been established, but correlations among each other and with temperate North Atlantic sites were partly hampered (Fig. 11, Mudie et al., 1990; see Stover et al., 1996 for review) by the inconsistent chronostratigraphic framework of some of the drill sites (see discussion in chapter 3).

Besides their stratigraphic utility, dinoflagellate cysts also provide the opportunity to reconstruct the paleoclimate history in unprecedented detail due to their relatively high abundance and diversity in subarctic marine sediments. Semiquantitative estimates of abundances indicated substantial changes in assemblage composition that were utilized to reconstruct Neogene paleoenvironments based on ODP Legs 104 (Manum et al., 1989; Mudie, 1989) and 105 (de Vernal and Mudie, 1989a,b; Head et al, 1989a,b,c), and a sediment core from the Central Arctic Ocean (Mudie, 1985). For example, Mudie (1989) and Mudie et al. (1990) reconstructed a succession of major paleoecological events in the Neogene Arctic Ocean and adjacent seas based on dinoflagellate cysts and acritarchs, reflecting a stepwise response of assemblage composition to global cooling at 15 Ma, 9 Ma, 4.2 Ma and 1.4 Ma. Notwithstanding, and although dinoflagellate cyst-based reconstructions of paleoenvironmental conditions have been proven a valuable tool in

the Quaternary where assemblages closely resemble modern ones (e.g. Mudie et al, 2001; de Vernal et al., 2005), they still remain inconclusive for Neogene deposits as assemblages are often dominated by extinct species. To decipher the paleoecological signal of extinct species different approaches such as statistical analyses (e.g. Versteegh and Zonneveld, 1994), definition of palaeoenvironmental indices (e.g. Edwards et al., 1991; Versteegh, 1994), and the deduction of climatic affinities from biogeographic distributions (e.g. Masure and Vrielynck, 2009) have been applied in the past two decades, and major progress was made by the correlation of abundance patterns to quantitative reconstructions of sea surface temperature (De Schepper et al., 2011).

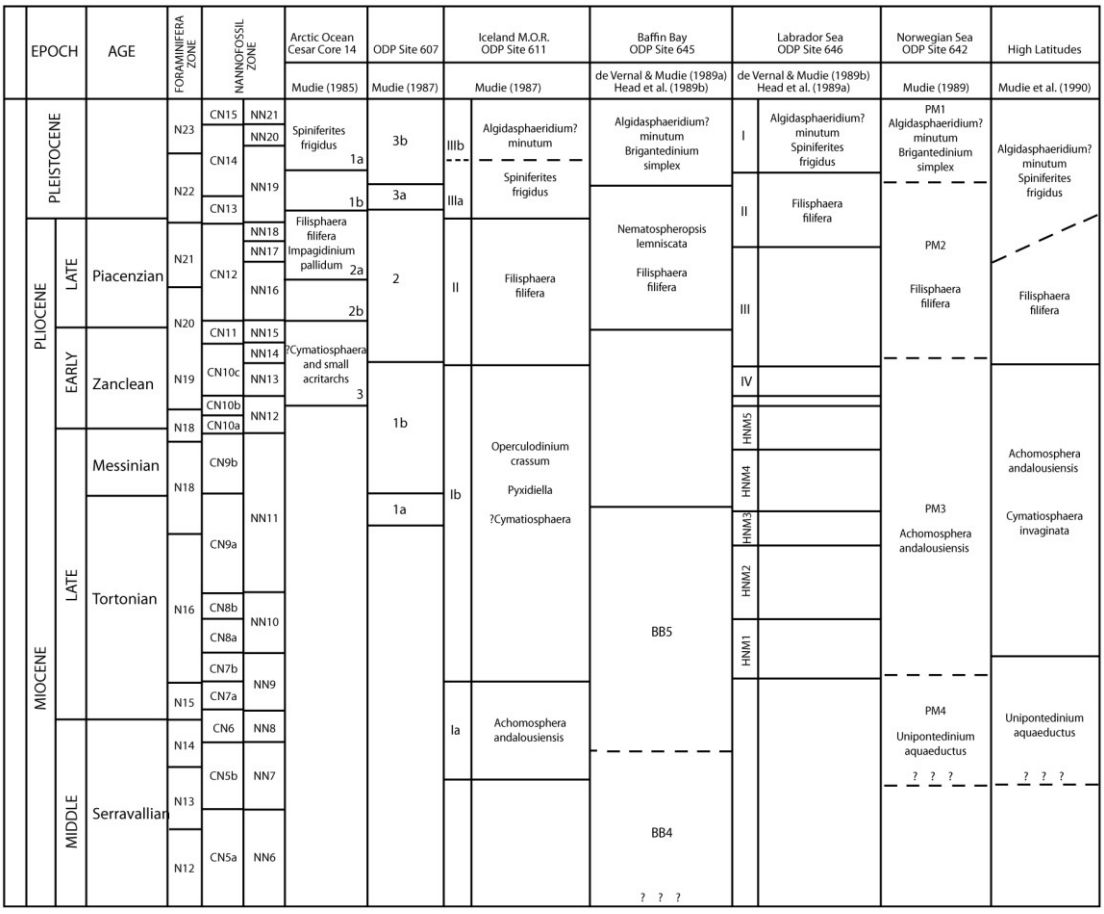

Figure 11: Neogene dinoflagellate cyst zonations of the Arctic and subarctic realm (modified from Stover et al., 1996).

In 1993 (ODP Leg 151) and 1995 (ODP Leg 162), new Neogene sequences have been recovered from the cold-water domain of the Nordic Seas in order to complement the records from the Norwegian Sea sites (ODP Leg 104), but dinoflagellate cyst studies (Matthiessen and Brenner, 1996; Poulsen et al., 1996; Smelror, 1999; Williams and Manum, 1999) basically conducted biostratigraphic correlations and did not further

proceed into the dinoflagellate cyst paleoecology.

Most recent advance in high latitude Neogene dinoflagellate cyst research was made in the framework of the IODP Expedition 302 (ACEX) in 2004, which retrieved Miocene through Pliocene sequences from the ice-covered Central Arctic Ocean for the first time. Dinoflagellate cysts and other palynomorphs are apparently more widely distributed than anticipated from core catcher samples (Backman et al., 2006, Sangiorgi et al., 2008; Matthiessen et al., 2009b; Matthiessen, unpubl. data), and the evaluation of palynomorph bioevents revealed that sedimentation rates are up to one magnitude higher in the Neogene than suggested by many studies on marine sediments from the Arctic Ocean (e.g. Clark et al., 1990). The presence of dinoflagellate cysts in the late Middle Miocene to Pliocene has been interpreted as seasonally open-water conditions and thus challenge the existence of perennial sea-ice cover based on sedimentology and mineralogy (Darby, 2008; Krylov et al., 2008). Moreover, based on the endemic acritarch *Decahedrella martinheadii* biostratigraphic and paleoenvironmental interpretations in the Neogene of the North Atlantic and Arctic Ocean have been revised (Matthiessen et al., 2009b), emphasizing the benefit of marine palynomorphs in the high latitudes.

Although dinoflagellate cysts are a valuable tool in Miocene through Pliocene stratigraphic and paleoenvironmental studies their overall potential is still not fully explored. A comprehensive Neogene biozonation including both the warm- and the cold-water domain of the high latitudes is still not available as the partly inconsistent chronostratigraphic framework of several ODP sites hampers precise absolute age determinations (Matthiessen et al., 2009b). Furthermore, it was only given little account on the taxonomy of more than 50 taxa that may partly be useful for biostratigraphy and paleoenvironmental interpretations (e.g. Poulsen et al., 1996), and different authors used various taxonomic concepts. The first palynological study on the Neogene of the Greenland Sea (Manum et al. 1976) revealed many new and distinctive dinoflagellate cyst species, but they were only illustrated and informally named. From the consecutive study on ODP Leg 104 in the Norwegian Sea, Mudie (1989) reported more than 100 late Cenozoic dinoflagellate cyst and acritarch morphotypes while Manum et al. (1989) recorded approximately 250 dinoflagellate cyst species for the early to late Cenozoic. Both authors refer only to half of the species as described and informal taxonomy was frequently used. In addition, Mudie (1989) mentioned many uncertainties regarding the equivalence of high northern latitude Neogene taxa reported by different workers

although a sound taxonomy is prerequisite for any biostratigraphic and paleoclimatic study.

Despite the utility of dinoflagellate cysts in the high northern latitudes, and although significant progress has been made in the past two decades essential tasks related to the taxonomy, paleoecology and biostratigraphy of Neogene dinoflagellate cysts yet remain to be addressed in order to fully grasp their potential for deep-time Arctic research.

2.4 Material and Methods

2.4.1 Study Material

This study focuses on sediments from Ocean Drilling Program Hole 907A, which was drilled in August 1993 during ODP Leg 151 „North Atlantic – Arctic Gateways". The site was planned as part of a paleoenvironmental transect from the Norwegian Sea (ODP Leg 104) to the Greenland continental margin in order to investigate the history of water mass exchange between the Arctic Ocean and the North Atlantic, in particular with regards to the climatically sensitive thermal gradient between the polar areas off East Greenland and temperate areas off Norway (Thiede and Myhre, 1996). Due to a medical emergency only Hole 907A was drilled in 1993, whereas the B, and C holes where drilled in 1995, when ODP Leg 162 reoccupied the drill site.

Hole 907A is located in the Iceland Sea as the southwestern part of the Nordic Seas, on the eastern Iceland Plateau (69°14.989´ N, 12°41.894´ W; 2035.7 m water depth). The Iceland Plateau is a flat-topped platform defined by the 1800-m contour, and Hole 907A was drilled on a relatively shallow part to provide an undisturbed, horizontal, pelagic sediment sequence (Shipboard Scientific Party, 1995). It reached a total depth of 224.1 mbsf with 216.3 m of sediment (recovery 102.6%) underlain by 8.7 m of basalts (recovery 60.2%) at the base of the hole. The recovered sediments mainly consist of unlithified, silty clays and clayey silts, which have been divided into five lithostratigraphic units by the Shipboard Scientific Party (1995) based on their siliciclastic, biogenic calcareous, and biogenic siliceous contents (Fig. 12). Unit III is furthermore subdivided into Subunit IIIA which is nannofossil ooze bearing, and Subunit IIIB that lacks calcareous nannofossils and has higher biogenic silica content.

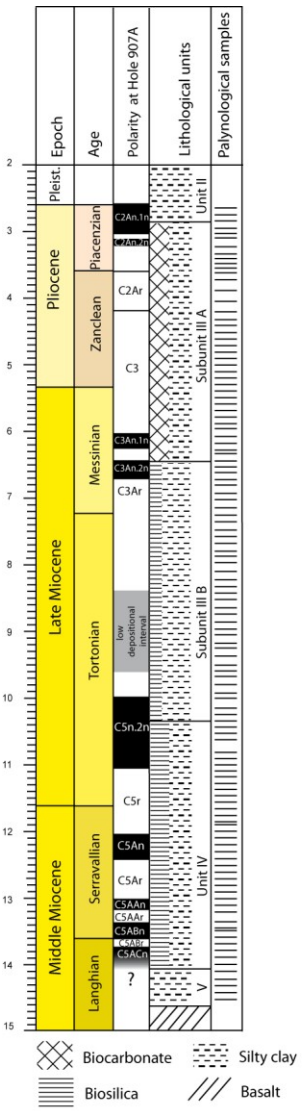

Figure 12: Magnetic polarity record (Channell et al., 1999) and lithological units (Shipboard Scientific Party, 1995) identified in the Pliocene through Miocene interval of Hole 907A. Also shown is the position of samples used in this study.

Samples used for this study were taken at the Bremen Core Repository in Spring 2008. Since the late Middle Miocene to Pliocene (*c.* 15–2.5 Ma) should be studied at a temporal resolution of ~ 100 kyr sample spacing varied with changes in sedimentation rates based on the revised age model for Site 907 (Channel et al., 1999a; Figs. 12, 15 and discussion of the age model in chapter 3.2.2), and due to preservation of the core material. Each sample (~ 30 cm^3) has been cleaned by scraping off all surfaces, which might have been contaminated by both drilling slurry and microbial growth, and was then divided into sub-samples for the different analytical methods. Out of these 120 samples a subset of 10 samples has been chosen for an initial study on alkenone biomarkers (chapter 5).

2.4.2 Methods

2.4.2.1 Palynological methods

Poulsen et al. (1996) reported that 2 cm^3 of sediment yielded only a small quantity of residue during a post-cruise palynological study. Thus the sample volume used for palynology was increased to ~ 15 cm^3. The samples were freeze-dried, weighed and processed using standard palynological methods (e.g. Wood et al., 1996). In a first step, samples were disaggregated using demineralised H_2O followed by adding 50 to 200 ml of cold 10% hydrochloric acid (HCl) to remove all carbonates. During this step, two *Lycopodium clavatum* tablets (Dept. of Quaternary Geology, Lund University, Sweden, batch no. 124961, X = 12542, s = ± 416 per tablet) were added to each sample to calculate palynomorph concentrations (Stockmarr, 1977). After chemical reaction had ceased, the material was neutralised with demineralised H_2O and sieved over a 6 μm polyester mesh to ensure that small palynomorphs (<15 μm) would be retained. In a second step, 200 ml cold 38–40% hydrofluoric acid (HF) was added in order to dissolve the siliciclastic components. The material was left in HF for 5–8 days, and has been thoroughly shaken at least once a day. Thereafter it was neutralised and sieved over 6 μm polyester mesh again. The procedure was repeated until all siliciclastic components had been removed. No ultrasound, oxidation or alkali treatments were applied, as these are known to damage some dinoflagellate cysts (e.g Schrank, 1988; de Schepper et al., 2004). The residue was finally mounted onto microscope slides using glycerine jelly. Depending on the amount of residue at least two permanent slides have been made. The coverslips have been sealed with non-caking paraffin in order to prevent the residue from drying out. All slides and residue are stored at the Alfred Wegener Institute for Polar and Marine Research, Bremerhaven, Germany. The slides containing the holotypes of new

species formally described in chapter 3 are curated at the Royal Ontario Museum, Toronto, Canada.

All palynological analysis have been conducted under a Zeiss Axioplan 2 microscope equipped with bright field, differential interference contrast, and phase contrast optics. The microscope slides were scanned along non-overlapping traverses using a 63x objective lens (barren samples have been scanned using a 40x objective lens), and wherever possible a minimum of at least 350 dinoflagellate cysts was counted to ensure statistical confidence. In addition, all other encountered palynomorphs (e.g. pollen, acritarchs, prasinophytes) have been enumerated. At least one slide was completely scanned for rare taxa not encountered during regular counts and for well-orientated specimens. Detailed morphological analysis of dinoflagellate cyst and small acritarch species has been performed using a 100x objective lens.

Autofluorescence of selected dinoflagellate cyst species has been determined by epifluorescence microscopy using a Zeiss Axiophot microscope equipped with the Zeiss filter set 9 (BP 450-490, FT 510; LP 515) in order to assess trophic affinity. In contrast to cysts of phototrophic dinoflagellates, cysts of heterotrophic species are known to be non-fluorescent (Brenner and Biebow, 2001).

Photomicrographs shown on plates I–IV were taken on a Leica DMR microscope equipped with a Leica DFC490 digital camera at the Department of Earth Science at Brock University, Canada. Photomicrographs shown on plate IV were taken on a Zeiss Axioplan 2 microscope equipped with a ProgRes C5 digital camera.

The dinoflagellate cyst nomenclature follows Fensome and Williams (2004 and reference therein) and Schreck et al. (chapter 3), and acritarch nomenclature follows Head et al. (1989a), Manum (1997), Head (2003), and de Schepper and Head (2008).

Palynomorph concentration has been calculated as:

$$N = \frac{(nC \times nS \times T)}{(nL \times sw)}$$ (Stockmarr, 1977)

N = Total number of palynomorphs per gram sample
nC = Number of palynomorphs counted
nS = Number of *Lycopodium clavatum* spores/tablet
T = Number of tablets added
nL = Number of *Lycopodium clavatum* spores counted
sw = sample weight in g (dry)

Two statistical indices have been used to characterise the dinoflagellate cyst assemblages. As a more simple measure for diversity species richness, which equals the number of dinoflagellate cyst species recorded in a sample, has been calculated. The Shannon-Wiener index was calculated as a statistical measure of species diversity. This index is based on information theory and tries to measure the amount of order (or disorder) contained in a system (Krebs, 1998). It is independent of sample size, but rare species increase the index (see also chapter 5). It was calculated as:

$$H' = \sum_{i=1}^{s} (p_i)(\log_2 p_i) \qquad \text{(Krebs, 1998)}$$

with s = species; p_i = proportion of total sample belonging to the ith species.

2.4.2.2 Organic geochemical bulk parameters

Organic geochemical bulk parameters have been determined to allow for a general characterisation of the amount and composition of organic matter preserved in the sediments. The sedimentary total organic carbon (TOC) content usually provides information on marine primary productivity and/or deposition of terrestrial material at a location (e.g. Stein and McDonald, 2004). The TOC contents were determined on ground freeze-dried samples by means of a carbon-sulfur determinator (CS-125, Leco) after the removal of carbonates by adding hydrochloric acid. Total carbon (TC) contents were measured by a CNS analyser (Elementar III, Vario) and used to calculate the carbonate ($CaCO_3$) content according to the formula:

$$CaCO_3 = (TC - TOC) \times 8.333$$

The amount of carbonate in the sediment also allows assumptions with respect to marine production of calcareous organisms and has been previously used to reconstruct the advection history of warmer Atlantic waters into the Norwegian Sea during the Neogene (Bohrmann et al., 1990). The carbon/nitrogen ratios (C/N) were measured and used to distinguish between a marine and a terrigenous source of the organic matter in the marine sediments. Marine plankton is generally characterised by ratios between 5-10, whereas values for terrigenous organic material commonly exceed 15 (e.g. Bordovskiy, 1965).

2.4.2.3 Alkenone paleothermometry

Alkenones are long-chained mono-ketones (Fig. 13). These highly resistant organic compounds are mainly produced by the ubiquitous coccolithophorid *Emiliania huxleyi*

(e.g. Volkman et al., 1995), a haptophyte that first appeared in the late Quaternary about 268 kyr ago (Thierstein et al., 1977). In pre-Quaternary sediments long-chain alkenones are attributed to the morphologically related genera of the family *Gephyrocapsaceae* (Marlowe et al., 1990). The degree of unsaturation of C_{37} alkenones is dependent from growth medium temperature (Brassel et al., 1986) and in combination with the global core-top calibration (Müller et al., 1998) this relationship can be used in the alkenone unsaturation index (Uk'_{37}) to accurately reconstruct mean annual sea surface temperatures (SST in °C) following:

$$U_{37}^{K'} = 0.333T + 0.04 \qquad \text{(Müller et al., 1998)}$$

The application and reliability of the Uk'_{37} index in Miocene through Pliocene sediments of the Iceland Sea is discussed in detail in chapter 5.

The freeze-dried and homogenised sediments (2 to 4g) were extracted with an Accelerated Solvent Extractor (DIONEX, ASE 200; 100°C, 1600 psi, 15min) using dichloromethane and methanol (99:1, v/v) as solvent. The neutral fraction was dissolved in hexane. The separation of compounds was carried out by open column chromatography (SiO_2) using *n*-hexane and dichloromethane (1:1, v/v), and dichloromethane. The composition of alkenones was analysed with a Hewlett Packard gas chromatograph (HP 6890, column 60 m x 0.32 mm; film thickness 0.25 μm; liquid phase: DB1-MS) using a temperature program as follows: 60°C (3 min), 150°C (rate: 20°C/min), 320°C (rate: 6°C/min), 320°C (40 min isothermal). For splitless injection a cold injection system (CIS) was used (60 °C [6 s], 340°C [rate: 12°C/s], 340°C [1 min isothermal]). Helium was used as carrier gas (1.2 ml/min). Individual alkenone ($C_{37:3}$, $C_{37:2}$) identification is based on retention time and the comparison with an external standard, which was also used for controlling the instrument stability.

The alkenone unsaturation index Uk'_{37} and hence the mean annual SST was calculated according to the above mentioned formula. The sample processing and the measurements were conducted by Marie Meheust (AWI).

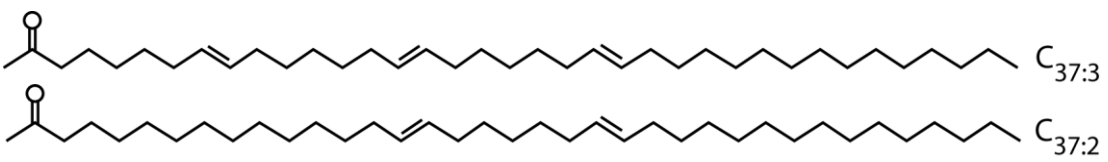

Figure 13: Molecular structure of the di- and tri-unsatured alkenone that is used in the alkenone unsaturation index Uk'_{37}.

3. A magnetostratigraphic calibration of Middle Miocene through Pliocene dinoflagellate cyst and acritarch events in the Iceland Sea (Ocean Drilling Program Hole 907A)

Michael Schreck[a,*], Jens Matthiessen[a] and Martin J. Head[b]

[a] Alfred Wegener Institute for Polar and Marine Research, 27568 Bremerhaven, Germany

[b] Department of Earth Sciences, Brock University, St. Catharines, Ontario L2S 3A1, Canada

Accepted in Review of Palaeobotany and Palynology.

Abstract

A detailed dinoflagellate cyst investigation of the almost continuous Middle Miocene through Pliocene of Ocean Drilling Program Hole 907A in the Iceland Sea has been conducted at 100-kyr resolution. The investigated section is well constrained by magnetostratigraphy, providing for the first time an independent temporal control on a succession of northern high-latitude dinoflagellate cyst bioevents.

Based on the highest/lowest occurrences (HO/LO) and highest common occurrence (HCO) of 20 dinoflagellate cyst taxa and one acritarch species, 26 bioevents have been defined and compared with those recorded in selected DSDP, ODP, and IODP sites from the North Atlantic and contiguous seas, and outcrops and boreholes from the onshore and offshore eastern U.S.A., and the North Sea and Mediterranean basins.

Comparisons reveal near-synchronous HOs of the dinoflagellate cysts *Batiacasphaera micropapillata* (3.8–3.4 Ma) and *Reticulatosphaera actinocoronata* (4.8–4.2 Ma) across the Nordic Seas and North Atlantic, highlighting their usefulness on a supraregional scale. This probably also applies to *Hystrichosphaeropsis obscura* when excluding ODP Hole 907A, as its upper stratigraphic range is presumably truncated on the Iceland Plateau. On a broader timescale, the HO of *Operculodinium piaseckii* most likely also permits correlation across the Nordic Seas and North Atlantic, whilst the HO of *Labyrinthodinium truncatum* appears to be valuable within the high latitudes of the Labrador and Nordic seas. Biostratigraphic markers useful for regional rather than supraregional correlation, are the HOs of *Batiacasphaera hirsuta* and *Unipontidinium aquaeductus*, the HCO of the acritarch *Decahedrella martinheadii*, and the LO of *Cerebrocysta irregulare* sp. nov. across

the Nordic Seas. Since *Habibacysta tectata, B. micropapillata, R. actinocoronata* and *D. martinheadii* have been observed in the Arctic Ocean they are potentially useful for high latitude correlations in the polar domain.

The LOs of *H. tectata and U. aquaeductus* suggest a mid- to late Langhian age (15.1–13.7 Ma) for deposits at the base of Hole 907A, thus providing new constraints on the maximum age of ODP Hole 907A.

The stratigraphically important dinoflagellate cysts *Cerebrocysta irregulare* sp. nov., and *Impagidinium elongatum* sp. nov. are described formally.

3.1 Introduction

Since Williams (1975) published the first Neogene dinoflagellate cyst (dinocyst) biozonation on drill holes from offshore eastern Canada, assemblages of Miocene to Pliocene age have been reported frequently from the Northern Hemisphere and our knowledge of their (paleo)ecology and stratigraphy has improved significantly (Stover et al., 1996; e.g. Williams and Bujak, 1985). It soon became evident that dinocysts are the only microfossil group with a continuous Neogene record in the high northern latitudes, and their relatively high diversity predisposes them for detailed and reliable biostratigraphic correlations in a region critical for understanding the development of Northern Hemisphere climate (De Schepper and Head, 2008). Despite these facts, and although Miocene and Pliocene sequences have been drilled successfully in the subpolar/polar North Atlantic and Arctic Ocean (Deep Sea Drilling Project [DSDP] Leg 38, Ocean Drilling Program [ODP] Legs 104, 105, 151, 162, and Integrated Ocean Drilling Program [IODP] Expedition 302), a consistent dinocyst biozonation for the Neogene is still not available.

The independent age calibration of dinocyst events is hampered partly by an incomplete chronostratigraphic framework of DSDP/ODP sites, as few holes have robust age control. First-order absolute age determinations using magnetic polarity reversals are often fragmentary due to incomplete core recovery and drilling disturbances caused by the technical difficulties of drilling at high latitudes. Where available, magnetostratigraphy is primarily supported by calcareous microfossil datums, but the paucity of biogenic carbonate in the high northern latitudes restricts their use and has relegated stable oxygen and carbon isotope stratigraphy to a subordinate role (Fronval and Jansen, 1996; Matthiessen et al., 2008). In addition, the low evolutionary turnover of these calcareous microfossil groups in high latitudes reduces the number of bioevents,

which themselves are not necessarily synchronous between high and low latitudes (Backman et al., 1984). These deficiencies are compounded by the susceptibility of foraminiferal tests and calcareous placoliths to dissolution in the colder waters of high northern latitude sites (e.g. Spiegler and Jansen, 1989).

Dinocysts are therefore crucial for high-latitude biostratigraphy, but to further enhance their utility it is necessary to study those sites with excellent chronostratigraphy as a means of independently calibrating the dinocyst datums (De Schepper and Head, 2008). ODP Hole 907A in the Iceland Sea (Fig. 14) is one of few high northern latitudes sites featuring a comparatively well-constrained magnetic polarity stratigraphy for the Middle and Upper Miocene (Channell et al., 1999a), in this case supported independently by silicoflagellate biostratigraphy (Amigo, 1999). Located today under the influence of cold water-masses exported from the Arctic Ocean, this site serves as a reference section for biostratigraphic correlation in the polar environments.

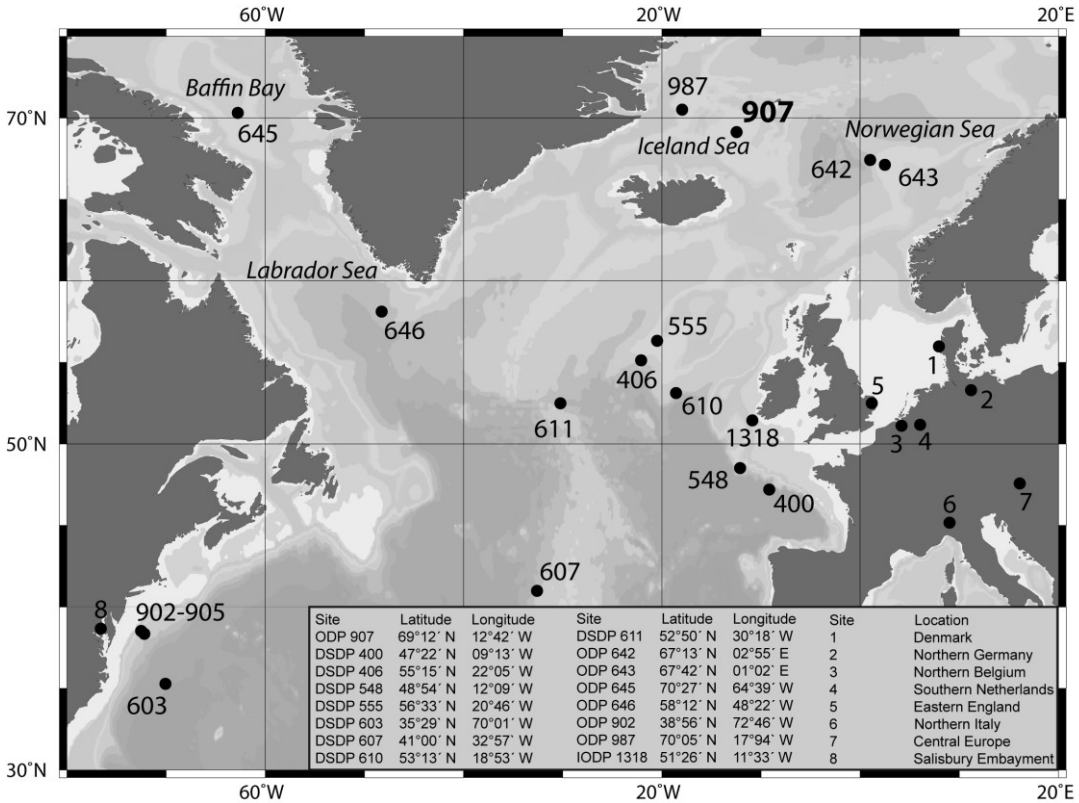

Site	Latitude	Longitude	Site	Latitude	Longitude	Site	Location
ODP 907	69°12´ N	12°42´ W	DSDP 611	52°50´ N	30°18´ W	1	Denmark
DSDP 400	47°22´ N	09°13´ W	ODP 642	67°13´ N	02°55´ E	2	Northern Germany
DSDP 406	55°15´ N	22°05´ W	ODP 643	67°42´ N	01°02´ E	3	Northern Belgium
DSDP 548	48°54´ N	12°09´ W	ODP 645	70°27´ N	64°39´ W	4	Southern Netherlands
DSDP 555	56°33´ N	20°46´ W	ODP 646	58°12´ N	48°22´ W	5	Eastern England
DSDP 603	35°29´ N	70°01´ W	ODP 902	38°56´ N	72°46´ W	6	Northern Italy
DSDP 607	41°00´ N	32°57´ W	ODP 987	70°05´ N	17°94´ W	7	Central Europe
DSDP 610	53°13´ N	18°53´ W	IODP 1318	51°26´ N	11°33´ W	8	Salisbury Embayment

Figure 14: North Atlantic and adjacent basins, showing the location of ODP Site 907 in the Iceland Sea and other sites discussed in the text.

For these reasons the Middle Miocene to Pliocene interval of Hole 907A has been selected for a detailed palynostratigraphic study. We present a suite of biostratigraphically useful dinocyst and acritarch bioevents that are correlated for the first time in the Nordic Seas to the astronomically-tuned Neogene time scale (ATNTS 2004,

Lourens et al., 2005) by using a revised magnetostratigraphy for Hole 907A (Channell et al., 1999a).

To identify those bioevents in Hole 907A that potentially extend biostratigraphic correlation into the high northern latitudes, we have compared the timing of our events with the published records of lower-latitude sites having independent age control. The most important of these sites are in the North Atlantic region, but we also compare our data with records from the North Sea and Mediterranean Sea basins and the on- and offshore eastern U.S.A. to evaluate possible ecologically or climatically induced asynchronies.

3.2 Material and Methods

ODP Leg 151 Hole 907A was drilled in the southwestern part of the Norwegian–Greenland Sea, on the eastern Iceland Plateau (69°14.989´ N, 12°41.894´ W; 2035.7 m water depth; Fig. 14), which is a flat-topped platform defined by the 1800-m contour. The drill hole penetrated a horizontal, undisturbed, pelagic sequence and reached a total depth of 224.1 meters below sea floor (mbsf). The lithology consists of 216.3 m of sediment (recovery 102.6%) underlain by 8.7 m of basalts (recovery 60.2%) at the base of the hole. The sediments mainly comprise unlithified silty clays and clayey silts, dark greyish brown in the upper half of the hole (0–56.3 mbsf) and olive grey, greenish grey, and greyish green in the lower half (56.3–216.3 mbsf; Shipboard Scientific Party, 1995). Five lithostratigraphic units (Fig. 15) were distinguished primarily by their siliciclastic, biogenic calcareous, and biogenic siliceous contents. Unit III is further subdivided into Subunit IIIA which is nannofossil ooze bearing, and Subunit IIIB that lacks calcareous nannofossils and has higher biogenic silica content. All units have pervasive bioturbation.

Previous studies on Hole 907A include an initial dinocyst stratigraphy for the Middle Miocene through middle Lower Pliocene by Poulsen et al. (1996). Based on 49 samples, these authors recognised three provisional biozones (Mio3, Mio4–5 and Mio6) but did not calibrate their informal biozones to the shipboard magnetostratigraphy (Shipboard Scientific Party, 1995).

3.2.1 Sampling and palynological methods

One hundred and twenty samples from Hole 907A (Fig. 16) were examined palynologically. Sample spacing varied with changes in the sedimentation rate and preservation of the core material. Based on the revised magnetostratigraphy of Channell

et al. (1999a), the sampling resolution was set at *c.* 100 kyr. The investigated interval (Sample 907A-6H-3, 82–84 cm to Sample 907A-23H-CC, 10–12 cm) extends from Subchrons C2An to C5ACn, spanning the entire Pliocene and extending back to the early Middle Miocene.

Since 2 cm^3 of sediment yielded only a small quantity of residue during post-cruise palynological studies (Poulsen et al., 1996), the sample volume used for this study was increased to 15 cm^3. Samples were freeze-dried, weighed, and processed using standard palynological techniques, including treatment with cold HCL (10%) and cold HF (38–40%), but without oxidation or alkali treatments. After each acid treatment the residue was neutralized with demineralised H_2O and sieved over a 6 μm polyester mesh to ensure that small palynomorphs (<15 μm) would be retained. Two *Lycopodium clavatum* tablets (Batch no. 124961, X = 12542, s = ± 416 per tablet) were added to each sample during HCl treatment to calculate palynomorph concentrations (Stockmarr, 1977). The residue was mounted on microscope slides with glycerine jelly and the coverslips sealed with non-caking paraffin wax. All slides are stored at the Alfred Wegener Institute for Polar and Marine Research, Bremerhaven, Germany, with the exception of six slides containing all illustrated specimens of *Cerebrocysta irregulare* sp. nov. and *Impagidinium elongatum* sp. nov. These slides are housed in the Invertebrate Section of the Department of Palaeobiology, Royal Ontario Museum, Toronto, Ontario, Canada, under the catalogue numbers ROM 61825–61830.

Wherever possible a minimum of 350 (average [Ø] = 272) dinocysts plus the acritarch *Decahedrella martinheadii* were enumerated, and the dinocysts identified to species level. At least one slide was completely scanned for rare taxa not seen during regular counts. All counts and scans were performed with a Zeiss Axioplan 2 microscope at 63x and 20x objective lens, respectively. Transmitted light photomicrographs (Plates I–IV) were taken on a Leica DMR microscope with a Leica DFC490 digital camera. Here we present data only for the species discussed (Fig. 16), as the full data set will be published elsewhere.

Nomenclature follows Fensome and Williams (2004) for the dinocysts and Manum (1997) for the acritarch. The full names of taxa are listed in Table 1.

3.2.2 Age Model

The initial shipboard magnetic polarity stratigraphy of Hole 907A was based entirely on inclination data supported by biostratigraphy (Shipboard Scientific Party, 1995).

Calcareous microfossils are rare to absent in the Miocene and Pliocene, and where they occur species diversity is low. In contrast, an initial radiolarian and diatom biostratigraphy was constructed for the Miocene and Pliocene (Shipboard Scientific Party, 1995), and a revised diatom biostratigraphy tied to an updated interpretation of the shipboard magnetostratigraphy was published by Koç and Scherer (1996), although these authors did not elaborate on the magnetostratigraphy in detail.

DINOFLAGELLATE CYSTS	Code	Plate
Batiacasphaera hirsuta Stover, 1977	Bhir	Plate III, 1–3
Batiacasphaera micropapillata Stover, 1977	Bmic	Plate III, 4–10
Cerebrocysta irregulare sp. nov.	Cirr	Plate III, 11–20
Cerebrocysta poulsenii de Verteuil and Norris, 1996	Cpou	Plate IV, 1–2
Cleistosphaeridium placacanthum (Deflandre and Cookson, 1955) Eaton et al., 2001	Cpla	Plate IV, 16–17
Corrudinium devernaliae Head and Norris, 2003	Cdev	Plate I, 11–12
Cordosphaeridium minimum sensu Benedek and Sarjeant (1981)	Cmin	Plate I, 1–3
Cristadinium cristatoserratum Head, Norris and Mudie, 1989a	Ccri	Plate IV, 10–12
Dapsilidinium pseudocolligerum (Stover 1977) Bujak et al., 1980	Dpseu	Plate IV, 9
Habibacysta tectata Head, Norris and Mudie, 1989a	Htec	Plate I, 19–20
Hystrichosphaeropsis obscura Habib, 1972	Hobs	Plate II, 1–5
Impagidinium elongatum sp. nov.	Ielo	Plate II, 6–20
Labyrinthodinium truncatum Piasecki, 1980 emend. de Verteuil and Norris, 1996	Ltru	Plate IV, 3–6
Operculodinium? *eirikianum* Head, Norris and Mudie, 1989a emend. Head, 1997	Oeir	Plate I, 4–5
Operculodinium piaseckii Strauss and Lund, 1992 emend. de Verteuil and Norris, 1996	Opia	Plate I, 6–7
Operculodinium tegillatum Head, 1997	Oteg	Plate I, 8–10
Palaeocystodinium spp. Alberti, 1961	Pspp	Plate IV, 13–15
Pyxidinopsis vesiculata Head and Norris, 2003	Pves	Plate I, 16–18
Reticulatosphaera actinocoronata (Matsuoka, 1983) Bujak and Matsuoka, 1986	Ract	Plate IV, 7–8
Unipontidinium aquaeductus (Piasecki, 1980) Wrenn, 1988	Uaqu	Plate I, 13–15
ACRITARCH		
Decahedrella martinheadii Manum, 1997	Dmar	Plate IV, 18–19

Table 1: Dinoflagellate cyst and acritarch species and their codes used in the present study of ODP Hole 907A.

Only Hole 907A was drilled at Site 907 during ODP Leg 151 in 1993, but this site was reoccupied in 1995 during ODP Leg 162 and Holes 907B and C were drilled. Channel et al. (1999a) used all three holes to establish a composite section for Site 907 and proposed a new magnetostratigraphy for Hole 907A (Fig. 15). The age model for Site 907 is based primarily on the interpretation of the paleomagnetic record obtained during Legs 151 and 162, as well as measurements of discrete samples on Hole 907B during post-cruise studies (Channell et al., 1999a). Two silicoflagellate datums identified at 193.79 and 152.4 mbsf in Hole 907B (Amigo, 1999) were now used to constrain the magnetostratigraphy in the Miocene interval. These datums were calibrated at Hole 982B (ODP Leg 162, Rockall Plateau) to a calcareous nannofossil stratigraphy (see Channell et al., 1999a for details). The revised interpretation of the magnetic polarity signal is

comparable to that suggested by Koç and Scherer (1996).

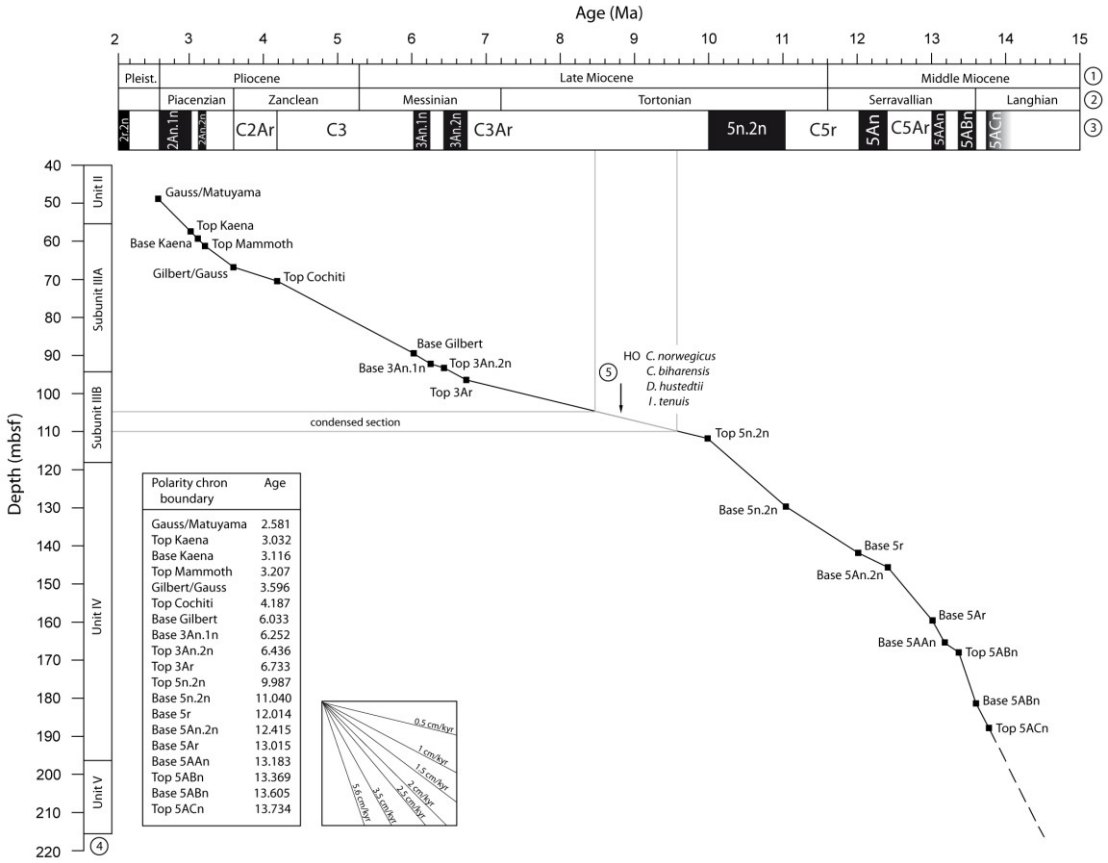

Figure 15: Age/depth plot for ODP Hole 907A. Solid black line: Age model of Channell et al. (1999) for ODP Hole 907A. Solid grey line: indicating possible unconformity/condensed section. Dashed black line: indicating our extrapolation of average sedimentation rates down-core (see Section 2.2). Symbols: ①Epoch/subepoch, ②Age, ③magnetic polarity zones of Hole 907A after Channel et al. (1999), ④lithological units and subunits identified (Shipboard Scientific Party, 1995), ⑤stratigraphic position of diatom events (Koç and Scherer, 1996) used for interpretation of unconformity/condensed section.

For the upper 100 m at Site 907, the shipboard pass-through inclination data indicate clearly-defined polarity zones that yield an excellent match with the magnetic polarity timescale (Shipboard Scientific Party, 1995; Channell et al., 1999a). However, the magnetostratigraphic interpretation of Channell et al. (1999a) indicates a condensed section or hiatus between ca. 105 and 110 mbsf, representing an interval between 8.4 and 9.6 Ma according to ATNTS 2004. This interpretation is based on a series of sawtooth-like steps in GRAPE density between 103 and 112 mbsf, associated with anomalously low magnetic susceptibility values for the same depth interval. Furthermore, the juxtaposition of the highest occurrences of the diatom species *Coscinodiscus norwegicus*, *Cymatosira biharensis*, *Ikebea tenuis,* and *Denticulopsis hustedtii* between 107.2 and 109.0 mbsf (113–115 mbsf according to Channell et al., 1999a) implies a hiatus at this level (Koç and

Scherer, 1996). As there is no sedimentological evidence for a hiatus, this interval probably instead represents a condensed section.

For the 110–185 mbsf interval, the correlation between the three holes of Site 907 is fairly straightforward (Channell et al., 1999a), although the Shipboard Scientific Party (1995) interpreted the absence of many of the C5An short normal Subchrons below 129 mbsf as another discontinuity. However, this is not supported by biostratigraphic data.

Although the paleomagnetic signal is well defined between 140 and 195 mbsf it is difficult to match with the polarity time scale. The Shipboard Scientific Party (1995) interpreted this interval as greatly expanded, and the four normal polarity zones were correlated to Subchrons C5AA to C5AD. However, Channel et al. (1999a) correlated the lowest polarity chron boundary at 187.85 mbsf to the top of Subchron C5ACn.

The maximum age of the sedimentary sequence is derived from $^{40}Ar/^{39}Ar$ dating of tholeiitic basalts recovered from the base of Hole 907A. The age of 13.2 ± 0.3 Ma represents the isochron of the low-temperature heating steps and is considered relatively accurate, but low potassium content and low radiogenic yields place limits on precision (Davis and McIntosh, 1996). The authors regarded their results as tentative because the dating has not yet been duplicated. The radiometric age is slightly younger than the top of Subchron C5ACn (13.7 Ma), implying that either the age or the magnetostratigraphy are in error. Even a slightly older age for the basalts would imply much higher sedimentation rates for the lowest *c.* 28 m than the average of 3.5–5.7 cm/ka for the lower part this hole. This is unlikely because no indications of mass transport have been found in that part of the hole (Shipboard Scientific Party, 1995). Therefore, we consider the paleomagnetic interpretation more reliable than a single $^{40}Ar/^{39}Ar$ date, and so have extrapolated sedimentation rates down-core. Sedimentation rates between the lowest three tie-points are fairly constant (Fig. 15), and we used these rates to calculate tentatively an age of 14.5 Ma for our lowermost sample (907A-23H-CC, 10–12 cm; 216.5 mbsf) at the base of the sedimentary sequence. The ages of the polarity chron boundaries given by Channel et al. (1999a) have been updated to ATNTS 2004 (Lourens et al., 2005). This age model has been used to calculate sedimentation rates and numerical ages for each sample and bioevent by linear interpolation between tie-points.

3.2.3 Definition of biostratigraphic events

We follow the concept of biostratigraphic datums used by De Schepper and Head

(2008). The abbreviations LO and HO indicate the lowest and highest in-situ stratigraphic occurrence of taxa, respectively. The HPO represents the highest persistent occurrence (i.e. in successive samples) of a taxon, even where such occurrences are marked by a few specimens only. Sporadic occurrences above a HPO might represent reworking (De Schepper and Head, 2008). A highest common occurrence (HCO) marks the highest sample in which a particular species is noticeably abundant, although it will occur above this level in much lower numbers.

3.2.4 Uncertainties in the assessment of bioevent ages

When calculating numerical ages for biostratigraphic events, those inaccuracies associated with the construction of the age model, sample spacing, and bioturbation must be considered (e.g. De Schepper and Head, 2008; Weaver and Clement, 1987). Furthermore, the temporal distribution and abundance variations of species may cause inaccurate definitions of bioevents.

Paleomagnetic boundaries are placed at the midpoint between two adjacent samples that record a reversal in inclination, thus introducing an error that can be as much as half the age difference between these samples (Weaver and Clement, 1987). For Hole 907A, the distance between two samples across a magnetic reversal varies from 10 to 20 cm (Ø 12 cm). With an average sedimentation rate of 2 cm/kyr, this accounts for an error of 5–10 kyr (Ø 6 kyr) on the age of the magnetic boundary.

The same applies for the highest and lowest occurrence (HO and LO) of a species, which might be anywhere between the lowest/highest sample containing a species and the next sample that does not contain that species. For Hole 907A sampled at 100 kyr resolution, this accounts for an average error of ± 50 kyr in the assessment of the true LO or HO of a species.

As mentioned previously, bioturbation was recorded in all lithological units (Shipboard Scientific Party, 1995). In several North Atlantic cores, Ruddiman and Glover (1972) found bioturbation of volcanic ash up to 44 cm below and 27 cm above the peak abundance of an ash layer. Based on these estimates for bioturbation and an average sedimentation rate of 2 cm/kyr for the studied interval in Hole 907A, the average errors for HOs and LOs due to bioturbation are 22 kyr (Ø 11 kyr) and 13.5 kyr (Ø 7 kyr), respectively.

Reworking of dinocysts is another potential source of error. This problem is not unique to dinocysts, but their durability makes them particularly susceptible. Aside from

preservational differences and other evidence, the stratigraphic pattern of cyst occurrences can be used to infer reworking. Species that are usually abundant through their stratigraphic range may occur in low numbers immediately above, invoking the possibility of reworking. Rare species might occur in low but persistent numbers to the top of their true stratigraphic range, with reworked specimens occurring only sporadically above it. The descriptive terms HCO and HPO can be useful in these two contexts. However, using such criteria to evaluate reworking in the published literature is difficult because raw counts or quantitative data are seldom made available.

Another complicating factor is that rare or discontinuous occurrences, especially at high latitude sites, may not represent reworking but relate to variable oceanographic/climatic conditions such as glacial/interglacial cycles. Thus, fixed-interval sampling will be biased towards colder conditions, and narrow intervals (e.g. interglacials) with high abundances of a warm-adapted species may not be sampled sufficiently. This introduces an unknown error into the calculations of ages for any bioevents, and HPOs and HCOs clearly must be treated with special caution in high-latitude regions.

3.3 Results

3.3.1 Chronostratigraphic summary of sites used for comparison

To test the biostratigraphic utility of bioevents calibrated in Hole 907A on a regional and supraregional scale, comparisons are made with the few relatively high-resolution Neogene palynostratigraphic studies from the North Atlantic region that have detailed and reliable magnetostratigraphy and/or independent biostratigraphy (Fig. 14). The age assignments of bioevents in the older literature have been revised where new chronostratigraphic control is available, and all datums are calibrated to the latest time scale, ATNTS 2004 (Lourens et al., 2005).

In general, Pliocene successions offer better magnetostratigraphic age control than Miocene successions, where magnetic polarity sequences tend to be complicated by hiatuses, drilling disturbances and high reversal frequencies. For the Pliocene, good paleomagnetic age control is available for Iceland Sea ODP Hole 987E (Channell et al., 1999b), Norwegian Sea ODP Site 642 (Bleil, 1989), eastern North Atlantic DSDP Holes 610A (Clement and Robinson, 1987; De Schepper and Head, 2008) and 400/400A (Hailwood, 1979), central North Atlantic DSDP Hole 607/607A (Clement and Robinson, 1987), and western North Atlantic DSDP Hole 603C (Canninga et al., 1987). For the Miocene, magnetostratigraphic age control is provided only for Norwegian Sea

ODP sites 642 and 643 (Bleil, 1989), and eastern North Atlantic IODP Site U1318 (Louwye et al., 2007b). At sites 642 and 643, the magnetic polarity record (Bleil, 1989) is fragmented by hiatuses identified primarily by a radiolarian stratigraphy (Goll, 1989; Goll and Bjørklund, 1989) that has since been re-interpreted based on unpublished data (Goll, 1997 in Williams and Manum, 1999). However, some putative hiatuses have been questioned by Bruns et al. (1998) who in fact suspected them to represent artefacts of calcareous and biosiliceous microfossil preservation due to reduced sedimentation rates. Our study therefore relies primarily on the magnetostratigraphic interpretation of Bleil (1989). IODP Site U1318 provides a well-constrained magnetostratigraphy that covers the Lower to Middle Miocene (Louwye et al., 2007b).

Other North Atlantic sites used for comparison in this study are dated less accurately or less completely, either through low resolution of the magnetostratigraphy and supporting microfossil datums or because biostratigraphy is the only age control.

Of the many palynostratigraphic studies published on sequences from the marginal North Atlantic and adjacent basins, relatively few have been selected for comparison. The continuous Miocene successions from northern Italy alone have a first-order paleomagnetic and biostratigraphic calibration (Zevenboom, 1995). The datums defined for the on- and offshore eastern U.S.A. and adjacent continental margin (de Verteuil, 1996, 1997; de Verteuil and Norris, 1996) have been widely accepted and frequently applied to European Neogene sequences because of their similar latitudinal position and comparable assemblages. However, while the U.S. continental margin and coastal plain sequences are placed within a detailed sequence stratigraphic framework, they have many hiatuses and lack the precise chronostratigraphic control of some deep-sea records.

The North Sea was a semi-enclosed basin connected only to the Nordic Seas during much of the Neogene (Rasmussen et al., 2008). A wealth of palynostratigraphic data has been compiled throughout the region in an attempt to correlate and date bioevents and zonations (for regional overviews see Dybkjær and Piasecki, 2010; Head, 1998; Köthe, 2003, 2005; Köthe and Piesker, 2007; Louwye et al., 2000, 2004, 2007; Munsterman and Brinkhuis, 2004). However, zonations have been established using comprehensive but geographically restricted data sets partly based on multiple boreholes or sections that may not be applicable between regions, e.g. the Netherlands and Germany (Köthe and Andruleit, 2007), and regional correlations have been hampered by the paucity of continuous sequences and a scarcity of calcareous planktonic microfossils

needed for independent control (for a detailed discussion see Head, 1998; Köthe, 2005; Dybkjaer and Piasecki, 2010). In the absence of such control, the Miocene dinocyst zonation established for the U.S. East Coast by de Verteuil and Norris (1996) has been used in Belgium (e.g. Louwye et al., 2000) and northern Germany (Köthe, 2003, 2005). For the North Sea Basin, Munsterman and Brinkhuis (2004) relied on a combination of stratigraphic data and the work of Zevenboom (1995) and de Verteuil and Norris (1996) for age-calibration of bioevents, and Donders et al. (2009) updated these ages to ATNTS 2004. In eastern England, the Miocene is missing, although a fragmentary Pliocene and Lower Pleistocene marine record has led to the definition of provisional highest occurrences and acme events for selected species (Head, 1998). A comprehensive stratigraphic assessment of bioevents defined in the separate studies is required to establish useful datums for the entire southern North Sea. In contrast to the southern North Sea Basin, few data are available from the northern North Sea (Head et al., 2004; Piasecki et al., 2002).

An unambiguous recalibration of datums identified from these studies is therefore not always possible, but approximate ages have been assigned below to species considered promising for future biostratigraphic investigations on a regional or supraregional scale.

3.3.2 Magnetostratigraphic calibration of dinocyst events

The studied section of Hole 907A yielded a diverse and well-preserved dinocyst record, comprising at least 155 species belonging to at least 44 genera, and most of the 120 samples analyzed yielded enough dinocysts to enumerate 350 cysts. Counts in 21 samples ranged between 14 and 194 cysts and 16 samples are virtually barren (<5 cysts per slide). Most barren samples cluster between 100 and 103 mbsf in the Upper Miocene (*c.* 7.5–8 Ma). A second low-productivity interval (<9 cysts per slide) is found in the Upper Pliocene between 2.6 and 3.3 Ma (49–62 mbsf). Reworking of pre-Miocene material is limited (M.S., unpubl. data).

For this study we focussed on 20 morphologically distinctive dinocyst taxa and one acritarch species (Table 1), many of which are already recognised biostratigraphic markers for the Miocene and Pliocene in the North Atlantic and adjacent seas (e.g. Stover et al., 1996; Williams et al., 1998, 2004).

Poulsen et al. (1996) recorded most of the taxa discussed here, but usually in a few samples only. Moreover, the age assignments of their three provisional biozones are

not consistent with age estimates calculated by Channell et al. (1999b) based on the well-defined magnetostratigraphy of ODP Hole 987E. Nonetheless, occurrences of important taxa reported by Poulsen et al. (1996) are discussed in the text where appropriate.

The datums identified in Hole 907A (Fig. 16) have been placed within a regional framework by comparison with suitable sites across the North Atlantic realm (Fig. 17). The source of dinocyst data, taxonomic information and the sample information used for the chronostratigraphic calibration of events at the various North Atlantic sites is given in Appendix A.

Langhian (Middle Miocene)

LO *Cristadinium cristatoserratum* (Plate IV, 10–12)

Occurrence: Sample 907A-23H-6, 97.5–99.5 cm; 215.30 mbsf.

Magnetostratigraphic calibration: extrapolated from top of Subchron C5ABn through top of Subchron C5ACn.

Age assessment: 14.3 Ma (mid-Langhian).

Discussion: The age of this datum should be regarded as a minimum owing to the rare and sporadic occurrence of this species in the lower part of Hole 907A.

This species has seldom been reported following its description by Head et al. (1989a) from ODP Hole 646B in the Labrador Sea. It extends to the base of Hole 646B, which is calibrated to the mid-Tortonian calcareous nannofossil zone NN10 (Head et al., 1989c; Knüttel et al., 1989).

It has been reported sporadically from offshore New Jersey, western North Atlantic, with a LO established from one sample in the Upper Oligocene of ODP Hole 906A and a LO in the Middle Miocene dinocyst zone DN5 of ODP Hole 905A (*c.* 13 Ma, de Verteuil, 1996; Gartner and Shyu, 1996). In western North Atlantic DSDP Hole 603C, this species occurs at the base of the hole at 5.82 Ma (upper Messinian) (M.J.H, unpubl. data; Canninga et al., 1987).

The only other published record of this species is from ODP Hole 908A, just west of Spitsbergen, where it was reported in a single sample from the lower Tortonian (Poulsen et al., 1996).

Figure 16 (next page): Raw counts and stratigraphic ranges of selected dinoflagellate cyst and acritarch taxa in ODP Hole 907A. * = species only encountered outside regular counts, (n) or (*) = suspected reworking. Light shading indicates total stratigraphic range, and dark shading indicates the 26 bioevents (LO, HCO, HO) recognised in the present study. Also shown is the magnetic polarity stratigraphy of Hole 907A (Channell et al., 1999a).

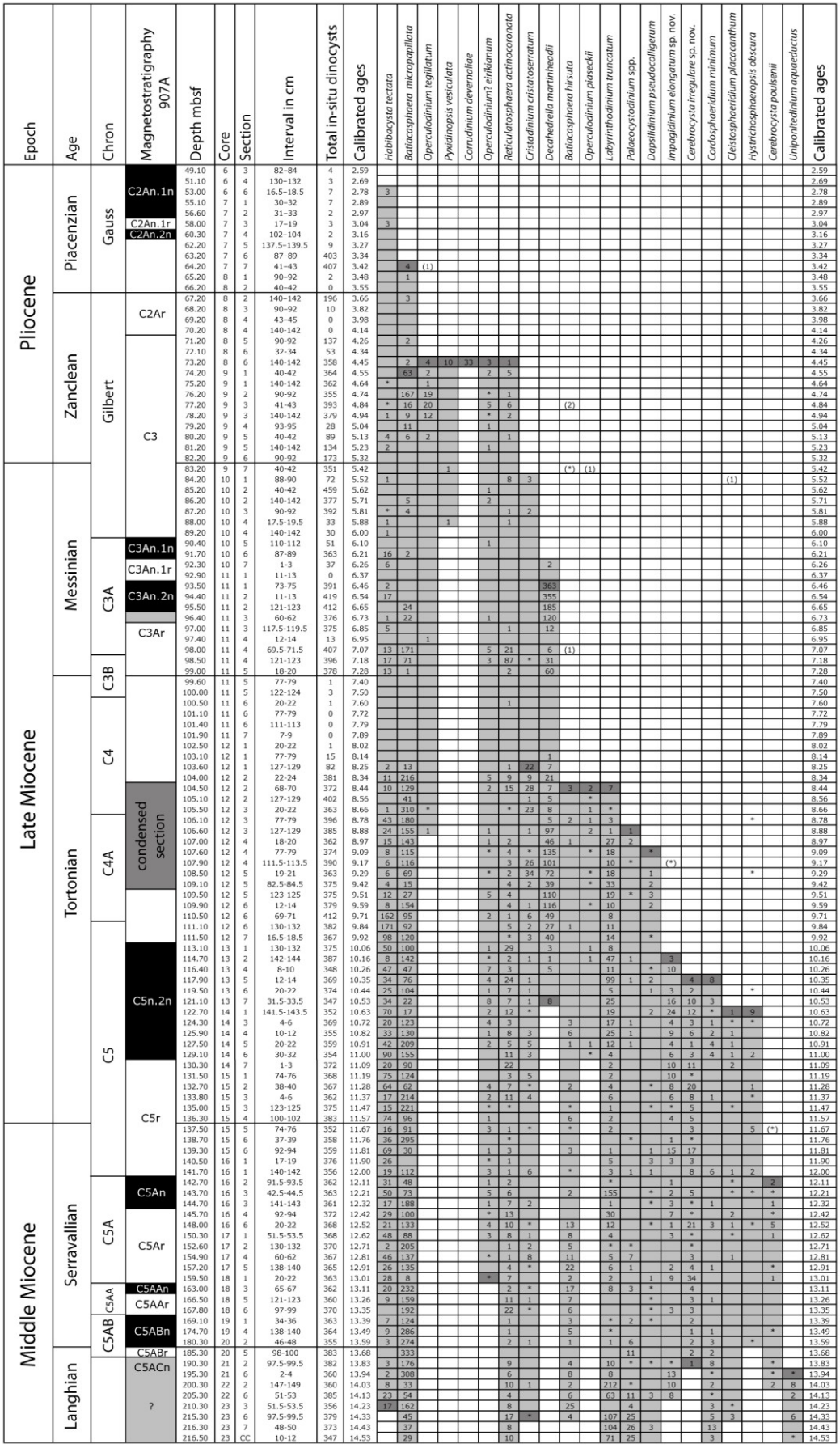

Epoch	Age	Chron	Magnetostratigraphy 907A	Depth mbsf	Core	Section	Interval in cm	Total in-situ dinocysts	Calibrated ages	*Habibacysta tectata*	*Batiacasphaera micropapillata*	*Operculodinium tegillatum*	*Pyxidinopsis vesiculata*	*Corrudinium devernaliae*	*Operculodinium? eirikianum*	*Reticulatosphaera actinocoronata*	*Cristadinium cristatoserratum*	*Decahedrella martinheadii*	*Batiacasphaera hirsuta*	*Operculodinium piaseckii*	*Labyrinthodinium truncatum*	*Palaeocystodinium* spp.	*Dapsilidinium pseudocolligerum*	*Impagidinium elongatum* sp. nov.	*Cerebrocysta irregulare* sp. nov.	*Cordosphaeridium minimum*	*Cleistosphaeridium placacanthum*	*Hystrichosphaeropsis obscura*	*Cerebrocysta poulsenii*	*Uniponitedinium aquaeductus*	Calibrated ages
Pliocene	Piacenzian	Gauss	C2An.1n	49.10	6	3	82–84	4	2.59																					2.59
				51.10	6	4	130–132	3	2.69																					2.69
				53.00	6	6	16.5–18.5	7	2.78	3																				2.78
				55.10	7	1	30–32	7	2.89																					2.89
				56.60	7	2	31–33	2	2.97																					2.97
			C2An.1r	58.00	7	3	17–19	3	3.04	3																				3.04
			C2An.2n	60.30	7	4	102–104	2	3.16																					3.16
				62.20	7	5	137.5–139.5	9	3.27																					3.27
				63.20	7	6	87–89	403	3.34																					3.34
				64.20	7	7	41–43	407	3.42		4	(1)																		3.42
				65.20	8	1	90–92	2	3.48		1																			3.48
				66.20	8	2	40–42	0	3.55																					3.55
	Zanclean	Gilbert	C2Ar	67.20	8	2	140–142	196	3.66		3																			3.66
				68.20	8	3	90–92	10	3.82																					3.82
				69.20	8	4	43–45	0	3.98																					3.98
				70.20	8	4	140–142	0	4.14																					4.14
				71.20	8	5	90–92	137	4.26		2																			4.26
				72.10	8	6	32–34	53	4.34																					4.34
				73.20	8	6	140–142	358	4.45		2	4	10	33	3	1														4.45
				74.20	9	1	40–42	364	4.55		63	2			2	5														4.55
				75.20	9	1	140–142	362	4.64	*	1																			4.64
				76.20	9	2	90–92	355	4.74		167	19			*	1														4.74
				77.20	9	3	41–43	393	4.84	*	16	20			5	6			(2)											4.84
				78.20	9	3	140–142	379	4.94	1	9	12			*	2														4.94
				79.20	9	4	93–95	28	5.04		11				1															5.04
			C3	80.20	9	5	40–42	89	5.13	4	6	2				1														5.13
				81.20	9	5	140–142	134	5.23	2					1															5.23
				82.20	9	6	90–92	173	5.32																					5.32
				83.20	9	7	40–42	351	5.42				1						(*)	(1)										5.42
				84.20	10	1	88-90	72	5.52	1						8	3											(1)		5.52
				85.20	10	2	40–42	459	5.62						1															5.62
				86.20	10	2	140–142	377	5.71		5				2															5.71
				87.20	10	3	90–92	392	5.81	*	4					1	2													5.81
				88.00	10	4	17.5–19.5	33	5.88	1			1			1														5.88
				89.20	10	4	140–142	30	6.00	1																				6.00
			C3An.1n	90.40	10	5	110–112	51	6.10						1															6.10
				91.70	10	6	87–89	363	6.21	16	2																			6.21
			C3An.1r	92.30	10	7	1-3	37	6.26	6								2												6.26
				92.90	11	1	11-13	0	6.37																					6.37
			C3An.2n	93.50	11	1	73-75	391	6.46	2								363												6.46
				94.40	11	2	11-13	419	6.54	17								355												6.54
				95.50	11	2	121-123	412	6.65		24							185												6.65
				96.40	11	3	60-62	376	6.73	1	22				1			120												6.73
			C3Ar	97.00	11	3	117.5-119.5	375	6.85	5						1		12												6.85
				97.40	11	4	12-14	13	6.95			1																		6.95
				98.00	11	4	69.5-71.5	407	7.07	13	171				5	21		6	(1)										7.07
		C3B		98.50	11	4	121-123	396	7.18	17	71				3	87	*	31												7.18
				99.00	11	5	18-20	378	7.28	13	1					2		60												7.28
	Messinian			99.60	11	5	77-79	1	7.40																					7.40
				100.00	11	5	122-124	3	7.50																					7.50
				100.50	11	6	20-22	1	7.60							1														7.60
				101.10	11	6	77-79	0	7.72																					7.72
				101.40	11	6	111-113	0	7.79																					7.79
				101.90	11	7	7-9	0	7.89																					7.89
				102.50	12	1	20-22	1	8.02																					8.02
				103.10	12	1	77-79	15	8.14									1												8.14
		C4		103.60	12	1	127-129	82	8.25	2	13					1	22	7												8.25
				104.00	12	2	22-24	381	8.34	11	216				5	9	9	21												8.34
			condensed section	104.50	12	2	68-70	372	8.44	10	129				2	15	28	7	3	2	7									8.44
				105.10	12	2	127-129	402	8.56		41						1	5		*										8.56
				105.50	12	3	20-22	363	8.66	1	310	*				*	23	8		1	*									8.66
				106.10	12	3	77-79	396	8.78	43	180							5	2	1	3							*		8.78
		C4A		106.60	12	3	127-129	385	8.88	24	155	1			1		1	97		2	1	1								8.88
				107.00	12	4	18-20	362	8.97	15	143				1	2		46	1		27	2								8.97
				107.60	12	4	77-79	374	9.09	8	115				*	4	*	135		*	18		*							9.09
				107.90	12	4	111.5-113.5	390	9.17	6	116					3	26	101			10	*		(*)						9.17
				108.50	12	5	19-21	363	9.29	6	69				*	2	34	72		*	18		1					*		9.29
				109.10	12	5	82.5-84.5	375	9.42	4	15					4	2	39		*	33		2							9.42
				109.50	12	5	123-125	375	9.51	12	27				5	4		110			19	*	3							9.51
				109.90	12	6	12-14	379	9.59	8	154					4	1	116		*	10		2							9.59
				110.50	12	6	69-71	412	9.71	162	95				2	1	6	49			8									9.71
				111.10	12	6	130-132	382	9.84	171	92					5	2	27	1		11									9.84
				111.50	12	7	16.5-18.5	367	9.92	98	120					*	3	40			14		*							9.92
				113.10	13	1	130-132	375	10.06	50	100				1	29		3		1	8									10.06
				114.70	13	2	142-144	387	10.16	8	142				*	2	1	1		1	47	1		3						10.16
				116.40	13	4	8-10	348	10.26	47	47				7	3		5			11		*	10						10.26
				117.90	13	5	12-14	369	10.35	34	76				4	24	1				99	1	2		4	8				10.35
				119.50	13	6	20-22	374	10.44	25	104				1	7	1				5		1	3	2			*		10.44
			C5n.2n	121.10	13	7	31.5-33.5	347	10.53	34	22				8	7	1	8			25			16	10	3				10.53
				122.70	14	1	141.5-143.5	352	10.63	70	17				2	12	*				19		2	24	12	*	1	9		10.63
				124.30	14	3	4-6	369	10.72	20	123				4	3			3		17	1		4	3	1	*	*		10.72
				125.90	14	4	10-12	355	10.82	33	130				1	8	3		6		25	1		9	6	2	1			10.82
				127.50	14	5	20-22	359	10.91	42	209				2	5	5		1	1	12	1		4	1	4	1			10.91
				129.10	14	6	30-32	354	11.00	90	155					11	3			*	4			6	3	4	1	2		11.00
				130.30	14	7	1-3	372	11.09	20	90					22					2			10	11		2			11.09
				131.50	15	1	74-76	368	11.19	75	124					3	5				2			10	*					11.19
				132.70	15	2	38-40	367	11.28	64	62				4	7	*		2		4		*	8	20			1		11.28
				133.80	15	3	4-6	362	11.37	17	214				2	11	4				6			6	8	1		*		11.37
				135.00	15	3	123-125	375	11.47	15	221				*	*			*		1		*	*	5		*			11.47
			C5r	136.30	15	4	100-102	383	11.57	74	96				1				6		2			4	5					11.57
				137.50	15	5	74-76	352	11.67	16	91				3	1	*		*		2				3			5	(*)	11.67
				138.70	15	6	37-39	358	11.76	36	295					*						*		1	*					11.76
				139.30	15	6	92-94	359	11.81	69	30				1	3			3		1		1	15	17					11.81
				140.50	16	1	17-19	376	11.90	26					*	1					5		3	3	3					11.90
				141.70	16	1	140-142	356	12.00	19	112				3	1	6		*		3	1	1		8	6	1	2		12.00
		C5A	C5An	142.70	16	2	91.5-93.5	362	12.11	31	48				1	2					*			1			*		2	12.11
				143.70	16	3	42.5-44.5	363	12.21	50	73				5	6			2		155		*	2	5		*	*	*	12.21
				144.70	16	3	141-143	361	12.32	17	188				1	7	2				1		*	3	*	1			1	12.32
				145.70	16	4	92-94	372	12.42	29	100				*	13					30			7	*		2		*	12.42
			C5Ar	148.00	16	6	20-22	368	12.52	21	133				4	10	*		13		12		*	1	21	3	1	*	5	12.52
				150.30	17	1	51.5-53.5	368	12.62	48	88				3	8	1		8		4			3	*		*		1	12.62
				152.60	17	2	130-132	370	12.71	2	205					1	2		5		*	*			*					12.71
				154.90	17	4	60-62	367	12.81	46	137				*	1	8		11		5	7			3		1			12.81
				157.20	17	5	138-140	365	12.91	26	135					4	*		22		6	1		2	4	1			*	12.91
				159.50	18	1	20-22	363	13.01	28	8				*	7			2		2		1	9	34				1	13.01
		C5AA	C5AAn	163.00	18	3	65-67	362	13.11	20	232					2	*		17		8	3	*		4					13.11
			C5AAr	166.50	18	5	121-123	360	13.26	9	159					11	1		7				*		3	1				13.26
		C5AB		167.80	18	6	97-99	370	13.35		192					22	*		6				*	3	3					13.35
			C5ABn	169.10	19	1	34-36	363	13.39	7	124					1			3		*	2	*		2					13.39
				174.70	19	4	138-140	364	13.49	9	286					1			5		*				1	1			*	13.49
				180.30	20	2	46-48	355	13.59	3	274					2	1		1		1	6			2	3		*		13.59
			C5ABr	185.30	20	5	98-100	383	13.68		333											11			2	2				13.68
	Langhian		C5ACn	190.30	21	2	97.5-99.5	382	13.83	3	176					9			4		10	*	*	*	1	8			*		13.83
Middle Miocene				195.30	21	6	2-4	360	13.94	2	308					6			8		8			13		*			*	*	13.94
				200.30	22	2	147-149	360	14.03	8	33					10	1		2		212	*		10		2			2	8	14.03
				205.30	22	6	51-53	385	14.13	23	54					4			6		63	11	3	8		*				2	14.13
			?	210.30	23	3	51.5-53.5	356	14.23	17	162					8			25			4				3	*				14.23
				215.30	23	6	97.5-99.5	379	14.33		45					17	*		4		107	25				5	3			6	14.33
				216.30	23	7	48-50	373	14.43		37					8					104	26	3			13					14.43
				216.50	23	CC	10-12	347	14.53		29					10					71	25				3				*	14.53

LO *Habibacysta tectata* (Plate I, 19–20)

Occurrence: Sample 907A-23H-3, 51.5–53.5 cm; 210.3 mbsf.

Magnetostratigraphic calibration: extrapolated from top of Subchron C5ABn through top of Subchron C5ACn.

Age assessment: 14.2 Ma (mid-Langhian).

Discussion: Habibacysta tectata has a well-defined LO four samples above the base of Hole 907A.

This species has been reported frequently across the North Atlantic (see Head, 1994 and references therein). The LO obtained from our data is consistent with its LO from the continental slope off New Jersey (de Verteuil, 1996) and the Salisbury Embayment (de Verteuil and Norris, 1996) but is lower than at eastern North Atlantic IODP Site U1318 (c. 13.5 Ma, Louwye et al., 2007b). In Baffin Bay ODP Hole 645E, the LO of *H. tectata* was recorded above the base of the combined calcareous nannofossil zones NN5 to NN15 (Head et al., 1989b; Knüttel et al., 1989) indicating an LO younger than 14.9 Ma. In Norwegian Sea ODP Holes 642B and 643C, it was possibly recorded from the Middle Miocene (as *T. pellitum* and Dinocyst sp. 1 in Mudie, 1989; Head, 1994). According to revised Re-Os isochron ages for IODP Hole M0002A (Poirier and Hillaire-Marcel, 2011), it has a LO at *c.* 15 Ma in the central Arctic Ocean (Expedition 302 Scientists), while ^{10}Be isotope stratigraphy (Frank et al., 2008) indicate an age of *c.* 12.9 Ma.

In the southern North Sea Basin, the LO of *H. tectata* is not well constrained but possibly lies within the lower part of calcareous nannofossil zone NN5 in northern Germany (as *Filisphaera minuta* in Strauss et al., 2001; see comments in Jiménez-Moreno et al., 2006). For two wells in northern Germany, Köthe and Piesker (2007) assigned the LO of *H. tectata* to the dinocyst zone DN8 (lower Tortonian) of de Verteuil and Norris (1996). Köthe (2003) attributed the late appearance of this and several other species to a strong facies-related control on bioevents.

In Belgium, the LO of *H. tectata* is within the mid-Langhian (Louwye et al., 2000) and below the HO of *Distatodinium paradoxum* in contrast to the succession observed by de Verteuil and Norris (1996) for the eastern U.S.A. However, it should be noted that in Belgium (Louwye et al., 2000) as well as elsewhere (e.g. de Verteuil and Norris, 1996; Munsterman and Brinkhuis, 2004) the LO of *H. tectata* is slightly higher than that of *Unipontidinium aquaeductus* which is provisionally constrained at 15.1–14.8 Ma (mid-Langhian; see discussion in Jiménez-Moreno et al., 2006).

Based on a subsurface investigation of the Netherlands, the LO of *H. tectata* was recorded within southern North Sea Miocene zone 7 of Munsterman and Brinkhuis (2004) that has an age of *c.* 15.0 Ma (mid-Langhian) at the base (D. Munsterman, pers. commun. 2012).

The relatively high LO of *H. tectata* in northern Italy (Subchron C5An, *c.* 12.2 Ma, upper Serravallian; Zevenboom, 1995) may not reflect the true LO because it was present since at least *c.* 14.8 Ma (mid-Langhian) in the Vienna and Pannonian basins (Jiménez-Moreno et al., 2006), and these were connected to the North Italian sites during most of the Middle and Late Miocene (Rögl, 1999).

Jiménez-Moreno et al. (2006) considered records older than calcareous nannofossil zone NN5 to result from caving or other contamination. This is presumably also true for Lower Miocene occurrences in Denmark (Dybkjær, 2004; for a revised age assignment of formations see Dybkjaer and Piasecki, 2010).

HO *Unipontidinium aquaeductus* (Plate I, 13–15)

Occurrence: Sample 907A-21H-6, 2–4 cm; 195.3 mbsf.

Magnetostratigraphic calibration: extrapolated from top of Subchron C5ABn through top of Subchron C5ACn.

Age assessment: 13.9 Ma (late Langhian).

Discussion: Poulsen et al. (1996) reported a comparable stratigraphic range for *U. aquaeductus* in Hole 907A from Section 907A-23H-4 (211.50 mbsf) up to Sample 21H-CC (197.38 mbsf).

This species has a rather poorly constrained HO in most sites selected for comparison, although the age appears to vary considerably between regions (Fig. 17). A HO is observed in the upper Langhian for Hole 907A but slightly higher near the Langhian/Serravallian boundary in deep-water sites in the Norwegian Sea (Hole 643A, Manum et al., 1989; Goll in Williams and Manum, 1999) and central North Atlantic (Site 406, Costa and Downie, 1979; Müller, 1979). A younger HO at *c.* 13.3 Ma (lower Serravallian) has been reported from the eastern U.S.A. and the continental slope off New Jersey (de Verteuil and Norris, 1996; de Verteuil, 1996); and for eastern North Atlantic IODP Site U1318, the HO is within Subchron C5An2n at *c.* 12.3 Ma, which is notably above the LO of *Cannosphaeropsis passio* (Louwye et al., 2007b). A similar overlap has been noted in Belgium (Louwye et al., 2000), but in the eastern U.S.A. (de Verteuil and Norris, 1996) and elsewhere (e.g. northern Germany; Strauss et al., 2001; Köthe and

Piesker, 2007), these two species do not overlap but have their stratigraphic ranges separated by a narrow interval represented by the dinocyst zone DN6 of de Verteuil and Norris (1996). This either implies strong ecological control on the distribution of one or both species, or reworking of *U. aquaeductus* into this atypical stratigraphic position. Mudie (1987) illustrated two specimens from the Upper Miocene and Lower Pliocene of central North Atlantic DSDP Sites 607 and 611, but neither is attributable to *U. aquaeductus* (de Verteuil and Norris, 1996).

In the Netherlands, Munsterman and Brinkhuis (2004) recorded a HO within the mid-Serravallian and Donders et al. (2009) calculated an age of 12.42 Ma which is comparable to that at IODP Site U1318. In Belgium it appears to range into the uppermost Serravallian (Louwye et al., 2000), although there is little independent stratigraphic control for this part of the sequence. In northern Germany, it has a HO in the upper Langhian or lower Serravallian (Strauss et al., 2001) while Dybkjær and Piasecki (2010) recorded a HO within the lower Serravallian in Denmark but stated that their *U. aquaeductus* zone is generally condensed in distal depositional settings. In Hungary, the HO is within the lower Serravallian (Jiménez-Moreno et al., 2006). As noted by Jiménez-Moreno et al. (2006), Zevenboom (1995) recorded the highest persistent occurrence of *U. aquaeductus* in the middle of his subzone Oei, an event calibrated to Subchron C5AAn and dated at *c.* 13.1 Ma (lower Serravallian). Rare and sporadic occurrences above this datum, in both the Cassinasco and Mazzapiedi sections (Zevenboom, 1995) and occurring as high as 12.0 Ma (upper Serravallian) in the Cassinasco section, were suspected by Jiménez-Moreno et al. (2006) of being reworked.

LO *Cerebrocysta irregulare* sp. nov. (Plate III, 11–20)

Occurrence: Sample 907A-21H-2, 97.5–99.5 cm; 190.3 mbsf.

Magnetostratigraphic calibration: extrapolated from top of Subchron C5ABn through top of Subchron C5ACn.

Age assessment: 13.8 Ma (late Langhian).

Discussion: Cerebrocysta irregulare has a rare but persistent occurrence through the lower part of its range in Hole 907A.

Tectatodinium sp. 4 of Manum et al. (1989) compares favourably with *Cerebrocysta irregulare* (see Systematic paleontology), and has a LO near the Langhian/Serravallian boundary in Norwegian Sea ODP Hole 643A (Manum et al., 1989; Goll in Williams and Manum, 1999). There are no other known records of this species.

Serravallian (Middle Miocene)

LO *Operculodinium*? *eirikianum* (Plate I, 4–5)

Occurrence: Sample 907A-18H-1, 20–22 cm; 159.5 mbsf.

Magnetostratigraphic calibration: Base of Subchron C5Ar (interpolation between base of Subchron C5Ar and base of Subchron C5An.2n).

Age assessment: 13.0 Ma (early Serravallian).

Discussion: This species has a LO within Subchron C5ACn at *c.* 14.0 Ma (upper Langhian) at eastern North Atlantic IODP Site U1318 (Louwye et al., 2007b), and the sporadic occurrence at this site suggests that its true LO may be yet lower. For the Cassinasco section of northern Italy, Zevenboom (1995) reported a LO at the top of Subchron C5ABr at *c.* 13.6 Ma (lowermost Serravallian).

Elsewhere, the LO of *O.*? *eirikianum* is not constrained directly to magnetostratigraphy and therefore subject to greater uncertainty, but records nonetheless show considerable disparity. From the Salisbury Embayment of eastern U.S.A., de Verteuil and Norris (1996) recorded the LO at the base of their zone DN9 which is calibrated to the base of calcareous nannofossil zone NN11 at *c.* 8.3 Ma (upper Tortonian). From offshore New Jersey, U.S.A. the LO was also recorded within zone DN9 (de Verteuil, 1996).

In Labrador Sea ODP Hole 646B (Head et al., 1989c) it was found in the lowermost sample of the cored interval within the mid-Tortonian (calcareous nannofossil zone NN10, Knüttel et al., 1989), this unlikely reflecting the real LO.

Its range base in the Norwegian Sea (ODP Leg 104), is poorly known because *O.*? *eirikianum* had not been described when the study was undertaken (Manum et al., 1989), and both *O.*? *eirikianum* and the superficially similar species *O. longispinigerum* were reported under the latter name. Head (in Head and Wrenn, 1992) confirmed the presence of *O. longispinigerum* in the Lower Miocene of ODP Hole 643A, but one specimen illustrated as *O. longispinigerum* by Manum et al. (1989, pl. 14, fig. 8) from the Upper Miocene or higher in ODP Hole 642C was assigned to *O.*? *eirikianum* by Head (in Head and Wrenn, 1992).

O.? *eirikianum* has a LO in the Middle Miocene of the Iberia Abyssal Plain, eastern North Atlantic, according to McCarthy and Mudie (1996), but the morphological description given by these authors indicates that some specimens were misidentified.

In the North Sea Basin, *O.*? *eirikianum* occurs in the Middle Miocene of Belgium in deposits assigned to the upper part of zone DN5 of de Verteuil and Norris (1996) and

probably of mid-Serravallian age (Louwye, 2005). From the Nieder Ochtenhausen borehole of northern Germany, Strauss et al. (2001) assigned the LO to their zone Cpl which is calibrated directly to the lower part of calcareous nannofossil zone NN5, indicating an upper Langhian age for this datum.

HO *Cerebrocysta poulsenii* (Plate IV, 1–2)

Occurrence: Sample 907A-16H-2, 91.5–93.5 cm; 142.7 mbsf.

Magnetostratigraphic calibration: upper part of Subchron C5An (interpolation between base of Subchron C5An.2n and base of Subchron C5r).

Age assessment: 12.1 Ma (late Serravallian).

Discussion: This species, recorded in the older literature as Gen. et sp. indet. of Piasecki (1980), has a diachronous HO in Iceland Sea Hole 907A and Norwegian Sea ODP Hole 643A (Subchron C4Ar, *c.* 9.5 Ma; mid-Tortonian; Manum et al., 1989; Bleil, 1989). In eastern North Atlantic DSDP Site 555 its HO has been observed in the upper Serravallian or lower Tortonian (Edwards, 1984; Backman, 1984). Its HO has also been recorded from the Salisbury Embayment, eastern U.S.A. within the lower part of zone DN8 (c. 10.4 Ma, early Tortonian; de Verteuil and Norris, 1996), and it has a well defined HO within zone DN6 (mid-Serravallian) of ODP Hole 905A on the New Jersey continental rise (de Verteuil, 1996; Gartner and Shyu, 1996). A single record in ODP Hole 903A on the New Jersey continental shelf within zone DN9 (late Tortonian, de Verteuil, 1996) is suspected of being reworked based on its unusually high stratigraphic position. Head et al. (1989b) reported rare occurrences of specimens assigned to a "Gen. et sp. indet of Piasecki, 1980 group" from the Lower, Middle and lower Upper? Miocene in Baffin Bay ODP Hole 645E. While this group's affiliation to *C. poulsenii* is not completely clear, the highest unquestioned occurrence in Hole 645E (Head et al., 1989b, pl. 12, figs. 10, 11) is here confirmed as being of *C. poulsenii*.

From Denmark the HO is recorded at *c.* 12.8 Ma, mid-Serravallian (Dybkjær and Piasecki, 2010), from the Netherlands at *c.* 11.8 Ma, upper Serravallian, (Munsterman and Brinkhuis, 2004), from the Serravallian of northern Germany (Straus et al., 2001), from the lower Serravallian of central Europe (Jiménez-Moreno et al., 2006), and from northern Italy in Subchron C5r.3r at *c.* 11.7 Ma, upper Serravallian (as "*Imperfectodinium septatum*" in Zevenboom, 1995).

Tortonian (Late Miocene)

HO *Cleistosphaeridium placacanthum* (Plate IV, 16–17)

Occurrence: Sample 907A-14H-1, 141.5–143.5 cm; 122.7 mbsf.

Magnetostratigraphic calibration: middle of Subchron C5n.2n (interpolation between base and top of Subchron C5n.2n).

Age assessment: 10.6 Ma (early Tortonian).

Discussion: For the Salisbury Embayment, eastern U.S.A., de Verteuil and Norris (1996) recorded a HO at *c.* 13.5 Ma (lower Serravallian), this datum defining the top of their zone DN5. In ODP Hole 905A offshore New Jersey, the HO has been observed at the same stratigraphic position (de Verteuil, 1996). At eastern North Atlantic IODP Site U1318 (Louwye et al., 2007b) and DSDP Site 555 (Edwards, 1984; Backman, 1984), the HCO and HO respectively are both at *c.* 13.0 Ma, with Louwye et al. (2007b) reporting only rare and isolated occurrences above 13.0 Ma, whereas in DSDP Hole 548A, *C. placacanthum* appears to extend into the Upper Miocene (as *Areoligera senonensis* complex in Brown and Downie, 1985; Müller, 1985) although a HCO/HPO cannot be defined.

De Verteuil and Norris (1996) considered a rare Upper Miocene record from Norwegian Sea ODP Hole 643A (c. 8.4 Ma, Manum et al., 1989; Bleil, 1989) to represent reworking, but Manum et al. (1989) recorded a HCO at the top of their *U. aquaeductus* zone, dated to *c.* 13.5 Ma (Goll unpubl. data in Williams and Manum, 1999) in the lower Serravallian.

For Denmark, Dybkjær and Piasecki (2010) noted a HO at the top of their *A. umbraculum* zone (*c.* 8.9 Ma, mid-Tortonian) and that the highest abundant occurrence of *C. placacanthum* is near the top of their *U. aquaeductum* zone (*c.* 13.3 Ma, lower Serravallian).

A comparatively high HO at *c.* 8.1 Ma is given for the Netherlands (Munsterman and Brinkhuis, 2004) but no quantitative data are available to evaluate whether this might be attributable to reworking. In northern Germany, the HPO of *C. placacanthum* is well defined (Strauss et al., 2001), and occurs below the LO of *Cannosphaeropsis passio* as it does in the eastern U.S.A. (de Verteuil and Norris, 1996) and eastern North Atlantic (Site 1318, Louwye et al., 2007b), implying a mid- to upper Serravallian age.

In northern Italian sections studied by Zevenboom (1995), the HCO is at *c.* 12.1 Ma (Subchron C5An.1n, upper Serravallian) in the Mazzapiedi section, but *C. placacanthum* is common to the top of the Cassinasco section, which is dated to *c.* 12.0–11.6 Ma (Subchron C5r.3r). Rare and sporadic occurrences at the top of the Mazzapiedi

section (*c.* 8.0 Ma, uppermost Tortonian) might at least in part represent reworking.

HCO *Hystrichosphaeropsis obscura* (Plate II, 1–5)

Occurrence: Sample 907A-14H-1, 141.5–143.5 cm; 122.7 mbsf.

Magnetostratigraphic calibration: middle of Subchron C5n.2n (interpolation between base and top of Subchron C5n.2n).

Age assessment: 10.6 Ma (early Tortonian).

Discussion: This species has a rare and somewhat sporadic occurrence throughout its range in Hole 907A. Elevated numbers occur in one sample here designated as the HCO, which is clearly a tentative datum. Above this, isolated specimens might be in place judging from the HO of this species elsewhere, although there is some evidence for ecological exclusion above the HCO (see Section 4.1).

Hystrichosphaeropsis obscura was first described from the Upper Miocene of the western North Atlantic (Habib, 1972). In Norwegian Sea ODP Hole 643A, its HO is at *c.* 7.4 Ma (Subchron C4n.1n, Manum et al., 1989; Bleil, 1989), and is at *c.* 7.2 Ma (Subchron C3Bn, Channel et al., 1999b) in Iceland Sea ODP Hole 987E (M. Smelror, pers. commun., 2007). De Verteuil and Norris (1996) used the HO of *H. obscura* to define the top of their DN9 zone in the upper Tortonian (*c.* 7.5 Ma) of the Salisbury Embayment, eastern U.S.A. A similar position at the top of zone DN9 was reported for the HO from the continental margin of New Jersey (de Verteuil, 1996; Gartner and Shyu, 1996). In eastern North Atlantic DSDP Site 555, the HO was reported within the lower part of nannofossil zone NN11 (upper Tortonian, Edwards, 1984; Backman, 1984), whereas *H. obscura* ranges to the nannofossil zone boundary NN5/6 in DSDP Hole 548A (Brown and Downie, 1985; Müller, 1985), although here the HO is probably lost within an apparent hiatus separating the upper Middle Miocene from middle Upper Miocene (Snyder et al., 1985). For eastern North Atlantic IODP Holes 1318B and C, Louwye et al. (2007b) reported *H. obscura* in low numbers fairly persistently throughout a Miocene succession that extends into the upper Serravallian. From northern North Atlantic DSDP Hole 408, Reykjanes Ridge, Engel (1992) recorded two isolated occurrences from foraminiferal zone N16 within the mid-Tortonian (Poore, 1979). Mudie (1987) found rare specimens in the Upper Pliocene of central North Atlantic DSDP Site 611 but attributed them to reworking.

In the North Sea Basin the HO of *H. obscura* seems to be in the upper Tortonian of both Denmark (Dybkjær and Piasecki, 2010) and Germany (Köthe, 2005; Köthe and

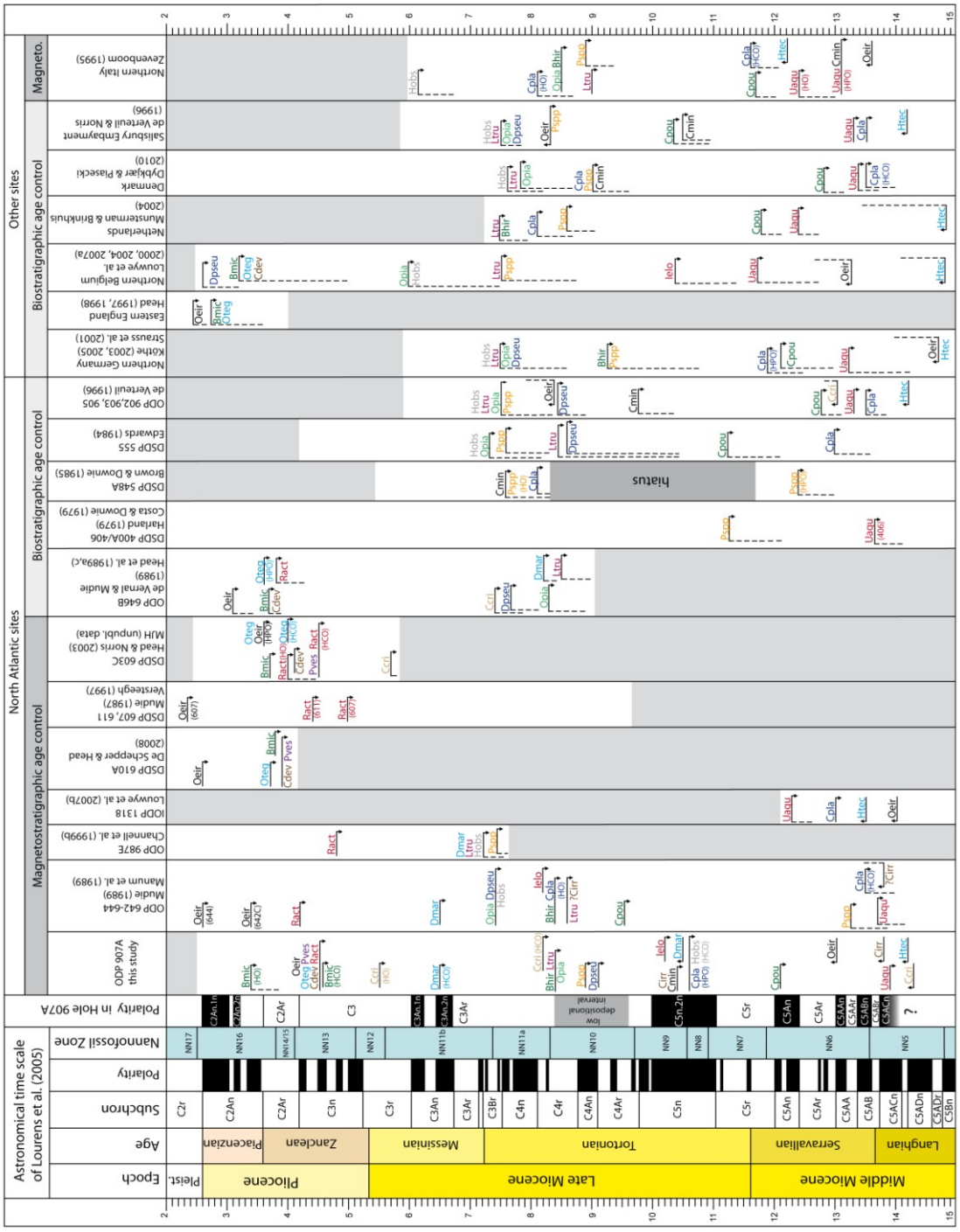

Figure 17: Dinocyst and acritarch bioevents identified in ODP Hole 907A and their corresponding positions in the various sites as discussed in the text. Dashed lines indicate uncertainties in the position of bioevents. The magnetic polarity zones for Hole 907A are from Channell et al. (1999) in Hole 907A. Light grey shaded areas mark the intervals not analysed at the various sites. Dark grey shaded area indicates hiatus. The names of species codes are given in Table 1.

Andruleit, 2007), and Louwye et al. (2007a) recorded *H. obscura* in the Belgian Kasterlee Formation which is indirectly dated at *c.* 7.5–6.0 Ma (uppermost Tortonian–mid-Messinian). An even younger Early Pliocene record in Dutch wells (Munsterman and Brinkhuis, 2004) is in conflict with its Late Miocene disappearance elsewhere and considered reworked (D. Munsterman, pers. commun., 2012).

For northwestern Italy, Zevenboom (1995) gave an undifferentiated mid-Messinian age for the HO in the Mazzapiedi/Perleto section. Based on the astronomical calibration of the sedimentary cycles on Crete (Greece), Santarelli et al. (1998) recorded the HO in the lower Messinian at *c.* 6.8 Ma. From the Atlantic coast of Morocco, its HO is in the upper part of Subchron C3r (*c.* 5.3 Ma, uppermost Messinian) just below the Miocene/Pliocene boundary (Warny and Wrenn, 2002).

LO *Decahedrella martinheadii* (Plate IV, 18–19)

Occurrence: Sample 907A-13H-7, 31.5–33.5 cm; 121.1 mbsf.

Magnetostratigraphic calibration: middle of Subchron C5n.2n (interpolation between base and top of Subchron C5n.2n).

Age assessment: 10.5 Ma (early Tortonian).

Discussion: This marine acritarch is restricted to the Upper Miocene and possible upper Middle Miocene, and was endemic to the high-latitude North Atlantic region and Arctic Ocean (Matthiessen et al., 2009). Matthiessen et al. (2009) compared its LO at numerous high northern latitude sites and suggested an age no greater than 13–12 Ma (Serravallian), with the oldest firm record at *c.* 11.0 Ma (lower Tortonian) from ODP Hole 909C in the Fram Strait. Matthiessen et al. (2009) also noted differences in its position between sites, even when allowing for uncertainties in age control. At Site 907 the LO would be at *c.* 10.1 Ma based on the observations of Poulsen et al. (1996) but here we record a slightly older LO at 10.5 Ma.

HO *Cordosphaeridium minimum* sensu Benedek and Sarjeant, 1981 (Plate I, 1–3)

Occurrence: Sample 907A-13H-5, 12–14 cm; 117.9 mbsf.

Magnetostratigraphic calibration: middle of Subchron C5n.2n (interpolation between base and top of Subchron C5n.2n).

Age assessment: 10.4 Ma (early Tortonian).

Discussion: The stratigraphic range of *C. minimum* sensu Benedek and Sarjeant (1981) is somewhat complicated by taxonomic uncertainties, although most Miocene records

apparently represent this taxon rather than *C.*? *minimum* (Morgenroth) Benedek 1972, which was described from the Lower Eocene of Germany as having coarsely fibrous to areolate body surface (Head et al., 1989b).

For Hole 907A, Poulsen et al. (1996) reported an isolated rare occurrence within Section 907A-12H-2 (104.08 mbsf, equivalent to an age of 8.4 Ma), and a common occurrence in Sample 13H-CC (121.62 mbsf, 10.5 Ma) which is close to our own observed HO for this hole.

The HO varies widely across the North Atlantic and adjacent seas, ranging from *c.* 13.1 Ma (lower Serravallian) in northern Italy (Zevenboom, 1995) to upper Tortonian in the eastern North Atlantic (Brown and Downie, 1985; Müller, 1985).

Our observations for Hole 907A are consistent with those of the Salisbury Embayment, eastern U.S.A. where this species disappeared at *c.* 10.5 Ma (early Tortonian, de Verteuil and Norris, 1996), and de Verteuil (1996) recorded a similar age within the middle of zone DN8 (mid-Tortonian, Gartner and Shyu, 1996) for its HO in the continental slope off New Jersey. For eastern North Atlantic IODP Site U1318, Louwye et al. (2007b) recorded this species rarely but persistently throughout the investigated Lower and Middle Miocene sequence which extends to 12.1 Ma (upper Serravallian).

Dybkjær and Piasecki (2010) gave an age of *c.* 9.0 Ma (mid-Tortonian) for its HO in Denmark, and Strauss et al. (2001) recorded this species from the Upper Miocene of northern Germany. From subsurface wells in the Netherlands, this species was recorded through and above southern North Sea Miocene zone 14 (*c.* 7.4–8.1 Ma; upper Tortonian) by Munsterman and Brinkhuis (2004).

HO *Cerebrocysta irregulare* sp. nov. (Plate III, 11–20)

Occurrence: Sample 907A-13H-5, 12–14 cm; 117.9 mbsf.

Magnetostratigraphic calibration: middle of Subchron C5n.2n (interpolation between base and top of Subchron C5n.2n).

Age assessment: 10.4 Ma (early Tortonian).

Discussion: A HO for this species is presently known with certainty only from this study. However, we tentatively synonymised this species with *Tectatodinium* sp. 4 of Manum et al. (1989), which has a magnetostratigraphically-calibrated HO at *c.* 8.6 Ma (mid-Tortonian) in Norwegian Sea ODP Hole 643A (Subchron C4r.2r, Manum et al., 1989; Bleil, 1989).

HO *Impagidinium elongatum* sp. nov. (Plate II, 6–20; Fig. 19, 20)

Occurrence: Sample 907A-13H-2, 142–144 cm; 114.7 mbsf.

Magnetostratigraphic calibration: interpolation between top C5n.2n and top C3Ar.

Age assessment: 10.2 Ma (mid-Tortonian).

Discussion: This species has a magnetostratigraphically-calibrated HO in Subchron C4r.1r at *c.* 8.2 Ma in Norwegian Sea ODP Hole 643A (as *Impagidinium* sp. 3 in Manum et al., 1989; Bleil, 1989). *Impagidinium* sp. 1 and 2 of Anstey (1992) from Baffin Bay ODP Hole 645E are probably conspecific with *Impagidinium elongatum*. Both morphotypes were recorded as rare to occasional, and confined to the lowest zone in Anstey's study, which is dated as late Middle? to early Late Miocene based on dinocyst biostratigraphy. It has been recorded also from the lower Tortonian Deurne Sands Member of the Diest Formation in Belgium (as *Impagidinium* sp. 1 in Louwye, 2002). *Impagidinium* sp. 1 of Manum et al. (1989) is questionably synonymised with *I. elongatum*, and has a HO in the upper Middle Miocene of Norwegian Sea ODP Hole 643A (Manum et al., 1989; Goll unpubl. data in Williams and Manum, 1999).

HO *Dapsilidinium pseudocolligerum* (Plate IV, 9)

Occurrence: Sample 907A-12H-4, 77–79 cm, 107.6 mbsf.

Magnetostratigraphic calibration: interpolation between top C5n.2n and top C3Ar.

Age assessment: 9.1 Ma (mid-Tortonian).

Discussion: This species has been reported commonly from the Miocene across the North Atlantic region along with *Dapsilidinium pastielsii*. It differs from *D. pastielsii* only by having processes that are somewhat longer, narrower and more widely separated (Stover, 1977) and hence rather less expanded proximally. However, McCarthy and Mudie (1996) noted that there may be intergrades between these species and we follow de Verteuil and Norris (1996) and Head and Westphal (1999) in not differentiating them in the Neogene literature.

For Hole 907A, Poulsen et al. (1996) reported a HO within section 12H-6 (109.99 mbsf, 9.6 Ma), which is slightly older than our own observation. In the Norwegian Sea, it has a magnetostratigraphically calibrated HO at *c.* 7.4 Ma in ODP Hole 643A (Subchron C4n.1n, Manum et al., 1989; Bleil, 1989). It has also been identified in ODP Hole 642C but its true HO is probably lost within a hiatus (Manum et al., 1989; Bleil, 1989). In Labrador Sea ODP Hole 646B, this species has a HO within calcareous nannofossil zone NN11a (upper Tortonian, Head et al., 1989c; Knüttel et al., 1989) but

that is based on sporadic occurrences; and it occurs in the lower Tortonian of Davis Strait (Piasecki, 2003) although age control is poor at this site. In eastern North Atlantic DSDP Site 555, it has a HO within combined calcareous nannofossil zone NN9/10 (lower to mid-Tortonian, Edwards, 1984; Backman, 1984). Engel (1992) observed the HO of this species in the Upper Miocene both of the Bay of Biscay (Müller, 1979) and Reykjanes Ridge (Poore, 1979). From the Iberia Abyssal plain, an early HO has been observed within the upper part of calcareous nannofossil zone NN2 (mid-Burdigalian, McCharty and Mudie, 1996; de Kaenel and Villa, 1996). For the Salisbury Embayment, eastern U.S.A., de Verteuil and Norris (1996) reported its HO at the top of their zone DN9 dated to *c.* 7.5 Ma (upper Tortonian). A HO at the top of zone DN8 has been reported from the continental slope off New Jersey (upper Tortonian, de Verteuil, 1996; Gartner and Shyu, 1996) whereas it is still present in the Lower Pleistocene of western North Atlantic DSDP Site 603C (M.J.H., unpubl. data; Canninga et al., 1987). Moreover, it is sporadically abundant in the Upper Pliocene or Lower Pleistocene of the Gulf of Mexico (as Dapsilidinium sp. A, Aubry, 1993; Wrenn and Kokinos, 1986) and ranges at least into the Lower Pleistocene of the Great Bahama Bank (Head and Westphal, 1999; Eberli et al., 1997).

In northern Germany, the HO has been placed at the top of zone DN9 (upper Tortonian, Köthe 2003, Köthe and Piesker, 2007) whereas in Belgium it is as high as the mid- to Upper Pliocene (Louwye et al., 2004; De Schepper et al., 2008), although both studies have poor independent age control.

HO *Palaeocystodinium* spp. (Plate IV, 13–15)

Occurrence: Sample 907A-12H-3, 127–129 cm; 106.6 mbsf.

Magnetostratigraphic calibration: interpolation between top C5n.2n and top C3Ar.

Age assessment: 8.9 Ma (mid-Tortonian).

Discussion: Palaeocystodinium golzowense was first described from the upper Paleogene of Germany by Alberti (1961), and was subsequently reported widely from the Miocene of the North Atlantic region and elsewhere, although reports of *Palaeocystodinium* species in open nomenclature increasingly acknowledged variations in morphology. In an attempt to explain this diversity, Strauss et al. (2001) proposed a phylogenetic lineage in which the ancestral *P. golzowense* gave rise to three new species that extended into the Middle Miocene (*P. miocaenicum*) and Late Miocene (*P. minor* and *P. powellii*). Some details of this lineage have since been questioned (Soliman et al., in press). Meanwhile, Zevenboom and

Santarelli (in Zevenboom, 1995) had already proposed two new manuscript names, "*P. striatogranulosum*" and "*P. ventricosum*", which subsequently found their way into the Miocene literature. To facilitate comparison between our Site 907 records and those elsewhere, particularly in the older literature, we have chosen simply to refer to the various species collectively as *Palaeocystodinium* spp.

Palaeocystodinium spp. is ubiquitous in the North Atlantic region and has been recorded from most sites considered here. For the Salisbury Embayment, eastern U.S.A., de Verteuil and Norris (1996) recorded its HO at the top of their zone DN8, which is dated to at *c.* 8.3 Ma (upper Tortonian). For the continental slope and rise off New Jersey it extends into zone DN9, which has a range of *c.* 8.3–7.5 Ma (de Verteuil, 1996). It extends into the Upper Miocene of the Davis Strait (Piasecki, 2003) and possibly also Baffin Bay (Head et al., 1989b) but age control is poor at both sites. For Iceland Sea ODP Hole 987E, a HO is recorded within the upper Tortonian at *c.* 7.4 Ma (M. Smelror, pers. commun., 2007; Channel et al., 1999b), although this species was recorded at the base of the cored interval, so it is impossible to know whether the HO represents a continuous or isolated occurrence. Within the high-latitude North Atlantic region, the lowest HO recorded is from ODP Site 643 in the Norwegian Sea (Manum et al., 1989) and has an estimated age of *c.* 13.6 Ma (lower Serravallian). According to the magnetostratigraphy of Bleil (1989), this event coincides with a hiatus, although a condensed section has also been proposed (Bruns et al., 1998). Without other chronostratigraphic evidence available, the age of this HO is based on the unpublished data of Goll (1997, in Williams and Manum, 1999) and should be treated with caution.

For eastern North Atlantic IODP Site U1318, it occurs mostly in low numbers throughout the Lower and Middle Miocene sequence studied by Louwye et al. (2007b) which extends to 12.1 Ma (upper Serravallian). A relatively high HO is recorded in eastern North Atlantic DSDP Site 555 (late Tortonian, Edwards, 1984; Backman, 1984) and eastern North Atlantic DSDP Site 548 (late Tortonian, Brown and Downie, 1985; Müller, 1985). At the latter site, an apparent hiatus of *c.* 5.0 Ma separates upper Middle Miocene from middle Upper Miocene (Snyder et al., 1985) and therefore the HPO (mid-Serravallian, Müller, 1985) from the HO, which is marked by a single occurrence only and hence potentially reworked. In this context, the true upper range is probably lost within the hiatus. However, the HPO is somewhat in the range of the single occurrence recorded at the nearby DSDP Site 400 (upper Serravallian-lower Tortonian, Harland, 1979; Müller, 1979). At Site 555, it is recorded persistently to its HO (Edwards, 1984),

which suggests that these specimens are in place. However, the large sample spacing and uncertainties in the biostratigraphic age control (Backman et al., 1984) may account for the observed differences.

Within Europe, the HO has been recorded at *c.* 9.0 Ma in Denmark (Dybkjær and Piasecki, 2010), *c.* 8.7 Ma in the Netherlands (Munsterman and Brinkhuis, 2004; Donders et al., 2009), and is placed within the mid-Tortonian (Louwye et al., 1999) or probable mid- to upper Tortonian (Louwye, 2002) in Belgium, and lower or middle Tortonian of northern Germany (Strauss et al., 2001); although these records lack precise independent age control. In the Mazzapiedi section of northern Italy, the HO occurs within the middle of Subchron C4An at *c.* 8.9 Ma (mid-Tortonian) although occurrences throughout this Serravallian–Tortonian section are rare and sporadic (Zevenboom, 1995).

HO *Labyrinthodinium truncatum* (Plate IV, 3–6)

Occurrence: Sample 907A-12H-2, 68–70 cm; 104.5 mbsf.

Magnetostratigraphic calibration: interpolation between top C5n.2n and top C3Ar.

Age assessment: 8.4 Ma (late Tortonian).

Discussion: The most common morphotype represented in Hole 907A has processes/ridges that are strongly expanded distally. This morphotype was recorded from the Miocene of the Norwegian Sea (as *L.* cf. *truncatum* in Manum et al., 1989, pl. 12, figs. 9, 10) and Baffin Bay (as *L.* cf. *truncatum* in Head et al., 1989b, pl. 10, figs. 2, 3). Because this morphotype intergrades with the more typical specimens in our material, and is not appreciably different from those illustrated, for example, from the Salisbury Embayment, eastern U.S.A. (as *L. truncatum* subsp. *truncatum* in de Verteuil and Norris, 1996, pl. 15, figs. 9–20), we include it within *L. truncatum.*

In Hole 907A its HO is slightly higher than that reported by Poulsen et al. (1996) but agrees with the high-latitude records of Labrador Sea ODP Hole 646B (calcareous nannofossil zone NN10, 9.7-8.3 Ma, Head et al., 1989c; Knüttel et al., 1989), Norwegian Sea ODP Hole 643A (Subchron C4r.2r, c. 8.6 Ma, Manum et al., 1989; Bleil, 1989), and eastern North Atlantic DSDP Hole 555 (mid-Tortonian, Edwards, 1984; Backman, 1984). In Iceland Sea ODP Hole 987E, the HO is magnetostratigraphically-calibrated to Subchron C3Bn (*c.* 7.2 Ma, Channell et al., 1999b), although no quantitative data are available to judge whether this relatively high position relates to a persistent or sporadic occurrence.

In the Salisbury Embayment, eastern U.S.A., *L. truncatum* has a HO at the top of zone DN9 which is dated at *c.* 7.5 Ma (de Verteuil and Norris, 1996), and it similarly ranges to the top of DN9 on the continental slope off New Jersey (upper Tortonian, de Verteuil, 1996; Gartner and Shyu, 1996).

In Belgium, the Netherlands, and northern Germany, this datum is at about the same stratigraphic level (Köthe, 2003, 2005; Louwye et al., 1999, 2007a) as in the Salisbury Embayment, while it is close to the top of zone DN9 and dated at *c.* 7.6 Ma in Denmark (Dybkjær and Piasecki, 2010). The early disappearance of this species in Italy (lower part of Subchron C4An, Mazzapiedi section, *c.* 9.0 Ma; Zevenboom, 1995) contrasts sharply with the North Sea records.

Pliocene records of this species at central North Atlantic DSDP Sites 607 and 611 (Mudie, 1987) have been acknowledged as misidentified (see Head et al., 1989c for details) and a record from the Pliocene of DSDP Site 408 on the Reykjanes Ridge (Engel, 1992) was attributed to reworking by de Verteuil and Norris (1996).

HO *Operculodinium piaseckii* (Plate I, 6–7)

Occurrence: Sample 907A-12H-2, 68–70 cm; 104.5 mbsf.

Magnetostratigraphic calibration: interpolation between top C3Ar and top C5n.2n.

Age assessment: 8.4 Ma (late Tortonian).

Discussion: This species was first described by Strauss and Lund (1992) but had been reported previously from across the North Atlantic and adjacent seas as *Operculodinium* sp. of Piasecki (1980).

In the Salisbury Embayment, eastern U.S.A. it has a HO within DN9, this zone being approximately coincident with Chron C4 (*c.* 8.8–7.5 Ma) in the western North Atlantic (de Verteuil and Norris, 1996). In ODP Hole 905A off New Jersey, the HO of *O. piaseckii* is at the top of zone DN9 (upper Tortonian, de Verteuil, 1996; Gartner and Shyu, 1996).

In Labrador Sea ODP Hole 646B, the HO is at *c.* 8.5 Ma (Head et al., 1989c), within the upper part of nannofossil zone NN10 (Knüttel et al., 1989). From offshore West Greenland, this species has a HO within the Tortonian (Piasecki, 2003), and at Norwegian Sea ODP Site 643, its HO is at least as high as *c.* 7.4 Ma (Manum et al., 1989; Bleil, 1989).

In eastern North Atlantic DSDP Hole 555, the HO is recorded within the upper Tortonian (Edwards, 1984; Backman, 1984). A single isolated lower Zanclean record

from eastern North Atlantic DSDP Hole 553A (Edwards, 1984; Backman, 1984) is considered reworked.

From the Danish sector of the eastern North Sea Basin, Dybkjær and Piasecki (2010) reported an HO within their *H. obscura* zone (*c.* 8.8–7.6 Ma); and in the Gram boring in Denmark, where this species was first described (as *Operculodinium* sp. in Piasecki, 1980), it ranges to the top of the Gram Formation which is dated as Tortonian (Piasecki, 1980, 2005). An unusually high occurrence was reported from the uppermost Tortonian–Messinian (*c.* 7.5–5.7 Ma) Kasterlee Formation of Belgium by Louwye et al. (2007a). However, in the Nieder Ochtenhausen borehole, Northern Germany, its HO coincides with that of *H. obscura* (Strauss et al. (2001) and is therefore assignable to zone DN9 (Köthe and Piesker, 2007).

From the Mazzapiedi section of northwestern Italy, Zevenboom (1995) recorded a HO at the top of the section, dated at *c.* 8.5 Ma within the lower part of Subchron C4r and within calcareous nannofossil zone NN11a.

Sporadic higher records include an isolated Upper Pliocene occurrence in the Gulf of Mexico (Wrenn and Kokinos, 1986) and rare occurrences in the uppermost Miocene or Lower Pliocene of DSDP Hole 408 in the Irminger Sea (Engel, 1992; Poore et al., 1979) that are likely all reworked.

HO *Batiacasphaera hirsuta* (Plate III, 1–3)

Occurrence: Sample 907A-12H-2, 68–70 cm; 104.5 mbsf.

Magnetostratigraphic calibration: interpolation between top C5n.2n and top C3Ar.

Age assessment: 8.4 Ma (late Tortonian).

Discussion: The HO obtained at Site 907 is tentative owing to the sporadic occurrence of this species in the upper part of its range. However, this position is consistent with that in Norwegian Sea ODP Hole 643A (Subchron C4r.2r, c. 8.4 Ma, Manum et al., 1989; Bleil, 1989). In Norwegian Sea ODP Hole 642C (Manum et al., 1989), the HO is within the Messinian (Goll, 1989) but based on a sporadic record. The HPO is within a possible hiatus (Bleil, 1989), thus hindering a reliable age determination. Poulsen et al. (1996) recorded a single, rare occurrence in the Lower Pliocene of Hole 907A (Section 9H-4 at 78.55 mbsf, *c.* 5.0 Ma based on our time scale), which we attribute to reworking.

In Iceland, this species occurs fairly persistently in low numbers in the Tjörnes beds which are dated as Zanclean, and it has a HO in the Lower Pleistocene Hörgi Formation (Verhoeven et al., 2011). We consider these Lower Pleistocene specimens

reworked, possibly from local Miocene deposits, as this formation is characterized by alternating glacial diamictites and interglacial marine deposits, and frequent occurrences of reworked clasts. In the Tjörnes beds, *B. hirsuta* occurs rarely but fairly persistently in the lower Serripes zone and upper Mactra zone, but is nearly absent from the underlying Tapes Zone. The two youngest units represent the deepest depositional environment, and hence an interval of increased subsidence (Verhoeven et al., 2011). Elevated sedimention rates in the lower Serripes and upper Mactra zones might have introduced reworked specimens of *B. hirsuta* from underlying Miocene strata, explaining the unusually high stratigraphic occurrence of this species in the Tjörnes beds.

Köthe and Piesker (2007) reported a HO from northern Germany within their zone DN8 (lower to mid-Tortonian; Köthe, 2005). Munsterman and Brinkhuis (2004) noted the presence of *B. hirsuta* in their Southern North Sea Miocene zones 6 and 9 (*c.* 15–12 Ma), but in many Dutch wells it ranges into zone 14 (*c.* 7.4–8.1 Ma; D. Munsterman, pers. commun., 2012). Louwye et al. (2000) reported this species from the Antwerp Sands in Belgium but this study is restricted to the Middle Miocene and a HO was not recognised.

Zevenboom (1995) recorded a HO at the top of the Mazzapiedi section of northwestern Italy, dated at *c.* 8.5 Ma within the lower part of Subchron C4r and within calcareous nannofossil zone NN11a.

HCO *Cristadinium cristatoserratum* (Plate IV, 10–12)

Occurrence: Sample 907A-12H-1, 127–129 cm; 103.6 mbsf.

Magnetostratigraphic calibration: interpolation between top C5n.2n and top C3Ar.

Age assessment: 8.3 Ma (mid-Tortonian).

Discussion: The HO observed from our data (5.5 Ma) is consistent with its HO in western North Atlantic DSDP Hole 603C at *c.* 5.7 Ma where it is restricted to the lowest two samples of the analysed section (M.J.H, unpubl. data; Canninga et al., 1987). However, we acknowledge that the HO is defined by sporadic occurrences in Hole 907A. In Hole 907A, the HCO of this species at 8.3 Ma is considered the more reliable datum, although we recognise that it coincides with the onset of (locally?) unfavourable conditions at Site 907 related to the deposition of ice-rafted debris (Fronval and Jansen, 1996).

In Labrador Sea ODP Hole 646B, the HO (Head et al., 1989a,c) is calibrated at *c.* 7.4 Ma (top of nannofossil zone NN11a; Knüttel et al., 1989), but inaccuracies in the age model presumably account for some of the observed age differences with other sites. De

Verteuil (1996) reported *C. cristatoserratum* from offshore New Jersey ODP Hole 903C in the lower and mid-Tortonian zone DN8 of de Verteuil and Norris (1996). However, it was recorded in the uppermost sample of the analysed interval preventing the complete stratigraphic range from being determined. This species occurs also in the Miocene of Baffin Bay ODP Hole 645E where it was recorded by Head et al. (1989b) in the highest sample analysed, and dated as Late Miocene, although independent age control is poor for this interval of Hole 645E.

Messinian (Late Miocene)

HCO *Decahedrella martinheadii* (Plate IV, 18–19)

Occurrence: Sample 907A-11H-1, 73–75 cm; 93.5 mbsf.

Magnetostratigraphic calibration: top of Subchron C3An.2n (interpolation between top of Subchron C3Ar and top of Subchron C3An.2n).

Age assessment: 6.5 Ma (mid-Messinian).

Discussion: The stratigraphic ranges of this acritarch species and their implications for North Atlantic biostratigraphy were discussed in detail by Matthiessen et al. (2009), who determined a HO at *c.* 6.2 Ma based on Norwegian Sea ODP Holes 642B/C and 985A and Iceland Sea Hole 907A. Our new studies from Hole 907A broadly confirm this datum, but because Poulsen et al. (1996) reported the HO slightly higher than us at 91.36 mbsf (not 91.26 mbsf as erroneously stated by Matthiessen et al., 2009b) we calculate a slightly older age of 6.3 Ma for the HO. However, this datum is marked by few specimens only and might result from reworking. Conversely, the HCO, which is marked by a remarkable acme where this species constitutes up to 90% of the assemblage (i.e., total dinocysts + *D. martinheadii*) in Hole 907A, is an unambiguous event. We therefore use the HCO, rather than the HO, as it is more robustly recognisable. Indeed, Matthiessen et al. (2009b) reported a possibly time equivalent acme from IODP Site M0002A (Arctic Ocean) and ODP Sites 908 and 909 (Fram Strait) and 985 (southern Norwegian Sea) that may allow the HCO of this species to be recognised between *c.* 6.7 and 6.3 Ma across the Norwegian–Greenland Sea.

Zanclean (Early Pliocene)

HCO *Batiacasphaera micropapillata* (Plate III, 4–10)

Occurrence: Sample 907A-9H-1, 40–42 cm; 74.2 mbsf.

Magnetostratigraphic calibration: upper part of Chron C3 (interpolation between base and top

of Chron C3).

Age assessment: 4.6 Ma (mid-Zanclean).

Discussion: Specimens in Hole 907A have a range of microreticulate, microvermiculate, and microrugulate ornamentation. *Batiacasphaera minuta* is exclusively microreticulate (Matsuoka and Head, 1992) but otherwise similar to *Batiacasphaera micropapillata,* which is described as having a range of micropapillate, finely granulate, to microreticulate ornament (Stover, 1977). A conceptual overlap therefore exists between these species (Matsuoka and Head, 1992). Although micropapillate forms were seen only rarely, we assign our specimens to *B. micropapillata* to encompass the range of ornament observed. Nonetheless, the HCO and HO in Hole 907A comprise microreticulate specimens assignable to *B. minuta*. To facilitate comparison with records elsewhere, we follow De Schepper and Head (2008) in treating both species together for purposes of stratigraphic synthesis.

This species has a HCO in Hole 907A at 4.6 Ma, with rare, sporadic occurrences extending to its HO at 3.4 Ma (lower Piacenzian). In Labrador Sea ODP Hole 646B, the HPO and HCO are near the nannofossil zone NN15/NN16 boundary dated at *c.* 3.7 Ma (as *Batiacasphaera sphaerica* in de Vernal and Mudie, 1989; Knüttel et al., 1989), with sporadic higher occurrences likely attributable to reworking (De Schepper and Head, 2008). Its HCO is magnetostratigraphically calibrated at *c.* 4.0 Ma in western North Atlantic DSDP Hole 603C (Subchron C2Ar, M.J.H., unpubl. data; Canninga et al., 1987).

HO *Reticulatosphaera actinocoronata* (Plate IV, 7–8)

Occurrence: Sample 907A-8H-6, 140–142 cm; 73.2 mbsf.

Magnetostratigraphic calibration: upper part of Chron C3 (interpolation between base and top of Chron C3).

Age assessment: 4.5 Ma (mid-Zanclean).

Discussion: The HO derived from our data agrees well with findings from Greenland Sea ODP Hole 987E (Subchron C3n.3n, *c.* 4.8 Ma, Channell et al., 1999b), Norwegian Sea ODP Hole 642C (*c.* 4.2 Ma; Mudie, 1989; Bleil, 1989), Labrador Sea ODP Hole 646B (lower nannofossil zone NN15, older than 3.7 Ma within the mid- to upper Zanclean, as *Impletosphaeridium* sp. in de Vernal and Mudie, 1989; Knüttel et al., 1989), central North Atlantic DSDP Site 607 (Subchron C3n.4n, *c.* 5.0 Ma, Mudie, 1987; Clement and Robinson, 1987), and central North Atlantic DSDP Site 611 (Subchron C3n.1r, *c.* 4.4 Ma, Mudie, 1987; Clement and Robinson, 1987). In western North Atlantic DSDP Hole

603C, this species has a HCO at *c.* 4.5 Ma and a HO at *c.* 4.0 Ma (M.J.H., unpubl. data; Canninga et al., 1987). It is uncertain whether specimens above the HCO are reworked. Judging from the above records, a HO recorded within the Matuyama Chron in Fram Strait ODP Hole 986D (Smelror, 1999; Channell et al., 1999b) must represent reworking. In the Tjörnes beds of Iceland the HO is recorded in the mid-Zanclean (Verhoeven et al., 2011).

HO *Operculodinium? eirikianum* (Plate I, 4–5)

Occurrence: Sample 907A-8H-6, 140–142 cm; 73.2 mbsf.

Magnetostratigraphic calibration: upper part of Chron C3 (interpolation between base and top of Chron C3).

Age assessment: 4.5 Ma (mid-Zanclean).

Discussion: In western North Atlantic DSDP Hole 603C, the HPO is recorded near the base of Subchron C2An.3n at *c.* 3.6 Ma, and it is uncertain whether rare and sporadic occurrences as high as the Olduvai Subchron at *c.* 1.8 Ma are reworked (M.J.H., unpubl. data; Canninga et al., 1987). In Labrador Sea ODP Hole 646B, the HO is recorded in the middle of calcareous nannofossil zone NN16 (mid-Piacenzian, as *Operculodinium longispinigerum* in de Vernal and Mudie, 1989; Knüttel et al., 1989). Off West Greenland, it was reported from the Upper Miocene but not from the unconformably overlying Zanclean (Piasecki, 2003).

In Norwegian Sea ODP Hole 642C, it was recorded in the highest sample investigated (as *Operculodinium longispinigerum* in Mudie, 1989), which was dated at *c.* 3.4 Ma (Subchron C2An.3n, Bleil, 1989), but in Hole 642B its HO seems to occur within the Olduvai Subchron at *c.* 1.8 Ma (as *Operculodinium longispinigerum* unillustrated in Mudie, 1989; Bleil, 1989), and in Norwegian Sea ODP Hole 644A it apparently has a HO at the top of the Gauss Chron at *c.* 2.6 Ma (Mudie, 1989; Bleil, 1989). Taxonomic uncertainties relating to this species in the Norwegian Sea are discussed by Mudie (in Head and Wrenn, 1992) and Head (1993, 1996).

In eastern North Atlantic DSDP Hole 610A, the HO is magnetostratigraphically-calibrated to *c.* 2.6 Ma (top C2An.1n, De Schepper and Head, 2008; Clement and Robinson, 1987), and this species ranges to at least MIS 91 (2.34 Ma) in central North Atlantic DSDP Hole 607/607A (Versteegh, 1997). A single, but apparently in-situ, specimen was reported from the warm-water St. Erth Beds of southwestern England, which are dated at *c.* 2.0 Ma (Head, 1993, 1999).

In the southern North Sea Basin, a HO is recorded at *c.* 2.4 Ma (Gelasian) both in eastern England (Head, 1996, 1998) and the offshore northern Netherlands sector of the southern North Sea (Kuhlmann et al., 2006a; 2006b).

HO *Pyxidinopsis vesiculata* (Plate I, 16–18)

Occurrence: Sample 907A-8H-6, 140–142 cm; 73.2 mbsf.

Magnetostratigraphic calibration: upper part of Chron C3 (interpolation between base and top of Chron C3).

Age assessment: 4.5 Ma (mid-Zanclean).

Discussion: This species has been reported previously only from western North Atlantic DSDP Hole 603C where it has a HO in Subchron C3n.2n at *c.* 4.5 Ma (Head and Norris, 2003; Canninga et al., 1987), and eastern North Atlantic DSDP Hole 610A where its HO is at *c.* 3.9 Ma (Subchron C2Ar, De Schepper and Head, 2008; Clement and Robinson, 1987). The re-examination of a specimen from the Upper Miocene (nannofossil zone NN11b, Knüttel et al., 1989) of Labrador Sea ODP Hole 646B illustrated as *Batiacasphaera/Cerebrocysta*? Group A by Head et al. (1989c, pl. 1, fig. 4) confirms that it is *P. vesiculata* (M.J.H., unpubl. data).

HO *Corrudinium devernaliae* (Plate I, 11–12)

Occurrence: Sample 907A-8H-6, 140–142 cm; 73.2 mbsf.

Magnetostratigraphic calibration: upper part of Chron C3 (interpolation between base and top of Chron C3).

Age assessment: 4.5 Ma (mid-Zanclean).

Discussion: This species is present in a single sample where it is common. Such an isolated occurrence clearly restricts the reliability of this event as a HO at Hole 907A (Fig. 16), but it falls within the narrow range recorded for this species from other sites. In western North Atlantic DSDP Hole 603C, it has a magnetostratigraphically-calibrated range of 4.7–4.1 Ma within the mid-Zanclean (Head and Norris, 2003; Canninga et al., 1987). In Labrador Sea ODP Hole 646B this species also has a narrow range, with a LO in nannofossil zone NN12, and a HPO calibrated to the nannofossil zone NN15/16 boundary dated at *c.* 3.7 Ma (as Corrudinium sp. 1 in de Vernal and Mudie, 1989; Knüttel et al., 1989). Sporadic higher occurrences in Hole 646B probably represent reworking (Head and Norris, 2003). In eastern North Atlantic DSDP Hole 610A, the HO is magnetostratigraphically calibrated to *c.* 3.9 Ma (Subchron C2Ar, De Schepper and Head,

2008; Clement and Robinson, 1987). In the southern North Sea basin, this species is restricted to the Belgian Kattendijk Formation (c. 5.0 to 4.7-4.4 Ma, De Schepper et al., 2008; Louwye et al., 2004), which is unconformably overlain by the Luchtbal Sands (*c.* 3.71–3.21 Ma, De Schepper et al., 2008).

HO *Operculodinium tegillatum* (Plate I, 8–10)

Occurrence: Sample 907A-8H-6, 140–142 cm; 73.2 mbsf.

Magnetostratigraphic calibration: upper part of Chron C3 (interpolation between base and top of Chron C3).

Age assessment: 4.5 Ma (mid-Zanclean).

Discussion: In western North Atlantic DSDP Hole 603C, the HCO is magnetostratigraphically-calibrated at *c.* 4.0 Ma, but this species extends continuously to its HO at *c.* 3.6 Ma (M.J.H., unpubl. data; Canninga et al., 1987). In Labrador Sea ODP Hole 646B, the HPO is recorded at *c.* 3.6 Ma close to the nannofossil zone NN15/16 boundary (as Operculodinium crassum in de Vernal and Mudie, 1989; Knüttel et al., 1989) with sporadic higher occurrences likely representing reworking. In eastern North Atlantic DSDP Hole 610A, the HO has a magnetostratigraphically-calibrated age of *c.* 3.7 Ma (Subchron C2Ar, De Schepper and Head, 2008; Clement and Robinson, 1987). In the Tjörnes beds of Iceland, the HO is within the mid-Zanclean (Verhoeven et al., 2011).

In eastern England, this species occurs within the Coralline Crag Formation (Head, 1997), which is dated biostratigraphically as mid- to late Zanclean (De Schepper et al., 2008; Head, 1998), but not in the unconformably overlain Walton Crag Formation dated *c.* 2.7 Ma (Head, 1998b). In Belgium, this species has been recorded within the Kattendijk Formation, which is dated biostratigraphically at (c. 5.0 to 4.7-4.4 Ma, De Schepper et al., 2008; Louwye et al., 2004), but is absent from the unconformably overlain Luchtbal Sands (*c.* 3.71–3.21 Ma, De Schepper et al., 2008).

Piacenzian (Late Pliocene)

HO *Batiacasphaera micropapillata* (Plate III, 4–10)

Occurrence: Sample 907A-7H-7, 41–43 cm; 64.2 mbsf.

Magnetostratigraphic calibration: lower part of Subchron C2An (interpolation between top of Subchron C2Ar and top of Subchron C2An.2r).

Age assessment: 3.4 Ma (early Piacenzian).

Discussion: Although we calibrate the HO at 3.4 Ma in Hole 907A, we acknowledge that

this datum is defined by sporadic occurrences only and therefore tentative. In Labrador Sea ODP Hole 646B, the HPO/HCO close to the calcareous nannofossil NN15/16 boundary at *c.* 3.7 Ma (as *Batiacasphaera sphaerica* in de Vernal and Mudie 1989; Knüttel et al., 1989) are taken to represent the upper stratigraphic range, as sporadic occurrences above that level have been attributed to reworking (De Schepper and Head, 2008). Its HO is magnetostratigraphically-calibrated at *c.* 3.8 Ma in eastern North Atlantic DSDP Hole 610A (Subchron C2Ar, De Schepper and Head, 2008; Clement and Robinson, 1987) and at *c.* 3.7 Ma in western North Atlantic DSDP Hole 603C (Subchron C2Ar, M.J.H., unpubl. data; Canninga et al., 1987). In the Tjörnes beds of Iceland, the HO is within the mid- to late Zanclean (Verhoeven et al., 2011).

Within the discontinuous Pliocene record of eastern England, this species has a highest occurrence in the Ramsholt Member of the Coralline Crag Formation (Head, 1997), which is biostratigraphically-dated at *c.* 4.4–3.8 Ma (De Schepper et al., 2008) but unconformably overlain by the Walton Crag Formation (Head, 1998b). In Belgium, this species has not been reported higher than the Kattendijk Formation (c. 5.0 to 4.7-4.4 Ma, Louwye et al., 2004), except for sporadic higher occurrences in the unconformably overlain Luchtbal Sands that are attributed to reworking (De Schepper et al., (2008).

3.4 Discussion

The appearance and disappearance datums of dinocyst species are rarely precisely synchronous worldwide (e.g. Williams et al., 2004), especially in the late Cenozoic owing to increasing latitudinal temperature gradients. De Schepper and Head (2008) recently compared mid-Pliocene through Pleistocene dinocyst events across the North Atlantic and, despite evident latitudinal control on the stratigraphic ranges of many species, they identified several bioevents for supraregional stratigraphic correlation.

Of the 26 bioevents defined in Hole 907A, 21 are HOs or HCOs, clearly reflecting a diminishing diversity of Miocene taxa in response to the deterioration of climate towards and into the Pliocene. Figure 18 shows those dinocyst and acritarch bioevents in Hole 907A that have potential to extend North Atlantic biostratigraphy into the higher latitudes.

3.4.1 Supraregional biostratigraphic correlation

For *Hystrichosphaeropsis obscura* (Plate II, 1–5), comprehensive literature reviews of the North Atlantic region show most HOs in the Middle and Upper Miocene (Head et al.,

1989c; Warny and Wrenn, 2002; Louwye et al., 2007a). Indeed, *H. obscura* has a HO at *c.* 7.4 Ma in the Norwegian Sea, within the lower part of nannofossil zone NN11 in the eastern North Atlantic, and at about *c.* 7.5 Ma in the western North Atlantic, all within the upper Tortonian; and most HOs in the North Sea basin are within the upper Tortonian, although there is little independent control on these records. In Iceland Sea ODP Hole 987E, it seems to disappear contemporaneously at *c.* 7.2 Ma although no quantitative data are available to judge whether this datum, which is close to the base of the core, is based on a persistent or sporadic occurrence. If the HO in Hole 987E is reliable, then the full stratigraphic range in Hole 907A may not have been detected. In Hole 907A, *H. obscura* has a scarce and somewhat sporadic occurrence through the Serravallian and lower Tortonian up to 10.6 Ma where it is relatively common in one sample (the HCO). Three higher isolated occurrences up to 8.8 Ma may be in place or reworked, although the latter is more likely because this species has an affinity for warm-temperate waters, judging from its stratigraphic distribution elsewhere (see also Head et al., 1989b) – and the lowest evidence of dropstones at 116.5 mbsf (Shipboard Scientific Party, 1995) just above the HCO at 123 mbsf indicates cooling that presumably led to ecological exclusion above this HCO in Hole 907A. Therefore, while our comparison suggests a high correlation potential for the HO of *H. obscura* across much of the North Atlantic region, the cold-water domain of Site 907 must be excluded.

Labyrinthodinium truncatum (Plate IV, 3–6) has an unusually high (*c.* 7.2 Ma, lowermost Messinian) and thus questionable record in Iceland Sea ODP Hole 987E, but otherwise a near-synchronous HO between 8.4 and 8.6 Ma (mid-Tortonian) in Hole 907A and the Norwegian Sea, which suggests good stratigraphic correlation potential within the Nordic Seas. Moreover, it does not range higher than calcareous nannofossil zone NN10 (mid-Tortonian) in the Labrador Sea and the eastern North Atlantic, which seems to permit supraregional correlations between the these high latitude sites. In contrast, from the mid-latitude sites of the Salisbury Embayment, offshore New Jersey, and in the North Sea Basin, this event is consistently recorded in the uppermost Tortonian at *c.* 7.5 Ma. While latitudinal control on the disappearance of *L. truncatum* might have contributed to this discrepancy, these mid-latitude sites represent shallow-water environments and have less reliable age control. Moreover, dinocyst datums are used in dating the North Sea Basin, possibly introducing bias through circular reasoning (see Section 3.1). Head et al. (1989c) reviewed the stratigraphic literature on *L. truncatum* and concluded that its HO was in the lower Upper Miocene, which is validated by this

study with no confirmed record above the uppermost Tortonian. Despite its offset between the mid- and high latitudes, *L. truncatum* appears to be a potentially useful stratigraphic marker for the mid- to upper Tortonian and for approximate correlations between both regions.

Reticulatosphaera actinocoronata (Plate IV, 7, 8) disappeared within a relatively short interval between *c.* 5.0 and 4.0 Ma in the Zanclean within the entire North Atlantic region, and if inaccuracies in age control and low sample resolution and the likelihood of reworking are all taken into consideration then this interval narrows to around *c.* 4.8–4.2 Ma in the mid-Zanclean. This species had a cosmopolitan distribution in the Miocene and apparently disappeared in other oceans within the Zanclean (Matsuoka et al., 1987; Udeze and Oboh-Ikuenobe, 2005; Williams et al., 2004) suggesting a global stratigraphic potential. This may include the marginal Arctic Ocean since it has been observed in Miocene sediments of the Beaufort Sea (Bujak and Davis, 1981).

Batiacasphaera micropapillata (Plate III, 4–10) exhibits a narrow range of HOs throughout the North Atlantic between *c.* 3.8 and 3.4 Ma, which suggests a good correlation potential across the various North Atlantic basins in the late Zanclean and earliest Piacenzian. A similar stratigraphic range in the North Sea, with no confirmed record above the Zanclean may allows for correlation between the North Atlantic and the North Sea. However, a comparison of HOs across the North Atlantic reveals a "reversed" succession of lower HOs at the southern sites (*c.* 3.8–3.7 Ma) and higher ones at the northern sites (*c.* 3.7–3.4 Ma), which is difficult to explain with a normal latitudinal gradient during the Neogene. However, as we cannot disregard the possibilities of reworking and inaccuracies in age control the interpretation of this pattern remains enigmatic, but is probably related to changes in warm water advection via the North Atlantic current (e.g. Lawrence et al., 2009; Naafs et al., 2010). The presence of *Batiacasphaera micropapillata* in the Middle and Upper Miocene of the central Arctic Ocean (J.M and M.S, unpubl. data) suggests its potential for use in correlation at very high northern latitudes.

3.4.2 Regional biostratigraphic correlation

Unipontidinium aquaeductus (Plate I, 13–15) disappeared somewhat consistently during the late Langhian in the Iceland and Norwegian seas, which allows stratigraphic correlation within the Nordic Seas. In the central North Atlantic, it disappeared near the Langhian/Serravallian boundary suggesting that this correlation might be extended

across this region, but more reliable records are needed. However, at these sites the HO

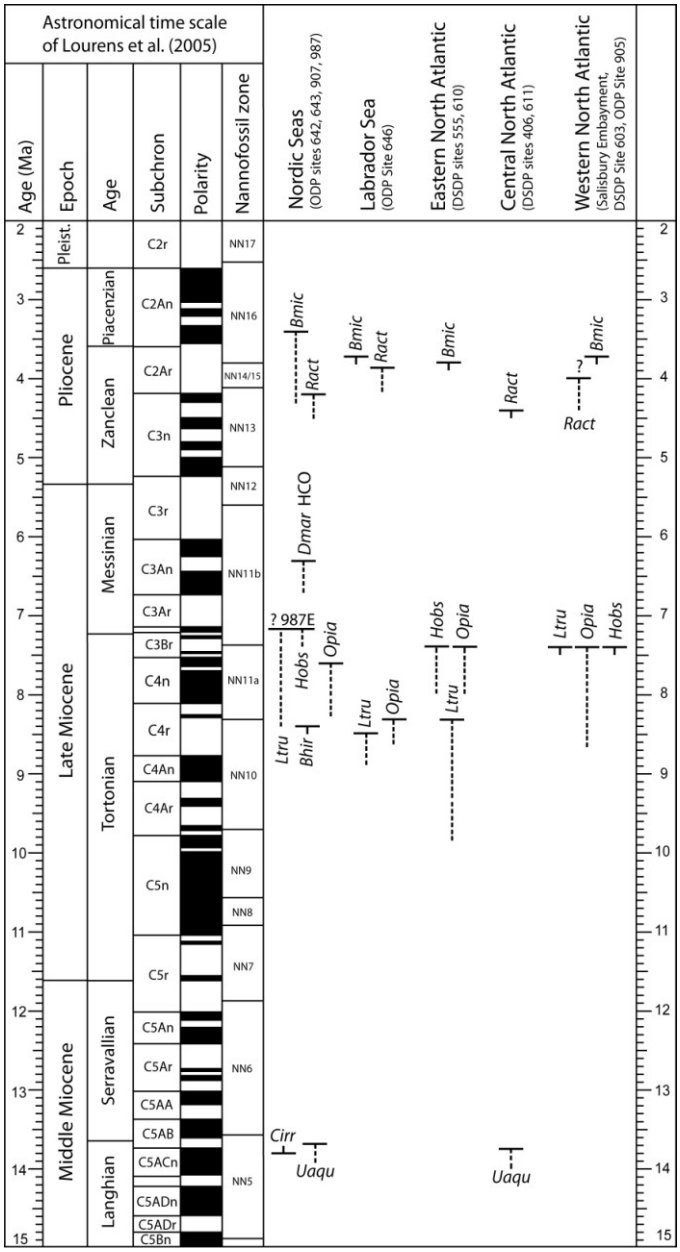

Figure 18: Correlation of key dinoflagellate cyst and acritarch bioevents across the North Atlantic region and the North Sea basin. Vertical dashed lines indicate the range of uncertainty in the position of a bioevent at the various sites (see section 3.2), and question marks indicate uncertainty in the assessment of a bioevent (for discussion see section 4). Data are from Manum et al. 1989; Mudie, 1989; Channel et al., 1999, and this study for the Nordic Seas; Head et al., 1989c; de Vernal and Mudie, 1989 for the Labrador Sea; Edwards, 1984; De Schepper and Head, 2008 for the eastern North Atlantic; Mudie, 1987; Costa and Downie, 1979 for the central North Atlantic; and de Verteuil, 1996; de Verteuil and Norris, 1996; and MJH (unpubl. data) for the western North Atlantic. Species codes are given in Table 1.

is considerably lower than the well-constrained HPO and HO of *c.* 13.1 Ma and *c.* 12.0 Ma in northern Italy and HO of *c.* 12.3 Ma in eastern North Atlantic IODP Site U1318, and also lower than HOs in the mid-latitude western North Atlantic and Europe. This

earlier disappearance from the northernmost sites is likely explained by a temperature threshold crossed during the cooling that occurred across the Middle Miocene climate transition (e.g. Flower and Kennett, 1994; Abels et al., 2005). It is nonetheless evident that *U. aquaeductus* does not range higher than calcareous nannofossil zone NN6 in the North Atlantic and adjacent seas.

The HO of the genus *Palaeocystodinium* (Plate IV, 13–15) is asynchronous across the various North Atlantic basins, ranging from lower Serravallian to upper Tortonian. In contrast, in the North Sea and Mediterranean basins a near-synchronous HO has been recognized in the mid-Tortonian between *c.* 9.0 and 8.7 Ma and suggests a similar timing of paleoenvironmental changes. In general, the HO of *Palaeocystodinium* spp. is recorded between the middle and upper Tortonian at both mid- and high northern latitudes, which agrees with its 8.9 Ma age in Hole 907A. This genus apparently does not range higher than the upper Tortonian across the North Atlantic region, which may be useful in high latitude regions where other biostratigraphic information is sparse.

Batiacasphaera hirsuta (Plate III, 1–3) appears to have disappeared contemporaneously at *c.* 8.4 Ma in the Iceland and Norwegian seas allowing for potential biostratigraphic correlations within the Nordic Seas. *Batiacasphaera hirsuta* occurs at least as high as *c.* 8.5 Ma in the Mediterranean Sea and had a wide distribution within the North Sea, where some evidence suggests a similar age for this bioevent. This indicates potential for supraregional correlations but more reliable data are needed on its HO in the North Sea.

The cold water acritarch *Decahedrella martinheadii* (Plate IV, 18, 19) has been reported with a tentative near-synchronous HO at *c.* 6.3–6.2 Ma from northern high latitude sites (Matthiessen et al., 2009) and appears to be an excellent marker across the subpolar/polar North Atlantic and Arctic Ocean. However, because the HO in Hole 907A is marked by a few specimens only and therefore strongly dependent on sample resolution, we use the HCO for correlations within the Nordic Seas. A HCO is recognised at 6.5 Ma in Hole 907A but further investigations of this event in other high latitude sites is needed to improve its constraints.

3.4.3 Potentially useful species for biostratigraphic correlation

Operculodinium piaseckii (Plate I, 6, 7) had a broad biogeographic distribution across the North Atlantic and adjacent seas, but all well-constrained records considered here show a broadly consistent HO within the upper Tortonian between *c.* 8.5 and 7.4 Ma. However,

this species is often rare and sporadic in its occurrence, which may affect its reliability as a biostratigraphic marker (de Verteuil and Norris, 1996). The scatter in positions of the HOs may reflect this deficiency, as will the less accurate age control and low sample spacing of some sites used here. Significantly, the well-dated Mediterranean and Iceland Sea sites yield a synchronous HO. The consistent highest occurrence in the upper Tortonian with no confirmed higher record demonstrates some potential for supraregional biostratigraphic correlations.

The HOs of *Operculodinium tegillatum* (Plate I, 8–10), *P. vesiculata* (Plate I, 16–18), and *C. devernaliae* (Plate I, 11, 12) at 4.5 Ma in Hole 907A are lower than elsewhere and likely related to the oceanographic and climatic changes that occurred in the Iceland Sea towards the intensification of northern hemisphere glaciations (e.g. Fronval and Jansen, 1996; Matthiessen et al., 2008). However, while the HOs of *P. vesiculata* and *C. devernaliae* are based on sporadic occurrences in Hole 907A, they agree well with those recorded in the western North Atlantic. Their higher occurrence in eastern North Atlantic DSDP Hole 610A may be due partly to the less accurate age control in that part of Hole 610A (De Schepper and Head, 2008) but also suggests different oceanographic/climatic conditions at this site presumably related to changes/variability in the North Atlantic current (cf. Lawrence et al., 2009). Due to sparse records of the extinct *P. vesiculata* and *C. devernaliae*, their paleoecological preferences are not well known although their observed biogeographic distribution pattern suggests an adaptation to more temperate conditions. *Operculodinium tegillatum* has a continuous record in Hole 907A but shows a similar trend with an earlier disappearance than at the other sites considered here.

Notwithstanding the above, *Operculodinium tegillatum, P. vesiculata*, and *C. devernaliae* appear to have HOs within the mid- to upper Zanclean (between 4.5 and 3.6 Ma) across the North Atlantic, and may therefore be helpful in distinguishing this time interval at high northern latitudes, where other stratigraphic age control is restricted. The presence of *C. devernaliae* even if sporadic may be of particular value at these high latitudes as its range is restricted to the Zanclean in the North Atlantic region.

3.4.4 Asynchronous last appearances

The HO of *Cerebrocysta poulsenii* (Plate IV, 1, 2) varies widely across the North Atlantic and adjacent seas, ranging from lower Serravallian to mid-Tortonian, although most HOs seem to center within the mid- to upper Serravallian. *Cerebrocysta poulsenii* is typically a scarce constituent of assemblages and this will have contributed to the uncertainty of its

HO, as will have the poor age control of some of the sequences. However, these factors alone do not explain discrepancies in the HO of *C. poulsenii*, especially the remarkable offset between the cold-water (Hole 907A) and warm-water domains (ODP Hole 643A) of the Norwegian–Greenland Sea. *Cerebrocysta poulsenii* seems to have been sensitive to the thermal gradient between these domains, restricting its biostratigraphic utility.

Cleistosphaeridium placacanthum (Plate IV, 16, 17) apparently has a diachronous HO in the North Atlantic, the North Sea Basin and the Mediterranean, ranging from *c.* 13.5 to 8 Ma. Because it is typically a common contributor to Miocene assemblages, and therefore particularly prone to reworking, those rare and sporadic specimens occurring higher in its observed range are often considered reworked (de Verteuil and Norris, 1996; Köthe, 2003). Our compilation of HCOs in the North Atlantic and adjacent seas at *c.* 13.5–13.0 Ma shows consistency but is tentative because this datum could not be recognised, or was not registered, at all sites. The HO of this species is obviously subject to greater uncertainty. Moreover, for the eastern North Sea, Dybkjær and Piasecki (2010) concluded that the highest occurrence of this species is not a distinct event but rather an attenuation over several meters. This species is continuously present but in very low numbers in the upper part of its stratigraphic range in Hole 907A, and its range top appears rather well defined. *Cleistosphaeridium placacanthum* is a neritic species, and given the high latitude and oceanographic setting of Hole 907A, this species might be near the limit of its ecological range, although reworking cannot be excluded. Jiménez-Moreno et al. (2006) discussed the HO of *C. placacanthum* across the North Atlantic region, and concluded that no reliable records exist above the uppermost Serravallian, as our survey also suggests. If this is correct, then the specimens from Hole 907A may be reworked.

Cordosphaeridium minimum (Plate I, 1–3) has a strongly asynchronous HO across the North Atlantic and marginal seas, ranging from lower Serravallian to upper Tortonian, although several studies record a HO within the lower to mid-Tortonian, which agrees with its well-defined range top in Hole 907A. Whether younger records may represent natural attenuation or even reworking remains speculative since few quantitative data are available. Uncertainties in age control and sample spacing are insufficient to account for the reported diachrony in the HO of this species, and thus regional changes in surface water masses and variable depositional settings at the different sites must also be considered. This suggests strong ecological control on its stratigraphic range, which, in combination with the taxonomic uncertainties mentioned previously, will have hindered its biostratigraphic utility.

Cerebrocysta irregulare sp. nov. (Plate 3, 11–20) is presently known only from this study and tentatively from the Norwegian Sea (questionably synonymised with *Tectatodinium* sp. 4 in Manum et al., 1989; see Systematic Paleontology). It apparently disappears earlier at Hole 907A than in the Norwegian Sea, and this might be attributable to the thermal gradient between the cold-water-influenced Iceland Sea and the more temperate Norwegian Sea. However, this species has a well-defined stratigraphic range in Hole 907A (Fig. 16) suggesting strong biostratigraphic potential in the cold-water domain of the high northern latitudes.

Impagidinium elongatum sp. nov. (Plate II, 6–20) has an asynchronous HO in the two well-dated Norwegian and Iceland sea sites, at 8.2 Ma and 10.2 Ma respectively, with a lower HO in the Iceland Sea that likely reflects the influence of the cold East Greenland Current. In Baffin Bay and Belgium, the HO seems broadly similar to that recorded for Hole 907A but is based on poorly dated sequences, and in the case of Baffin Bay the identification is not certain. Regardless, the range top of *I. elongatum* sp. nov. in Hole 907A is well-defined and may be stratigraphically significant in the polar domain of the Arctic and Subarctic seas.

The asynchronous HO of *Dapsilidinium pseudocolligerum* (Plate IV, 9) is a clear response to Late Miocene cooling, as this species persisted into the Late Pliocene and Early Pleistocene in the mid- to low-latitude North Atlantic whereas it had already disappeared from high-latitude sites by the middle Late Miocene. This confirms the tropical to warm-temperate affinities of *D. pseudocolligerum* as recognised by Head and Westphal (1999) and is consistent with the observed discrepancy in the Nordic Seas, where it disappeared earlier in the colder Iceland Sea (9.1 Ma; mid-Tortonian) than in the more temperate Norwegian Sea (*c.* 7.4 Ma; late Tortonian). The distribution of this species elsewhere accords with its North Atlantic pattern, as it occurs persistently in the Pliocene of the eastern Indian Ocean (McMinn, 1992) and has a HO in the Upper Pliocene of the northeast Australian margin (McMinn, 1993), but does not range higher than early Middle Miocene in northern Japan (Bujak and Matsuoka, 1986). Although it has a well-defined HO in Hole 907A, the strong climatic control on the distribution of *D. pseudocolligerum* would seem to hinder its biostratigraphic utility even on a regional scale.

Cristadinium cristatoserratum (Plate IV, 10–12) has a fairly synchronous HO in the upper Messinian of the western North Atlantic and Iceland Sea, although sporadic records define this datum at the latter site. The uppermost Tortonian HO in the

Labrador Sea is lower than recorded at other sites, but higher than the mid-Tortonian HCO in Hole 907A. Imprecise age control for Labrador Sea ODP Site 646 might have contributed to the discrepancy. These being the only sites where the upper stratigraphic range of this species is recorded unambiguously, it is likely that this species does not range higher than the uppermost Miocene.

Operculodinium? *eirikianum* (Plate I, 4, 5) clearly has an asynchronous highest occurrence across the North Atlantic and the North Sea Basin, with a somewhat time-transgressive trend in the succession of HOs. It disappears earlier in the high latitude sites (Norwegian–Greenland Sea, Labrador Sea) than in the mid-latitude eastern and eastern North Atlantic and North Sea basin, where comparatively warmer waters presumably prevailed longer due to the influence of the North Atlantic current. Head (1993, 1997) and De Schepper and Head (2008) regarded *O.*? *eirikianum* as a mid- to high-latitude cold-intolerant species, which supports the interpretation of an asynchronous last appearance across the North Atlantic in response to differential cooling.

3.4.5 First appearances

The only presently well constrained records for the LO of *Cristadinium cristatoserratum* (Plate IV, 10–12) are from the Iceland Sea (Langhian) and western North Atlantic (Upper Oligocene). However, the LOs at both sites are based on sporadic occurrences that may not reflect the true stratigraphic range, and all other studies considered here do not record a LO due to inadequate coring depth. This species is evidently adapted to higher-latitude environments and its LO might be climatically controlled, but until more records become available, it is difficult to assess the stratigraphic potential of this datum.

Although relatively few LOs of *Habibacysta tectata* (Plate I, 19, 20) have good independent stratigraphic control, most published studies record this datum slightly above the LO of *U. aquaeductus* which is provisionally constrained at 15.1–14.8 Ma (Jiménez-Moreno et al., 2006a). Therefore, an LO across the North Atlantic and adjacent seas within calcareous nannofossil zone NN5 (mid- and late Langhian) appears most likely, which accords with the conclusion of Jiménez-Moreno et al. (2006). Suspected contamination likely explains a Lower Miocene record from northern Belgium (S. Louwye, pers. commun. in Jiménez-Moreno et al., 2006). *Habibacysta tectata* seems to have a relatively good stratigraphic potential for integrating North Atlantic and North Sea records at higher latitudes because of its tolerance of cooler temperatures (De Schepper et al., 2011; Head, 1994; Head et al., 1989a), and its similar LO in IODP Hole M0002A

suggests that this may be extended into the central Arctic Ocean.

Cerebrocysta irregulare sp. nov. (Plate III, 11–20) has been recorded only from the Iceland and possibly the Norwegian Sea (as *Tectatodinium* sp. 4 in Manum et al., 1989) where it has a near-synchronous LO close to the Langhian/Serravallian boundary. This and its well-defined range in Hole 907A suggest a strong stratigraphic potential for this bioevent in the Nordic Seas.

Operculodinium? *eirikianum* (Plate I, 4, 5) has a broad range of LOs ranging from lower Langhian to upper Tortonian, which cannot be explained solely by inaccurate age control and sample resolution solely. These reported discrepancies may in part reflect confusion with the similar *Operculodinium*? *borgerholtense* (see Soliman et al., 2009) and *O.*? *longispinigerum* (see Head and Westphal, 1999), both of which range into the Lower Miocene. Magnetostratigraphically dated records from the Iceland Sea, eastern North Atlantic and the Mediterranean place the LO of *O.*? *eirikianum* between *c.* 14 and 13 Ma. Indeed, except for the Salisbury Embayment and offshore New Jersey, this species seems to have appeared not later than early Serravallian across the North Atlantic and adjacent seas. However, more well-constrained records are needed to critically evaluate this species utility for regional and supraregional stratigraphic correlations.

For the first time, the LO of *Decahedrella martinheadii* (Plate IV, 18, 19) has been magnetostratigraphically-calibrated in the Nordic Seas, to 10.5 Ma. At other high latitude sites, with the exception of an LO at *c.* 11.0 Ma in the Fram Strait, its range base cannot be defined unambiguously due to inadequate coring depth or recovery (Matthiessen et al., 2009b), thus preventing an opportunity to critically evaluate the stratigraphic utility of this event. The first appearance of *D. martinheadii* may have been related to the fundamental reorganisation of the surface and deep-water circulation in the northernmost North Atlantic due to the deepening of the Fram Strait (Matthiessen et al., 2009b) and the onset of an East Greenland current precursor (Wolf-Welling et al., 1996).

3.4.6 Age assignment for the base of Hole 907A

Age estimates for the lowermost sediments of Hole 907A based on magnetostratigraphy (Channell et al., 1999a) and $^{40}Ar/^{39}Ar$ dating of the underlying tholeiitic basalts (Davis and McIntosh, 1996) do not fully agree (Section 2.2); with extrapolation from magnetostratigraphy giving an age of 14.53 Ma and $^{40}Ar/^{39}Ar$ measurements suggesting 13.3 ± 0.3 Ma. Two dinocyst occurrences call into question the $^{40}Ar/^{39}Ar$ age. *Unipontidinium aquaeductus* occurs in the lowermost Sample 23H-CC, 10–12 cm (216.5

mbsf). The LO of *U. aquaeductus* elsewhere is rather well constrained, and Jiménez-Moreno et al. (2006) placed this event provisionally at 15.1–14.8 Ma (mid-Langhian). The LO of *Habibacysta tectata* occurs in Sample 907A-23H-3, 51.5–53.5 cm between the magnetostratigraphic and $^{40}Ar/^{39}Ar$ ages. Elsewhere, it is generally placed slightly higher than the LO of *U. aquaeductus* in the mid- to upper Langhian calcareous nannofossil zone NN5, with the oldest well-constrained record being dated at no younger than *c.* 14.8 Ma (Jiménez-Moreno et al., 2006). Because *H. tectata* is a cool-tolerant species, its LO at Hole 907A might be expected to be at least as old as in lower latitudes. Therefore, the basal deposits at Hole 907A are no older than 15.1–14.8 Ma (mid-Langhian) based on the LO of *U. aquaeductus* which is at or slightly predates the basal deposits, and probably no younger than mid- to late Langhian (*c.* 14.8–13.7 Ma) based on the LO of *H. tectata* which is just above the basal deposits. A mid- to late Langhian age (15.1–13.7 Ma) is accordingly suggested for the basal deposits. This biostratigraphic constraint, while tentative, more closely agrees with the extrapolated magnetostratigraphic age of *c.* 14.5 Ma than with the radiometric age of 13.2 Ma.

As noted by the Shipboard Scientific Party (1995, but adjusting ages to the time scale of Lourens et al., 2005), Site 907 was drilled either on Magnetic Anomaly 6B crust between 22.6 and 21.8 Ma (Talwani and Eldholm, 1977) or Anomaly 5B crust between 16.0 and 14.8 Ma (Vogt et al., 1980), depending on whether sea-floor spreading from the Kolbeinsey Ridge was symmetrical (Vogt et al., 1980) or not (Talwani and Eldholm, 1977). It is not certain whether the basalt at the base of Hole 907A represents oceanic crust or a later submarine eruption (Davis and McIntosh, 1996). If oceanic crust is represented, then both magnetostratigraphy and dinocyst stratigraphy imply that Site 907 sits on Anomaly 5A between 14.8 and 12.0 Ma. A younger part of Anomaly 5B, as proposed by Vogt et al. (1980), would also be possible if the extrapolated magnetostratigraphic age of *c.* 14.5 Ma is slightly underestimated.

3.5 Conclusions

Based on the palynological analyses of 120 samples spanning the interval between *c.* 14.5–2.5 Ma in ODP Hole 907A at *c.* 100 kyr temporal resolution, a magnetostratigraphic calibration of a suite of 26 potentially biostratigraphic useful dinocyst and acritarch events has been conducted for the first time in the Miocene and Pliocene of the high northern latitudes. Most events are last appearances and reflect a progressive extinction of species in response to long-term cooling from the Middle Miocene towards the

intensification of Northern Hemisphere glaciation in the Late Pliocene.

The calibrated events have been compared with other sites in the North Atlantic and adjacent basins to evaluate their utility for correlations within the high northern latitudes. Our comparison reveals that seven datums are useful within the Nordic Seas, but only four events are suitable for supraregional correlations. This understandably results from a strong latitudinal control on the stratigraphic range of species, often through the earlier disappearance in the cold-water Iceland Sea than elsewhere.

The HOs of *B. micropapillata* and *R. actinocoronata* have been shown to represent useful bioevents for improving supraregional biostratigraphic correlations between the Nordic Seas and the various North Atlantic basins, and the HO of *L. truncatum* for supraregional correlation between the Labrador and the Nordic seas. However, only *B. micropapillata* may allows integration of North Atlantic and North Sea records. Although the HO of *H. obscura* seems useful on a supraregional scale it is of restricted use in the Iceland Sea as its HO is somewhat contradictory at the two sites located within this region. Additionally, the HOs of *U. aquaeductus*, *B. hirsuta*, and the HCO of *D. martinheadii* are good stratigraphic markers within the Nordic Seas, and this is probably also true for the LO of *C. irregulare* sp. nov. Furthermore, our comparison suggest that the HOs of *O. piaseckii*, *O. tegillatum*, *P. vesiculata*, and *C. devernaliae* may be potentially useful stratigraphic markers across the North Atlantic on a broader timescale.

Most events are clearly diachronous across the North Atlantic, showing no clear pattern of appearance or disappearance and hence presumably representing local or regional paleoenvironmental conditions. *Operculodinium*? *eirikianum* disappears earlier in the high-latitude sites than in the mid-latitudes presumably in response to progressive Pliocene cooling within the Northern Hemisphere. Overall, however, the evaluated dinocyst datums of ODP Hole 907A provide an improved, magnetostratigraphically-calibrated temporal framework for future analyses of Neogene sequences in the high and mid-northern latitudes. Our records are generated from a site critical for understanding paleoclimatic and paleoceanographic evolution, and at a time when Earth's climate finally changed from a "greenhouse" to an "icehouse" world.

Dinocyst stratigraphy shows the basal sediments of Hole 907A to be no younger than the LO of *H. tectata* (mid- to late Langhian; *c.* 14.8–13.7 Ma) and no older than the LO of *Unipontidinium aquaeductus* (mid-Langhian, around 15.1–14.8 Ma). These constraints, while tentative, more closely agree with the extrapolated magnetostratigraphic age of *c.* 14.5 Ma than with the radiometric age of 13.2 Ma for the underlying basalts. If

the underlying basalts represent oceanic crust, which is by no means certain, then Site 907 sits on Magnetic Anomaly 5A, or perhaps a younger part of Anomaly 5B.

3.6 Systematic paleontology

Division DINOFLAGELLATA (Butschli, 1885) Fensome et al., 1993
Subdivision DINOKARYOTA Fensome et al., 1993
Class DINOPHYCEAE Pascher, 1914
Subclass PERIDINIPHYCIDAE Fensome et al., 1993
Order Gonyaulacales Taylor, 1980
Suborder Gonyaulacineae (Autonym)
Family Gonyaulacaceae Lindemann, 1928
Subfamily Gonyaulacoideae (Autonym)
Genus Cerebrocysta Bujak in Bujak et al., 1980
Type: *Cerebrocysta bartonensis* Bujak in Bujak et al., 1980

Cerebrocysta irregulare sp. nov. (Plate III, 11–20)

? 1989 *Tectatodinium* sp. 4; Manum et al., pl. 20, figs 6,7.

Holotype: Sample 907A-17H-5, 138–140 cm; slide 1; England Finder reference P43/4; Plate III, 11–14.

Repository: Invertebrate Section of the Department of Palaeobiology, Royal Ontario Museum, Toronto, Ontario; catalogue number ROM 61830.

Type locality: ODP Site 907, eastern Iceland Plateau (69°14.989'N, 12°41.894'W).

Stratigraphic horizon: ODP Hole 907A, 157.2 mbsf; Serravallian (Middle Miocene), Subchron C5Ar, calibrated age 12.9 Ma.

Etymology: Latin *irregularis*, irregular, with reference to the nature of the muri that characterizes this species.

Diagnosis: A species of *Cerebrocysta* having an almost spherical, ovoidal shape; and surface ornamented with sinuous and discontinuous muri of irregular width (up to ca. 1.5 μm) that form a surface pattern varying from microrugulate to an incomplete and irregular microreticulation; with spacing between muri up to *c.* 2.0 to 3.0 μm. The archeopyle, formed by loss of plate 3", has well-defined angles.

Description: Proximate cyst with ovoidal shape that is close to spherical, occasionally with a low apical protuberance. Wall ornament consists of sinuous, discontinuous muri that form a surface pattern varying from microrugulate to an incomplete and irregular microreticulation. The muri are of irregular width that varies between *c.* 1.5 μm and < 0.2 μm, this variation occurring on the same cyst. Muri often

widen at intersections. Muri are up to about 1.5 μm high; but height varies, with narrower muri often lower than wider muri. Crests are flat-topped (especially at intersections) or taper distally. The lacunae between muri are usually up to about 2.0 μm diameter (on the holotype mostly 1.5 μm or less; occasionally reaching 3.0 μm in other specimens), and vary from rounded polygonal to rectangular. The underlying pedium is about 0.2–0.3 μm thick, and both pedium and overlying muri appear solid and continuous under light microscopy. The ornament covers the entire surface of the cyst without variation, and extends to the archeopyle margins without modification. The archeopyle is formed by loss of plate 3", and has well-defined angles. There is no other expression of tabulation.

Discussion: The holotype has a slight (0.5 μm) apical protuberance, and one specimen was found to have an unusually pronounced apical protuberance (Plate III, 16), a feature that is absent or very weakly developed in other specimens. *Tectatodinium* sp. 4 of Manum et al. (1989), from the Miocene of the Norwegian Sea, is questionably synonymised with *Cerebrocysta irregulare* on account of its similar ornament but more pronounced apical protuberance.

Cerebrocysta irregulare differs from all other validly described species of the genera *Cerebrocysta*, *Corrudinium* and *Pyxidinopsis* by its relatively small size and irregularly-shaped muri that form an incomplete and irregular microreticulate to microrugulate pattern. *Cerebrocysta 'cassinascoensis'* Zevenboom and Santarelli in Zevenboom, 1995 (unpublished manuscript name), from the Langhian through base Serravallian of Italy, is very similar to *Cerebrocysta irregulare* but differs in having a coarser microreticulation, and apparently larger overall size range of 40–50 μm (Zevenboom and Santarelli in Zevenboom, 1995), although the illustrations of this species somewhat contradict its description. Specimens reported rarely from the upper Langhian of Hungary as *Cerebrocysta 'cassinascoensis'* Zevenboom and Santarelli in Zevenboom, 1995 by Jiménez-Moreno et al. (2006) have slightly coarser ornament than *Cerebrocysta irregulare* but are of similar size (maximum diameter 37–39 μm based on three specimens; M.J.H., unpubl. data). Further research on these Mediterranean–Paratethyan morphotypes is needed to assess their relationship fully with *Cerebrocysta irregulare*.

Dimensions: Holotype: length (including ornament), 39 μm; wall thickness, ca. 1.4 μm. Range: maximum diameter (including ornament), 32 (38.4) 42 μm; wall thickness, ca. 0.9–1.8 μm. Eighteen specimens measured.

Stratigraphic occurrence: In Hole 907A, *Cerebrocysta irregulare* ranges almost

continuously from the uppermost Langhian (13.8 Ma) to lower Tortonian (10.4 Ma).

Tectatodinium sp. 4 of Manum et al. (1989), which we questionably synonymise with *Corrudinium irregulare*, ranges from the uppermost Langhian through mid-Tortonian in the Norwegian Sea.

Genus Impagidinium Stover and Evitt, 1978
Type: *Impagidinium dispertitum* (Cookson and Eisenack, 1965) Stover and Evitt, 1978

Impagidinium elongatum sp. nov. (Plate II, 6–20; Figs. 19, 20)

1989 *Impagidinium* sp. 3; Manum et al., pl. 12, figs 2–4.
? 1989 *Impagidinium* sp. 1; Manum et al., pl. 17, figs 7, 8.
? 1992 *Impagidinium* sp. 1; Anstey, text-fig. 8, pl. 5, fig. 1–3; pl. 18, fig. 1.
? 1992 *Impagidinium* sp. 2; Anstey, text-fig. 9, pl. 5, fig. 4–6; pl. 18, fig. 2.
2002 *Impagidinium* sp. 1; Louwye, fig. 5 (9, 10).

Holotype: Sample 907A-13H-6, 20–22 cm; slide 2; England Finder reference P52/2; Plate II, 6–10.
Repository: Invertebrate Section of the Department of Palaeobiology, Royal Ontario Museum, Toronto, Ontario; catalogue number ROM 61826.

Type locality: ODP Site 907, eastern Iceland Plateau (69°14.989'N, 12°41.894'W).

Stratigraphic horizon: ODP Hole 907A, 119.50 mbsf; lower Tortonian (lower Upper Miocene), Subchron C5n.2n, calibrated age 10.4 Ma.

Etymology: Late Latin *elongare*, elongate, with reference to the characteristic shape of the central body of this species.

Diagnosis: A mid-sized to large species of *Impagidinium* of variable morphology with strongly elongated central body bearing low crests, some elevated at intersections. The surface is granulate, to granulo-punctate, to nearly smooth. Plate 6" is strongly triangular, owing to a steeply descending plate 6c, and narrowly contacts plate 1'+4' (Fig. 19). Sulcal plates are usually weakly and incompletely expressed. Individual cingular plates are usually clearly demarcated, and the cingulum narrows towards boundaries between adjacent cingular plates. The development of sutural crests can be strongly reduced, especially in the equatorial and ventral areas.

Description: Proximate to proximochorate cysts with ovoidal to ovoidal–ellipsoidal central body having a length vs. equatorial diameter usually between 1.5 and 2.3 (a single exception registering 1.2). The central body wall is moderately thick (ca. 0.6–1.3 μm) and

the outer wall varies from distinctly granulate, to granulo-punctate, to nearly smooth, with thicker-walled specimens usually having more pronounced ornament. A low (up to 2.0 μm) apical protuberance may be present (Plate II, 13). Wall stratification is indistinguishable over most of the central body under LM. Low sutural crests demarcate with variable completeness a gonyaulacacean tabulation typical of the genus. Crests are developed from the outer layer of the central body wall, and usually arise steeply from the central body surface, the two layers being closely appressed distally and for most or all of the height of the crests. However, slight cavation is occasionally developed at the base of crests, particularly where they intersect. Surface of crests varies from distinctly granulate, to granulo-punctate, to nearly smooth, as for the central body; and crests occasionally have small (up to 2–3 μm) perforations, or may even be fenestrate (Plate II, 18). Distal margins of crests may be straight, smoothly undulating, to irregular and occasionally serrated, with several types of margin often present on the same cyst. Crests may be mostly of even height, but all specimens have some crests raised at intersections, particularly between adjacent precingular and postcingular plates. Crests may be lower in mid-ventral and mid-dorsal areas. Crests usually demarcate the tabulation quite fully except within the sulcus, where plates are weakly and incompletely expressed by narrow lineations. In the apical area, the boundary between 1' and 4' is usually not expressed (Fig. 19), but rarely indicated by a faint and discontinuous line.

The precingular and postcingular plates are mostly elongate. Plates 3" and *4"" are both mid-dorsally centred (Fig. 19) indicating neutral torsion. Plate 6" is strongly triangular, owing to a steeply descending plate 6c, and narrowly contacts plate 1'+4'. Plate *1"" is very narrow and located inside the sulcus, and is seldom expressed (Plate II, 16, 17). The sulcus is only slightly sigmoidal and is bordered by a non-overhanging cingulum although the strongly triangular 6" conforms to an S-type ventral organization (Fig. 19). The anterior margin of the posterior sulcal plate (ps) is usually expressed by a faint line, and the right sulcal plate may be also. The cingulum is laevorotatory and descends steeply where it approaches the sulcus from the right (plate 6c), resulting in an offset of about two widths. Both upper and lower margins of the cingulum are usually expressed on the ventral surface. Individual cingular plates are usually well demarcated, and the cingulum characteristically narrows towards boundaries between adjacent cingular plates, this being particularly evident on the dorsal surface. The archeopyle is reduced and elongated, and formed by loss of the third precingular plate.

Discussion: While the elongate central body, the tabulation, and low crests that in places slightly rise gonally are stable features, the morphology in general is very variable, and is probably a response to environmental change. In particular, specimens at the top of its range in Hole 907A, in Sample 13H-2, 142–144 cm, have extremely reduced crests in the equatorial region so that almost no tabulation can be discerned in this region (Plate II, 19–20). Samples 21H-6, 2–4 cm, 22H-2, 147–149 cm, and 22H-6, 51–53 cm, at the bottom of this species' range, also contain specimens with reduced crests. We interpret this feature as a response to unfavourable conditions, probably reduced salinity judging from other septate species (e.g. the cysts of *Gonyaulax baltica*; Ellegaard et al., 2002). A specimen illustrated by Manum et al. (1989, pl. 12, figs 2–4, as *Impagidinium* sp. 3) is intermediate between morphotypes with extremely reduced equatorial tabulation and those with normally expressed tabulation.

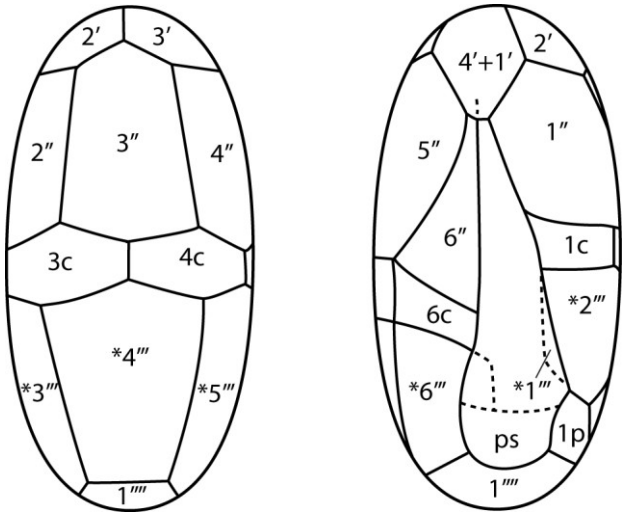

Figure 19: Generalized tabulation for *Impagidinium elongatum* sp. nov., using Kofoid labelling with homologues indicated by an asterisk. A dashed line indicates weakly and occasionally expressed plate boundaries. Dorsal (left) and ventral views are shown.

A change in the dominant morphotype occurs at around 132 mbsf (11.24 Ma), with specimens in sample 15H-1, 74–76 cm and above being on average larger, with thicker central body walls, and with more strongly ornamented surfaces (e.g. Plate II, 6–10). This morphotype ranges down to sample 16H-1, 17–19 cm. Specimens in sample 15H-2, 38–40 cm (e.g. Plate II, 11–16) and below tend to be smaller, with thinner central body walls and faintly granulate to almost smooth surfaces (see Dimensions, and Fig. 20). However, there is overlap between these morphologies, and we therefore treat them as a single species.

Dimensions: Holotype: central body length, 56 μm, central body width, 33 μm; maximum crest height, 4.5 μm, wall thickness, *c.* 1.0 μm. Range for specimens from samples 21H-6, 2–4 cm to 15H-2, 38–40 cm: central body length 39(47.7)59 μm, central body width 26(29.5)34 μm, central body length/width ratio 1.2(1.62)2.2, maximum crest height 1.5(4.1)7.0 μm, wall thickness ca. 0.6(0.8)1.2 μm; 18 specimens measured. Range for specimens from samples 15H-1, 74–76 cm to 13H-2, 142–144 cm: central body length 52(56.0)62 μm, central body width 23(30.9)37 μm, central body length/width ratio 1.5(1.83)2.3, maximum crest height 3.8(4.7)5.5 μm, wall thickness ca. 0.8(1.0)1.3 μm; 14 specimens measured. Overall range: central body length 39(51.3)62 μm, central body width 23(30.1)37 μm, central body length/width ratio 1.2(1.71)2.3, maximum crest height 1.5(4.3)7 μm, wall thickness ca. 0.6(0.9)1.3 μm; 32 specimens measured (see also Fig. 20).

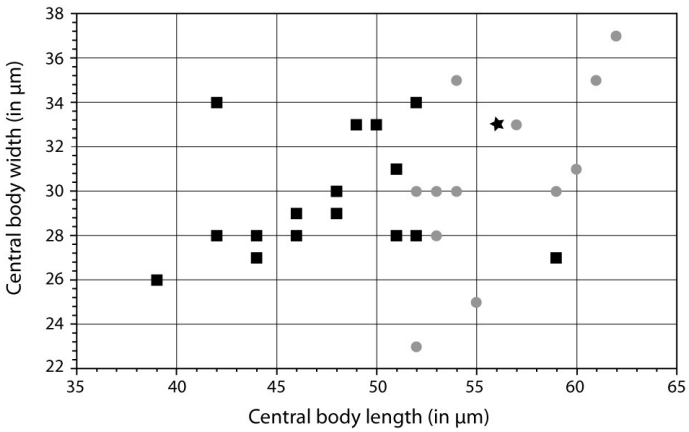

Figure 20: Central body length vs. central body width for *Impagidinium elongatum* sp. nov. Black squares = specimens from Sample 907A-21H-6, 2–4 cm to 15H-2, 38–40 cm (faintly granulate to almost smooth surfaces). Grey circles = specimens from Sample 907A-15H-1, 74–76 cm to 13H-2, 142–144 cm (strongly ornamented surfaces). Black star = holotyp.

Stratigraphic occurrence: In Hole 907A, *Impagidinium elongatum* ranges from the Langhian (14.1 Ma) through lower Tortonian (10.2 Ma); with occurrences below 12.6 Ma being sporadic, and an isolated specimen at 9.2 Ma considered reworked.

Elsewhere recorded as *Impagidinium* sp. 3 in Manum et al. (1989) from the Lower through Upper Miocene of Norwegian Sea ODP Hole 643A (Manum et al., 1989; Bleil, 1989) and Middle Miocene of Norwegian Sea ODP Hole 642C (Manum et al., 1989; Bleil, 1989). Also recorded from the lower Tortonian Deurne Sands of Belgium (as *Impagidinium* sp. 1 in Louwye (2002).

Impagidinium sp. 1 of Manum et al. (1989) from the Upper Oligocene through upper Middle Miocene of Norwegian Sea ODP Hole 643A (Manum et al., 1989; Goll in Williams and Manum, 1999) and Lower Miocene of Norwegian Sea ODP Hole 642D

(Manum et al., 1989; Bleil et al., 1989), is questionably synonymised with *Impagidinium elongatum*. *Impagidinium* sp. 1 and 2 of Anstey (1992) from the late Middle? to early Late Miocene of Baffin Bay ODP Hole 645E are probably conspecific with *Impagidinium elongatum*.

Acknowledgements

This research uses samples and data provided by DSDP and ODP and we thank Walter Hale and Alex Wülbers for technical support while sampling at the IODP Core Repository, Bremen. We are grateful to Morten Smelror who shared unpublished data, and Stijn De Schepper for comments on an earlier draft of this manuscript. Support was provided by the German Research Foundation (DFG MA 3913/2) to J.M. and M.S., and a Natural Sciences and Engineering Research Council of Canada Discovery Grant to M.J.H. Dirk Munsterman and an anonymous reviewer improved the manuscript with their constructive comments.

4. *Batiacasphaera micropapillata* – Palaeobiogeographic distribution and palaeoecological implications of a critical Neogene species complex

Michael Schreck and Jens Matthiessen

Alfred Wegener Institute for Polar and Marine Research, 27568 Bremerhaven, Germany

Accepted in The Geological Society London, Special Publications.

Abstract

The extinct dinoflagellate cyst complex *Batiacasphaera micropapillata* (comprising *B. micropapillata* and *B. minuta*) has been frequently reported from Miocene through Pliocene sediments of the North Atlantic region, but little is known about its palaeoecological affinity. To utilise it for future palaeoenvironmental interpretations, biogeographic distribution maps for middle Miocene to Pliocene time slices have been generated by using new data from ODP Hole 907A (Iceland Sea) and IODP Hole M0002A (Central Arctic Ocean) supplemented by published data.

This species complex is apparently adapted to outer-neritic to oceanic marine environments judged by its high abundance at many deep-water sites in comparison to marginal marine settings, and the co-occurrence of well-known oceanic species. The centre of distribution is located in the high-latitude North Atlantic, but it probably tolerates a broad range of mean annual sea-surface temperatures from 7–10°C to > 20°C. The relatively low concentration in the Central Arctic Ocean presumably represent an occurrence close to its ecological (thermal) limit, and suggests that it may occur in regions with possible pronounced seasonal temperature gradients and winter sea-ice. Increased nutrient availability may be a second important ecological factor under optimum living conditions.

A distinct decline in the Late Miocene of the Iceland Sea and Central Arctic Ocean and a near-synchronous disappearance in the North Atlantic region in the Pliocene suggest a strong response to the global late Cenozoic cooling. In the high northern latitudes the Late Miocene decline might have been associated with the initial formation of small-scale glaciers on Greenland and/or the expansion of winter sea ice from the Arctic Ocean into the Nordic Seas.

4.1 Introduction

Environmental parameters such as sea-surface temperature, salinity and nutrient availability determine the distribution of dinoflagellates and their resting cysts and thus also the composition of fossil dinoflagellate cyst (dinocyst) assemblages (e.g. Taylor, 1987). Although dinocyst-based reconstructions of palaeoenvironmental conditions have been proven a valuable tool in the Quaternary (e.g. Mudie et al., 2001; Matthiessen et al., 2005) they still remain inconclusive for Neogene deposits, as assemblages are often dominated by extinct species. To decipher the palaeoecological signal of extinct species different approaches such as statistical analyses (e.g. Versteegh and Zonneveld, 1994), definition of palaeoenvironmental indices (e.g. Edwards et al., 1991; Versteegh, 1994), the deduction of climatic affinities from biogeographic distributions (e.g. Masure and Vrielynck, 2009), and correlation of abundance patterns to quantitative reconstructions of sea-surface temperatures (De Schepper et al., 2011) have been applied.

In the past two decades, the extinct *B. micropapillata* and *B. minuta* have been frequently reported from Miocene through Pliocene deposits in the northern hemisphere (Appendix B), and the highest occurrence (HO) is a stratigraphically important marker on supraregional scale in the North Atlantic (3.8–3.4 Ma, De Schepper and Head, 2008; Schreck et al., chapter 3). These species may dominate Middle through Late Miocene dinocyst assemblages in the Baffin Bay and Iceland Sea, and its abundance pattern is characterised by a general long-term decrease superimposed by short-term variations of varying magnitude (Head et al., 1989a; Poulsen et al., 1996). These changes in abundance are most likely of palaeoenvironmental significance, but to date exceptionally little is known about its (palaeo)ecological preferences (Poulsen et al., 1996). The global distribution in the Neogene has not been studied yet, which obviously hampers accurate ecological interpretations. Furthermore, published records are presumably biased by the inaccurate taxonomic definition of these species.

In order to assess the palaeoecology of *B. micropapillata* and *B. minuta* (*B. micropapillata* complex hereafter, see Taxonomy), we generated a set of palaeo-biogeographic maps from new and published data for three time slices in the Neogene. These compilations are used to describe the latitudinal gradients that may allow assumptions on relative temperature affinities. Furthermore, zonal gradients in these distribution patterns may be interpreted in relation to possible salinity gradients and/or the trophic state of the environment.

4.2 Material

For this study we analyzed 120 samples from ODP Hole 907A in the Iceland Sea (69°15´ N, 12°42´ W) spanning the Middle Miocene through Pliocene on a 100 kyr temporal resolution. In addition, we examined 132 samples covering the same critical time interval in IODP Hole M0002A (87°55´ N, 139°22` E, Central Arctic Ocean). All samples were processed using standard palynological techniques (Wood et al., 1996), including acid treatment (cold HCL [10%], cold HF [38-40%]) but without oxidation or alkali treatments. Specimens have been studied with a Zeiss Axioplan 2 microscope at 63x and 100x magnification respectively in order to assess critical features of the surface ornamentation (see Taxonomy). In addition, autofluorescence has been determined with the Zeiss filter set 9 (BP 450-490, FT 510; LP 515). We calculated both relative abundance (in %, only for Hole 907A) and cyst concentration (cysts/g sediment, Stockmarr, 1977) to evaluate the observed changes in *Batiacasphaera* abundance independent from variable relative abundances of other species.

In order to derive a comprehensive picture of the spatio-temporal distribution of the *B. micropapillata* complex on a global scale, a literature review has been carried out to supplement our data. We have focused on three time slices that encompass the time interval documented in Hole 907A and M0002A, but have not considered records referring to *Batiacasphaera* spp. (or species in open nomenclature), as these not necessarily contain species of the *B. micropapillata* complex. Sites used to generate the biogeographic distribution maps are given in Appendix B. The descriptive terms rare, common, and abundant are used throughout the text, as quantitative data is seldom available.

4.3 Taxonomy

The genus *Batiacasphaera* was erected by Drugg (1970) for proximate cysts with various ornamentation and an apical archeopyle. Besides *B. micropapillata*, *B. minuta* and *B. sphaerica*, which have closely related morphologies, another five species occur in Miocene and Pliocene deposits (Table 1), but these may easily be distinguishable from the former three species. *Batiacasphaera micropapillata* and *B. sphaerica* were described from Middle Oligocene, and Lower Miocene deposits of the Blake Plateau, offshore North Carolina, respectively (Stover, 1977). Both species are characterized by variations in surface ornamentation ranging from finely papillate, finely granulate to microreticulate for *B. micropapillata*, and granulate to punctoreticulate or combination thereof for *B. sphaerica*; and they only differ in that *B. sphaerica* being more coarsely ornamented, having a

generally thicker autophragm and thus maintaining its spherical to subspherical shape (Stover, 1977). However, the holotype of *B. micropapillata* is micropapillate (Edwards, written commun. in Matsuoka and Head, 1992). De Verteuil and Norris (1996) observed microreticulate luxuriae based on light microscopy on *B. sphaerica*, which is in contrast to their illustration (pl. 1, fig. 3-4), and micropunctate to pseudoreticulate luxuriae based on scanning electron microscopy (pl. 11, fig. 4,5,7,8) but stated that "this difference in wall ultrastructure can be perceived, but not resolved, in transmitted light" (de Verteuil and Norris, 1996, p. 78).

B. baculata	Drugg 1970
B. cooperi	Hannah et al. 1998
B. deheinzelinii	Louwye 1999
B. gemmata	Head et al. 1989
B. hirsuta	Stover 1977
B. micropapillata	Stover 1977
B. minuta	(Matsuoka 1983) Matsuoka and Head 1992
B. sphaerica	Stover 1977

Table 2: Compilation of Miocene and Pliocene *Batiacasphaera* species.

The taxonomy is further complicated because re-examination of the holotype of *Batiacasphaera minuta* revealed a microreticulate ornamentation and an apical archeopyle (Matsuoka and Head, 1992). This species was first described from Middle Miocene sediments of central Japan as *Tectatodinium minutum* (Matsuoka, 1983) having a granular periphragm and a precingular archeopyle. Matsuoka and Head (1992, p. 168) already stated that "the somewhat subtle differences that separate *B. minuta*, *B. micropapillata*, and *B. sphaerica* present a need for careful documentation of fine surface ornament among specimens of this species complex by means of light microscopy ideally supplemented by SEM".

In consequence, restudy of specimens resulted in identification of *B. minuta* in the *B. micropapillata* complex of Head et al., 1989a (Lower through ?Upper Miocene of ODP Site 645, Baffin Bay) and in the *Batiacasphaera*/*Cerebrocysta* group A of Head et al. 1989b (Upper Miocene of ODP Site 646, Labrador Sea) (see Matsuoka and Head, 1992), but also in the reassignment based on illustrations; for example *B. sphaerica* figured from the Pliocene of ODP Site 646 (de Vernal and Mudie, 1989) has been transferred to *B. minuta* by Head (1997).

These taxonomic uncertainties prohibit a consistent assignment of specimens to a particular species and may cause lumping of species, which inevitably complicates the accurate definition of the stratigraphic range of the species. The existing conceptual overlap in the definition of these species requires a careful revision, including holotype and paratype material of all three species.

An additional factor obscuring the (upper) stratigraphic range of this species complex became evident during the DINO9 Conference taxonomic workshop in Liverpool 2011. Species of the genus *Pyxidinopsis* (e.g. *P. pastilliformis*, *P. braboi*) and *Cerebrocysta* are overall similar to species of *Batiacasphaera* with respect to surface ornamentation and thus are often difficult to differentiate if archeopyle style cannot be determined with certainty due to crumpling of cysts (see also Matsuoka and Head, 1992).

Specimens in Hole 907A have a range of microreticulate, vermiculoreticulate–vermiculate and rugulate ornamentation that go far beyond *B. minuta* sensu stricto (Plate V). In Hole M0002A, specimens also show a variety of microreticulate, pseudoreticulate to microrugulate surface ornamentation and transitions between different ornaments. Although papillate forms were only seen rarely at both sites, we refer all specimens to the *B. micropapillata* complex, as *B. minuta* must be considered a taxonomic junior synonym if the broad circumscription of *B. micropapillata* is accepted (Head in Head and Wrenn, 1992, p. 3). The term complex is used in order to integrate the various ornamentations observed, and we do not differentiate between both species in Neogene literature as the *B. minuta* morphology will almost certainly also have been recorded as *B. micropapillata*. However, we acknowledge that microreticulate specimens assignable to *B. minuta* sensu strictu form the stratigraphic useful HO in Hole 907A (Schreck et al., chapter 3). *Batiacasphaera sphaerica* is not considered part of the species complex as the described granulate to punctate to punctoreticulate ornamentation does not overlap with *B. micropapillata* and *B. minuta*. Moreover, it reveals only rare occurrences at most sites considered here and therefore its paleobiogeographic distribution is not discussed below.

4.4 The *Batiacasphaera* record in ODP Hole 907A and IODP Hole M0002A

The *Batiacasphaera micropapillata* complex is predominant in the Middle through Late Miocene sequence of Hole 907A, partly contributing more than 50% to the dinocyst assemblage (Fig. 21). Its abundance pattern is characterised by short-term recurrent changes of varying magnitude superimposed on a long-term change shown by the upward decrease, which is mirrored in cyst concentration and thus excludes a decline in

this species complex due to relative increase of other species. It is conspicuously abundant from ~ 14 Ma (upper Langhian) until its highest persistent occurrence (HPO) at ~ 8.2 Ma (upper Tortonian). The most obvious change occurs subsequent to an enigmatic interval virtually barren of palynomorphs, after which concentrations of the *B. micropapillata* complex decrease and it is replaced by *Nematosphaeropsis labyrinthus* as dominant species (M.S. unpubl. data). However, it ranges almost continuously to ~ 4.5 Ma (mid-Zanclean), where a highest common occurrence (HCO) can be defined, but occurs sporadically until its HO at ~ 3.4 Ma (lower Piacenzian).

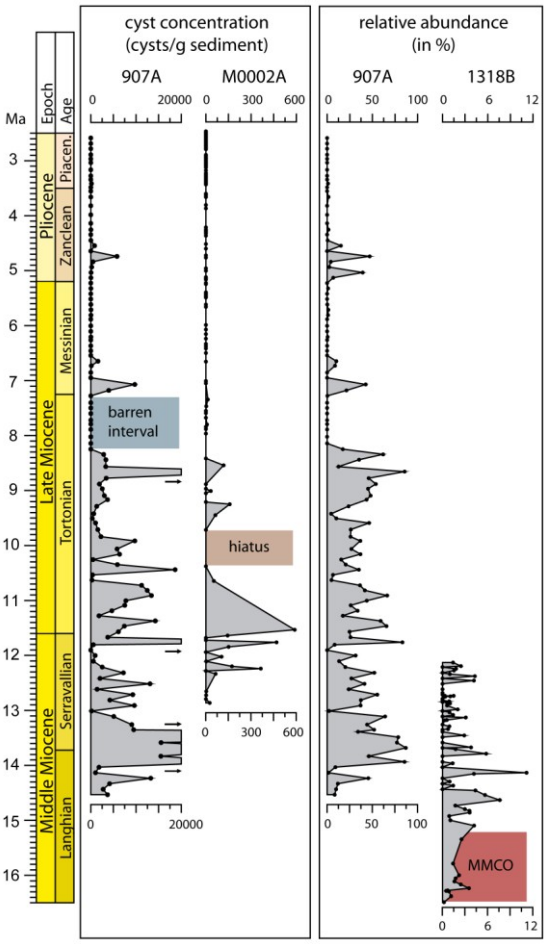

Figure 21: Relative abundance (%) of *B. micropapillata* complex in ODP Hole 907A, and IODP Hole U1318B; and absolute concentrations (cysts/g sediment) in ODP Hole 907A, and IODP Hole M0002A. Red shaded area = middle Miocene climate optimum (MMCO). Grey shade area = barren interval in Hole 907A. Brown shaded area = possible hiatus in Hole M0002A.

In Hole M0002A the *B. micropapillata* complex shows a comparable variability in concentrations (Fig. 21) and dominates dinocyst assemblages in the upper Serravallian and Tortonian, and a HO has been recorded at ~ 7 Ma according to the age model of Frank et al. (2008). Although cyst concentrations are generally less by two orders of

magnitude when compared with Hole 907A, both records show a pronounced decline in the Late Miocene indicating that ecological conditions have deteriorated almost coeval in both regions.

4.5 Palaeobiogeographic distribution and its interpretation

This complex has a widespread distribution during the Middle to Late Miocene but the distribution pattern shows a clear center in the Atlantic sector of the northern hemisphere to where it is apparently restricted in the Pliocene (Fig. 22).

The only southern hemisphere records are from Middle Miocene deposits of eastern Indian Ocean ODP Site 765, where McMinn (1992) recorded a few isolated specimens of *B. micropapillata* until close to the Middle/Upper Miocene boundary, and from Middle through Upper Miocene deposits of the Colorado Basin off Argentina (Guerstein and Junicel, 2001; Guler and Guerstein, 2003) where it is never abundant (V. Guler, pers. comm. 2012). Macphail and Truswell (2004) reported specimens similar to *B. minuta* (as *Batiacasphaera* sp. A) from undifferentiated Middle Miocene deposits of southern high latitudes ODP Site 1165 (Prydz Bay, Antarctica), but an unequivocal assignment based on their illustrations is not possible. Thus this species complex is possibly absent from the southern hemisphere in the Pliocene and there are no unambiguous Neogene low latitude records from both hemispheres as all other records pertain to *Batiacasphaera* spp. not necessarily comprising species of the *B. micropapillata* complex, although it may be included (Appendix B). Zegarra and Helenes (2011) reported only low concentrations of *B. minuta* and related morphotypes in the Eastern Equatorial Pacific, but photomicrographs provided by M. Zegarra (pers. comm. 2012) suggest that the figured specimens are not the morphotypes that we assigned to the *B. micropapillata* complex. Therefore this record has not been included in our compilation.

In the North Pacific, the species complex is rare in shallow-water ?Lower through Upper Miocene deposits of central Japan (as *Tectatodinium minutum* in Matsuoka 1983; Matsuoka et al., 1987), just like in the central and eastern Bering Sea (as *Tectatodinium minutum* in Matsuoka and Bujak, 1988). By contrast, Kurita and Obuse (2003) reported common to abundant *B. minuta* from the lower Middle to lower Upper Miocene of ODP Site 1151 (~ 2500 m water depth) off the northeast coast of Japan. This species complex is apparently absent from the Pacific Ocean in the Pliocene.

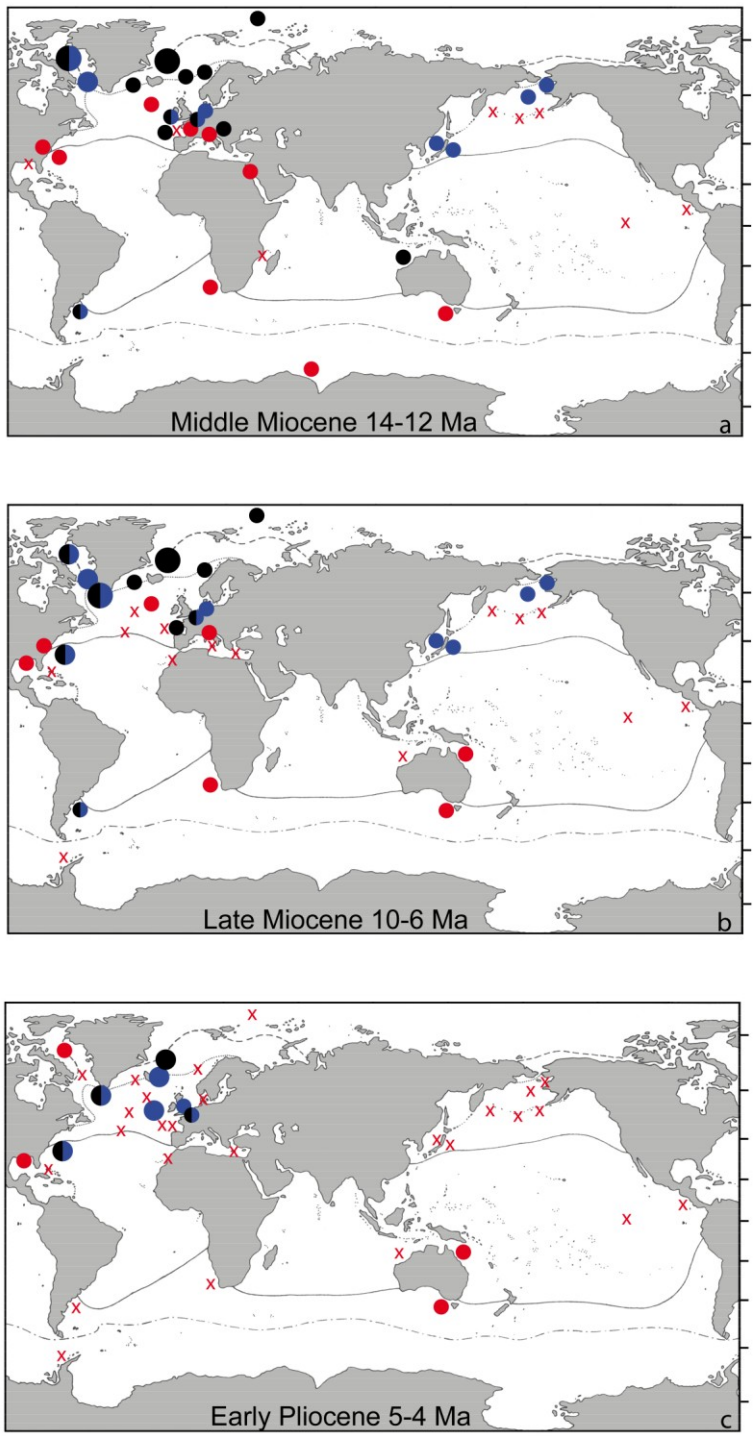

Figure 22: Palaeobiogeographic distribution of *B. minuta* (blue dots) and *B. micropapillata* (black dots) during a) Middle Miocene, b) Late Miocene, and c) Early Pliocene. Red dots indicate records of other *Batiacasphaera* species, and x indicates the absence of *Batiacasphaera* species. Abundance: • = rare, ● = common, ⬤ = abundant.

All other records are confined to the Central Arctic Ocean, the mid- to high-latitude North Atlantic, and the North Sea Basin (Fig. 22). It has been regularly reported from Miocene and Pliocene deposits at several North Sea sites (Appendix B), but is only rare

in most sites (< 5%). Likewise low percentages have been reported from the relatively shallow (409 m water depth) IODP Site U1318 in the Porcupine Basin (Louwye et al., 2008). It reaches highest abundances in the high-latitude North Atlantic, particularly at deep-water sites e.g. Baffin Bay ODP Site 645 (Head et al., 1989b), Labrador Sea ODP Site 646 (de Vernal and Mudie, 1989; Head et al., 1989c), Davis Strait (Qulleq-1 well, Piasecki, 2003), and Iceland Sea (Poulsen et al. 1996; this study), but is also common within the Central Arctic Ocean (this study), and rare to common in Vøring Plateau ODP Site 643 (Manum et al., 1989).

The high abundance in the oceanic environments of the Central Arctic Ocean, Baffin Bay, Labrador Sea, Iceland Sea, and off northeast Japan, and its generally rare occurrence in the shallow-water Porcupine Basin Site U1318, the North Sea and central Japan suggest a preference for oceanic to outer-neritic conditions. This is supported by the co-occurrence of the generally outer-neritic to oceanic genera *Impagidinium* spp. and *Nematosphaeropsis* spp. (Marret and Zonneveld, 2003) at most of these sites. Furthermore, its high abundance in these oceanic environments in contrast to the North Sea which was a semi-enclosed basin during most of the Neogene (Rasmussen et al., 2008) indicates an affinity for somewhat higher salinities.

The occurrence not only during the comparatively warm Middle Miocene Climate Optimum (MMCO, 17–15 Ma, Zachos et al., 2008), but also during the considerably cooler Late Miocene through Early Pliocene indicates a tolerance for a broad range of temperatures. Numerical mean annual sea surface temperature (SST) estimates based on alkenone data from Hole 907A (Schreck et al., chapter 5) allow to roughly define the temperature range from > 20°C to ~ 7°C. The cyst concentration clearly show a centre of distribution at Hole 907A in the Iceland Sea, whereas those in IODP Hole M0002A are less by up to two orders of magnitude (Fig. 21) probably representing an occurrence at the lower end of its temperature range. In the Arctic Ocean, a perennial (Darby, 2008) or at least a seasonal (St. John, 2008) sea ice cover might have been present throughout the Neogene, and presumably had an adverse effect on the living conditions as well. Early Miocene alkenone SSTs where around 10–15°C (Weller and Stein, 2008), which are somewhat comparable to the lower temperature limit at Hole 907A. If the global Middle Miocene temperature decrease (Zachos et al., 2008) has also been recorded in the Arctic Ocean then SSTs during the Late Miocene occurrence of the *B. micropapillata* complex might have been even lower, presumably causing the low concentration in the Late Miocene and the disappearance at ~ 7 Ma at

Hole M0002A. The significant decrease in the Late Miocene in Hole 907A is associated with a SST drop below 10°C and co-occurs with first significant ice-rafted debris (IRD) pulses (Fronval and Jansen, 1996), suggesting that this species complex may sustain some sea-ice cover associated with SSTs around 7°C.

Although the species complex is apparently not adapted to cold waters, the available data suggest that it may occur at temperatures as low as 7–10°C associated with (seasonal) sea ice that is in the range of modern SSTs in the northeast Atlantic Ocean and Norwegian Sea, but sea ice is absent from these regions today. The upper temperature limit is difficult to estimate because the MMCO is not recorded in Hole 907A, but occurrence in Site U1318 suggest adaptation even to warmer SSTs during the MMCO (Fig. 21). The possible absence at low latitudes might be caused by too high SSTs, but might also reflect adaptation to the prevailing light regimes in the mid- to high latitudes. Therefore, the *B. micropapillata* complex may be considered cool- to warm-temperate, but additional taxonomic studies of low latitude records are required to prove this hypothesis.

In Hole 907A, the remarkable abundance of this species complex during most of the Middle to middle Late Miocene seems to be related to enhanced nutrient availability as suggested by total diatom abundance and *Chaetoceros* resting spore frequency (Stabell and Koç, 1996), but also by palynomorph concentrations (Schreck et al., chapter 5). In turn, a low nutrient supply might have caused the low abundance/absence of this complex at sites that probably had comparable temperatures as Hole 907A. However, autofluorescence of these cysts (cf Brenner and Biebow, 2001) precludes an exclusive heterotrophic affinity. Moreover, Middle to Late Miocene dinocyst assemblages are highly diverse at Hole 907A with more than 30 taxa recovered routinely, thus excluding a lack of intra-species competition as another cause for the high abundance of the *B. micropapillata* complex in the Iceland Sea.

Few quantitative data are available to decipher the long-term evolution of this species complex during the Neogene climate deterioration that occurred after the MMCO. Despite the cyst concentration being less by two orders of magnitude at Hole M0002A than at Hole 907A, distinct similarities in the long-term pattern can be observed, which are independent from variable relative abundances of other species, and differences in assemblage composition. Noteworthy, cyst concentrations decrease drastically at both sites in the middle Late Miocene (Fig. 21), and *Nematosphaeropsis* replaced the *B. micropapillata* complex as the dominant species at both sites (MS and JM

unpubl. data). The similar timing of this decrease at both environmentally different sites suggest a strong response of the *B. micropapillata* complex to global climate perturbations related to the Late Miocene growth of ice-sheets and sea-ice in the northern hemisphere as recorded by IRD-events at several North Atlantic sites (see Thiede et al., 2011 for review), and changes in ocean circulation (e.g Butzin et al., 2011). Semi-quantitative data from other sites (e.g. Head et al., 1989a, b; Louwye and Laga, 1998; Louwye et al., 2007) reflect these changes by generally higher abundances in the Middle to Upper Miocene, and only common to rare occurrences in the Lower Pliocene. A response of this species complex to global Late Miocene cooling is also suggested by its possible absence from Pliocene deposits of the North Pacific and the southern hemisphere.

Notwithstanding the above, we acknowledge that the global distribution pattern may be biased due to the few southern hemisphere dinocyst studies available, but also due to the paucity of continuous Miocene through Pliocene sediment sequences in general, and the frequent record of *Batiacasphaera* spp. in literature.

4.6 Conclusions

New quantitative data from ODP Hole 907A and IODP Hole M0002A have been combined with an literature review on the palaeobiogeographic distribution of the stratigraphically important Neogene dinocyst complex *Batiacasphaera micropapillata* (HO 3.8–3.4 Ma; De Schepper and Head, 2008; Schreck et al., chapter 3) in order to decipher its palaeoecological affinities. This compilation revealed a pronounced emphasis towards the northern hemisphere, but shows a clear latitudinal gradient with focus on the high-latitude North Atlantic, where it reaches highest abundances. In contrast, it is rare in the Middle to Late Miocene of the southern hemisphere and even absent in the Pliocene. Cyst concentrations suggest a preferred habitat for the *B. micropapillata* complex within the Iceland Sea where it occurs in a broad range of temperatures from 7–10°C to > 20°C. The record in the Central Arctic Ocean probably present an occurrence close to the lower limit of thermal requirements, whereas an upper temperature limit likely accounts for the absence in the low latitudes. With reference to its wide distribution but high abundance in the subarctic North Atlantic, we consider it a warm- to cool-temperate species that is apparently well adapted to the prevailing light regime in the high latitudes. A significant zonal gradient from neritic to oceanic environments, with higher abundance in the latter is evident when comparing the North Atlantic deep-water sites with the comparatively shallow-water Porcupine Basin, North Sea, and central Japan

sites, and suggest an affinity for outer-neritic to oceanic conditions and somewhat higher salinities. It occurs continuously from the comparatively warm Middle Miocene through cooler Late Miocene until the Early/Late Pliocene boundary in Hole 907A, but exhibits a gradual long-term decrease in abundance throughout this time interval. The general Late Miocene decline and its disappearance in the Pliocene are likely related to late Cenozoic cooling, and may be associated with the formation of sea-ice in the high northern latitudes. However, sea-ice cover is apparently a restricting but not excluding factor.

Ultimately, we propose *B. micropapillata*, *B. minuta* and *B. sphaerica* to be restudied by means of detailed LM and SEM work on the holotype and paratype material due to the taxonomic uncertainties and conceptual overlap that exists between these species.

Acknowledgements

This research uses samples provided by ODP and IODP, and M.S. and J.M. are grateful to the German Research Foundation for financial support (DFG MA 3913/2). We acknowledge S. De Schepper and an anonymous reviewer for constructive comments improving this manuscript.

5. Response of marine palynomorphs to Neogene climate cooling in the Iceland Sea (ODP Hole 907A)

Michael Schreck, Marie Meheust, Ruediger Stein and Jens Matthiessen

Alfred Wegener Institute for Polar and Marine Research, 27568 Bremerhaven, Germany

Submitted to Marine Micropaleontology.

Abstract

The present study on ODP Leg 151 Hole 907A combines a detailed analysis of marine palynomorphs (dinoflagellate cysts, prasinophytes, acritarchs) and a low-resolution alkenone-based sea surface temperature (SST) record for the interval between 14.5 and 2.5 Ma, and allows to investigate the relationship between palynomorph assemblages and the paleoenvironmental evolution of the Iceland Sea.

A high marine productivity is indicated in the Middle Miocene, and palynomorphs and SSTs both mirror the subsequent long-term Neogene climate deterioration while the diverse Middle Miocene palynomorph assemblages clearly diminish towards the impoverished assemblages of the Late Pliocene; parallel with a somewhat gradual decrease of SSTs being as high as 20°C at ~ 13.5 Ma to around 8°C by ~ 3 Ma.

Superimposed, palynomorph assemblages not only reflect Middle to Late Miocene climate variability partly coinciding with the short-lived global Miocene isotope events, but also the initiation of a proto-thermohaline circulation across the Middle Miocene Climate Transition, which led to increased meridionality in the Nordic Seas. Three extinction events were observed within the Late Miocene to Early Pliocene and are ascribed to the progressive strengthening and freshening of the proto-East Greenland Current towards modern conditions. A significant high latitude cooling between 6.5 and 6 Ma is depicted by the supraregional "*Decahedrella* event", lowest Miocene productivity, and a SST decline of ~ 5°C.

In the Early Pliocene, a transient warming is accompanied by surface water stratification and increased productivity that likely reflects a high latitude response to the global biogenic bloom. The succeeding crash in palynomorph productivity, and a subsequent interval virtually barren of marine palynomorphs may indicate enhanced

bottom water oxygenation and substantial sea-ice cover, and suggests that conditions seriously affecting marine productivity in the Iceland Sea have already been established well before the marked expansion of the Greenland ice sheet at 3.3 Ma.

5.1 Introduction

The Neogene is a crucial epoch for the evolution of Earth's climate as it went through the fundamental transition from a relatively warm Early Miocene to the colder conditions at the end of the Pliocene (Zachos et al., 2008). After the Miocene Climate Optimum (MCO, 17–15 Ma), when Earth experienced warmest temperatures since the Middle Eocene (Zachos et al., 2008), global surface and deep ocean temperatures cooled significantly (Wright et al., 1992; Billups and Schrag, 2002; Shevenell et al., 2004; Kuhnert et al., 2009) across the Middle Miocene Climate Transition (MMCT, 14.2–13.7 Ma), and the East Antarctic Ice Sheet experienced major expansion (e.g. Flower and Kenneth, 1994; John et al., 2011; Passchier et al., 2011). This transition marked the onset of progressive long-term cooling both on land (Pound et al., 2012) and in the sea (Zachos et al., 2008) that ultimately pushed the climate system into the bipolar glaciated mode of today. Superimposed, distinct short-term climate variability has been observed in marine records (Miller et al., 1991; Turco et al., 2001; Anderson and Jansen, 2003; Westerhold et al., 2005; John et al., 2011) and partly attributed to ice sheet growth on Antarctica and/or bottom-water cooling (Mi events sensu Miller et al., 1991). Notwithstanding, the high northern latitude oceans are of eminent relevance to decipher causes and consequences of the Neogene climate variability (e.g. Thiede et al. 1998) since they influence global climate through feedback mechanisms related to the formation of perennial/seasonal sea-ice cover (Miller et al., 2010b; Serreze and Barry, 2011), and production of northern-sourced deep-water (Flower and Kenneth, 1994; Rahmstorf, 2006).

The timing of the onset of glaciations in the northern hemisphere is still debated but ice-rafted debris (IRD) has been recorded as early as the Middle Eocene in the Arctic Ocean (Stickley et al., 2009) and the Greenland Sea (Eldrett et al., 2007; Tripati et al., 2008). Although it has been speculated that an Neogene Greenland ice sheet has existed since at least 18 Ma (Thiede et al., 2011), published records suggest that small scale glaciations large enough to reach sea-level might have occurred on Greenland not before the early to middle Late Miocene (Schaeffer and Spiegler, 1986; Wolf and Thiede, 1991; Fronval and Jansen, 1996; Wolf-Welling et al., 1996; Helland and Holmes, 1997; Winkler et al., 2002). In contrast, ice sheets probably developed in the northern Barents Sea and

on Scandinavia already in the Middle Miocene (Fronval and Jansen, 1996; Knies and Gaina, 2008).

The formation of glacial ice on the circum-arctic continents might have been linked to the fundamental reorganisation of the circulation in the Nordic Seas. The opening of Fram Strait and the subsidence of the Greenland-Scotland Ridge (GSR) have led to an enhanced exchange of water masses between the Arctic Ocean and the North Atlantic via the Nordic Seas (Bohrmann et al., 1990; Poore et al., 2006; Jakobsson et al., 2007; Knies and Gaina, 2008). Jakobsson et al. (2007) assumed that Fram Strait reached sufficient width (40–50km; present-day width 400km) to efficiently ventilate the Arctic Ocean at ~ 17.5 Ma, and began to open at greater depth by ~ 14 Ma, which is supported by benthic foraminiferal evidence from the Lomonosov Ridge and Fram Strait (Kaminski et al., 2006; Kaminski, 2007). Simultaneously, a prominent shift from biosiliceous to calcareous-rich sediments in the Norwegian Sea (Bohrmann et al., 1990; Cortese et al., 2004) was likely coupled to the subsidence of the Greenland-Scotland Ridge (GSR), which consequently modulated exchange of North Atlantic and Arctic water masses. Reduced fluxes in Northern Component Water (NCW) have been correlated with uplifts of the GSR and vice versa (Wright and Miller, 1996; Poore et al., 2006; Abelson et al., 2008), and Bohrmann et al. (1990) related periodic changes in biogenic carbonate and opal accumulation in the Norwegian Sea to variable exchange of surface waters between the Nordic Seas and the North Atlantic. The initiation of an proto-East Greenland Current may coincide with the establishment of modern-like ice drift pattern through Fram Strait (Knies and Gaina, 2008), but Wei et al. (1998) suggest an onset around 12 Ma based on calcareous nannofossils from the Irminger Basin whereas Wolf-Welling et al. (1996) set this event at around 10.5 Ma based on changes in bulk accumulation rates in the Fram Strait. The modern EGC was probably first established during the intensification of Northern hemisphere glaciations with the thermal isolation of Greenland due to the final closure of the Isthmus of Panama and the opening of Bering Strait at the Pliocene-Quaternary transition (Sarnthein et al., 2009).

However, to date most information are derived from a few Neogene sections located along the path of the inflowing North Atlantic waters in the Norwegian Sea (Fig. 23) while the Neogene paleoceanography of the Greenland and Iceland seas is almost unknown due to the discontinuous occurrence of calcareous microfossils in these sediments (e.g. Fronval and Jansen, 1996). Here we present a comparatively high-resolution record of organic-walled microfossils (e.g. dinoflagellate cysts, prasinophytes,

acritarchs) from the almost continuous middle Miocene to upper Pliocene sequence of ODP Hole 907A in the Iceland Sea, an area close to the growing Greenland and Iceland ice sheets, which experienced the effects of sea-ice cover, migrating wind fronts and ocean currents. The pristine paleomagnetic record of Hole 907A provides the unique opportunity for detailed investigations on the response of palynomorph assemblages to the MMCT and subsequent long-term cooling, and thus to derive complementary information on the Neogene of the Nordic Seas cold-water domain. Palynomorph-based interpretations have been supplemented with a low-resolution alkenone SST record that provides new constrains on its thermal evolution.

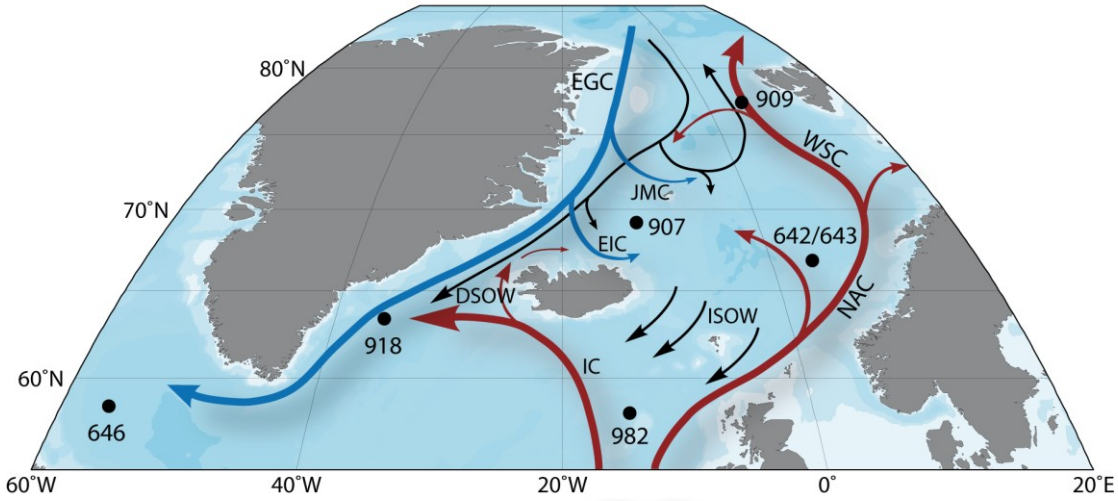

Figure 23: Schematic representation of the present day ocean circulation in the Nordic Seas, and location of ODP Leg 151 Site 907, as well as sites discussed in the text (black dots). Blue arrows refer to Arctic Ocean derived cold surface waters: EGC = East Greenland Current, JMC = Jan Mayen Current, EIC = East Iceland Current. Red arrows indicate Atlantic Ocean derived warm surface water: WSC = West Spitzbergen Current, NAC = Norwegian Atlantic Current, IC = Irminger Current. Black arrows show pathways of deep/bottom water: DSOW = Denmark Strait Overflow Water; ISOW = Iceland Scotland Overflow Water (modified from Blindheim and Østerhus, 2005).

5.2 Material and Methods

ODP Hole 907A is located on the eastern Iceland Plateau (69°14.989´ N, 12°41.894´ W; 2035.7 m water depth; Fig. 23), and was drilled in an undisturbed hemipelagic sequence that mainly consists of unlithified silty clays and clayey silts (Shipboard Scientific Party, 1995). Based on the revised magnetostratigraphy (Channell et al., 1999), which has been adjusted to the latest astronomically-tuned Neogene timescale (ATNTS 2004, Lourens et al., 2005), a total of 120 samples spanning the Pliocene to early Middle Miocene (Samples 6H-3, 82-84 cm to 23H-CC, 10–12 cm), has been selected at ~ 100 kyr resolution. The

stratigraphic occurrence of a selected number of dinocyst and acritarch species has been discussed by Schreck et al. (chapter 3).

5.2.1 Palynological methods

Subsamples (~ 15 cm^3) were processed using standard palynological techniques (e.g. Wood et al., 1996), including acid treatment (HCl [10%], HF [38-40%]), but without oxidation or alkali treatments. 2 *Lycopodium clavatum* tablets (Batch no. 124961, X = 12542, s = ± 416 per tablet) were added to each sample during the HCl treatment to calculate palynomorph concentrations (Stockmarr, 1977). The residue was sieved over a 6 µm polyester mesh to ensure that small palynomorphs (< 15µm) would be retained, and mounted with glycerine jelly on microscope slides.

Generally, marine palynomorphs have been counted until a minimum of 350 (Ø = 272) dinoflagellate cysts (dinocysts) had been enumerated. At least one slide was completely scanned for rare taxa not encountered during regular counts. All counts and scans were conducted on a Zeiss Axioplan 2 microscope at 63x and 20x magnification, respectively. Autofluorescence has been determined by epifluorescence microscopy using a Zeiss Axiophot microscope equipped with the Zeiss filter set 9 (BP 450-490, FT 510; LP 515).

The dinocyst nomenclature follows Fensome and Williams (2004 and references therein) and Schreck et al. (chapter 3), and acritarch and prasinophyte nomenclature follows Head et al. (1989a), Manum (1997), Head (2003), and De Schepper and Head (2008).

The Shannon-Wiener index was calculated for the dinocysts assemblage as a statistical measure of diversity as

$$H' = \sum_{i=1}^{s} (p_i)(\log_2 p_i)$$

with s = number of species, and p_i = proportion of total sample belonging to *i*th species. As a more simple measure for diversity, we present species richness, which equals the number of dinocyst taxa recorded in a sample. The Shannon-Wiener Index is based on information theory and independent of sample size, and tries to measure the amount of order (or disorder) contained in a system (Krebs, 1998). Therefore, this index also provides information on the heterogeneity of an assemblage. As the total number of species is known by species richness, the observed differences between both diversity measures are partly on account of relative shifts within the dinocyst assemblage.

5.2.2 Organic geochemical methods

Sedimentary total organic carbon (TOC) contents were determined for all 120 samples by means of a carbon-sulfur determinator (CS-125, Leco) after the removal of carbonates by adding hydrochloric acid. Total carbon and nitrogen contents were measured by a CNS analyser (Elementar III, Vario) and used to calculate C/N ratios.

For an initial study on alkenones, a subset of 10 samples has been selected (Table 3). The freeze-dried and homogenised sediments (2 to 4g) were extracted with an Accelerated Solvent Extractor (DIONEX, ASE 200; 100°C, 1600 psi, 15min) using dichloromethane and methanol (99:1, v/v) as solvent. The neutral fraction was dissolved in hexane. The separation of compounds was carried out by open column chromatography (SiO_2) using *n*-hexane and dichloromethane (1:1, v/v), and dichloromethane. The composition of alkenones was analysed with a Hewlett Packard gas chromatograph (HP 6890, column 60 m x 0.32 mm; film thickness 0.25 μm; liquid phase: DB1-MS) using a temperature program as follows: 60°C (3 min.), 150°C (rate: 20°C/min.), 320°C (rate: 6°C/min.), 320°C (40 min. isothermal). For splitless injection a cold injection system (CIS) was used (60 °C [6 s], 340°C [rate: 12°C/s], 340°C [1 min. isothermal]). Helium was used as carrier gas (1.2 ml/min.). Individual alkenone ($C_{37:3}$, $C_{37:2}$) identification is based on retention time and the comparison with an external standard, which was also used for controlling the instrument stability.

Core, section, interval (cm)	Depth (mbsf)	Age (Ma)	UK'37	SST (°C)
7H-4, 102-104	60.32	3.16	0.325	8.5
9H-2, 90-92	76.20	4.74	0.436	11.9
10H-3, 90-92	87.20	5.80	0.278	7.1
11H-3, 117.5-119.5	96.98	6.85	0.443	12.1
11H6, 77-79	101.07	7.72	0.550	15.3
12H4, 111.5-113.5	107.92	9.17	0.545	15.2
13H6, 20-22	119.50	10.44	0.643	18.1
16H3, 42.5-44.5	143.72	12.21	0.500	13.8
19H1, 34-36	169.14	13.39	0.718	20.4
23H6, 97.5-99.5	215.27	14.33	-	-

Table 3: Alkenone results from Hole 907A.

The alkenone unsaturation index Uk'_{37} and hence the mean annual sea-surface temperature (SST in °C) was calculated as $Uk'_{37} = 0.033T + 0.044$ according to Müller et al. (1998). The Uk_{37} index may be more appropriate in the present-day Nordic Seas (Bendle and Rosell-Melé, 2004) but could not be calculated due to low abundance of tetra-unsaturated alkenones.

5.2.3 Reliability of the Uk'_{37} index in the Neogene

In recent sediments alkenones are mainly produced by the ubiquitous coccolithophorid *Emiliania huxleyi* (e.g. Volkman et al., 1995), a haptophyte that first appeared in the late Quaternary about 268 kyr ago (Thierstein et al., 1977). In pre-Quaternary sediments long-chain alkenones are attributed to the morphologically related genera of the family Gephyrocapsaceae (Marlowe et al., 1990). Previous studies have shown that these species can be used for Uk'_{37} and global core-top calibration without significant differences in SST dependence to *E. huxleyi* (e.g. Villanueva et al., 2002; McClymont et al., 2005). SST records for the Pliocene (Lawrence et al., 2009, 2010; Naafs et al., 2010), Miocene (Herbert and Schuffert, 1998; Mercer and Zhao, 2004; Huang et al., 2007; Rommerskirchen et al., 2011), and lowermost Miocene and Eocene (Weller and Stein, 2008) demonstrate the capability to obtain reliable temperature estimates on pre-Quaternary time scales.

The input of allochthonous alkenones seems to be of some importance in the modern Nordic Seas (Bendle et al., 2005). However, coccolithophorids, dinoflagellates and prasinophytes are flagellates sharing the same habitat and thus biotic and abiotic processes should affect the communities in the same way. As reworking of dinocysts is very low (< 1%) the input of allochthonous alkenones should be restricted and likely not significantly affect our SST estimates. Furthermore, post-depositional processes may affect the preservation of organic matter and alkenones (e.g. Rommerskirchen et al., 2011), with oxygen as one of the most destructive agents (Zonneveld et al., 2010a). Since dinocysts, which are sensitive to oxygenic degradation (Zonneveld et al., 2008), exhibit high concentration throughout most of the sequence, this effect is assumed to have a minor influence on the record.

On global scale, Uk'_{37} shows the best statistical relationship to mean annual SST, as the production of alkenones is not limited to summer in most regions (Müller et al., 1998). In the Nordic Seas, however, coccolithophorid production today is considerably higher during summer than in the "non-production" period from autumn to early summer (e.g. Samtleben et al., 1995; Andruleit, 1997; Schröder-Ritzrau et al., 2001). These seasonal fluctuations in alkenone production may cause a shift towards a summer bias in temperature (Conte et al., 2006). We also acknowledge that alkenone production may have shifted during the time span of our study and that alkenone production might have been less seasonal in the warm Miocene.

5.3 Results

5.3.1 Palynomorph assemblages

Hole 907A yielded a diverse and moderate to well preserved palynomorph assemblage, where 84 samples contained enough material to enumerate the statistical relevant 350 cysts. Counts in 36 samples ranged between 0 and 196 cysts of which 21 samples are virtually barren of dinocysts (< 10 cysts/slide). The majority of these samples cluster in two distinctive intervals between *c.* 8.1–7.4 Ma (Late Miocene, 100–103 mbsf) and *c.* 4.1–2.6 Ma (Late Pliocene, 49–62 mbsf; Fig. 24). Both intervals are also barren of acritarchs and prasinophytes. The relative abundance and concentration of the palynomorph groups and the distribution of selected dinocyst taxa in Hole 907A are given in Fig. 24 and Fig. 25. Raw counts and stratigraphic ranges of all taxa encountered are provided in Appendix C1. To avoid spurious abundance peaks all samples with less than 50 dinocysts counted have been omitted from all figures.

In-situ dinocysts

Dinocysts are the most abundant and diverse palynomorph group (Fig. 24), comprising at least 151 species belonging to at least 43 genera. A large number of these species are apparently not formally described, and only 23 are extant (Appendix C1).

The *Batiacasphaera micropapillata* complex and *Nematosphaeropsis labyrinthus* represent more than 50% of the assemblages in most samples, but are usually inversely correlated (Fig. 25). Accompanying taxa regularly recorded are shown in Fig. 25, but only *Batiacasphaera sphaerica*, *Habibacysta tectata*, *Labyrinthodinium truncatum*, *Spiniferites* spp. and *Protoperidinium* spp. continuously contribute more than 10% to the assemblage in some intervals. Moreover, 99 species occur in five or less samples and 33 of these are recovered in one sample only. Another 14 species are recorded only outside the regular counts (Appendix C1). Additionally, 81 of these 99 species occur in very low numbers (< 2%) whereas seven species occur in considerably high numbers (> 15%) in one sample but are rarely recorded in adjacent samples, which seriously restrict the utility of most species for interpretation.

The middle to middle Late Miocene assemblages are characterized by a high species richness with more than 30 taxa recovered routinely, accompanied by concentrations ranging from 10.000 to 40.000 cysts/g sediment, being exceptionally even higher (Fig. 24). The highest concentrations are attributed to low counts of *Lycopodium* spores. Thus absolute values are subject to statistical uncertainty but trends are reliable.

After maximum values in the Langhian, concentration decreases in the Serravallian to a minimum around 5.000 cysts/g sediment, but reaches average values higher than 20.000 cysts/g again in the lower to mid-Tortonian before it declines to an average of 15.000 cysts/g during the mid-Tortonian to mid-Messinian. Latest Miocene and Pliocene cyst concentration is comparatively low (ø 1340 cysts/g sediment), and the number of encountered taxa rarely exceeds 20 per sample, with the majority varying around 10 species. Late Pliocene assemblages usually contain less than 10 species (Fig. 24).

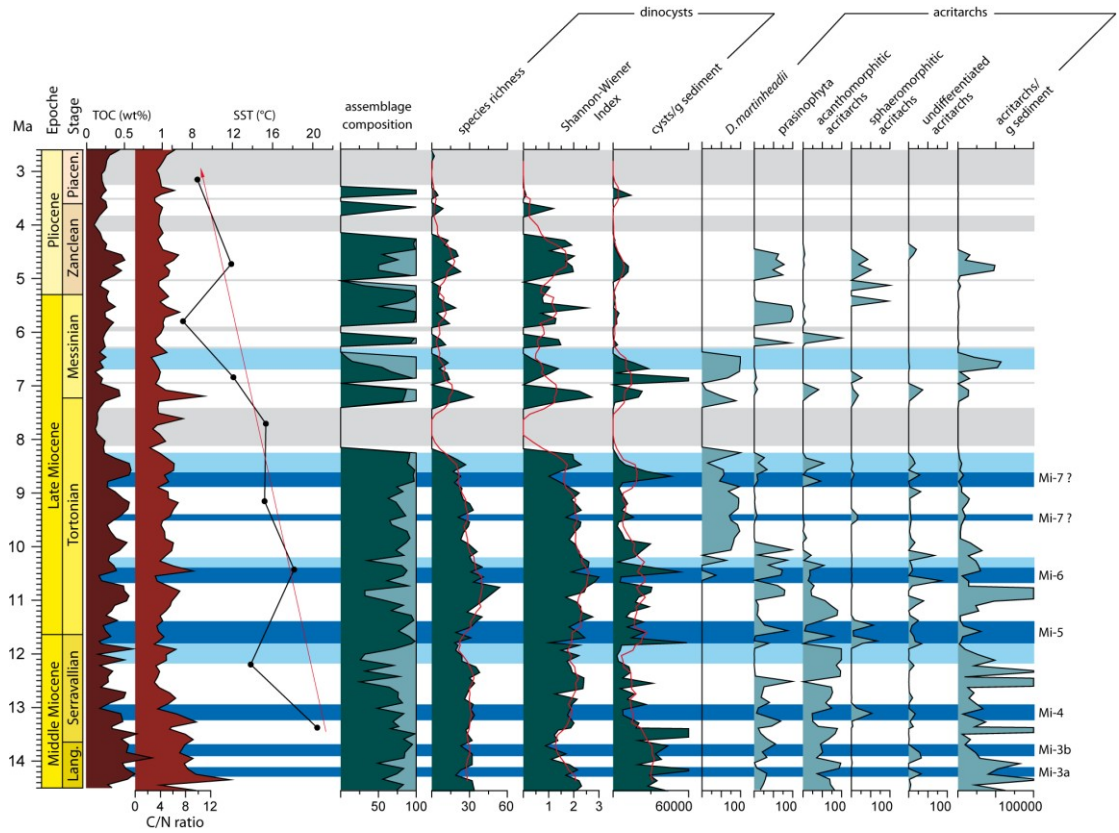

Figure 24: Total organic carbon (TOC) in weight percentage (wt%), C/N ratio and sea-surface temperature (SST in °C, red line illustrating the long-term trend) in ODP Hole 907A. The relative abundance (%) and concentration (specimen/g sediment) of dinocysts (dark green) and acritarchs (light green), and relative abundance (%) of the five acritarch groups within the acritarch assemblage in Hole 907A are shown. For the dinocysts, the diversity indices (species richness, Shannon-Wiener index) are shown. Horizontal grey bars indicate the position of the barren samples in Hole 907A. Dark blue bars indicate the position of the confirmed and orbitally tuned Mi-events. Mi-3a = 14.2 Ma (Abels et al., 2005), Mi-3b = 13.9–13.7 Ma (Mourik et al., 2011), Mi-4 = 13.2–13.0 Ma, Mi-5 = 11.8–11.4 Ma, Mi-6 = 10.7–10.4 Ma (all Westerhold et al. 2005). For Mi-7, the two possible positions discussed in Westerhold et al. (2005) are shown. Light blue bars indicate additional cooling phases identified in Hole 907A.

Although dinocyst diversity is comparatively high throughout middle to late Miocene times three distinctive events are highlighted by the Shannon-Wiener index: 1) a significant decrease between 14.5 and 13.7 Ma, followed by 2) an increase to maximum values at ~ 10.7 Ma, and 3) a subsequent long-term decline until a significant drop ~ 7.0

Ma, which is interrupted by a prominent barren interval between 8.1 and 7.4 Ma (Fig. 24). The species richness generally displays the same trend. The crucial difference, however, is a distinct short-term decline between 12.3 and 11.7 Ma, which is not clearly reflected in the Shannon-Wiener index.

The lowermost part of the hole is characterized by abundant to dominant *B. sphaerica* and *L. truncatum*, and common *Palaeocystodinium* spp., which all decrease until ~ 14.0 Ma when the *B. micropapillata* complex increase significantly. This complex exhibits cyclic variations with temporarily reduced abundances but is characterized by a general decrease towards the middle Late Miocene (Fig. 25). A distinct shift is marked by a minimum at ~ 13 Ma associated with a minimum of *B. sphaerica*, and *N. labyrinthus*, *H. tectata*, *Impagidinium pallidum*, *Impagidinium* cf. *pacificum*, and *Cerebrocysta irregulare* were considerably abundant for the first time.

	age	event	species
extinction event I (10.6–10.2 Ma)	10.6	HCO	*Hystrichosphaeropsis obscura*
	10.6	HO	*Cleistosphaeridium placacanthum*
	10.5	HO	*Spiniferites* sp. B
	10.4	HO	*Cerebrocysta irregulare*
	10.4	HO	*Cordosphaeridium minimum*
	10.4	HO	*Impagidinium* sp. A
	10.4	HO	*Operculodinium giganteum*
	10.4	HPO	*Selenopemphix brevispinosa*
	10.2	HO	*Impagidinium* aff. *aculeatum*
	10.2	HO	*Impagidinium elongatum*
extinction event II (9.0–8.3 Ma)	9.0	HO	*Dapsilidinium pseudocolligerum*
	8.9	HO	*Palaeocystodinium golzowense*
	8.8	HO	*Hystrichosphaeropsis obscura*
	8.8	HO	*Spiniferites* sp. A
	8.5	HPO	*Selenopemphix nephroides*
	8.4	HPO	*Melitasphaeridium choanophorum*
	8.4	HO	*Batiacasphaera hirsuta*
	8.4	HO	*Labyrinthodinium truncatum*
	8.4	HO	*Operculodinium piaseckii*
	8.4	HO	*Selenopemphix brevispinosa*
	8.3	HCO	*Cristadinium cristatoserratum*
	8.3	HO	*Lingoludinium machaerophorum*
extinction event III (4.5–4.3 Ma)	4.6	HO	*Corrudinium? labradori*
	4.5	HCO	*Batiacapshaera micropapillata*
	4.5	HO	*Batiacasphaera sphaerica*
	4.5	HO	*Corrudinium devernaliae*
	4.5	HO	*Invertocysta lacrymosa*
	4.5	HO	*Melitasphaeridium choanophorum*
	4.5	HO	*Pyxidinopsis vesiculata*
	4.5	HO	*Operculodinium? eirikianum*
	4.5	HO	*Operculodinium tegillatum*
	4.5	HO	*Reticulatosphaera actinocoronata*
	4.3	HO	*Corrudinium harlandii*
	4.3	HO	*Spiniferites elongatus*

Table 4: List of dinocyst datums associated with the three extinction events. HO = highest occurrence, HCO = highest common occurrence, HPO = highest persistent occurrence. For stratigraphic ranges of species not shown in Figure 3 see Appendix C1.

The gradual Late Miocene decline in diversity is punctuated by major transitions in assemblage composition at ~ 10.6–10.2 Ma and ~ 9–8.3 Ma, when several species became extinct (Table 4, Fig. 25). *Batiacasphaera sphaerica* and *Reticulatosphaera actinocoronata* have their highest common occurrence at ~ 10 whilst *Spiniferites* spp. and *H. tectata* decrease during this interval, the latter significantly after a remarkable acme at ~ 10 Ma (Fig. 25).

After the barren interval, the *B. micropapillata* complex is still present but in considerably lower numbers, and *N. labyrinthus* is predominant in most of the samples. Another major turnover at ~ 4.5 to 4.3 Ma is marked by a cluster of last occurrences (Table 4, Fig. 25), and the highest common occurrence of the *B. micropapillata* complex. At ~ 4.2 Ma *N. labyrinthus* disappears abruptly and succeeding samples are virtually

barren, interrupted by almost mono-specific *Spiniferites spp.* samples at 3.6 Ma, 3.4 Ma and 3.3 Ma only.

Ecology: For the interpretation of ecological affinities of extant species a vast data set has been compiled in the past decade (e.g Rochon et al, 1999; Marret and Zonneveld, 2003; Bonnet et al., 2012). Since most species recorded in this study are extinct, however, it has been attempted to derive their ecological preferences based on paleobiogeographic compilations and thermal preferences determined by comparison to Mg/Ca temperatures of co-occurring foraminifera *Globigerina bulloides* (De Schepper et al., 2011). The paleoenvironmental interpretations are principally based on a few common to abundant taxa, and index-species with relatively well-constrained (paleo) ecological preferences. Appendix C2 provides a summary of ecological preferences of extant and extinct species that have been utilized for interpretation (Fig. 24). The only ecological group erected is *Protoperidinium* spp., which includes all species of the genera *Trinovantedinium, Barssidinium, Sumatradinium, Selenopemphix, Lejeunecysta, Xandarodinium, Brigantedinium* and *Cristadinium*, as there is a positive correlation between heterotrophic taxa and productivity (e.g. Devillers and de Vernal, 2000; Reichart and Brinkhuis, 2003; Radi and de Vernal, 2008). Their heterotrophic affinity has been proven by autofluorescence microscopy (Brenner and Biebow, 2001; Appendix C1).

For interpretation of the diversity indices it has to be considered that diversity of marine phytoplankton is generally lowest at the poles and higher at lower latitudes (Barton et al., 2010). On global scale, dinocyst diversity is positively correlated with sea surface temperature, particularly pronounced in cooler water < 13°C, and accounts for most of the correlation observed between diversity and latitude (Chen et al., 2011). Moreover, dinocyst diversity does not decrease with decreasing nutrient concentration (Chen et al., 2011), thus may provides independent estimates for relative temperature changes. In surface samples from the modern Nordic Seas (Matthiessen et al., 1995) it has also been shown that species diversity is higher in the comparatively temperate western domain off Norway when compared to the cold-water influenced Iceland Sea and East Greenland margin; and in the Pliocene of the Labrador Sea diverse dinocyst assemblages correspond to interglacial stages while low diversity assemblages correlate with glacial periods (de Vernal and Mudie, 1989b).

Figure 25 (next page): Detailed diagram showing relative percentages (% out of the total sum of dinocysts counted) of selected dinocyst species in Hole 907A. For colour coding of horizontal bars see Fig. 24.

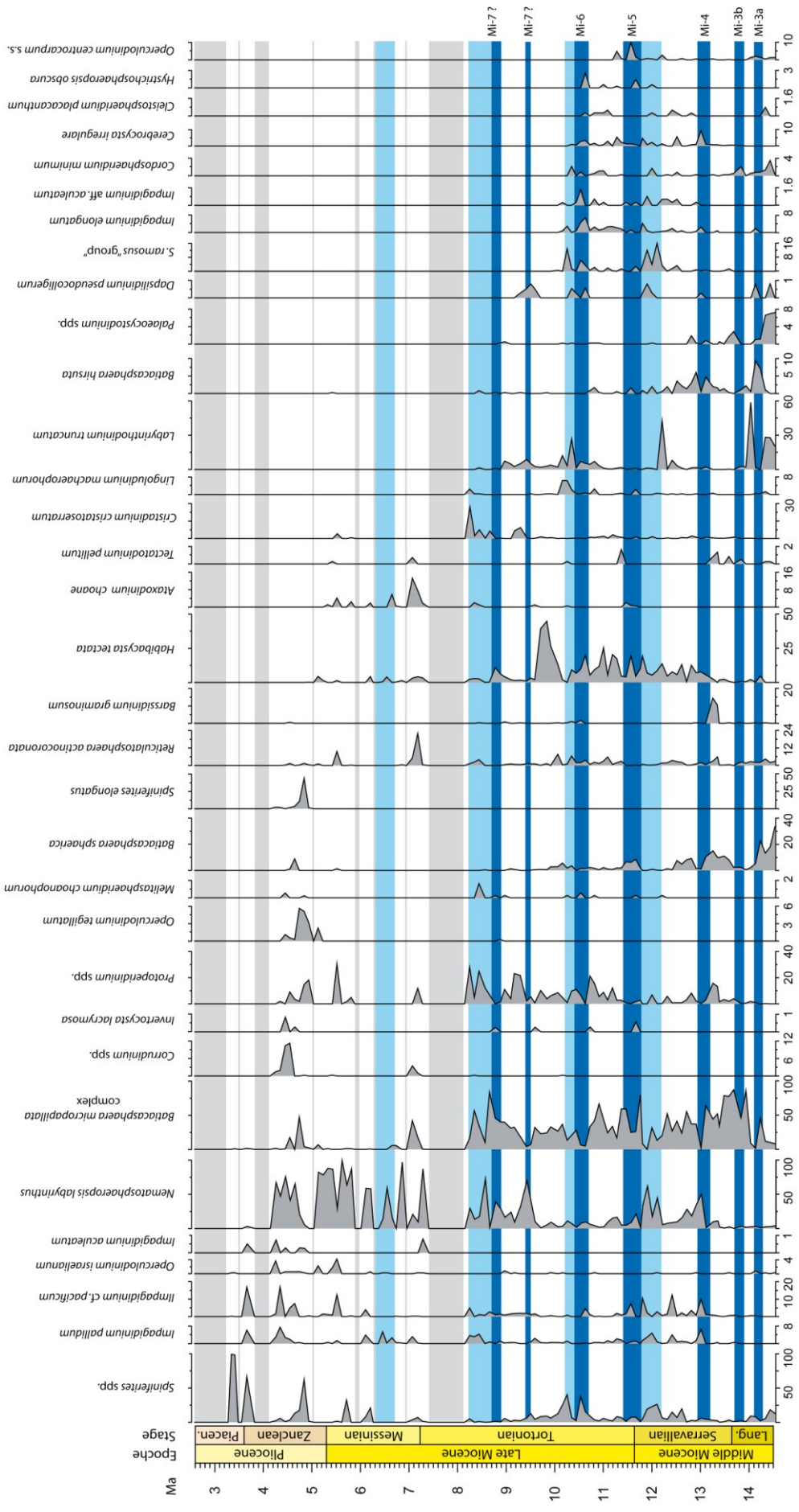
Mi-7 ?
Mi-7 ?
Mi-6
Mi-5
Mi-4
Mi-3b
Mi-3a
Operculodinium centrocarpum s.s.
Hystrichosphaeropsis obscura
Cleistosphaeridium placacanthum
Cerebrocysta irregulare
Cordosphaeridium minimum
Impagidinium aff. aculeatum
Impagidinium elongatum
S. ramosus "group"
Dapsilidinium pseudocolligerum
Palaeocystodinium spp.
Batiacasphaera hirsuta
Labyrinthodinium truncatum
Lingolusdinium machaerophorum
Cristadinium cristatoserratum
Tectatodinium pellitum
Ataxodinium choane
Habibacysta tectata
Barssidinium graminosum
Reticulatosphaera actinocoronata
Spiniferites elongatus
Batiacasphaera sphaerica
Melitasphaeridium choanophorum
Operculodinium tegillatum
Protoperidinium spp.
Invertocysta lacrymosa
Corrudinium spp.
Batiacasphaera micropapillata complex
Nematosphaeropsis labyrinthus
Impagidinium aculeatum
Operculodinium israelianum
Impagidinium cf. pacificum
Impagidinium pallidum
Spiniferites spp.
Ma
Epoche
Stage
Middle Miocene
Late Miocene
Pliocene
Lang.
Serravallian
Tortonian
Messinian
Zanclean
Piacen.

Reworked dinocysts

Reworking of Neogene sediments is of minor importance as well-known stratigraphic marker species occur only rarely above their range tops (Schreck et al., chapter 3). Limited reworking of pre-Neogene material constantly occurs in Langhian and Serravallian sediments but only sporadically above that interval. However, the number of reworked dinocysts never exceeds 1% of the assemblage. Only Sample 6H-3, 82–84 cm (49.1 mbsf, ~2.6 Ma) contains abundant reworked dinocysts. Reworked Paleogene species include *Deflandrea phosphoritica*, *Svalbardella* spp., *Eatonicysta ursulae*, *Enneadocysta spp.*, *Homotryblium* spp., *Oligosphaeridium* spp. and *Wetziella* spp.

Acritarchs

Acritarchs constitute a significant part of the palynomorph assemblage throughout most of the analysed interval and partly even outnumber dinocyst (Fig. 24, Appendix C1). This diverse complex has been roughly subdivided into five distinctive morphological groups.

a) *Decahedrella martinheadii*

This morphologically characteristic acritarch has a restricted range in Hole 907A. It first occurs at 10.5 Ma, and is continuously present until its last occurrence at 6.3 Ma (Fig. 24; Schreck et al., chapter 3). It reveals high relative abundances from 9.9 to 8.9 Ma, but constitutes up to 90% of the palynomorph assemblage between 6.7 and 6.5 Ma.

Ecology: This species is endemic for the high northern latitudes and considered a cool-temperate to cold-water oceanic species (Manum, 1997; Matthiessen et al., 2009).

b) *Prasinophyta*

This group is mainly composed of species that could be assigned to the genera *Cymatiosphaera* and *Lavradosphaera* (mainly *Cymatiosphaera*? *invaginata*, *Lavradosphaera crista*). Other specimens broadly resemble different *pterosphaeridiaceaen* and *cymatiosphaeridiaceaen* species, but have not been determined to species level. Prasinophytes are common between 14.5 and 12.6 Ma, but most abundant at 12.5 Ma, and between 10.9 and 10.1 Ma. *Cymatiosphaera*? *invaginata* and *L. crista* dominate the acritarchs between 5.5 and 4.5 Ma. (Fig. 24).

Ecology: Fossil prasinophytes are just as cosmopolitan as their modern relatives (Fensome et al., 1990; Guy-Ohlson, 1996). However, exceptionally light $\delta^{13}C$ values of fossil phycomata suggest deposition under low temperature and reduced salinity (Prauss and

Riegel, 1989). In modern and Quaternary sediments prasinophytes (in particular *Cymatiosphaera* species) are often associated with less saline and/or cool surface water (Wall et al., 1973; Tappan, 1980), and may be typical for stratified surface water in the Plio-Pleistocene (Mudie et al., 1990). The (paleo)biogeographic distribution of the genus *Lavradosphaera* suggests a cool water affinity (De Schepper, pers. comm. 2012).

c) *Acanthomorphitic acritarchs*

In the lower part of the hole this group is mainly composed of 2 morphotypes that may be attributed to the genus *Micrhystridium*, complemented by *Nannobarbophora gedlii*. This morphological complex dominates the acritarch assemblage during the Middle to early Late Miocene, actually reaching more than 50% of the whole palynomorph assemblage between 12.5 and 12.0 Ma (Fig. 24), but disappears abruptly at ~ 10.8 Ma. Acanthomorphitic acritarchs sporadically recorded above this stratigraphic level broadly resemble the cyst of the dinoflagellate *Pentapharsodinium dalei* but an unambiguous assignment could not be made. However, the latter complex only plays a subordinate role.

Ecology: The ecology of this group is yet poorly constrained (Strother, 1996) since our knowledge is mainly based on occurrences in Palaeozoic and Mesozoic deposits (Batten, 1996). The Neogene *Nannobarbophora gedlii* is associated with warm-water conditions (Head, 2003) as is the genus. The ecology of *Micrhystridium* spp. is unknown, but Jimenez-Moreno et al. (2006) recorded abundant *Micrhystridium* spp. in the earliest Serravallian of central Europe probably indicating a more temperate distribution of these spinous forms.

d) *Sphaeromorphitic acritarchs*

This group comprises discoidal to spherical forms similar to the extant genera *Halosphaera* and *Leiosphaeridia*. Due to unfavourable orientation and recurrent folding of specimens these taxa could not be determined to genus level. They only occur sporadically throughout but are common at 13 Ma, 11.5 Ma, and between 5.5 and 4.5 Ma (Fig. 24).

Ecology: In modern sediments of high latitude environments, spherical forms such as *Leiosphaeridia* spp. occur frequently in vicinity to sea-ice margins (Mudie et al., 1990; Mudie, 1992). By analogy, they have been associated with colder and less saline conditions, sea-ice, and/or the inflow of Arctic waters in the Late Miocene through Pliocene of the subarctic North Atlantic (e.g. Mudie et al., 1990).

e) *Undifferentiated acritarchs*

This group encloses morphotypes, which could not be attributed to one of the other groups due to diverging morphology and/or preservational reasons.

Ecology: The uncertain taxonomy prevents the assignment of ecological preferences.

5.3.2 The Uk'_{37} sea surface temperature record

All but the lowermost sample (23H-6, 97.5–99.5 cm, 215.27 mbsf) yielded alkenones to allow the application of the Uk'_{37} index to calculate SSTs (Table 3, Fig. 24). Although core top samples close to our study site yielded Uk'_{37} values for a given SST that fall within the Müller et al. (1998) 99% data envelope (Bendle and Rosell-Melé, 2004) we acknowledge that absolute temperatures should not be taken at face values. The results from Site 907 indicate conditions considerably warmer than at present day (mean annual temperature ~ 2.5°C) with SSTs as high as 20°C at ~13.5 Ma decreasing towards 8°C by around ~3 Ma (Fig. 24). Further comparisons are hampered by the scarcity of high latitude Neogene SST time series, which all focus on the Plio-Pleistocene (e.g. Robinson, 2009; Lawrence et al., 2009, 2010; Naafs et al., 2010), or older epochs (Weller and Stein, 2008).

5.4 Discussion

Superimposed on the general long-term trend from a highly diverse Middle Miocene palynomorph assemblage towards the impoverished assemblages of the Late Pliocene significant fluctuations in abundance and composition have been observed. The palynological data are here complemented with alkenone SSTs and TOC data (Fig. 24) to characterize and discuss the paleoenvironmental evolution of the Iceland Sea between 14.5 and 2.5 Ma.

The Middle Miocene transition (14.5–13.0)

Sedimentation at Site 907 commenced shortly after the MCO and palynomorph concentration suggests a high net primary productivity (Zonneveld et al., 2010), which has also been inferred from abundant diatoms and their resting spores after 14 Ma (Stabell and Koç, 1996). However, as *protoperidiniacean* dinocysts are usually abundant in upwelling areas (Reichart and Brinkhuis, 2003; Holzwarth et al., 2007, 2010), their low abundance during this interval in the Iceland Sea does not support substantial upwelling as suggested by Stabell and Koç (1996). Since selective degradation is excluded due to

light to dark brown colours and no evidence of oxidative damage of *Barssidinium* and *Cristadinium* specimens encountered, the high paleoproductivity likely resulted from increased nutrient input due to enhanced chemical weathering during a much warmer and humid climate (Wan et al., 2009; Ma et al., 2011; Pound et al., 2012). The significant decline in the Shannon-Wiener index towards lowest Miocene values at 13.7 Ma likely depicts the impact of subsequent cooling during the MMCT (14.2–13.7 Ma, Shevenell et al., 2004). As species richness appears to be rather constant across this interval, the decline in the Shannon-Wiener Index also indicates a drastic shift of relative abundances within the dinocyst assemblage, which may represent the increase of opportunistic species (i.e. the *B. micropapillata* complex) during times of ecosystem perturbation. However, the richness exhibit two transient minima centred at 14.2 and 13.7 Ma, which may denote the two-step character of the MMCT (Mi-3a/b, Miller et al., 1996; Abels et al., 2005; Mourik et al., 2011). A short-term decrease in acritarch abundance, but a relative shift in assemblage composition from more warm-temperate acanthomorphitic acritarchs (*N. gedlii*, *Micrhystridium* spp.) to prasinophytes characterizes both steps. The MMCT is also reflected by a decline in *B. sphaerica, Labyrinthodinium truncatum* and *Palaeocystodinium* spp. accompanied by the first occurrence of the cool-water species *H. tectata* at ~ 14.2 Ma (temperature range *c.* 9–17°C, De Schepper at al., 2011). *Batiacasphaera hirsuta* and the *B. micropapillata* complex both increase during the early phase of this transition followed by a significant drop at ~ 14.1 and ~ 14.2 Ma respectively. The latter is common in the Middle to Late Miocene of the high northern latitudes and Arctic Ocean, and is considered a cool- to warm-temperate species complex, which may sustain some sea-ice cover (Schreck and Matthiessen, accepted for publication). Its drastic increase at ~ 13.9 Ma thus suggests the establishment of somewhat cooler conditions, whereas the occurrence of sea-ice in the Iceland Sea during the MMCT as reported from Fram Strait (Knies and Gaina, 2008; Thiede et al., 2011) remains speculative because IRD has only been studied from ~ 8 Ma (Fronval and Jansen, 1996). Nonetheless, the low abundance/absence of (sub)tropical *Impagidinium* species, large gonyaulacoids and species with expanded wall coverings (e.g. *Hystrichosphaeropsis pontiana*, *Hystrichosphaeropsis obscura*, *Hystrichokolpoma rigaudiae*, *Lingoludinium machaerophorum*, *Melitasphaeridium choanophorum*, *Tuberculodinium vancampoae*, *Dapsilidinium pseudocolligerum*, *Invertocysta spp.*) suggest colder surface waters than in the Norwegian Sea and other North Atlantic sites where these taxa dominate coeval assemblages (Harland, 1979; Costa and Downie, 1979; Mudie, 1987; Manum et al., 1989; see Mudie et al., 1990 for discussion). These taxa are

also absent from Baffin Bay (Head et al., 1989c), which might be related to the onset of cooler conditions as inferred from the drop in accumulation rates of terrigenous organic carbon around 14.5 Ma (Stein, 1991; Stein, 2008).

The cooler surface waters in the Iceland than in the Norwegian Sea may be attributed to enhanced exchange of water masses between the Arctic Ocean and the Nordic Seas since ~ 14 Ma (Jakobsson et al., 2007). Since the Transpolardrift has been active in the past 15 Ma (Haley et al., 2008), the opening of the Fram Strait led to the establishment of a modern-like ice drift pattern with export from the Arctic Ocean into the western Nordic Seas (Fig. 26; Knies and Gaina, 2008), most likely via the Transpolardrift and a proto-East Greenland Current (EGC). Indeed, judging from the occurrence of septate species such as *Gonyaulax baltica* in low salinity environments (Ellegaard et al., 2002), the strongly reduced crests of *I. elongatum* specimens in that interval (Schreck et al., chapter 3) may indicate less saline Arctic waters transported as far south as the Iceland Sea by a proto-EGC. This presumably led to the development of a temperature gradient across the Nordic Seas as early as Middle Miocene (cf. Fronval and Jansen, 1996), as supported by differences in dinocyst assemblages. In concert with the proposed onset of a Norwegian-Atlantic Current precursor (Henrich et al., 1989), this may points towards the initiation of a proto-thermohaline circulation in the Nordic Seas around this time as also indicated by a prominent switch from biosiliceous to carbonate-rich sedimentation on Vøring Plateau (Bohrmann et al., 1990; Cortese et al., 2004; Knies and Gaina, 2008). However, paleobotanical studies on Iceland revealed that a land bridge between Europe and Greenland must have been present (Denk et al., 2011; Fig. 26) restricting the water mass exchange with the North Atlantic.

A brief (~ 500 kyr) warming is indicated subsequent to Mi-3b by an increased Shannon-Wiener index, recurrent *Palaeocystodinium* spp., a single peak of *Barssidinium graminosum*, and a significant increase in acanthomorphitic acritarchs. The rare but continuous occurrence of *Tectatodinium pellitum* indicates summer SSTs > 15–25°C (De Schepper et al., 2011) consistent with our reconstructed mean annual SST of 20°C at 13.4 Ma. The observed warming of surface waters may result from temporary westward deflection of warmer North Atlantic waters into the Iceland Sea.

The highest persistent occurrence of the warm water species *T. pellitum*, and peaks of typical high latitude species such as *N. labyrinthus*, *H. tectata*, *I. pallidum, I.* cf. *pacificum* and *C. irregulare* (Fig. 25) indicate iterative cooling presumably associated with the Miocene isotope event Mi-4 (13.2–13.0 Ma, Westerhold et al., 2005). Likewise the

shift that occurred across the MMCT, a pronounced minimum in the *B. micropapillata* complex is accompanied by a decline in *B. sphaerica* and *B. hirsuta*, but now co-occurs with very abundant *N. labyrinthus*. The minimum in acanthomorphitic acritarchs, which is similar to that observed during Mi-3a and b, is coeval with an increase in sphaeromorphitic acritarchs (Fig. 24), which may evince first sea-ice reaching the Iceland Sea. *Impagidinium pallidum* has been frequently considered an indicator for cold surface water conditions and a variable range of sea-ice cover (e.g. Rochon et al., 1999; de Vernal et al., 2001; Marret and Zonneveld, 2003), and its common occurrence (~ 10%) has been associated with summer SSTs < 15°C (de Schepper et al., 2011). Since *H. tectata* requires summer SSTs > 9°C (De Schepper et al., 2011) and abundances of *N. labyrinthus* > 50% are correlated to SSTs < 14°C (Bonnet et al., 2012), SSTs might have been in the range of > 9 to < 14°C. Today, *N. labyrinthus* is abundant to dominant (40–60%) in regions where colder, polar waters mixes with warmer Atlantic waters (Rochon et al., 1999). As SSTs are still comparatively warm sea-ice likely originated in the Arctic Ocean (St. John, 2008) and has been exported via Fram Strait (Knies and Gaina, 2008) into the western Nordic Seas.

Late Middle to early Late Miocene (13.0–10.7 Ma)

After the incisive changes that occurred across the MMCT and the Mi-4 event comparatively stable conditions prevailed on the Iceland Plateau after ~ 13 Ma. Concentration indicates palynomorph productivity similar to the modern western North Atlantic margin (Rochon et al., 1999), but higher when compared to the modern Iceland Sea (Matthiessen, 1995). A more temperate environment is indicated by the somewhat continuous occurrence of *Cleistosphaeridium placacanthum*, *H. obscura*, *Operculodinium centrocarpum* s.s., *Impagidinium* aff. *aculeatum*, common *Spiniferites ramosus* s.l., and very abundant acanthomorphitic acritarchs (Fig. 24, 25). Consistently, both dinocyst diversity measures show a general increase across the latest Middle through early Late Miocene, only interrupted by a transient decline between 12.3 and 11.6 Ma as also observed in the cyst concentration. Although the age model is well constrained in this interval (Channell et al., 1999), these brief minima, and a coeval minimum of the *B. micropapillata* complex slightly precede the global Mi-5 cooling (11.8–11.4 Ma, Westerhold et al., 2005), which might be attributed to insufficient sample resolution. However, the minima coincide with peak abundance of *N. labyrinthus* (≥ 50%) which suggests SSTs < 14°C (Bonnet et al., 2012) and temporary enhanced mixing of Atlantic and polar water (cf. Rochon et al.,

1999). Wei (1998) inferred time-equivalent cooling of surface waters along the southeast Greenland margin from calcareous nannofossils, which he attributed to the (proto) EGC. Therefore, the inverse correlation between *N. labyrinthus* and *B. micropapillata* complex may indicate cooling but further studies are needed to test this assumption. Notwithstanding, alterations in the acritarch assemblage resembling those observed during the MMCT occur contemporaneously with Mi-5, whereas the dinocyst diversity and productivity apparently recovers. On continental Iceland, pollen data also suggest that markedly warm conditions persisted at least until the Late Miocene (Denk et al., 2011). These temperate conditions might be related to a generally enhanced inflow of

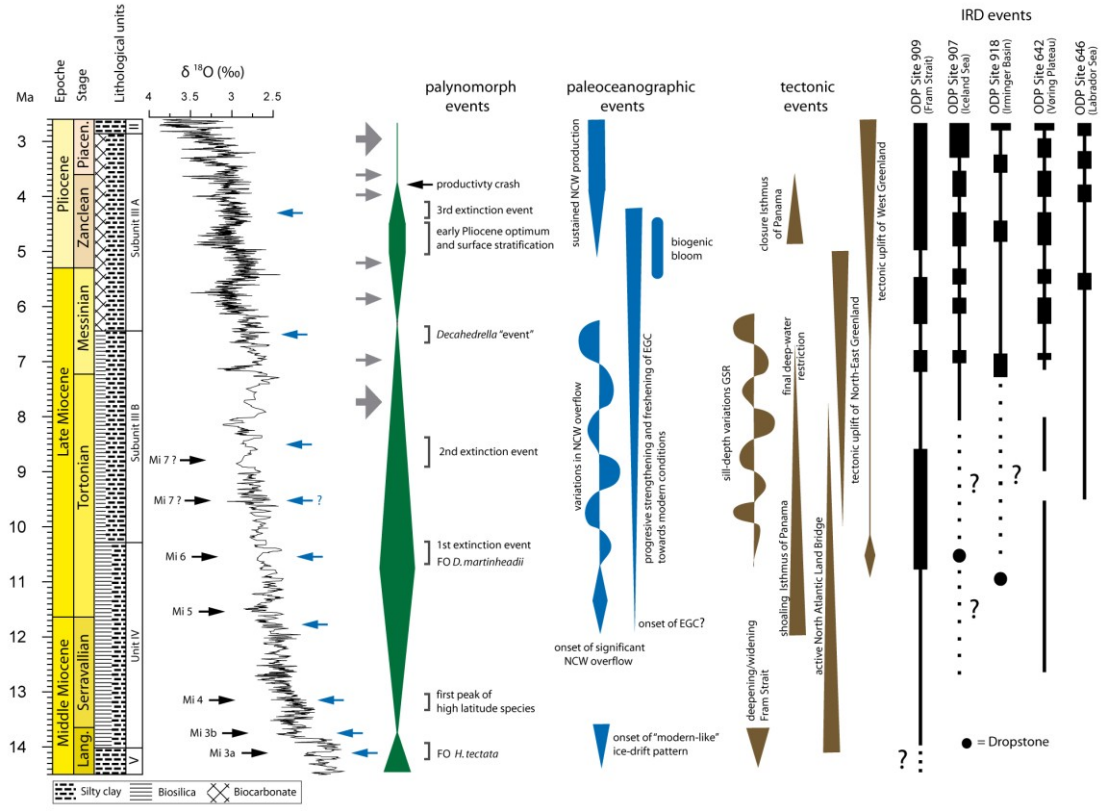

Figure 26: Palynomorph events identified in this study in relationship to paleoceanographic, tectonic, and IRD events (for references see text). Note that signatures for variations in NCW and GSR are only schematic representations, and do not indicate direction or quantity. Lithological units are from the Shipboard Scientific Party (1995). Grey arrows show position of the palynologically barren samples. Black arrows refer to the Mi-events as numbered (see Fig. 2 for details). Blue arrows indicate cooling events identified in Hole 907A. Also shown the global benthic oxygen isotope record (Zachos et al., 2001). Schematic representation of IRD events are redrawn from Wolf and Thiede (1991) for ODP Site 646; from Fronval and Jansen (1996) for ODP sites 642 and 907; from Wolf-Welling et al. (1996) for ODP Site 909; and from Helland and Holms (1997) and St. John and Krissek (2002) for ODP Site 918. NCW = Northern Component Water; EGC = East Greenland Current; GSR = Greenland-Scotland Ridge.

North Atlantic waters into the Nordic Seas as suggested by the renewal of NCW production around 13–12 Ma (Fig. 26; Bohrmann et al., 1990; Wright and Miller, 1996; Poore et al., 2006).

Glacial inception in the Iceland Sea (~ 10.7–10.2 Ma)

Both diversity measures start to decline within this interval accompanied by the first occurrence of the endemic cold-water acritarch *D. martinheadii* (Manum, 1997; Matthiessen et al., 2009) at ~ 10.5 Ma, and a significant cluster of species last occurrences (Table 4, Fig. 25). The *B. micropapillata* complex shows a significant minimum as previously during Mi-3, Mi-4, and shortly prior to Mi-5 whilst cool-water *H. tectata*, and *I. elongatum* and *Spiniferites* spp. (mainly *S. ramosus* s.l.) contribute significantly to the dinocyst assemblage. Whereas *S. ramosus* s.l. is a cosmopolitan species that may not be `monospecific` (see Marret and Zonneveld, 2003 and references therein for discussion) the occurrence of *I. elongatum* appears to be restricted to the high northern latitudes (Schreck et al., chapter 3). In alignment with common to abundant prasinophytes, and the disappearance of *Micrhystridium* spp. and warm-temperate *N. gedlii*, all this suggest a cooling of surface waters that may correspond to the glacial Mi-6 event (10.7–10.4 Ma, Westerhold et al., 2005), which is thought to reflect the growth of continental ice sheets (Miller et al., 1991; Turco et al., 2001). Indeed, the onset of predominantly siliciclastic deposition (120 mbsf, 10.5 Ma) and the occurrence of the first dropstone (116.5 mbsf, 10.3 Ma) at Site 907 (Fig. 26; Shipboard Scientific Party, 1995) prove ice rafting since that time, and suggest a link between observed assemblage changes and the Mi-6 glacial event. Increased bulk accumulation rates at ODP Site 909 supposedly reflect intensification of water mass exchange through Fram Strait (Wolf-Welling et al., 1996; Winkler et al., 2002), which would have resulted in enhanced advection of comparatively cold, low saline, and presumably sea-ice covered waters into the Iceland Sea, forcing the observed changes in the palynomorph assemblage. The occurrence of *I. elongatum* specimens with strongly reduced crests on the cyst wall might have been caused by these somewhat reduced salinities (Schreck et al., chapter 3). The increased advection of colder waters may have triggered the coeval collapse in accumulation of *Chaetoceros* resting spores reflecting a diminished diatom production (Koç and Stabell, 1996). Moreover, benthic $\delta^{18}O$ values on Vøring Plateau indicate substantial deep water cooling ~ 11 Ma (Fronval and Jansen, 1996), and increased circum-arctic IRD fluxes between 11.0 and 9.5 Ma (Schaeffer and Spiegler, 1986; Thiébault et al., 1989; Wolf and Thiede, 1991; Fronval and

Jansen, 1996; Wolf-Welling et al., 1996; Helland and Holmes, 1997; Winkler et al., 2002) prove general cooling in the high northern latitudes. The timing of IRD events broadly correspond to a major uplift phase on Greenland (Thomson et al., 1999; Japsen et al., 2006) suggesting a pivotal role in establishing the Greenland ice sheet during Late Miocene times, when pCO_2 stabilized at pre-industrial values (Pagani et al., 1999). A similar onset of cooling at ~ 10.5 Ma has been reported from northeast North Atlantic ODP Site 982 (Andersson and Jansen, 2003), but also from shallow marine deposits in northwest Europe (Donders et al., 2009). Based on pollen from continental Iceland, Mudie and Helgason (1983) proposed a drastic drop in atmospheric temperature (~10°C) at around 10 Ma, but this magnitude has been recently challenged by Denk et al. (2011) who suggest a more continuous climate deterioration starting around that time. A drastic change in atmospheric temperature, however, should have been recorded in the alkenone SST as well, that, instead show only a moderate decrease throughout the Late Miocene (Fig. 24).

Late Miocene cooling and variable surface water conditions (~ 10.2–6.7 Ma)

Subsequently, the prevalence of colder Arctic derived waters in the Iceland Sea is proven by continuously high abundances of the cold-water acritarch *D. martinheadii* (Fig. 24), and the gradual decline in both diversity measures indicate progressive Late Miocene cooling. *Habibacysta tectata* declines drastically after a massive acme (~ 10 Ma), whereas *N. labyrinthus* and the high northern latitude dinocyst *Cristadinium cristatoserratum* (Schreck et al., chapter 3) reveal generally higher abundances. As such high abundance of *H. tectata* occurs within its usual temperature range (De Schepper et al., 2011) other factors such as nutrient availability or salinity changes might have been responsible. However, the temporary influence of warmer, more saline Atlantic waters is indicated by low numbers of prasinophytes and the sporadic occurrence of warm-water species (e.g. *M. choanophorum, Operculodinium israelianum, D. pseudocolligerum, L. machaerophorum*). The alternating influence of different source water masses is also shown by large fluctuations of *N. labyrinthus* between 10 and 6.8 Ma. At ~ 9.5 Ma increased abundance of *N. labyrinthus* coincides with a minimum in the *B. micropapillata* complex. Interestingly, such reversed correlation has already between observed during Mi-4 and slightly prior to Mi-5; suggesting similar conditions around 9.4–9.5 Ma. Indeed, both diversity measures show a short-lived minimum accompanied by sphaeromorphitic acritarchs; and this timing coincides with the Mi-7 event as proposed by Wright and Miller (1992; 9.45 Ma), but its

identification in high-resolution benthic $\delta^{18}O$ records, however, remains uncertain (see Westerhold et al., 2005 for discussion). Notwithstanding, this points towards Arctic water inflow that presumably caused the subsequent disappearance of the warm-water *Dapsilidinium pseudocolligerum*. Consequently, the variations in surface waters caused a variable pattern of nutrient availability and paleoproductivity as revealed by contemporaneous changes in *Protoperidinium* spp. and TOC (Fig. 24). The TOC is predominately of marine origin as shown by C/N ratios between 6 and 8 (Fig. 24; e.g. Bordowskiy, 1965), although they should be interpreted cautiously due to low TOC contents of ≤ 0.5% (Stein and Macdonald, 2004). However, diatoms also show a distinctive shift from a continuously high to a more variable abundance pattern ~ 10 Ma (Stabell and Koç, 1996). Variable surface and deep-water circulation and progressive Late Miocene cooling has also been reported from the Norwegian Sea (Bohrmann et al., 1990; Ciesielski and Case, 1989; Locker and Martini, 1989), and the former is likely coupled to GSR sill depth variations (Poore et al., 2006). Accordingly, Iceland pollen data suggest an active North Atlantic Land Bridge via a partly subaerial exposed GSR until ~ 8 Ma (Denk et al., 2011), and thus varying surface and deep-water exchange (Fig. 26). Moreover, moist and cool-temperate conditions continuously established on continental Iceland between 10 and 7–6 Ma (Denk et al., 2005, 2011). These variations in ocean circulation might have caused the waxing and waning of circum-continental ice-sheets indicated by repetitive IRD events during this time in the Fram Strait (Wolf-Welling et al., 1996), the Vøring Plateau (Jansen and Sjoholm, 1991), Labrador Sea (Wolf and Thiede, 1991) and the Irminger Sea (Schaeffer and Spiegler, 1986).

Enhanced cold-water advection into the Iceland Sea (~ 9–8.4 Ma)

Superimposed on the progressive decline in dinocyst diversity a pronounced cluster of species last occurrences co-occurred with very abundant cold-water *D. martinheadii* between 9.0–8.4 Ma. The disappearance and/or highest persistent occurrence of several taxa, including those with warm-water affinity and/or longer stratigraphic ranges elsewhere in lower latitudes (Fig. 25, Table 4), and common *I. pallidum* and *C. cristatoserratum* indicate cooling in the Iceland Sea. This is supported by the contemporaneous record of IRD at Site 907 (Fig. 26; Fronval and Jansen, 1996), and the reversed correlation of *N. labyrinthus* and the *B. micropapillata* complex at 8.6 Ma as observed in the vicinity of previous cooling events. Despite highest *Protoperidinium* spp. abundance between 8.5 and 8.2 Ma, which is usually associated with elevated productivity

(Reichart and Brinkhuis, 2003; Radi and de Vernal, 2008) dinocyst concentration drops significantly at 8.6 Ma. Thus the dominance of *protoperidiniacean* taxa (mainly *C. cristatoserratum*, round brown cysts, Fig. 25, Appendix C1) may result from harsh sea surface conditions with sea-ice cover (Rochon et al., 1999; Radi and de Vernal, 2008). Coincidently, Engel (1989) reported a shift to a cold-adapted dinocyst assemblage transported from polar regions to DSDP Site 408, located just south of the Denmark Strait, and $\delta^{18}O$ data (Aksu and Hillaire-Marcel, 1989) and changes in the coiling ratio of *Neogloboquadrina atlantica* (Aksu and Kaminski, 1989) at ODP Site 646 in the Labrador Sea prove strengthened influence of cold water at this time. Accordingly, the last occurrence of several species and abundant *D. martinheadii* at Site 907 presumably record the amplification of southward transport of colder Arctic waters via the proto-EGC, and thus its progressive development towards modern conditions. Moreover, Wold (1994) inferred the onset of deep Denmark Strait overflow due to initial formation of the Eirik Drift at the same time, suggesting modern-like conditions of surface and deep-water circulation in the Iceland Sea. Interestingly, cold-indicative silicoflagellate assemblages from the Vøring Plateau suggest a plunge in temperature at ~ 8.5 Ma (Cieslielski and Case, 1989), as does the strong decrease in SSTs in northwest Europe ~ 8.4 Ma (Donders et al., 2009). Moreover, in North Atlantic ODP Site 982 a marked increase in $\delta^{18}O$ occurs around 9 Ma (Andersson and Jansen, 2003), in North Atlantic ODP Site 904 at 8.7 Ma (Miller et al., 1998), in South Atlantic ODP Site 1085 at 8.8 Ma (Westerhold et al., 2005), and in the global $\delta^{18}O$ composite between 8.9–8.7 Ma (Zachos et al., 2008), which may suggest an alternate timing for the Mi-7 event (see discussion in Westerhold et al., 2005) that broadly correspond to the changes observed in the palynomorph assemblage.

The palynologically barren interval (8.1–7.4 Ma)

The disappearance of marine palynomorphs, as well as pollen and spores (not shown), is apparently not related to sedimentation rate changes, as deposition is low but constant in that part of Hole 907A. Moreover, diatoms are present throughout this interval (Stabell and Koç, 1996; Koç and Scherer, 1996) thus excluding low sedimentation rates as a single cause. However, diatoms were studied at low resolution in this part (3 samples) and no overlap exists when compared to our samples. Hence sample spacing may partly explain the observed differences. In addition, we assume prolonged exposure to oxygen due to the low sedimentation rates an important factor preventing the accumulation of

palynomorphs, as it would result in aerobic degradation of organic-walled microfossils (e.g. Zonneveld et al., 2008). However, the reason for enhanced oxygen contents of bottom-waters remains enigmatic particularly in context of its sudden nature and temporal extent, but must involve circulation changes in the study area that may be related to the onset of Denmark Strait overflow (Wold, 1994) or final collapse of the North Atlantic land bridge (Denk et al., 2011).

The "Decahedrella event" and pronounced cooling (6.7–6.3 Ma)

A pronounced reorganisation of the oceanography in the Iceland Sea starting at ~ 6.7 Ma is unveiled by a significant acme of the endemic cold-water acritarch *D. martinheadii* (Fig. 24), succeeded by its abrupt disappearance. Dinocyst concentration drops significantly and species richness reaches lowest Miocene values at ~ 6.2 Ma, suggesting unfavourable conditions for dinoflagellates on the Iceland Plateau. Besides *D. martinheadii* (up to 90% of the palynomorph assemblage) only rare *N. labyrinthus* and *I pallidum* have been recorded. This acme can be traced across the Iceland and Greenland seas into the Arctic Ocean, but although there is some uncertainty in the exact timing of this event at different sites (see Matthiessen et al., 2009 for discussion) it portrays its supraregional prevalence. The comparable composition of the dinocyst assemblage in the Central Arctic Ocean (Matthiessen et al., 2009) and the Iceland Sea suggest an increased advection of cold waters via the proto-EGC. Contemporaneously increased IRD fluxes (Fig. 26) in the Iceland Sea, on Vøring Plateau (Fronval and Jansen, 1996), and in Fram Strait (Wolf-Welling et al., 1996), and increased $\delta^{18}O$ values of planktonic foraminifera suggest a major cooling event in the Nordic Seas between 7 and 6 Ma (Fronval and Jansen, 1996), thus proving the relationship between the "*Decahedrella* event" and surface water cooling. As SSTs are still significantly higher than annual mean temperatures today they are probably biased to summer temperatures due to a generally increased seasonality in the Late Miocene as shown by Mosbrugger et al. (2005) for continental Europe. However, the observed cooling significantly precedes the establishment of large-scale glaciations in the northern hemisphere, and the vegetation changes in the high latitudes (Pound et al., 2012) and particularly on Iceland (Denk et al., 2011) are in agreement with these findings and reveal a general impoverishment and cool-temperate climate.

The Miocene/Pliocene transition (6.3–5.1 Ma)

The palynomorph record becomes patchy with low dinocyst diversity, whilst concentration and thus production is somewhat comparable to the modern Iceland Sea (Matthiessen, 1995; Marret et al., 2004). The impoverished dinocyst assemblage is dominated by *N. labyrinthus* with abundances usually associated with mean annual temperatures around 5°C in modern surface sediments (Marret and Zonneveld, 2003), which is in accordance with our reconstructed SST of 7°C at 5.8 Ma (Fig. 24). The occurrence of accessory species such as cool-water *H. tectata* and cold to temperate *Ataxodinium choane* (Edwards and Andrle, 1992; Rochon et al., 1999) depicts the prevalence of cold conditions in the Iceland Sea after ~ 6.3 Ma, as also shown for ODP Site 982 just south of the Greenland-Scotland Ridge (Hodell et al., 2001). Likewise depleted arctic-subarctic assemblages have been reported from the Miocene/Pliocene of the Labrador Sea (Head et al., 1989b; de Vernal and Mudie, 1989b; de Vernal and Mudie, 1992), Davis Strait (Piasecki, 2003), and Baffin Bay (de Vernal and Mudie, 1989a), and a Late Miocene temperature decrease has been inferred for the Norwegian Sea based on silicoflagellates (Locker and Martini, 1989). Abundant prasinophytes (mainly *C.? invaginata*) and presumably sea-ice indicative sphaeromorphitic acritarchs co-occur with significant IRD at ~ 5.4 Ma (Fronval and Jansen, 1996) and suggest colder, but also less saline and probably stratified surface waters between 5.5–5.3 Ma, a time of major global cooling and intense glaciations (Hodell and Kennett, 1986). However, sporadic advection of relatively warmer North Atlantic water to the Iceland Plateau is indicated by the occurrence of *Operculodinium israelianum* and *T. pellitum,* which both prefer summer SST > 10°C (De Schepper et al., 2011).

Early Pliocene surface stratification and elevated productivity (5.0–4.5 Ma)

The Early Pliocene is characterized by elevated marine productivity as indicated by an increase in cyst concentration, the common occurrence of *Protoperidinium* spp., and an increase in TOC, which is presumably of marine origin (Fig. 24). Coeval IRD pulses (Fig. 26; Fronval and Jansen, 1996) indicate freshwater input via melting sea-ice/icebergs likely causing surface water stratification as suggested by abundant prasinophytes (*C.? invaginata, L. crista*; Fig, 24, Appendix C1), and triggering the productivity increase. The enhanced Early Pliocene productivity in the Iceland Sea appears to be in concert with the global biogenic bloom (see Cortese et al., 2004 for discussion), but also with observations on dinocysts from the Labrador Sea (de Vernal and Mudie, 1989b) and the Vøring

Plateau (Mudie, 1989). Furthermore, common to abundant *C.*? *invaginata* in the Labrador Sea (de Vernal and Mudie, 1989b), Davis Strait (Piasecki, 2003) and Baffin Bay (de Vernal and Mudie, 1989a) indicates somewhat similar surface water conditions with temporary freshening and/or stratification on both sides of Greenland presumably related to the waxing and waning of the Greenland ice sheet.

Furthermore, the Early Pliocene SST might have been somewhat higher than in the latest Miocene, which agrees with the general consensus of a warm Early Pliocene (e.g. Lawrence et al., 2009; Salzmann et al., 2011). *Spiniferites elongatus*, a major component of the dinocyst assemblage during this phase, is usually associated with cool-temperate surface waters (Rochon et al., 1999; Marret and Zonneveld, 2003), but has highest abundances in recent sediments around Iceland underlain by the comparatively warm Irminger Current (Marret et al., 2004), and off North Norway underlain by the Norwegian-Atlantic Current (Matthiessen, 1995). Common *S. elongatus* have been also recorded during MIS5e from the Vøring Plateau (Van Nieuwenhoven et al., 2007) and the Eurasian continental margin (Matthiessen et al., 2001) associated with Atlantic water inflow. The sporadic occurrence of *Invertocysta lacrymosa*, *Impagidinium aculeatum*, *M. choanophorum*, *Corrudinium* spp., *Operculodinium tegillatum*, and *O. israelianum* indeed indicate temporary advection of North Atlantic derived warm water presumably linked to the restriction of the Panama Isthmus (Fig. 26; Haug and Tiedemann, 1998; Butzin et al., 2011).

Early Pliocene species turnover (4.5–4.3 Ma)

A pronounced last occurrence of species occurred between 4.5 and 4.3 Ma (Fig. 25, Table 4), and the longer stratigraphic range of most taxa elsewhere in lower latitudes suggests a strong climatic control on this event. Although Site 907 received only little IRD between 4.4 and 4.2 Ma (Fig. 26; Fronval and Jansen, 1996) this demonstrates a pronounced adjustment of the Iceland Sea palynomorph assemblage to changing oceanographic conditions prior to the intensification of Northern Hemisphere glaciations. Recent studies (Sarntheim et al., 2009; Verhoeven et al., 2011) indicate the onset of a northward flow of Pacific waters through Bering Strait into the Arctic Ocean at that time caused by the further restriction of the Panama Isthmus, which resulted in a considerably fresher, modern like EGC and the thermal isolation of Greenland (Sarntheim et al., 2009). Thus this species turnover is the result of both decreasing temperature and salinity, and likely reflects the establishment of the modern EGC.

Early through Late Pliocene: productivity crash and pronounced deep-water formation (4.2–2.5 Ma)
The most distinctive feature of the Pliocene is a crash in palynomorph productivity at 4.2 Ma, which significantly precedes the diatom productivity crash between 3.5 and 3.3 Ma (Stabell and Koç, 1996) and antedates the first major IRD peak at 3.3 Ma that marks the expansion of the Greenland ice sheet (Jansen et al., 2000; Kleiven et al., 2002). Thus, conditions that seriously affected palynomorph productivity have already been established in the Iceland Sea well before the onset of large-scale glaciations on Greenland.

Besides almost mono-specific *Spiniferites* spp. assemblages at 3.6 Ma, 3.4 Ma and 3.3 Ma all subsequent samples are virtually barren of marine palynomorphs (< 10 cysts/sample). Dilution by high input of terrigenous material is an unlikely cause for this barren interval, as it would have affected all microfossil groups. Moreover, as sedimentation rates are fairly constant between 7.0 and 2.5 Ma (1.5–2.5 cm/kyr) accumulation of biogenic material must have been altered by processes at the sea surface (e.g. nutrient availability, sea-ice cover) or within the deeper waters such as selective degradation and dissolution (Jansen et al., 1996). Species recorded just below this interval (*N. labyrinthus*, *I. pallidum*, *S. elongatus*) survive harsh conditions with up to 12 month per year sea-ice cover (de Vernal et al., 2001; Marret and Zonneveld, 2003) excluding sea-ice as a single cause, and nutrient availability might be excluded since diatoms have been constantly recorded in this interval (Stabell and Koc, 1996). Recent studies demonstrate a species dependent selective aerobic degradation (Zonneveld et al. 2008, 2010), and "*Impagidinium* and *Nematosphaeropsis* are clearly more resistant than TOC" (Versteegh et al., 2010; p. 177), but all other dinocysts degrade considerably faster. However, *N. labyrinthus* and *Impagidinium* spp. disappear abruptly whereas TOC even shows a slight increase (Fig. 24). Therefore, post-depositional aerobic degradation due to sinking of well-oxygenated surface waters during times of enhanced deep-water formation probably played an important role, but is unlikely the single cause. In addition, sampling might have been biased towards unfavourable conditions, and narrow intervals with abundant palynomorphs might have not been sampled. Nevertheless, this barren interval might indicate increased Pliocene overturning circulation in the Iceland Sea related to the closure of the Panama Isthmus (Haug and Tiedemann, 1998) or a submerged Greenland-Scotland Ridge (Robinson et al., 2011), as also indicated by sustained NCW production during this time (Poore et al., 2006).

5.5 Conclusions

For the interval between 14.5 and 2.5 Ma, ODP Hole 907A has been palynologically investigated on ~ 100 kyr resolution in order to provide new constraints on the Neogene paleoenvironmental evolution of the Iceland Sea. In addition, an alkenone based SST record has been constructed to portray its long-term thermal development. In general, our findings are in good accordance with the few Neogene high northern latitude proxy records available highlighting the potential for palynomorph based paleoenvironmental reconstruction.

The Middle Miocene Iceland Sea is characterized by a high marine productivity, and distinctive differences in assemblage composition compared to the Norwegian Sea suggest the prevalence of cooler waters and the establishment of a temperature gradient between both regions across the MMCT. Palynological and geochemical methods both reveal a gradual cooling trend that initiated after the MCO, and using the $U^{k'}_{37}$ index, the maximum cooling of surface waters during this period is estimated to be ~ 12°C. Superimposed, our palynomorph record depicts Miocene climate variability and transient alterations in the assemblages coincide with the MMCT (Mi-3a and Mi-3b) and the Mi-4 event, both presumably reflecting short-lived cooling periods in the Iceland Sea. Changes in dinocyst diversity and assemblage composition, however, slightly precede Mi-5 event. Substantial changes in the surface water characteristics and the onset of progressive Late Miocene cooling is indicated between 10.6 and 10.2 Ma (equivalent to Mi-6) by a pronounced cluster of species last occurrences and the first occurrence of the endemic cold-water acritarch *D. martinheadii*. In concert with a second major disappearance event between 9 and 8.4 Ma, which may coincide with Mi-7, this reflects the progressively strengthened influence of a proto-East Greenland Current in the Iceland Sea. The subsequent supraregional "*Decahedrella* event", and a contemporaneous SST decrease mark a general Late Miocene climate deterioration in the high northern latitudes at ~ 6.5 Ma. Indeed, most Neogene cooling occurred prior to 5.5 Ma, well before the initiation of large-scale northern hemisphere glaciations.

The earliest Pliocene is characterised by a transient warming, and enhanced productivity is likely related to surface stratification caused by freshwater discharge of melting icebergs/sea-ice. However, the most distinctive feature of the Pliocene palynomorph record is a pronounced species disappearance between 4.5 and 4.3 Ma, probably related to the establishment of the modern East Greenland Current, and a subsequent crash of palynomorph productivity that results in a conspicuous barren

interval. Possible explanations for this interval invoke enhanced bottom-water oxygenation due to increased Mid-Pliocene overturning circulation, and sea-ice cover but probably also a bias introduced by sample resolution. However, the timing of these events significantly precede the marked expansion of the Greenland ice-sheet and suggests a sensible adaptation of the palynomorph assemblage to climate deterioration of a magnitude that does not led to traceable records in deep-sea sediments.

Acknowledgements

This research used samples and data provided by the Ocean Drilling Program (ODP), and Walter Hale and Alex Wülbers are thanked for technical support while sampling at the IODP Core Repository Bremen. J.M. and M.S. acknowledge support by the German Research Foundation (DFG MA 3913/2).

6. Conclusions and Future perspectives

The main goal of this thesis was to thoroughly evaluate and to improve the utility of Neogene organic-walled marine palynomorphs (dinoflagellate cysts, prasinophyte algae, acritarchs) for both biostratigraphic correlation and paleoenvironmental interpretation in the (cold-water domain) high northern latitudes, an area critical for understanding the late Cenozoic development of northern hemisphere climate. To achieve this goal, Iceland Sea ODP Hole 907A, a key location due to its continuous Miocene through Pliocene sediment sequence and its pristine paleomagnetic record, has been palynologically investigated at ~ 100 kyr resolution, and the palynomorph inventory has been documented in great detail. This chapter summarizes the results of this thesis (chapters 3–5) and addresses some remaining questions and future research perspectives.

Based on the highest/lowest occurrences and highest common occurrence of 20 dinoflagellate cyst taxa and one acritarch species, 26 bioevents have been defined and calibrated to the well-defined magnetostratigraphy of Site 907. This study therefore provides first-order independent absolute age determinations on Neogene dinoflagellate cyst bioevents in the high northern latitudes for the first time (chapter 3). These bioevents have been placed into a (supra)regional framework by defining or revising events based on those published data for North Atlantic sites with independent age control. To help identify species promising for future biostratigraphic correlation with lower latitudes of the Northern Hemisphere, the data has also been compared with records from the North Sea and Mediterranean Sea basins, and the eastern U.S.A.

This study revealed that seven events are useful on a regional scale within the Nordic Seas (LO of *C. irregulare* sp. nov, HOs of *U. aquaeductus*, *B. hirsuta*, *D. martinheadii, B. micropapillata*, *R. actinocoronata*, and *L. truncatum*), but only the latter three events are suitable for supraregional correlations between mid- and high latitudes. The HO of *Hystrichosphaeropsis obscura* also allows for supraregional correlations when excluding the cold-water domain, as its position in the Iceland Sea yet remains uncertain. Furthermore, the HOs of *O. piaseckii*, *O. tegillatum*, *P. vesiculata*, and *C. devernaliae* may be potentially useful stratigraphic markers across the North Atlantic on a broader timescale, and *H. tectata, D. martinheadii, R. actinocoronata*, and *B. micropapillata* yield the potential for correlations into the Central Arctic Ocean. Most events are clearly diachronous across the North Atlantic, showing no clear pattern of appearance or disappearance, which

understandably results from a strong latitudinal control on the stratigraphic range of species, often through the earlier disappearance in the cold-water Iceland Sea than elsewhere. Finally, two important Neogene dinoflagellate cysts species have been formally described (*Cerebrocysta irregulare*, *Impagidinium elongatum*), and critically evaluated for their biostratigraphic utility. The evaluated dinoflagellate cyst and acritarch datum events of ODP Hole 907A provide an improved, magnetostratigraphically-calibrated temporal framework for analyses of Neogene sequences in the high and mid-northern latitudes, and will be of great value for future deep drilling in the northernmost North Atlantic and Arctic Ocean, in particular with respect to post-2013 IODP activities.

Future perspectives: Although this study highlights the utility of marine palynomorphs for biostratigraphy in the northernmost North Atlantic and Arctic Ocean their full potential has not been completely explored yet. Detailed high-resolution palynostratigraphic correlations are still hampered by an inconsistent taxonomy, and even more crucial, by the large number of undescribed taxa that might be potentially useful due to short stratigraphic ranges. This is particularly true for the diverse complex of prasinophytes and acritarchs. It is therefore pivotal that future work focuses on a sound taxonomy, which is prerequisite for a consistent biozonation. Furthermore, this study clearly demonstrated that our knowledge on palynomorph bioevents is biased towards the warm-water domain of the Nordic Seas and to the North Atlantic south of the Greenland-Scotland Ridge. Additional records from the Nordic Seas cold-water domain (nowadays influenced by the East Greenland Current) and the Arctic Ocean are needed to robustly confirm the findings of this study, and to define a reference biozonation for the cold-water domain. Reasonable sites for future investigations include ODP sites 987 (due to its robust magnetostratigraphy in the Late Miocene), 909, 918, and IODP Site M0002. Full geographical coverage is crucial to ultimately integrate both cold- and warm-water domain in a consistent high latitude palynomorph biochronology.

A second fundamental issue of high northern latitude Neogene palynology is the paleoecology of extinct species. Exemplarily, the paleoecological preferences of the Neogene dinoflagellate cyst complex *Batiacasphaera micropapillata*, the predominant taxon in Miocene assemblages in the Iceland Sea and Central Arctic Ocean, has been described (chapter 4). This stratigraphically important species complex has been frequently reported from Miocene through Pliocene sediments of the North Atlantic region, but its global distribution has not been studied yet, which obviously hampered accurate

ecological interpretations. To overcome this obstacle, the ODP Hole 907A record has been supplemented with new quantitative data from IODP Hole M0002A (Central Arctic Ocean), and published literature to generate global distribution maps. Distribution pattern and abundances revealed a significant zonal gradient from neritic to oceanic environments, suggesting an adaptation to outer-neritic to oceanic marine conditions and a preference for somewhat higher salinities. This species complex occurs in a broad range of temperatures from > 7°C to > 20°C, and with reference to its high abundance in the subarctic North Atlantic it is considered a warm- to cool-temperate species that is well adapted to enhanced nutrient availability and the prevailing light conditions in the high latitudes. Its general Late Miocene decline and stratigraphically important disappearance in the Pliocene are likely related to late Cenozoic cooling, and may be associated with the formation of local sea-ice in the high northern latitudes. This study demonstrated that the combination of biogeographic distribution maps with organic geochemical temperature proxies is a valid approach to decipher the paleoecology of extinct species, prerequisite for any paleoenvironmental application.

Future perspectives: It is likely that species of the *Batiacasphaera micropapillata* complex represent a phylogenetic lineage originating from one common ancestor, thus carrying distinctive stratigraphic information. The stratigraphic utility, but also the paleoecological affinities of this species complex might be refined by detailed taxonomic work including the re-examination of holotype and paratype material by means of scanning electron microscopy. A second important (high priority) issue that should be addressed in future studies is the establishment of a reference dataset for the Neogene high northern latitudes, where absolute species abundance is calibrated against independent sea-surface temperature estimates (cf. De Schepper et al., 2011). That will significantly improve the application of extinct Neogene taxa for reliable paleoenvironmental interpretations in the Arctic and subarctic seas.

The relationship between palynomorph assemblages and the paleoenvironmental evolution of the Iceland Sea has been investigated in chapter 5. In order to shed light on the long-term thermal development of the Iceland Sea surface waters the detailed palynological analysis was supplemented by the first continuous high northern latitude Neogene SST record. Both palynomorphs and geochemical methods mirror the general long-term Neogene climate deterioration that initiated after the Middle Miocene Climate Optimum, and approximate the global $\delta^{18}O$ record. The Middle Miocene is characterized

by high marine productivity and differences in assemblage composition suggest the establishment of a temperature gradient across the Nordic Seas around that time, which is likely associated with the initiation of a proto-Thermohaline Circulation. Subsequently, the diverse middle Miocene palynomorph assemblages clearly diminish towards the impoverished assemblages of the Late Pliocene whilst maximum cooling of surface waters during this period is estimated to be ~ 12°C. Superimposed on that long-term trend, changes in assemblage composition indicate a sensible response of marine palynomorphs to Miocene climate variability, and major alterations seem to partly coincide with the global Miocene isotope events (Mi-events), which reflect initial cooling trends in the Iceland Sea. Three distinctive extinction events in the Late Miocene through Early Pliocene reflect the progressive development (cooling and freshening) of a proto-East Greenland Current towards modern conditions, which finally led to thermal isolation of Greenland. The "*Decahedrella*-event" is of supraregional prevalence and marks a general Late Miocene cooling phase in the high northern latitudes at ~ 6.5 Ma associated with ice growth on the surrounding continents (as documented by increased IRD deposition) well before the initiation of large-scale northern hemisphere glaciations. The Early Pliocene is characterised by transient warming and enhanced productivity due to surface stratification caused by freshwater discharge of melting icebergs/sea-ice, whilst the succeeding productivity crash presumably depicts sustained deep-water formation, enhanced bottom-water oxygenation, and sea-ice cover due to increased meridional overturning related to the closure of the Panama Isthmus. The combinatory approach of organic-walled microfossils and alkenone paleothermometry suggests that both major alterations in marine productivity and most Neogene cooling significantly precede the marked expansion of the Greenland ice-sheet at 3.3 Ma, and it yields great potential for detailed paleoclimatic reconstructions in the largely biogenic carbonate free Neogene sediments of the high northern latitudes.

Future perspective: Marine palynomorphs from the Iceland Sea indicate a high latitude response to short-term climate variability, possibly the Miocene isotope events, and it is assumed that changes in diversity, abundance pattern, and assemblage composition might be sensitive indicators for them. However, to resolve this relationship in more detail high-resolution studies focussing on specific intervals, such as the Mi-events or the *Decahedrella* acme, are crucial. Special emphasize should be given to the very abundant and diverse complex of prasinophytes and acritarchs, as they seem to response rapidly to short-term environmental changes. The two distinctive barren intervals observed during

this study remain enigmatic but should be investigated in more detail to resolve the actual trigger for these intervals.

Alkenone-based SST reconstructions have been proven applicable in the Miocene to Pliocene of the high northern latitudes and should now be used to generate high resolution records in order to resolve the orbital- and/or millennial scale variability that occurred superimposed on the long-term Neogene cooling, and to decipher their role within the initiation of northern hemisphere glaciations during the Miocene.

Although the northern hemisphere ice-sheets are a major player within the global climate system their Miocene history, in particular the initiation of small-scale continental glaciations, is still a matter of intense debate. The Miocene (short-term) climate variability has been frequently associated with variations in the Antarctic ice-sheet, but the response of the Greenland ice-sheet to this variability yet remains enigmatic. Due to its location close to the Greenland and Iceland ice-sheets and its well-constrained age model, Site 907 is ideally suited to address this important issue at the necessary high resolution.

7. References

Aagaard, K., Swift, J.H., Carmack, E., 1985. Thermohaline circulation in the Arctic Mediterranean Seas. Journal of Geophysical Research. 90, 4833–4846.

Aagaard, K., Foldvik, A., Hillman, S.R., 1987. The West Spitsbergen Current: Disposition and Water Mass Transformation. Journal of Geophysical Research. 92, 3778–3784.

Abels, H.A., Hilgen, F.J., Krijgsman, W., Kruk, R.W., Raffi, I., Turco, E., Zachariasse, W.J., 2005. Long-period orbital control on middle Miocene global cooling: Integrated stratigraphy and astronomical tuning of the Blue Clay Formation on Malta. Paleoceanography. 20, PA4012.

Abelson, M., Agnon, A., Almogi-Labin, A., 2008. Indications for control of the Iceland plume on the Eocene-Oligocene "greenhouse-icehouse" climate transition. Earth and Planetary Science Letters. 265, 33-48.

Adl, S.M., Simpson, A.G.B., Farmer, M.A., Andersen, R.A., Anderson, O.R., Barta, J.R., Bowser, S.S., Brugerolle, G.U.Y., Fensome, R.A., Fredericq, S., James, T.Y., Karpov, S., Kugrens, P., Krug, J., Lane, C.E., Lewis, L.A., Lodge, J., Lynn, D.H., Mann, D.G., McCourt, R.M., Mendoza, L., Moestrup, Ø., Mozley-Standridge, S.E., Nerad, T.A., Shearer, C.A., Smirnov, A.V., Spiegel, F.W., Taylor, M.F.J.R., 2005. The New Higher Level Classification of Eukaryotes with Emphasis on the Taxonomy of Protists. Journal of Eukaryotic Microbiology. 52, 399–451.

Aksu, A.E. and Kaminski, M.A., 1989. Neogene and Quaternary planktonic foraminifera biostratigraphy and biochronology in Baffin Bay and Labrador Sea. In: Srivastava, S.P., Arthur, M., Clement, B. (Eds.), Proceedings of the Ocean Drilling Program, Scientific Results 105. College Station, TX, pp. 287–304.

Aksu, A.E., Hillaire-Marcel, C., 1989. Upper Miocene to Holocene oxygen and carbon isotopic stratigraphy of Sites 646 and 647, Labrador Sea. In: Srivastava, S.P., Arthur, M., Clement, B. et al., Proceedings of the Ocean Drilling Program, Scientific Results 105. College Station, TX, pp. 689–704.

Alberti, G., 1961. Zur Kenntnis mesozoischer and alttertiärer Dinoflagellaten und Hystrichosphaerideen von Nord- und Mitteldeutschland sowie einigen anderen europäischen Gebieten. Palaeontographica Abteilung A. 116, 1–58.

Amigo, A.E., 1999. Miocene silicoflagellate stratigraphy: Iceland and Rockall Plateaus. In: Raymo, M.E., Jansen, E., Blum, P., Herbert, T.D. (Eds.), Proceedings of the Ocean Drilling Program, Scientific Results 162. College Station, TX, pp. 63–81.

Anderson, D.M., Lively, J.J., Reardon, E.M., Price, C.A., 1985. Sinking characteristics of dinoflagellate cysts. Limnology and Oceanography. 30, 1000–1009.

Andersson, C., Jansen, E., 2003. A Miocene (8–12 Ma) intermediate water benthic stable isotope record from the northeastern Atlantic, ODP Site 982. Paleoceanography. 18, 1013.

Andruleit, H., 1997. Coccolithophore fluxes in the Norwegian-Greenland Sea: seasonality and assemblage alterations. Marine Micropaleontology. 31, 45–64.

Anstey, C.E., 1992. Biostratigraphic and paleoenvironmental interpretation of upper middle Miocene through lower Pleistocene dinoflagellate cyst, acritarch, and other algal palynomorph assemblages from Ocean Drilling Program Leg 105, Site 645, Baffin Bay. Unpublished MSc thesis, University of Toronto, 257 pp.

Aubry, M.P., 1993. Neogene allostratigraphy and depositional history of the De Soto Canyon area, northern Gulf of Mexico. Micropaleontology. 39, 327–366.

Backman, J., Westberg-Smith, M.J., Brown, S., Bukry, D., Edwards, L.E., Harland, R., Huddlestun, P., 1984. Biostratigraphy of Leg 81 sediments - A high latitude record. In: Roberts, D.G., Schnitker, D. et al., Initial Reports DSDP 81. U.S. Government Printing Office, Washington, D.C., pp. 855–860.

Backman, J., Moran, K., McInroy, D.B., Mayer, L.A., and the Expedition 302 Scientists, 2006. Proceedings of the Integrated Ocean Drilling Program, Volume 302. 1–43.

Backman, J., Jakobsson, M., Frank, M., Sangiorgi, F., Brinkhuis, H., Stickley, C., O'Regan, M., Løvlie, R., Pälike, H., Spofforth, D., Gattacecca, J., Moran, K., King, J., Heil, C., 2008. Age model and core-seismic integration for the Cenozoic Arctic Coring Expedition sediments from the Lomonosov Ridge. Paleoceanography. 23, PA1S03.

Barton, A.D., Dutkiewicz, S., Flierl, G., Bragg, J., Follows, M.J., Patterns of Diversity in Marine Phytoplankton. Science. 327, 1509–1511.

Batten, D.J., 1996. Colonial Chlorococcales. In: Jansonius, J. McGregor, D.C. (Eds.), Palynology: Principles and Application, Volume 1 Principles. American Association of Stratigraphic Palynologists Foundation, Dallas, pp. 191–204.

Baumann, K., H., Meggers, H., Henrich, R., 1996. Variations in surface water mass conditions in the Norwegian-Greenland Sea: evidence from Pliocene/Pleistocene calcareous plankton records (Sites 644, 907, 909). In: Thiede, J., Myhre, A.M., Firth, J.V., Johnson, G.L., Ruddiman, W.F. (Eds.), Proceedings of the Ocean Drilling Program, Scientific Results 151. College Station, TX, pp. 493–514.

Bendle, J., Rosell-Melé, A., 2004. Distributions of UK37 and UK´37 in the surface waters and sediments of the Nordic Seas: Implications for paleoceanography. Geochemistry Geophysics Geosystem. 5, Q11013.

Bendle, J., Rosell-Melé, A., Ziveri, P., 2005. Variability of unusual distributions of alkenones in the surface waters of the Nordic seas. Paleoceanography. 20, PA2001.

Benedek, P.N., Sarjeant, W.A.S., 1981. Dinoflagellate cysts from the middle and upper Oligocene of Tönisberg (Niederrheingebiet): a morphological and taxonomical restudy. Nova Hedwigia. 35, 313–356.

Berggren, W.A., Schnitker, D., 1983. Cenozoic marine environments in the North Atlantic and Norwegian-Greenland Sea. In: Bott, M.H.P., Saxov, S., Talwani, M., Thiede, J. (Eds.), Structure and development of the Greenland-Scotland Ridge: New methods and concepts. Plenum Press, New York, pp. 495–548.

Billups, K., Schrag, D.P., 2002. Paleotemperatures and ice volume of the past 27 Myr revisited with paired Mg/Ca and 18O/16O measurements on benthic foraminifera. Paleoceanography. 17, 1003.

Bleil, U., 1989. Magnetostratigraphy of Neogene and Quaternary sediment series from the Norwegian Sea: Ocean Drilling Program, Leg 104. In: Eldholm, O., Thiede, J., Taylor, E. et al., Proceedings of the Ocean Drilling Program, Scientific Results 104. College Station, TX, pp. 829–901.

Blindheim, J., 2004. Oceanography and Climate In: Skjoldal, H.R. (Eds.), The Norwegian Sea Ecosystem. Tapir Academic Press, Trondheim.

Blindheim, J., Østerhus, S., 2005. The Nordic Seas, main oceanographic features. In: Drange, H., Dokken, T., Furevik, T., Gerdes, R. (Eds.), The Nordic Seas - An integrated perspective. American Geophysical Union, Washington D.C., pp. 11–38.

Bohrmann, G., Henrich, R., Thiede, J., 1990. Miocene to Quaternary paleoceanography in the northern North Atlantic: Variability in carbonate and biogenic opal accumulation In: Bleil, U., Thiede, J. (Eds.), Geological History of Polar Oceans: Arctic versus Antarctic. Kluwer Academic Publisher, Dordrecht, pp. 647–675.

Bonnet, S., de Vernal, A., Gersonde, R., Lembke-Jene, L., 2012. Modern distribution of dinocysts from the North Pacific Ocean (37–64N, 144E–148W) in relation to hydrographic conditions, sea-ice and productivity. Marine Micropaleontology. 84, 87–113.

Bordovskiy, O.K., 1965. Sources of organic matter in marine basins. Marine Geology. 3, 5–31.

Bott, M.H.P., 1983. Deep structure and geodynamics of the Greenland-Scotland Ridge: An introductory review. In: Bott, M.H.P., Saxov, S., Talwani, M., Thiede, J. (Eds.), Structure and development of the Greenland-Scotland Ridge: New methods and concepts. Plenum Press, New York, pp. 3–10.

Brassell, S.C., Eglinton, G., Marlowe, I.T., Pflaumann, U., Sarnthein, M., 1986. Molecular stratigraphy: a new tool for climatic assessment. Nature. 320, 129–133.

Brenner, W., Biebow, N., 2001. Missing autofluorescence of rcent and fossil dinoflagellate cysts - an indicator of heterotrophy? Neues Jahrbuch für Geologie und Paläntologie, Abhandlungen. 219, 229–240.

Brinkhuis, H., Munsterman, D.K., Sengers, S., Sluijs, A., Warnaar, J., Williams, G.L., 2003. Late Eocene-Quaternary dinoflagellate cysts from ODP Site 1168, off Western Tasmania. In: Exon, N.F., Kennett, J.P. & Malone, M.J. (Eds.), Proceedings of the Ocean Drilling Program, Scientific Results 189. College Station, TX, pp. 1–36.

Broecker, W.S., 1991. The great ocean conveyor. Oceanography. 4, 79–89.

Brown, S., Downie, C., 1985. Dinoflagellate cyst stratigraphy of Paleocene to Miocene sediments from the Goban Spur (Sites 548–550, Leg 80). In: Graciansky, P.C., Poag, C.W. et al., Initial Reports DSDP 80. U.S. Government Printing Office, Washington, D.C., pp. 643–651.

Bruns, P., Dullo, W.-C., Hay, W.W., Frank, M., Kubik, P., 1998. Hiatuses on Vøring Plateau: sedimentary gaps or preservation artifacts? Marine Geology. 145, 61–84.

Bujak, J.P. 1984. Cenozoic dinoflagellate cysts and acritarchs from the Bering Sea and northern North Pacific, DSDP Leg 19. Micropaleontology. 30, 180–212.

Bujak, J.P., Davis, D.H., 1981. Neogene dinoflagellate cysts from the Hunt Dome KOPANOAR M-13 Well, Beaufort Sea, Canada. Bulletin of Canadian Petroleum Geology. 29, 420–425.

Bujak, J.P., Matsuoka, K., 1986. Late Cenozoic dinoflagellate cyst zonation in the western and northern Pacific. In: Wrenn, J.H., Duffield, S.L., Stein, J.A. (Eds.), Papers from the first symposium on Neogene dinoflagellate cyst biostratigraphy. AASP Contributions Series 17. American Association of Stratigraphic Palynologists Foundation, Dallas, Texas, pp. 7–25.

Butt, F.A., Elverhøi, A., Forsberg, C.F., Solheim, A., 2001. Evolution of the Scoresby Sund Fan, central East Greenland - evidence from ODP Site 987. Norwegian Journal of Geology. 81, 3–15.

Butzin, M., Lohmann, G., Bickert, T., 2011. Miocene ocean circulation inferred from marine carbon cycle modeling combined with benthic isotope records. Paleoceanography. 26, PA1203.

Canninga, G., Zijderveld, J.D.A., van Hinte, J., 1987. Late Cenozoic magnetostratigraphy of Deep Sea Drilling Project Hole 603C, Leg 93, on the North American continental rise off Cape Hatteras. In: van Hinte, J., Wise, S.W.J. et al., Initial Reports DSDP 93. U.S. Government Printing Office, Washington, D.C., pp. 839–848.

Channell, J.E.T., Amigo, A.E., Fronval, T., Rack, F., Lehman, B., 1999a. Magnetic stratigraphy at Sites 907 and 985 in the Norwegian–Greenland Sea and a revision of the Site 907 composite section. In: Raymo, M.E., Jansen, E., Blum, P., Herbert, T.D. (Eds.), Proceedings of the Ocean Drilling Program, Scientific Results 162, College Station, TX, pp. 131–148.

Channell, J.E.T., Smelror, M., Jansen, E., Higgins, S.M., Lehman, B., Eidvin, T., Solheim, A., 1999b. Age models for glacial fan deposits off East Greenland and Svalbard (Sites 986 and 987). In: Raymo, M.E., Jansen, E., Blum, P., Herbert, T.D. (Eds.), Proceedings of the Ocean Drilling Program, Scientific Results 162. College Station, TX, pp. 149–166.

Ciesielski, P.F., Case, M.S., 1989. Neogene paleoceanography of the Norwegian Sea based upon silicoflagellate assemblage changes in ODP Leg 104 sedimentary sequences. In: O. Eldholm, O., Thiede, J. Taylor, E. (Eds), Proceedings of the Ocean Drilling Program, Scientific Results 104. College Station, TX, pp. 527–542.

Clark, D.L., Chern, L.A., Hogler, J.A., Mennicke, C.M., Atkins, E.D., 1990. Late Neogene climate evolution of the central Arctic Ocean. Marine Geology. 93, 69–94.

Clark, P.U., Pisias, N.G., Stocker, T.F., Weaver, A.J., 2002. The role of the thermohaline circulation in abrupt climate change. Nature. 415, 863–869.

Clement, B., Robinson, F., 1987. Magnetostratigraphy of Leg 94 sediments. In: Ruddiman, W.F., Kidd, R.B., Thomas, E. et al., Initial Reports DSDP 94. U.S. Government Printing Office, Washington, D.C., pp. 635–650.

Conte, M.H., Sicre, M.-A., Rühlemann, C., Weber, J.C., Schulte, S., Schulz-Bull, D., Blanz, T., 2006. Global temperature calibration of the alkenone unsaturation index (UK´37) in surface waters and comparison with surface sediments. Geochemistry Geophysics Geosystem. 7, Q02005.

Cortese, G., Gersonde, R., Hillenbrand, C.-D., Kuhn, G., 2004. Opal sedimentation shifts in the World Ocean over the last 15 Myr. Earth and Planetary Science Letters. 224, 509–527.

Costa, L.I., Downie, C., 1979. Cenozoic dinocyst stratigraphy of Sites 403 to 406 (Rockall Plateau) IPOD, Leg 48. In: Montadert, L., Roberts, D.G. et al., Initial Reports DSDP 48. U.S. Government Printing Office, Washington, D.C., pp. 513–529.

Crane, K., Eldholm, O., Myhre, A.M., Sundvor, E., 1982. Thermal implications for the evolution of the Spitsbergen transform fault. Tectonophysics. 89, 1–32.

Dale, B., 1976. Cyst formation, sedimentation, and preservation: Factors affecting dinoflagellate assemblages in recent sediments from trondheimsfjord, Norway. Review of Palaeobotany and Palynology. 22, 39–60.

Dale, B., 1992. Dinoflagellate contributions to the open ocean sediment flux. In: Dale, B., Dale, A. L. (Eds.), Dinoflagellate contributions to the dep sea, Ocean Biocenosis Series 5. Woods Hole Oceanographic Institution, Woods Hole.

Dale, B., 1996. Dinoflagellate cyst ecology: modelling and geological applications. In: Jansonius, J., McGregor, D.C. (Eds.), Palynology: Principles and Applications, Volume 3 Applications. American Association of Stratigraphic Palynologists Foundation, Dallas, pp. 1249–1275.

Dale, B., Dale, A., 2002. Environmental applications of dinoflagellate cysts and acritarchs. In: K. Haslett (Editor), Quaternary environmental micropaleontology. Oxford University Press, London, pp. 207–240.

Darby, D.A. 2008. Arctic perennial ice cover over the last 14 million years. Paleoceanography. 23, PA1S07.

Davis, L.L., McIntosh, W.C., 1996. The petrology and 40Ar/39Ar age of tholeiitic basalt recovered from Hole 907A, Iceland Plateau. In: Thiede, J., Myhre, A.M., Firth, J.V., Johnson, G.L., Ruddiman, W.F. (Eds.), Proceedings of the Ocean Drilling Program, Scientific Results 151. College Station, TX, pp. 351–365.

de Boer, B., van de Wal, R.S.W., Bintanja, R., Lourens, L.J., Tuenter, E., 2010. Cenozoic global ice-volume and temperature simulations with 1-D ice-sheet models forced by benthic ^{18}O records. Annals of Glaciology. 51, 23–33.

de Kaenel, E., Villa, G., 1996. Oligocene–Miocene calcareous nannofossil biostratigraphy and paleoecology from the Iberia Abyssal Plain. In: Whitmarsh, R.B., Sawyer, D.S., Klaus, A., Masson, D.G. (Eds.), Proceedings of the Ocean Drilling Program, Scientific Results 149. College Station, TX, pp. 79–145.

de Leeuw, J.W., Versteegh, G.J.M., van Bergen, P.F., 2006. Biomacromolecules of plants and algae and their fossil analogues. Plant Ecology. 189, 209–233.

De Schepper, S., Head, M.J., 2008. Age calibration of dinoflagellate cyst and acritarch events in the Pliocene–Pleistocene of the eastern North Atlantic (DSDP Hole 610A). Stratigraphy. 5, 137–161.

De Schepper, S. & Head, M.J. 2009. Pliocene and Pleistocene dinoflagellate cyst and acritarch zonation of DSDP Hole 610A, eastern North Atlantic. Palynology. 33, 179–218.

De Schepper, S., Head, M.J. and Louwye, S., 2004. New dinoflagellate cyst and incertae sedis taxa from the Pliocene of northrn Belgium, southern North Sea basin. Journal of Paleontology. 78, 625–644.

De Schepper, S., Head, M.J., Louwye, S., 2008. Pliocene dinoflagellate cyst stratigraphy, palaeoecology and sequence stratigraphy of the Tunnel-Canal Dock, Belgium. Geological Magazine. 146, 92–112.

De Schepper, S., Fischer, E., Groeneveld, J., Head, M.J., Matthiessen, J., 2011. Deciphering the palaeoecology of Late Pliocene and Early Pleistocene dinoflagellate cysts. Palaeogeography, Palaeoclimatology, Palaeoecology. 309, 17–32.

de Vernal, A., Mudie, P., 1989a. Late Pliocene to Holocene palynostratigraphy at ODP Site 645, Baffin Bay. In: Srivastava, S.P., Arthur, M., Clement, B. et al., Proceedings of the Ocean Drilling Program, Scientific Results 105. College Station, TX, pp. 387-399.

de Vernal, A., Mudie, P., 1989b. Pliocene and Pleistocene palynostratigraphy at ODP Sites 646 and 647, eastern and southern Labrador Sea. In: Srivastava, S.P., Arthur, M., Clement, B. et al., Proceedings of the Ocean Drilling Program, Scientific Results 105. College Station, TX, pp. 401–422.

de Vernal, A., Mudie, P., 1992. Pliocene and Quaternary dinoflagellate cyst stratigraphy in the Labrador Sea: paleoenvironmental implications. In: Head, M.J., Wrenn, J.H. (Eds.),

Neogene and Quaternary Dinoflagellate Cysts and Acritarchs. American Association of Stratigraphic Palynologists Foundation, Dallas, Texas, pp. 329– 346.

de Vernal, A., Rochon, A., Turon, J.-L., Matthiessen, J., 1997. Organic-walled dinoflagellate cysts: Palynological tracers of sea-surface conditions in middle to high latitude marine environments. Geobios. 30, 905–920.

de Vernal, A., Henry, J., Matthiessen, J., Mudie, P., Rochon, A., Boessenkool, K.P., Eynaud, F., Grosfjeld, K., Guiot, J., Hamel, D., Harland, R., Head, M.J., Kunz-Pirrung, M., Levac, E., Loucheur, V., Peyron, O., Pospelova, V., Radi, T., Turon, J.L., Voronina, E., 2001. Dinflagellate cyst assemblages as tracers of sea-surface conditins in the northern North Atlantic, Arctic, and sub-Arctic seas: the new "n=677" data base and its application for quantitative paleoceanographic reconstruction. Journal of Quaternary Science. 16, 681–698.

de Vernal, A., Eynaud, F., Henry, M., Hillaire-Marcel, C., Londeix, L., Mangin, S., Matthiessen, J., Marret, F., Radi, T., Rochon, A., Solignac, S., Turon, J.L., 2005. Reconstruction of sea-surface conditions at middle to high latitudes of the Northern Hemisphere during the Last Glacial Maximum (LGM) based on dinoflagellate cyst assemblages. Quaternary Science Reviews. 24, 897–924.

de Verteuil, L., 1996. Data Report: Upper Cenozoic dinoflagellate cysts from the continental slope and rise off New Jersey. In: Mountain, G.S., Miller, K.G., Blum, P., Poag, C.W. (Eds.), Proceedings of the Ocean Drilling Program, Scientific Results 150. College Station, TX, pp. 439–454.

de Verteuil, L., 1997. Palynological delineation and regional correlation of Lower through Upper Miocene sequences in the Cape May and Atlantic City boreholes, New Jersey coastal plain. In: Miller, K.G., Snyder, S.W. (Eds.), Proceedings of the Ocean Drilling Program, Scientific Results 150X. College Station, TX, pp. 129–145.

de Verteuil, L., Norris, G., 1996. Miocene dinoflagellate stratigraphy and systematics of Maryland and Virginia. Micropaleontology. 42(supplement), 1–172.

DeConto, R.M., Pollard, D., Wilson, P.A., Palike, H., Lear, C.H., Pagani, M., 2008. Thresholds for Cenozoic bipolar glaciation. Nature, 455, 652–656.

Denk, T., Grímsson, F., Kvaček, Z., 2005. The Miocene floras of Iceland and their significance for late Cainozoic North Atlantic biogeography. Botanical Journal of the Linnean Society. 149, 369–417.

Denk, T., Grímsson, F., Zetter, R. and Símonarson, L.A., 2011. Late Cenozoic floras of Iceland - 15 million years of vegetation and climate history in the northern North Atlantic. Springer, Heidelberg, 854 pp.

Devillers, R., de Vernal, A., 2000. Distribution of dinoflagellate cysts in surface sediments of the northern North Atlantic in relation to nutrient content and productivity in surface waters. Marine Geology. 166, 103-124.

Doré, A.G., 1991. The structural foundation and evolution of Mesozoic seaways between Europe and the Arctic. Palaeogeography, Palaeoclimatology, Palaeoecology. 87, 441–492.

Drange, H., Dokken, T., Furevik, T., Gerdes, R., Berger, W., Nesje, A., Orvik, K.A., Skagseth, O., Skjelvan, I. and Osterhus, S., 2005. The Nordic Seas: An Overview. In: H. Drange, T. Dokken, T. Furevik, R. Gerdes et al. (Editors), The Nordic Seas - An integrated perspective. American Geophysical Union, Washington, D.C., pp. 1–10.

Drugg, W. S. 1970. Some new genera, species and combinations of phytoplankton from the Lower Tertiary of the Gulf Coast, U.S.A. Proceedings of the North American Paleontological Convention, Chicago, September 1969, part G, 809–843.

Dybkjær, K., 2004. Dinocyst stratigraphy and palynofacies studies used for refining a sequence stratigraphic model – uppermost Oligocene to lower Miocene, Jylland, Denmark. Review of Palaeobotany and Palynology. 131, 201–249.

Dybkjær, K., Piasecki, S., 2010. Neogene dinocyst zonation for the eastern North Sea Basin, Denmark. Review of Palaeobotany and Palynology. 161, 1–29.

Eberli, G.P., Swart, P.K., McNeill, D.F., Kenter, J.A.M., Anselmetti, F.S., Melim, L.A., Ginsburg, R.N., 1997. A synopsis of the Bahamas Drilling Project: Results from two deep core borings drilled on the Great Bahamas Bank. In: Eberli, G.P., Swart, P.K., Malone, M.J.

(Eds.), Proceedings of the Ocean Drilling Program, Initial Reports 166. College Station, TX, pp. 23–41.

Edwards, L.E., 1984. Miocene dinocysts from Deep Sea Drilling Project Leg 81, Rockall Plateau, eastern North Atlantic. In: Roberts, D.G., Schnitker, D. et al.., Initial Reports DSDP 81. U.S. Government Printing Office, Washington, D.C., pp. 581–594.

Edwards, L.E., 1986. Late Cenozoic dinoflagellate cysts from South Carolina, U.S.A. In: Wrenn, J.H., Duffield, S.L., Stein, J.A. (Eds.), Papers from the first symposium on Neogene dinoflagellate cyst biostratigraphy. AASP Contributions Series 17. American Association of Stratigraphic Palynologists Foundation, Dallas, Texas, pp. 47-57.

Edwards, L. E., Mudie, P., de Vernal, A., 1991. Pliocene paleoclimatic reconstruction using dinoflagellate cysts: Comparison of methods. Quaternary Science Reviews. 10, 259–274.

Ehlers, B.M., Jokat, W., 2009. Subsidence and crustal roughness of ultra-slow spreading ridges in the northern North Atlantic and Arctic Ocean. Geophysical Journal International. 177, 451–462.

Eldholm, O., Skogseid, J., Sundvor, E., Myhre, A.M., 1990. The Norwegian Greenland Sea. In: Grantz, A., Johnson, L., Sweeney, J.L. (Eds.), The Arctic Ocean Region. Geological Society of America, pp. 351–364.

Eldrett, J.S., Harding, I.C., Wilson, P.A., Butler, E., Roberts, A.P., 2007. Continental ice in Greenland during the Eocene and Oligocene. Nature. 446, 176–179.

Ellegaard, M., Lewis, J., Harding, I., 2002. Cyst–theca relationship, life cycle, and effects of temperature and salinity on the cyst morphology of *Gonyaulax baltica* sp. nov. (Dinophyceae) from the Baltic Sea area. Journal of Phycology. 38, 775–789.

Engel, E.R., 1992. Palynologische Evidenz klimarelevanter Ereignisse in miozänen Sedimenten des Nordatlantiks. Geologisches Jahrbuch A. 125, 3–39.

Engen, Ø., Faleide, J.I., Dyreng, T.K., 2008. Opening of the Fram Strait gateway: A review of plate tectonic constraints. Tectonophysics. 450, 51-69.

Evitt, W.R., 1985. Sporopollenin dinoflagellate cysts. their morphology and interpretation. American Association of Stratigraphic Palynologists, Dallas, 333 pp.

Esper, O. and Zonneveld, K.A.F., 2007. The potential of organic-walled dinoflagellate cysts for the reconstruction of past sea-surface conditions in the Southern Ocean. Marine Micropaleontology, 65(3-4): 185-212.

Faleide, J.I., Vågnes, E., Gudlaugsson, S.T., 1992. Late Mesozoic-Cenozoic evolution of the southwestern Barents Sea in a regional rift-shear tectonic setting. Marine and Petroleum Geology. 10, 186–214.

Fensome, R.A., Williams, G.L., 2004. The Lentin and Williams index of fossil dinoflagellates 2004 Edition. AASP Contributions Series 42. American Association of Stratigraphic Palynologists Foundation, Dallas, Texas, 909 pp.

Fensome, R.A., Williams, G.L., Barss, M.S., Freeman, J.M., Hill, J.M., 1990. Acritarchs and fossil prasinophytes: an index to genera, species and infraspecific taxa. American Association of Stratigraphic Palynologists, Contributions Series 25. 1–771.

Fensome, R.A., Taylor, F.J.R., Norris, G., Sarjeant, W.A.S., Wharton, D.I., Williams, G.L., 1993. A classification of living and fossil dinoflagellates. Micropaleontology, Special Publication Number 7. 351 pp.

Firth, J.V., 1996. Upper middle Eocene to Oligocene dinofagellate biostratigraphy and assemblage variations in Hole 913B, Greenland Sea. In: Thiede, J., Myhre, A.M., Firth, J.V., Johnson, G.L., Ruddiman, W.F. (Eds.), Proceedings of the Ocean Drilling Program, Scientific Results 151. College Station, TX, pp. 203–242.

Flower, B.P., Kennett, J.P., 1994. The middle Miocene climatic transition: East Antarctic ice sheet development, deep ocean circulation and global carbon cycling. Palaeogeography, Palaeoclimatology, Palaeoecology. 108, 537–555.

Frank, M., Backman, J., Jakobsson, M., Moran, K., O'Regan, M., King, J., Haley, B.A., Kubik, P.W., Garbe-Schönberg, D., 2008. Beryllium isotopes in central Arctic Ocean sediments over the past 12.3 million years: Stratigraphic and paleoclimatic implications. Paleoceanography. 23, PA1S02.

Fronval, T., Jansen, E., 1996. Late Neogene paleoclimates and paleoceanography in the Iceland–Norwegian Sea: Evidence from the Iceland and Vøring Plateaus. In: Thiede, J., Myhre,

A.M., Firth, J.V., Johnson, G.L., Ruddiman, W.F. (Eds.), Proceedings of the Ocean Drilling Program, Scientific Results 151. College Station, TX, pp. 455–468.

Gartner, S., Shyu, J.-P., 1996. Aspects of calcareous nannofossil biostratigraphy and abundance in the Pliocene and Late Miocene of Site 905. In: Mountain, G.S., Miller, K.G., Blum, P., Poag, C.W. (Eds.), Proceedings of the Ocean Drilling Program, Scientific Results 150. College Station, TX, pp. 53–62.

Goll, R.M., 1989. A synthesis of Norwegian Sea biostratigraphies: ODP Leg 104 on the Vøring Plateau. In: Eldholm, O., Thiede, J., Taylor, E. et al., Proceedings of the Ocean Drilling Program, Scientific Results 104. College Station, TX, pp. 777–826.

Goll, R.M., Bjørklund, K., 1989. A new radiolarian biostratigraphy for the Neogene of the Norwegian Sea: ODP Leg 104. In: Eldholm, O., Thiede, J., Taylor, E. et al., Proceedings of the Ocean Drilling Program, Scientific Results 104. College Station, TX, pp. 697–737.

Guerstein, R. G., Junciel, G. J. 2001. Quistes de Dinoflagelados del Cenozoico de la Cuneca del Colorado, Argentina. Ameghiniana. 38, 299–316.

Guiot, J., De Vernal, A., 2007. Transfer functions: methods for quantitative paleoceanography. Quaternary Science Reviews. 30, 1965–1972.

Guler, V. M., Guerstein, R. G. 2003., Quistos de dinoflagelados (Cladopyxiaceae, Gonyaulacaceae, Goniodomaceae e Incierta) del Oligoceno-Plioceno temperano de la Cuenca del Colorado, Argentina. Revista Española de Paleontologìa. 18, 23–47.

Guy-Ohlson, 1996. Prasinophycean algae. In: Jansonius, J., McGregor, D.C. (Eds.), Palynology: Principles and Application, Volume 1 Principles. American Association of Stratigraphic Palynologists Foundation, Dallas, pp. 181–190.

Hailwood, E.A., 1979. Paleomagnetism of late Mesozoic to Holocene sediments from the Bay of Biscay and Rockall Plateau, drilled on IPOD Leg 48. In: Montadert, L., Roberts, D.G. et al., Initial Reports DSDP 48. U.S. Government Printing Office, Washington, D.C., pp. 305–339.

Haley, B.A., Frank, M., Spielhagen, R., Fietzke, J., 2008. Radiogenic isotope record of Arctic Ocean circulation and weathering inputs of the past 15 million years. Paleoceanography 23, PA1S13.

Hannah, M.J., 2006. The palynology of ODP site 1165, Prydz Bay, East Antarctica: A record of Miocene glacial advance and retreat. Palaeogeography, Palaeoclimatology, Palaeoecology. 231, 120–133.

Hannah, M.J., Wrenn, J.H., Wilson, G.J., 1998. Early Miocene and Quaternary marine palynomorphs from Cape Roberts Project CRP-1, McMurdo Sound, Antarctica. Terra Antarctica. 5, 527–538.

Hansen, B., Østerhus, S., 2000. North Atlantic–Nordic Seas exchanges. Progress in Oceanography. 45, 109–208.

Harland, R., 1979. Dinoflagellate biostratigraphy of Neogene and Quaternary sediments at Holes 400/400A in the Bay of Biscay (Deep Sea Drilling Project Leg 48). In: Montadert, L., Roberts, D.G. et al., Initial Reports DSDP 48. U.S. Government Printing Office, Washington, D.C., pp. 531–545.

Harland, R., 1982. Recent dinoflagellate cysts from the southern Barents Sea. Palynology. 6, 9–18.

Harland, R., 1983. Distribution maps of recent dinoflagellate cysts in bottom sediments from the North Atlantic Ocean and adjecant seas. Paleontology. 26, 321–387.

Harland, R., Pudsey, C.J., 1999. Dinoflagellate cysts from sediment traps deployed in the Bellingshausen, Weddell and Scotia seas, Antarctica. Marine Micropaleontology. 37, 77–99.

Harland, R., Reid, J.R., Dobell, P., Norris, G., 1980. Recent and sub-recent dinoflagellate cysts from the Beaufort Sea, Canadian Arctic. Grana. 19, 211–225.

Haug, G.H., Tiedemann, R., 1998. Effect of the formation of the Isthmus of Panama on Atlantic Ocean thermohaline circulation. Nature. 393, 673–676.

Head, M.J., 1993. Dinoflagellates, sporomorphs, and other palynomorphs from the Upper Pliocene St. Erth Beds of Cornwall, southwestern England. Journal of Paleontology. 67, 1–61.

Head, M.J., 1994. Morphology and paleoenvironmental significance of the Cenozoic dinoflagellate genera Tectatodinium and Habibacysta. Micropaleontology. 40, 289–321.

Head, M.J., 1996. Late Cenozoic dinoflagellates from the Royal Society borehole at Ludham, Norfolk, eastern England. Journal of Paleontology. 70, 543–570.

Head, M.J., 1997. Thermophilic dinoflagellate assemblages from the mid Pliocene of eastern England. Journal of Paleontology. 71, 165–193.

Head, M.J., 1998a. Marine environmental change in the Pliocene and early Pleistocene of eastern England: the dinoflagellate evidence reviewed. Mededelingen Nederlands Institut voor Toegepaste Geowetenschappen TNO. 60, 199–226.

Head, M.J, 1998b. Pollen and dinoflagellates from the Red Crag at Walton-on-the Naze, Essex: evidence for a mild climatic phase during the early late Pliocene of eastern England. Geological Magazine. 135, 803–817.

Head, M.J., 1999. The Late Pliocene St. Erth Beds of Cornwall: a review of the palynology and reappraisal of the dinoflagellates. In: Scource, J., Furze, M.F.A. (Eds.), The Quaternary of West Cornwall. Field Guide. Quaternary Research Association, Durham, U.K., pp. 88–92.

Head, M.J., Wrenn, J.H., 1992. A forum on Neogene and Quaternary dinoflagellate cysts: the edited transcript of a round table discussion held at the Second Workshop on Neogene dinoflagellates. In: Head, M.J., Wrenn, J.H. (Eds.), Neogene and Quaternary Dinoflagellate Cysts and Acritarchs. American Association of Stratigraphic Palynologists Foundation, Dallas, Texas, pp. 1–31.

Head, M.J., Westphal, H., 1999. Palynology and paleoenvironments of a Pliocene carbonate platform: The Clino core, Bahamas. Journal of Paleontology. 73, 1–25.

Head, M.J., Norris, G., 2003. New species of dinoflagellate cysts and other palynomorphs from the latest Miocene and Pliocene of DSDP Hole 603, western North Atlantic. Journal of Paleontology. 77, 1–15.

Head, M.J., Norris, G., Mudie, P., 1989a. New species of dinocysts and a new species of acritarch from the upper Miocene and lowermost Pliocene, ODP Leg 105, Site 646, Labrador Sea. In: Srivastava, S.P., Arthur, M., Clement, B. et al., Proceedings of the Ocean Drilling Program, Scientific Results 105. College Station, TX, pp. 453–466.

Head, M.J., Norris, G., Mudie, P., 1989b. Palynology and dinocyst stratigraphy of the Miocene in ODP Leg 105, Hole 645E, Baffin Bay. In: Srivastava, S.P., Arthur, M., Clement, B. et al., Proceedings of the Ocean Drilling Program, Scientific Results 105. College Station, TX, pp. 467–514.

Head, M.J., Norris, G., Mudie, P., 1989c. Palynology and dinocyst stratigraphy of the upper Miocene and lowermost Pliocene, ODP Leg 105, Site 646, Labrador Sea. In: Srivastava, S.P., Arthur, M., Clement, B. et al., Proceedings of the Ocean Drilling Program, Scientific Results 105. College Station, TX, pp. 423–451.

Head, M.J., Riding, J.B., Eidvin, T., Chadwick, R.A., 2004. Palynological and foraminiferal biostratigraphy of (Upper Pliocene) Nordland Group mudstones at Sleipner, northern North Sea. Marine and Petroleum Geology. 21, 277–297.

Heinrich, S., Zonneveld, K.A.F., Bickert, T., Willems, H., 2011. The Benguela upwelling related to the Miocene cooling events and the development of the Antarctic Circumpolar Current: Evidence from calcareous dinoflagellate cysts. Paleoceanography. 26, PA3209.

Helland, P.E., Holmes, M.A., 1997. Surface textural analysis of quartz sand grains from ODP Site 918 off the southeast coast of Greenland suggests glaciation of southern Greenland at 11 Ma. Palaeogeography, Palaeoclimatology, Palaeoecology. 135, 109-121.

Henrich, R., Wolf, T., Bohrmann, G. and Thiede, J., 1989. Cenozoic paleoclimatic and paleoceanographic changes in the northern hemisphere revealed by variability of coarse-fraction composition in sediments from the Vøring Plateau - ODP Leg 104 drill sites. In: Eldholm, O., Thiede, J., Taylor, E. et al., Proceedings of the Ocean Drilling Program, Scientific Results 104. College Station, TX, pp. 75–188.

Henrich, R, Baumann, K.-H., Huber, R., Meggers, H., 2002. Carbonate preservation records of the past 3 Myr in the Norwegian-Greenland Sea and the northern North Atlantic: implications for the history of NADW production. Marine Geology. 184, 17–39.

Herbert, T.D., Schuffert, J.D., 1998. Alkenone unsaturation estimtes for Late Miocene through Late Pliocene sea-surface temperatures at Site 985. In: J.V. Firth, J.V. (Eds.), Proceedings of the Ocean Drilling Program, Scientific Results 159T. College Station, TX, pp. 17–21.

Herold, N., Huber, M., Müller, R.D., Seton, M., 2012. Modeling the Miocene climatic optimum: Ocean circulation. Paleoceanography. 27, PA1209.

Holzwarth, U., Esper, O., Zonneveld, K., 2007. Distribution of organic-walled dinoflagellate cysts in shelf surface sediments of the Benguela upwelling system in relationship to environmental conditions. Marine Micropaleontology. 64, 91–119.

Holzwarth, U., Esper, O., Zonneveld, K.A.F., 2010. Organic-walled dinoflagellate cysts as indicators of oceanographic conditions and terrigenous input in the NW African upwelling region. Review of Palaeobotany and Palynology. 159, 35–55.

Honjo, S., 1996. Fluxs of particles to the interior of the open oceans. In: Ittekkot, V., Schäfer, P., Honjo, S., Depetris, P.J. (Eds.), Particle flux in the ocean. John Wiley & Sons, Chichester, pp. 91–154.

Huang, Y., Clemens, S.C., Liu, W., Wang, Y., Prell, W.L., 2007. Large-scale hydrological change drove the late Miocene C4 plant expansion in the Himalyan foreland and Arabian Peninsula. Geology. 35, 531–534.

Hull, D.M., 1996. Paleoceanography and biostratigraphy of Paleogene radiolarians from the Norwegian-Greenland Sea. In: Thiede, J., Myhre, A.M., Firth, J.V., Johnson, G.L., Ruddiman, W.F. (Eds.), Proceedings of the Ocean Drilling Program, Scientific Results 151. College Station, TX, pp. 125–152.

Ikehara, M., Kawamura, K., Ohkouchi, N., Asahiko, T., 1999. Organic geochemistry of greenish clay and organic-rich sediments since the Early Miocene from Hole 985A, Norway Basin. In: Raymo, M.E., Jansen, E., Blum, P., Herbert, T.D. (Eds.), Proceedings of the Ocean Drilling Program, Scientific Results 162, College Station, TX, pp. 209–216.

Jakobsson, M., Backman, J., Rudels, B., Nycander, J., Frank, M., Mayer, L., Jokat, W., Sangiorgi, F., O'Regan, M., Brinkhuis, H., King, J., Moran, K., 2007. The early Miocene onset of a ventilated circulation regime in the Arctic Ocean. Nature. 447, 986–990.

Jansen, E., Sjøholm, J., 1991. Reconstruction of glaciation over the past 6 Myr from ice-born deposits in the Norwegian Sea. Nature. 349, 600–603.

Jansen, E., Fronval, T., Rack, F., Channell, J.E.T., 2000. Pliocene-Pleistocene Ice Rafting History and Cyclicity in the Nordic Seas During the Last 3.5 Myr. Paleoceanography. 15, 709–721.

Jansen, E., Raymo, M.E. and Blum, P., 1996. Proceedings of the Ocean Drilling Program, Initial Reports 162. 1182 pp.

Jansen, E., Fronval, T., Rack, F., Channell, J.E.T., 2000. Pliocene-Pleistocene Ice Rafting History and Cyclicity in the Nordic Seas During the Last 3.5 Myr. Paleoceanography. 15, 709–721

Japsen, P., Bonow, J.M., Green, P.F., Chalmers, J.A., Lidmar-Bergström, K., 2006. Elevated, passive continental margins: Long-term highs or Neogene uplifts? New evidence from West Greenland. Earth and Planetary Science Letters. 248, 330–339.

Jarvis, J.I., Tocher, B.A., 1985. Neogene and Quaternary dinoflagellate biostratigraphy of the Eastern Equatorial Pacific: Deep Sea Drilling Project Leg 85. In: Mayer, L., Theyer, F. (Eds.), Initial Reports DSDP 85. College Station, TX, pp. 407–412.

Jiménez-Moreno, G., Head, M.J., Harzhauser, M., 2006. Early and Middle Miocene dinoflagellate cyst stratigraphy of the Central Paratethys, Central Europe. Journal of Micropalaeontology. 25, 113–119.

Johannessen, O.M., 1986. Brief overview of the physical oceanography. In: Hurdle, B.G. (Eds.), The Nordic Seas, Springer Verlag, Heidelberg, pp. 103–124.

John, C.M., Karner, G.D., Browning, E., Leckie, R.M., Mateo, Z., Carson, B., Lowery, C., 2011. Timing and magnitude of Miocene eustasy derived from the mixed siliciclastic-carbonate stratigraphic record of the northeastern Australian margin. Earth and Planetary Science Letters. 304, 455–467.

Kaminski, M.A., 2007. Fauna contraints for the timing of the Fram Strait opening: The record of Miocene deep-water agglutinated foraminifera from IODP Hole M0002A, Lomonosov Ridge. IODP Newsletter UK. 32, 18–20.

Kaminski, M.A., Gradstein, F.M., Scott, B.D., Mackinnon, K.D., 1989. Neogene benthic foraminifer biostratigraphy and deep-water history of Sites 645, 646, and 647, Baffin Bay and Labrador Sea. In: Srivastava, S.P., Arthur, M., Clement, B. et al., Proceedings of the Ocean Drilling Program, Scientific Results 105. College Station, TX, pp. 731–757.

Kaminski, M.A., Silye, L., Kender, S., 2006. Miocene deep-water agglutinated foraminifera from ODP Hole 909C: Implications for the paleoceanography of the Fram Strait Area, Greenland Sea. Micropaleontology. 51, 373–403.

Kleiven, H.F., Jansen, E., Fronval, T., Smith, T.M., 2002. Intensification of Northern Hemisphere glaciations in the circum Atlantic region (3.5–2.4 Ma) - ice-rafted detritus evidence. Palaeogeography, Palaeoclimatology, Palaeoecology. 184, 213–223.

Knies, J., Gaina, C., 2008. Middle Miocene ice sheet expansion in the Arctic: Views from the Barents Sea. Geochemistry Geophysics Geosystems. 9, Q02015.

Knies, J., Matthiessen, J., Vogt, C., Laberg, J.S., Hjelstuen, B.O., Smelror, M., Larsen, E., Andreassen, K., Eidvin, T., Vorren, T.O., 2009. The Plio-Pleistocene glaciation of the Barents Sea-Svalbard region: a new model based on revised chronostratigraphy. Quaternary Science Reviews. 28, 812–829.

Knies, J., Matthiessen, J., Vogt, C., Stein, R., 2002. Evidence of 'Mid-Pliocene (3 Ma) global warmth' in the eastern Arctic Ocean and implications for the Svalbard/Barents Sea ice sheet during the late Pliocene and early Pleistocene (3-1.7 Ma). Boreas. 31, 82–93.

Knüttel, S., Russel, M.D., Firth, J.V., 1989. Neogene calcareous nannofossils from ODP Leg 105: Implications for Pleistocene paleoceanographic trends. In: Srivastava, S.P., Arthur, M., Clement, B. et al., Proceedings of the Ocean Drilling Program, Scientific Results 105. College Station, TX, pp. 245–262.

Koç, N., Scherer, R.P., 1996. Neogene diatom biostratigraphy of the Iceland Sea Site 907. In: Thiede, J., Myhre, A.M., Firth, J.V., Johnson, G.L., Ruddiman, W.F. (Eds), Proceedings of the Ocean Drilling Program, Scientific Results 151. College Station, TX, pp. 61–74.

Kodrans-Nsiah, M., de Lange, G.J., Zonneveld, K.A.F., 2008. A natural exposure experiment on short-term species-selective aerobic degradation of dinoflagellate cysts. Review of Palaeobotany and Palynology. 152, 32–39.

Kokinos, J.P., Eglinton, T.I., Goñi, M.A., Boon, J.J., Martoglio, P.A., Anderson, D.M., 1998. Characterization of a highly resistant biomacromolecular material in the cell wall of a marine dinoflagellate resting cyst. Organic Geochemistry. 28, 265–288.

Köthe, A., 2003. Dinozysten-Zonierung im Tertiär Norddeutschlands. Revue Palèbiologie. 22, 895–923.

Köthe, A., 2005. Biostratigraphie an der Oligozän/Miozän-Grenze und im Unter-Miozän der Forschungsbohrung Wursterheide (Kalknannoplankton, Dinozysten, Norddeutschland). Senckenbergiana lethaea. 85, 201–229.

Köthe, A., Andruleit, H., 2007. Late Miocene dinoflagellate cysts and calcareous nannoplankton from the eastern North Sea Basin margin: biostratigraphy and palaeoenvironmental interpretation (Breklum research borehole, Germany). Journal of Nannoplankton Research. 29, 5–18.

Köthe, A., Piesker, B., 2007. Stratigraphic distribution of Paleogene and Miocene dinocysts in Germany. Revue Palèbiologie. 26, 1–39.

Krebs, C.J., 1998. Ecological Methodology. Addison-Welsey Educational Publishers, Menlo Park. 620 pp.

Kristoffersen, Y., 1990. On the tectonic evolution and paleoceanographic significance of the Fram Strait gateway. In: Bleil, U., Thiede, J. (Eds.), Geological history of the Polar Oceans: Arctic versus Antarctic. Kluwer Academic Publishers, Dordrecht, pp. 63–76.

Krylov, A.A., Andreeva, I.A., Vogt, C., Backman, J., Krupskaya, V.V., Grikurov, G.E., Moran, K., Shoji, H., 2008. A shift in heavy and clay mineral provenance indicates a middle Miocene onset of a perennial sea ice cover in the Arctic Ocean. Paleoceanography. 23, PA1S06.

Kuhlmann, G., Langereis, C., Munsterman, D., Van Leeuwen, R.J, Verreussel, R., Meulenkamp, J., Wong, T., 2006a. Chronostratigraphy of Late Neogene sediments in the southern North Sea Basin and paleoenvironmental interpretations. Palaeogeography, Palaeoclimatology, Palaeoecology. 239, 426–455.

Kuhlmann, G., Langereis, C.G., Munsterman, D.K., Van Leeuwen, R.J., Verreussel, R., Meulenkamp, J.E., Wong, T.E., 2006b. Integrated chronostratigraphy of the Pliocene–Pleistocene interval and its relation to the regional stratigraphic stages in the southern North Sea region. Geologie en Mijnbouw. 85, 19–35.

Kuhnert, H., Bickert, T., Paulsen, H., 2009. Southern Ocean frontal system changes precede Antarctic ice sheet growth during the middle Miocene. Earth and Planetary Science Letters. 284, 630–638.

Kurita, H., Obuse, A., 2003. Middle Miocene-uppermost Lower Pliocene dinoflagellate cyst biostratigraphy, ODP Leg 186 Hole 1151A, off Sanriku coast of Northern Japan, northwestern Pacific. In: Suyehiro, K., Sacks, I.S., Acton, G.D. & Oda, E. (Eds.), Proceedings of the Ocean Drilling Program, Scientific Results 186. College Station, TX, pp. 1–19.

Larsen, J., Sournia, A., 1991. The diversity of heterotrophic dinoflagellates. In: Patterson, D., Larsen. J. (Eds.), The biology of free-living heterotrophic flagellates. Clarendon Press, Oxford, pp. 313–332.

Lawrence, K.T., Herbert, T.D., Brown, C.M., Raymo, M.E., Haywood, A.M., 2009. High-amplitude variations in North Atlantic sea surface temperature during the early Pliocene warm period. Paleoceanography. 24, PA2218.

Lawrence, K.T., Sosdian, S., White, H.E., Rosenthal, Y., 2010. North Atlantic climate evolution through the Plio-Pleistocene climate transitions. Earth and Planetary Science Letters. 300, 329–342.

Lawver, L.A., Müller, R.D., Srivastava, S.P., Roest, W., 1990. The opening of the Arctic Ocean. In: Bleil, U., Thiede, J. (Eds.), Geological history of the Polar Oceans: Arctic versus Antarctic. Kluwer Academic Publisher, Dordrecht, pp. 29–62.

Lewis, J., Harris, A.S.D., Jones, K.J., Edmonds, R.L., 1999. Long-term survival of marine planktonic diatoms and dinoflagellates in stored sediment samples. Journal of Plankton Research. 21, 343–354.

Lisiecki, L.E., Raymo, M.E., 2005. A Pliocene-Pleistocene stack of 57 globally distributed benthic $\delta^{18}O$ records. Paleoceanography. 20, PA1003.

Locker, S. and Martini, E., 1989. Cenozoic silicoflagellates, ebridians, and actiniscidians from the Vøring Plateau (ODP Leg 104). In: Eldholm, O., Thiede, J., Taylor, E. et al., Proceedings of the Ocean Drilling Program, Scientific Results 104, College Station, TX, pp. 543–586.

Londeix, L., Jan du Chène, R. 1998. Burdigalian dinocyst stratigraphy of the stratotypic area (Bordeaux, France). Geobios. 30, 283–294.

Londeix, L., Benzakour, M., Suc, J.-P., Turon, J.-L., 2007. Messinian palaeoenvironments and hydrology in Sicily (Italy): The dinoflagellate cyst record. Geobios. 40, 233–250.

Lourens, L., Hilgen, F., Shackleton, N.J., Laskar, J., Wilson, J., 2005. The Neogene. In: Gradstein, F.M., Ogg, J.G., Smith, A.G. (Eds.), A geological timescale 2004. Cambridge University Press, Cambridge, U.K., pp. 409–430 [Imprinted 2004].

Louwye, S., 2002. Dinoflagellate cyst biostratigraphy of the Upper Miocene Deurne Sands (Diest Formation) of northern Belgium, southern North Sea Basin. Geological Journal. 37, 55–67.

Louwye, S., 2005. The Early and Middle Miocene transgression at the southern border of the North Sea Basin (northern Belgium). Geological Journal. 40, 441–456.

Louwye, S., Laga, P., 1998. Dinoflagellate cysts of the shallow marine Neogene succession in the Kalmthout well, northern Belgium. Bulletin of the Geological Society of Denmark. 45, 73–86.

Louwye, S., Laga, P., 2008. Dinoflagellate cyst stratigraphy and palaeoenvironment of the marginal marine Middle and Upper Miocene of the eastern Campine area, northern Belgium (southern North Sea Basin). Geological Journal. 43, 75–94.

Louwye, S., De Schepper, S., 2010. The Miocene–Pliocene hiatus in the southern North Sea Basin (northern Belgium) revealed by dinoflagellate cysts. Geological Magazine. 147, 1–17.

Louwye, S., De Coninck, J., Verniers, J., 1999. Dinoflagellate cyst stratigraphy and depositional history of Miocene and Lower Pliocene formations in northern Belgium (southern North Sea Basin). Geologie en Mijnbouw. 78, 31–46.

Louwye, S., De Coninck, J., Verniers, J., 2000. Shallow marine Lower and Middle Miocene deposits at the southern margin of the North Sea Basin (northern Belgium): dinoflagellate cyst biostratigraphy and depositional history. Geological Magazine. 137, 381–394.

Louwye, S., Head, M.J., De Schepper, S., 2004. Dinoflagellate cyst stratigraphy and palaeoecology of the Pliocene in northern Belgium, southern North Sea Basin. Geological Magazine. 141, 353–378.

Louwye, S., De Schepper, S., Laga, P., Vandenberghe, N., 2007a. The Upper Miocene of the southern North Sea Basin (northern Belgium): a palaeoenvironmental and stratigraphical reconstruction using dinoflagellate cysts. Geological Magazine. 144, 33–52.

Louwye, S., Foubert, A., Mertens, K., Van Rooij, D. and the IODP Expedition 307 Scientific Party, 2007b. Integrated stratigraphy and palaeoecology of the Lower and Middle Miocene of the Porcupine Basin. Geological Magazine. 145, 1–24.

Louwye, S., Marquet, R., Bosselaers, M. & Lambert, O. 2010. Stratigraphy of an Early-Middle Miocene sequence near Antwerp in northern Belgium (southern North Sea basin). Geologica Belgica, 13, 269–284.

Ma, W., Tian, J., Li, Q., Wang, P., 2011. Simulation of long eccentricity (400-kyr) cycle in ocean carbon reservoir during Miocene Climate Optimum: Weathering and nutrient response to orbital change. Geophysical Research Letters. 38, L10701.

Macphail, M. K., Truswell, E. M., 2004. Palynology of Neogene slope and rise deposits from ODP Sites 1165 and 1167, East Antarctica. In: Cooper, A. K., O´Brian, P. E., Richter, C. (Eds.), Proceedings of the Ocean Drilling Program, Scientific Results 188. College Station, TX, pp. 1–20.

Mahmoud, M.S., 1993. Dinocyst stratigraphy of the Middle Miocene from Shagar-1 borehole, SW Gulf of Suez (Egypt). Newsletter on Stratigraphy. 28, 79–92.

Manabe, S., Stouffer, R.J., 1980. Sensitivity of a global climate model to an increase of CO_2 in the atmosphere. Journal of Geophysical Research. 85, 5529–5554.

Manum, S.B., 1976. Dinocyst in Tertiary Norwegian-Greenland Sea sediments (Deep Sea Drilling Project leg 38) with observations on palynomorphs and palynodebris in relation to environment. In: Talwani, M., Udintsev, G. et al., Initial Reports DSDP 38. U.S. Government Printing Office, Washington, D.C., pp. 897–919.

Manum, S.B., 1997. *Decahedrella martinheadii* gen. et sp. nov. – a problematic palynomorph from the Northern Atlantic Miocene. Palynology. 21, 67–77.

Manum, S.B., Boulter, M.C., Gunnarsdottir, H., Rangnes, K., Scholze, A., 1989. Eocene to Miocene Palynology of the Norwegian Sea (ODP Leg 104). In: Eldholm, O., Thiede, J., Taylor, E. et al., Proceedings of the Ocean Drilling Program, Scientific Results 104. College Station, TX, pp. 611–662.

Marlowe, I.T., Brassell, S.C., Eglinton, G., Green, J.C., 1990. Long-chain alkenones and alkyl alkenoates and the fossil coccolith record of marine sediments. Chemical Geology. 88, 349–375.

Marret, F., Zonneveld, K. A. F., 2003. Atlas of modern organic-walled dinoflagellate cyst distribution. Review of Palaeobotany and Palynology. 125, 1–200.

Marret, F., EirÌksson, J., Knudsen, K.L., Turon, J.-L., Scourse, J.D., 2004. Distribution of dinoflagellate cyst assemblages in surface sediments from the northern and western shelf of Iceland. Review of Palaeobotany and Palynology. 128, 35–53.

Martini, E., Müller, C., 1976. Eocene to Pleistocene silicoflagellates from the Norwegian-Greenland Sea (DSDP Leg 38). In: Talwani, M., Udintsev, G. et al., Initial Reports DSDP 38. U.S. Government Printing Office, Washington, D.C., pp. 857–895.

Masure, E., Vrielynck, B., 2009. Late Albian dinoflagellate cyst paleobiogeography as indicator of asymmetric sea surface temperature gradient on both hemispheres with southern high latitudes warmer than northern ones. Marine Micropaleontology. 70, 120–133.

Matsuoka, K., 1983. Late Cenozoic dinoflagellates and acritarchs in the Niigata District, central Japan. Palaeontographica Abt. B. 187, 89–154.

Matsuoka, K., Bujak, J. P. 1988. Cenozoic dinoflagellate cysts from the Navarin Basin, Norton Sound and St. George Basin, Bering Sea. Bulletin of the Faculty of Liberal Arts, Nagasaki University. 29, 1–147.

Matsuoka, K., Bujak, J.P., Shimazaki, T., 1987. Late Cenozoic dinoflagellate cyst biostratigraphy from the west coast of northern Japan. Micropaleontology. 33, 214–229.

Matsuoka, K., Head, M.J., 1992. Taxonomic revision of the Neogene marine palynomorphs *Cyclopsiella granosa* (Matsuoka) and *Batiacasphaera minuta* (Matsuoka), and a new species of *Pyxidinopsis* Habib (Dinophyceae) from the Miocene of the Labrador Sea. In: Head, M.J., Wrenn, J.H. (Eds.), Neogene and Quaternary Dinoflagellate Cysts and Acritarchs. American Association of Stratigraphic Palynologists Foundation, Dallas, Texas, pp. 165–180.

Matthiessen, J., 1995. Distribution patterns of dinoflagellate cysts and other organic-walled microfossils in recent Norwegian-Greenland Sea sediments. Marine Micropaleontology. 24, 307–334.

Matthiessen, J., Brenner, W., 1996. Dinoflagellate cyst ecostratigraphy of Pliocene/Pleistocene sediments from Yermak Plateau, Arctic Ocean (ODP Leg 151, Site 911A). In: Thiede, J., Myhre, A.M., Firth, J.V., Johnson, G.L., Ruddiman, W.F. (Eds.), Proceedings of the Ocean Drilling Program, Scientific Results 151. College Station, TX, pp. 243–254.

Matthiessen, J., Knies, J., Nowaczyk, N.R., Stein, R., 2001. Late Quaternary dinoflagellate cyst stratigraphy at the Eurasian continental margin, Arctic Ocean: indications for Atlantic water inflow in the past 150,000 years. Global and Planetary Change. 31, 65–86.

Matthiessen, J., de Vernal, A., Head, M. J., Okolodkov, Y., Puerto, A., Zonneveld, K. A. F. Harland, R., 2005. Modern organic-walled dinoflagellate cysts in Arctic marine environments and their (paleo-) environmental significance. Paläontologische Zeitschrift. 79, 3–51.

Matthiessen, J., Knies, J., Vogt, C., Stein, R., 2009a. Pliocene palaeoceanography of the Arctic Ocean and subarctic seas. Philosophical Transactions of the Royal Society A. 367, 21–48.

Matthiessen, J., Brinkhuis, H., Poulsen, N.E., Smelror, M., 2009b. *Decahedrella martinheadii* Manum 1997 – a stratigraphically and paleoenvironmentally useful Miocene acritarch of the northern high latitudes. Micropaleontology. 55, 171–186.

McCarthy, F.M.G., Mudie, P., 1996. Palynology and dinoflagellate biostratigraphy of Upper Cenozoic sediments from Sites 898 and 900, Iberia Abyssal Plain. In: Whitmarsh, R.B., Samyer, D.S., Klaus, A., Masson, D.G. (Eds.), Proceedings of the Ocean Drilling Program, Scientific Results 149. College Station, TX, pp. 241–265.

McClymont, E.L., Rosell-Melé, A., Giraudeau, J., Pierre, C., Lloyd, J.M., 2005. Alkenone and coccolith records of the mid-Pleistocene in the south-east Atlantic: Implications for the index and South African climate. Quaternary Science Reviews. 24, 1559–1572.

McKenna, M.C., 1983. Cenozoic paleogeography of North Atlantic Land Bridges. In: Bott, M.H.P., Saxov, S., Talwani, M., Thiede, J. (Eds.), Structure and development of the Greenland-Scotland Ridge: New methods and concepts. Plenum Press, New York, pp. 351–400.

McMinn, A., 1992. Neogene Dinoflagellate distribution in the eastern Indian Ocean from Leg 123, Site 765. In: Gradstein, F.M., Ludden, J.N. et al., Proceedings of the Ocean Drilling Program, Scientific Results 123. College Station, TX, pp. 429–441.

McMinn, A., 1993. Neogene Dinoflagellate Cyst biostratigraphy from Sites 815 and 823, Leg 133, Northeastern Australian Margin. In: McKenzie, J.A., Davies, P.J., Palmer-Julson, A. et al., Proceedings of the Ocean Drilling Program, Scientific Results 133. College Station, TX, pp. 97–105.

Mercer, J.L.,Zhao, M., 2004. Alkenone stratigraphy of the northern South China Sea for the past 35 m.y., Sites 1147 and 1148, ODP Leg 184. In: W.L. Prell, W.L.,Wang, P., Blum, P., D.K. Rea, D.K. (Eds.), Proceedings of the Ocean Drilling Program, Scientific Results 184. College Station, TX, pp. 1–17.

Mertens, K.N., Ribeiro, S., Bouimetarhan, I., Caner, H., Combourieu Nebout, N., Dale, B., De Vernal, A., Ellegaard, M., Filipova, M., Godhe, A., Goubert, E., Grøsfjeld, K., Holzwarth, U., Kotthoff, U., Leroy, S.A.G., Londeix, L., Marret, F., Matsuoka, K., Mudie, P.J., Naudts, L., PeÒa-Manjarrez, J.L., Persson, A., Popescu, S.-M., Pospelova, V., Sangiorgi, F., van der Meer, M.T.J., Vink, A., Zonneveld, K.A.F., Vercauteren, D., Vlassenbroeck, J., Louwye, S., 2009. Process length variation in cysts of a dinoflagellate,

Lingulodinium machaerophorum, in surface sediments: Investigating its potential as salinity proxy. Marine Micropaleontology. 70, 54-69.

Mertens, K.N., Bradley, L.R., Takano, Y., Mudie, P.J., Marret, F., Aksu, A.E., Hiscott, R.N., Verleye, T.J., Mousing, E.A., Smyrnova, L.L., Bagheri, S., Mansor, M., Pospelova, V., Matsuoka, K., 2012. Quantitative estimation of Holocene surface salinity variation in the Black Sea using dinoflagellate cyst process length. Quaternary Science Reviews. 39, 45–59.

Miller, K.G., Tucholke, B.E., 1983. Development of Cenozoic abyssal circulation south of the Greenland-Scotland Ridge. In: Bott, M.H.P., Saxov, S., Talwani, M., Thiede, J. (Eds.), Structure and development of the Greenland-Scotland Ridge: New methods and concepts. Plenum Press, New York, pp. 549–590.

Miller, K.G., Mountain, G.S., 1996. Drilling and Dating New Jersey Oligocene-Miocene Sequences: Ice Volume, Global Sea Level, and Exxon Records. Science. 271, 1092–1095.

Miller, K.G., Wright, J.D., Fairbanks, R.G., 1991. Unlocking the Ice House: Oligocene-Miocene oxygen isotopes, eustasy, and margin erosin. Journal of Geophysical Research. 96, 6829–6848.

Miller, K.G., Mountain, G.S., Browning, J.V., Kominz, M., Sugarman, P.J., Christie-Blick, N., Katz, M.E., Wright, J.D., 1998. Cenozoic global sea level, sequences, and the New Jersey Transect: Results From coastal plain and continental slope drilling. Revue of Geophysics 36, 569–601.

Miller, G.H., Brigham-Grette, J., Alley, R.B., Anderson, L., Bauch, H.A., Douglas, M.S.V., Edwards, M.E., Elias, S.A., Finney, B.P., Fitzpatrick, J.J., Funder, S.V., Herbert, T.D., Hinzman, L.D., Kaufman, D.S., MacDonald, G.M., Polyak, L., Robock, A., Serreze, M.C., Smol, J.P., Spielhagen, R., White, J.W.C., Wolfe, A.P., Wolff, E.W., 2010a. Temperature and precipitation history of the Arctic. Quaternary Science Reviews. 29, 1679–1715.

Miller, G.H., Alley, R.B., Brigham-Grette, J., Fitzpatrick, J.J., Polyak, L., Serreze, M.C., White, J.W.C., 2010b. Arctic amplification: can the past constrain the future? Quaternary Science Reviews. 29, 1779–1790.

Mudelsee, M., Raymo, M.E., 2005. Slow dynamics of the Northern Hemisphere glaciation. Paleoceanography. 20, PA4022.

Mountain, G.S., Tucholke, B.E., 1985. Mesozoic and Cenozoic geology of the U.S. Atlantic continental slope and rise. In: Poag, C.W. (Eds.), Geologic evolution of the United States Atlantic margin. Reinhold van Nostrand, New York, pp. 231–243.

Mosbrugger, V., Utescher, T., Dilcher, D., 2005. Cenozoic continental climatic evolution of Central Europe. Proceedings of the National Academy of Science. 102, 14964–14969.

Mourik, A.A., Abels, H.A., Hilgen, F.J., Di Stefano, A., Zachariasse, W.J., 2011. Improved astronomical age constraints for the middle Miocene climate transition based on high-resolution stable isotope records from the central Mediterranean Maltese Islands. Paleoceanography. 26, PA1210

Mudie, P., 1985. Palynology of the CEASAR cores, Arctic Ocean. In: Jackson, H.R., Mudie, P.J., Blasco, S.M. (Eds.), Initial geological reports on CEASAR-The Canadian expedition to study the Alpha Ridge, Arctic Ocean. Geological Survey Canada Paper 84-22, pp. 149–174.

Mudie, P., 1987. Palynology and dinoflagellate biostratigraphy of Deep Sea Drilling Project Leg 94, Sites 607 and 611, North Atlantic Ocean. In: Ruddiman, W.F., Kidd, R.B., Thomas, E. et al., Initial Reports DSDP 94. U.S. Government Printing Office, Washington, D.C., pp. 785–812.

Mudie, P., 1989. Palynology and dinocyst biostratigraphy of the Late Miocene to Pleistocene, Norwegian Sea: ODP Leg 104, Sites 642 to 644. In: Eldholm, O., Thiede, J., Taylor, E. et al., Proceedings of the Ocean Drilling Program, Scientific Results 104. College Station, TX, pp. 587–610.

Mudie, P., 1992. Circum-arctic Quaternary and Neogene marine palynofloras: paleoecology and statistical analysis. In: Head M.J., Wrenn, J.H. (Eds.), Neogene and Quaternary Dinoflagellate Cysts and Acritarchs. American Association of Stratigraphic Palynologists Publications, Dallas, pp. 347–390.

Mudie, P., 1996. Pellets of dinoflagellate-eating zooplankton. In: Jansonius, J., McGregor, D.C., (Eds.), Palynology: Principles and Application, Volume 3 New directions, other

applications and floral history. American Assosciation of Stratigraphic Palynologists, Dallas, pp. 1087–1089.

Mudie, P., Helgason, J., 1983. Palynological evidence for Miocene climatic cooling in eastern Iceland about 9.8 Ma. Nature. 303, 689–692.

Mudie, P., Short, S.K., 1985. Marine palynology of Baffin Bay. In: J.T. Andrew (Eds.), Quaternary environments. Allen & Unwin, Boston, pp. 263–308.

Mudie, P., Harland, R., 1996. Aquatic Quaternary. In: Jansonius, J., McGregor, D.C., (Eds.) Palynology: Principles and Application, Volume 2 Applications. American Association of Stratigraphic Palynologists, Dallas, pp. 843–879.

Mudie, P., de Vernal, A., Head, M.J., 1990. Neogene to recent palynostratigraphy of circum-Arctic basins: Results of ODP Leg 104, Norwegian Sea, Leg 105, Baffin Bay, and DSDP Site 611, Irminger Sea. In: Bleil, U., Thiede, J. (Eds.), Geological History of Polar Oceans: Arctic versus Antarctic. Kluwer Academic Publisher, Dordrecht, pp. 609–646.

Mudie, P., Harland, R., Matthiessen, J., de Vernal, A., 2001. Marine dinoflagellate cysts and high latitude Quaternary paleoenvironmental reconstructions: an introduction. Journal of Quaternary Science. 16, 595–602.

Müller, C., 1979. Calcareous nannofossils from the North Atlantic (Leg 48). In: Montadert, L., Roberts, D.G. et al., Initial Report DSDP 48. U.S. Government Printing Office, Washington, D.C., pp. 589–639.

Müller, C., 1985. Biostratigraphic and paleoenvironmental interpretation of the Goban Spur region based on a study of calcareous nannoplankton. In: Graciansky, P.C., Poag, C.W. et al., Initial Reports DSDP 80. U.S. Government Printing Office, Washington, D.C., pp. 573–599.

Müller, P.J., Kirst, G., Ruhland, G., von Storch, I., Rosell-Melé, A., 1998. Calibration of the alkenone paleotemperature index UK'_{37} based on core-tops from the eastern South Atlantic and the global ocean (60°N-60°S). Geochimica et Cosmochimica Acta. 62, 1757–1772.

Munsterman, D.K., Brinkhuis, H., 2004. A southern North Sea Miocene dinoflagellate cyst zonation. Geologie en Mijnbouw. 83, 267–285.

Myhre, A.M., Thiede, J., 1995. North Atlantic-Arctic Gateways. In: Myhre, A.M., Thiede, J., Firth, J.V. et al., Proceedings of the Ocean Drilling, Initial Reports 151. College Station, TX, pp. 5–26.

Naafs, B.D.A., Stein, R., Hefter, J., Khèlifi, N., De Schepper, S., Haug, G.H., 2010. Late Pliocene changes in the North Atlantic Current. Earth and Planetary Science Letters. 298, 434–442.

Ocean Drilling Program: http//www-odp.tamu.edu/sitemap

O'Regan, M., Moran, K., Backman, J., Jakobsson, M., Sangiorgi, F., Brinkhuis, H., Pockalny, R., Skelton, A., Stickley, C., Koç, N., Brumsack, H.-J., Willard, D., 2008. Mid-Cenozoic tectonic and paleoenvironmental setting of the central Arctic Ocean. Paleoceanography. 23, PA1S20.

Okolodkov, Y., 1999. Species range types of recent marine dinoflagellates recorded from the Arctic. Grana. 38, 162–169.

Osterman, L.E., Spiegler, D., 1996. Agglutinated benthic foraminiferal biostratigraphy of Sites 909 and 913, northern North Atlantic. In: Thiede, J., Myhre, A.M., Firth, J.V., Johnson, G.L., Ruddiman, W.F. (Eds.), Proceedings of the Ocean Drilling Program, Scientific Results 151. College Station, TX, pp. 169–187.

Pagani, M., Freeman, K.H., Arthur, M.A., 1999. Late Miocene Atmospheric CO2 Concentrations and the Expansion of C4 Grasses. Science. 285, 876-879.

Paschier, S., Browne, G., Field, B., Fielding, C.R., Krissek, L.A., Panter, K., Pekar, S.F., and the Andrill Science Team, 2011. Early and middle Miocene Antarctic glacial history from the s edimentary facies distribution in the AND-2A drill hole, Ross Sea, Antarctica. Geological Scociety of America Bulletin. 123, 2352–2365.

Persson, A., Rosenberg, R., 2003. Impact of grazing and bioturbation of marine benthic deposit feeders on dinoflagellate cysts. Harmful Algae. 2, 43–50.

Piasecki, S., 1980. Dinoflagellate cyst stratigraphy of the Miocene Hodde and Gram Formations, Denmark. Bulletin of the Geological Society of Denmark. 29, 53–76.

Piasecki, S., 2003. Neogene dinoflagellate cysts from Davis Strait, offshore West Greenland. Marine and Petroleum Geology. 20, 1075–1088.

Piasecki, S., 2005. Dinoflagellate cysts of the Middle–Upper Miocene Gram Formation, Denmark. In: Roth, F., Hoedemakers, K. (Eds.), The marine Gram Formation at Gram, Denmark: Late Miocene Geology and Palaeontology. Palaeo Publishing and Library vzw, Antwerpen, pp. 29–45.

Piasecki, S., Gregersen, U., Johannessen, P.N., 2002. Lower Pliocene dinoflagellate cysts from cored Utsira Formation in the Viking Graben, northern North Sea. Marine and Petroleum Geology. 19, 55–67.

Poirier, A., Hillaire-Marcel, C., 2011. Improved Os-isotope stratigraphy of the Arctic Ocean. Geophysical Research Letters. 38, L14607.

Polyak, L., Alley, R.B., Andrews, J.T., Brigham-Grette, J., Cronin, T.M., Darby, D.A., Dyke, A.S., Fitzpatrick, J.J., Funder, S., Holland, M., Jennings, A.E., Miller, G.H., O'Regan, M., Savelle, J., Serreze, M., St. John, K., White, J.W.C., Wolff, E., 2010. History of sea ice in the Arctic. Quaternary Science Reviews. 29, 1757–1778.

Poore, R.Z., 1979. Oligocene through Quaternary planktonic foraminiferal biostratigraphy of the North Atlantic: DSDP Leg 49. In: Luyendyk, B.P., Cann, J.R., Sharman, G.S. et al., Initial Reports DSDP 49. U.S. Government Printing Office, Washington, D.C., pp. 447–517.

Poore, H.R., Samworth, R., White, N.J., Jones, S.M., McCave, I.N., 2006. Neogene overflow of Northern Component Water at the Greenland-Scotland Ridge. Geochemistry Geophysics Geosystems. 7, Q06010.

Poore, H.R., White, N., Jones, S., 2009. A Neogene chronology of Iceland plume activity from V-shaped ridges. Earth and Planetary Science Letters. 283, 1–13.

Poulsen, N.E., Manum, S.B., Williams, G.L., Ellegaard, M., 1996. Tertiary dinoflagellate biostratigraphy of Sites 907, 908, and 909 in the Norwegian–Greenland Sea. In: Thiede, J., Myhre, A.M., Firth, J.V., Johnson, G.L., Ruddiman, W.F. (Eds.), Proceedings of the Ocean Drilling Program, Scientific Results 151. College Station, TX, pp. 255–287.

Pound, M.J., Haywood, A.M., Salzmann, U., Riding, J.B., Global vegetation dynamics and latitudinal temperature gradients during the Mid to Late Miocene (15.97–5.33 Ma). Earth-Science Reviews. 112, 1–22.

Powell, J.A. 1986. The stratigraphic distribution of Late Miocene dinoflagellate cysts from the Castellanian superstage stratotyp, northwest Italy. In: Wrenn, J.H., Duffield, S.L., Stein, J.A. (Eds.), Papers from the first symposium on Neogene dinoflagellate cyst biostratigraphy. AASP Contributions Series 17. American Association of Stratigraphic Palynologists Foundation, Dallas, Texas, pp. 129–149.

Prauss, M., Riegel, W., 1989. Evidence from phytoplankton associations for causes of black shale formation in epicontinental seas. Neues Jahrbuch für Geologie und Paläontologie. 11, 671–682.

Pudsey, C.J., Harland, R. 2001., Data Report: Dinoflagellate cyst analysis of Neogene sediments from sites 1095 and 1096, Antarctic Peninsula continental rise. In: Barker, P.F., Camerlenghi, A., Acton, G.D., Ramsey, A.T.S. (Eds.), Proceedings of the Ocean Drilling Program, Scientific Results 178. College Station, TX, pp. 1–10.

Quattrocchio, M., Guerstein, R.G., Sbadellati, S.M., 1986. Neogene dinoflagellate cysts from the Colorado Basin, Argentina. In: Wrenn, J.H., Duffield, S.L., Stein, J.A. (Eds.), Papers from the first symposium on Neogene dinoflagellate cyst biostratigraphy. AASP Contributions Series 17. American Association of Stratigraphic Palynologists Foundation, Dallas, Texas, pp. 151–157.

Radi, T., de Vernal, A., 2008. Dinocysts as proxy of primary productivity in mid-high latitudes of the Northern Hemisphere. Marine Micropaleontology. 68, 84–114.

Radi, T., de Vernal, A., Peyron, O., 2001. Relationships between dinoflagellate cyst assemblages in surface sediment and hydrographic conditions in the Bering and Chukchi seas. Journal of Quaternary Science. 16, 667–680.

Rahmstorf, S., 2006. Thermohaline Ocean Circulation. In: Elias, A. (Eds.), Encyclopedia Quaternary Sciences. Elsevier, Amsterdam, pp. 1–10.

Rasmussen, E.S., Heilmann-Clausen, C., Waagstein, R., Eidvin, T., 2008. The Tertiary of Norden. Episodes. 31, 66–72.

Raymo, M.E., Hodell, D. and Jansen, E., 1992. Response of Deep Ocean Circulation to Initiation of Northern Hemisphere Glaciation (3-2 MA). Paleoceanography. 7, 645–672.

Reichart, G.-J., Brinkhuis, H., 2003. Late Quaternary Protoperidinium cysts as indicators of paleoproductivity in the northern Arabian Sea. Marine Micropaleontology. 49, 303-315.

Ribeiro, S., Berge, T., Lundholm, N., Andersen, T.J., Abrantes, F., Ellegaard, M., 2011. Phytoplankton growth after a century of dormancy illuminates past resilience to catastrophic darkness. Nature Communication. 2, 311–318.

Robinson, M.M., 2009. New quantitative evidence of extreme warmth in the Pliocene Arctic. Stratigraphy. 6, 265–275.

Robinson, M.M., Valdes, P.J., Haywood, A.M., Dowsett, H.J., Hill, D.J., Jones, S.M., 2011. Bathymetric controls on Pliocene North Atlantic and Arctic sea surface temperature and deepwater production. Palaeogeography, Palaeoclimatology, Palaeoecology. 309, 92–97.

Rochon, A., De Vernal, A., Turon, J.L., Matthiessen, J., Head, M.J., 1999. Distribution of recent dinoflagellate cysts in surface sediments from the North Atlantic Ocean and adjacent seas in relation to sea-surface parameters. AASP Contribution Series No. 35. American Association of Stratigraphic Palynologists Foundation, Dallas, 1–152 pp.

Rögl, F., 1999. Mediterranean and Paratethys. Facts and Hypotheses of an Oligocene to Miocene Paleogeography (short overview). Geologica Carpathica. 50, 339–349.

Rommerskirchen, F., Condon, T., Mollenhauer, G., Dupont, L., Schefuss, E., 2011. Miocene to Pliocene development of surface and subsurface temperatures in the Benguela Current system. Paleoceanography. 26, PA3216.

Ruddiman, W.F., Glover, L.K., 1972. Vertical mixing of ice-rafted volcanic ash in North Atlantic sediments. Geological Society of America Bulletin. 83, 2817–2836.

Rudels, B., Quadfasel, D., 1991. Convection and deep water formation in the Arctic Ocean-Greenland Sea System. Journal of Marine Systems. 2, 435–450.

Rudels, B., J. Friedrich, H., Quadfasel, D., 1999. The Arctic Circumpolar Boundary Current. Deep Sea Research Part II: Topical Studies in Oceanography. 46, 1023–1062.

Rudels, B., Fahrbach, E., Meincke, J., Budeus, G., Eriksson, P., 2002. The East Greenland Current and its contribution to the Denmark Strait overflow. ICES Journal of Marine Science: Journal du Conseil. 59, 1133–1154.

Rudels, B., Björk, G., Nilsson, J., Winsor, P., Lake, I., Nohr, C., 2005. The interaction between waters from the Arctic Ocean and the Nordic Seas north of Fram Strait and along the East Greenland Current: results from the Arctic Ocean-02 Oden expedition. Journal of Marine Systems. 55, 1–30.

Rusbült, J., Strauss, C., 1992. Mikrofossilen des Unter- und Mittelmiozän in der Braunkohlenbohrung Lübtheen 46/84 (Südwestt-Mecklenburg). Neues Jahrbuch für Geologie-Paläontologie – Mitteilungen. 3, 150–170.

Salzmann, U., Williams, M., Haywood, A.M., Johnson, A.L.A., Kender, S.,Zalasiewicz, J., 2011. Climate and environment of a Pliocene warm world. Palaeogeography, Palaeoclimatology, Palaeoecology. 309, 1–8.

Samtleben, C., Schäfer, P., Andruleit, H., Baumann, A., Baumann, K.H., Kohly, A., Matthiessen, J., Schröder-Ritzrau, A., 1995. Plankton in the Norwegian-Greenland Sea: from living communities to sediment assemblages - an actualistic approach. Geologische Rundschau. 84, 108–136.

Sangiorgi, F., Brumsack, H.-J., Willard, D.A., Schouten, S., Stickley, C.E., O'Regan, M., Reichart, G.-J., Sinninghe-Damsté, J.S., Brinkhuis, H., 2008. A 26 million year gap in the central Arctic record at the greenhouse-icehouse transition: Looking for clues. Paleoceanography. 23, PA1S04.

Santarelli, A., Brinkhuis, H., Hilgen, F.J., Lourens, L.J., Versteegh, G.J.M., Visscher, H., 1998. Orbital signatures in a Late Miocene dinoflagellate record from Crete (Greece). Marine Micropaleontology. 33, 273–297.

Sarnthein, M., Bartoli, G., Prange, M., Schmittner, A., Schneider, B., Weinelt, M., Andersen, N., Garbe-Schönberg, D., 2009. Mid-Pliocene shifts in ocean overturning circulation and the onset of Quaternary-style climates. Climate of the Past. 5, 269–283.

Schaeffer, R., Spiegler, D., 1986. Neogene Kälteeinbrüche und Vereisungsphasen im Nordatlantik. Zeitschrift der Deutschen Geolgischen Gesellschaft. 137, 537–552.

Schauer, U., Rudels, B., Jones, E.P., Anderson, L.G., Muench, R.D., Björk, G., Swift, J.H., Ivanov, V., Larsson, A.M., 2002. Confluence and redistribution of Atlantic water in the Nansen, Amundsen and Makarov basins. Annale Geophysicae. 20, 257–273.

Scherer, R.P., Koç, N., 1996. Late Paleogene diatom biostratigraphy and paleoenvironments of the northern Norwegian-Greenland Sea. In: Thiede, J., Myhre, A.M., Firth, J.V.,Johnson, G.L., WRuddiman, W.F. (Eds.), Proceedings of the Ocean Drilling Program, Scientific Results 151. College Station, TX, pp. 75–100.

Schnepf, E., Elbrächter, M., 1992. Nutritional strategies in dinoflagellates. A review with emphasis on cell biological aspects. European Journal of Protistology. 28, 3–24.

Schnitker, D., 1980. North Atlantic oceanography as possible cause of Antarctic glaciation and eutrophication. Nature. 284, 615–616.

Schnitker, D., 1986. North-east Atlantic Neogene benthic foraminiferal faunas: tracers of deep-water palaeoceanography. Geological Society, London, Special Publications. 21, 191–203.

Schrank, E., 1988. Effects of chemical processing on the preservation of peridinioid dinoflagellates: A case from the late Cretaceous of NE Africa. Review of Palaeobotany and Palynology. 56, 123–140.

Serreze, M.C., Barry, R.G., 2011. Processes and impacts of Arctic amplification: A research synthesis. Global and Planetary Change. 77, 85–96.

Shipboard Scientific Party, 1995. Site 907. In: Myhre, A.M., Thiede, J., Firth, J.V. et al., Proceedings of the Ocean Drilling Program, Initial Reports 151. College Station, TX, pp. 57–111.

Shor, A.N., Poore, R.Z., 1979. Bottom curents and ice rafting in the North Atlantic: Interpretation of Neogene depositional environments of Leg 49 cores. In: Luyendyk, B.P. Cann, J.R. (Eds.), Initial Reports DSDP 49. pp. 859–872.

Smayda, T.J., Reynolds, C.S., 2001. Community Assembly in Marine Phytoplankton: Application of Recent Models to Harmful Dinoflagellate Blooms. Journal of Plankton Research. 23, 447–461.

Smelror, M., 1999. Pliocene–Pleistocene and redeposited dinoflagellate cysts from the western Svalbard Margin (Site 986): biostratigraphy, paleoenvironment, and sediment provenance. In: Raymo, M.E., Jansen, E., Blum, P., Herbert, T.D. (Eds.), Proceedings of the Ocean Drilling Program, Scientific Results 162. College Station, TX, pp. 83–97.

Snyder, S.W., Müller, C., Townsend, H., Poag, C.W., 1985. Biostratigraphy, paleoenvironmental, and paleomagnetic synthesis of the Goban Spur region, Deep Sea Drilling Project Leg 80. In: Graciansky, P.C., Poag, C.W. (Eds.), Initial Reports DSDP 80. College Station, TX, pp. 1169–1186.

Soliman, A., Head, M.J., Louwye, S., 2009. Morphology and distribution of the Miocene dinoflagellate cyst *Operculodinium*? *borgerholtense* Louwye 2001, emend. Palynology. 33, 73–85.

Soliman, A., Ćorić, S., Head, M.J., Piller, W., El Beialy, S.Y. (In press). Lower and Middle Miocene biostratigraphy, Gulf of Suez, Egypt, based on dinoflagellate cysts and calcareous nannofossils. Palynology.

Spiegler, D., Jansen, E., 1989. Planktonic foraminifer biostratigraphy of Norwegian Sea sediments: ODP Leg 104. In: Eldholm, O., Thiede, J., Taylor, E. (Eds.), Proceedings of the Ocean Drilling Program, Scientific Results 104. College Station, TX, pp. 681–696.

St. John, K., 2008. Cenozoic ice-rafting history of the central Arctic Ocean: Terrigenous sands on the Lomonosov Ridge. Paleoceanography. 23, PA1S05.

Stabell, B., Koç, N., 1996. Recent to Middle Miocene diatom productivity at Site 907, Iceland Plateau. In: Thiede, J., Myhre, A.M., Firth, J.V. & Johnson G.L. (Eds.), Proceedings of the Ocean Drilling Program, Scientific Results, 151, 483–492.

Stein, R., 1991. Organic carbon accumulation in Baffin Bay and paleoenvironment in high northern latitudes during the past 20 m.y. Geology 19, 356–359.

Stein, R., 2008. Arctic Ocean sediments – Processes, proxies and paleoenvironment. Elsevier, Amsterdam. 592 pp.

Stein, R., Macdonald, R.W., 2004. The organic carbon cycle in the Arctic Ocean. Springer, Heidelberg. 363 pp.

Stickley, C.E., St John, K., Koç, N., Jordan, R.W., Passchier, S., Pearce, R.B., Kearns, L.E., 2009. Evidence for middle Eocene Arctic sea ice from diatoms and ice-rafted debris. Nature. 460, 376–379.

Stockmarr, J., 1977. Tablets with spores used in absolute pollen analysis. Pollen et Spores. 13, 615–621.

Stover, L.E., 1977. Oligocene and Early Miocene dinoflagellates from Atlantic corehole 5/5B, Blake Plateau. AASP Contributions Series 5A. American Association of Stratigraphic Palynologists Foundation, Dallas, Texas, pp. 66–89.

Stover, L.E., Brinkhuis, H., Damassa, S.P., de Verteuil, L., Helby, R.J., Monteil, E., Partridge, A.D., Powell, J.A., Riding, J.B., Smelror, M., Williams, G.L., 1996. Mesozoic–Tertiary dinoflagellates, acritarchs and prasinophytes. In: Jansonius, J., McGregor, D.C. (Eds.), Palynology: Principles and Application, Volume 2 Application. American Association of Stratigraphic Palynologists Foundation, Dallas, Texas, pp. 641–750.

Strauss, C., Lund, J.J., 1992. A Middle Miocene dinoflagellate cyst microflora from Papendorf near Hamburg, Germany. Mitteilung Geologisch-Paläontologisches Institut Universität Hamburg. 73, 159–189.

Strauss, C., Lund, J.J., Lund-Christensen, J., 2001. Miocene dinoflagellate cyst biostratigraphy of the Nieder Ochterhausen research borehole (NW Germany). Geologisches Jahrbuch A. 152, 395–447.

Strother, P.K., 1996. Acritarchs. In: Jansonius. J., McGregor, D.C. (Eds.), Palynology: Principles and Application, Volume 1 Principles. American Association of Stratigraphic Palynologists Foundation, Dallas, pp. 81–106.

Susek, E., Zonneveld, K.A.F., Fischer, G., Versteegh, G.J.M., Willems, H., 2005. Organic-walled dinoflagellate cyst production in relation to upwelling intensity and lithogenic influx in the Cape Blanc region (off north-west Africa). Phycological Research. 53, 97–112.

Suto, I., 2006. The explosive diversification of the diatom genus Chaetoceros across the Eocene/Oligocene and Oligocene/Miocene boundaries in the Norwegian Sea. Marine Micropaleontology. 58, 259–269.

Swift, J.H., 1984. The circulation of the Denmark Strait and Iceland-Scotland overflow waters in the North Atlantic. Deep Sea Research Part A. Oceanographic Research Papers. 31, 1339–1355.

Talwani, M., Eldholm, O., 1977. Evolution of the Norwegian-Greenland Sea. Geological Society of America Bulletin. 88, 969–999.

Tappan, H., 1980. The paleobiology of plant protists. W.H. Freeman and Company, San Francisco, 1028 pp.

Taylor, F.J.R. 1987. The biology of dinoflagellates. Blackwell Scientific Publications, Oxford, 785 pp.

Telford, R.J., 2006. Limitations of dinoflagellate cyst transfer functions. Quaternary Science Reviews. 25, 1375–1382.

Telford, R.J., Birks, H.J.B., 2005. The secret assumption of transfer functions: problems with spatial autocorrelation in evaluating model performance. Quaternary Science Reviews. 24, 173–2179.

Thiébault, F., Cremer, M., Debrabant, P., Foulon, J., Nielsen, O.B., Zimmerman, H., 1989. Analysis of sedimentary facies, clay mineralogy, and geochemistry of the Neogene_Quaternary sediments in ODP Site 645, Baffin Bay, in: Srivastava, S.P., Arthur, M., Clement, B. et al., Proceedings of the Ocean Drilling Program, Scientific Results 105. College Station, TX, pp. 83–100.

Thiede, J., Eldholm, O., 1983. Speculations about the paleodepth of the Greenland-Scotland Ridge during the Late Mesozoic and Cenozoic times. In: Bott, M.H.P., Saxov, S., Talwani, M., Thiede, J. (Eds.), Structure and development of the Greenland-Scotland Ridge: New methods and concepts. Plenum Press, New York, pp. 445–456.

Thiede, J., Myhre, A.M., 1996. Introduction to the North Atlantic-Arctic Gateways: plate tectonic-paleoceanographic history and significance. In: J. Thiede, A.M. Myhre, J.V. Firth, G.L. Johnson, Ruddiman, W.F. (Eds.), Proceedings of the Ocean Drilling Program, Scientific Results 151. College Station, TX, pp. 3–23.

Thiede, J., Eldholm, O., Tayler, E., 1989. Variability of Cenozoic Norwegian-Greenland Sea paleoceanography and northern hemisphere climate. In: Eldholm, O., Thiede, J., Taylor, E. et al., Proceedings of the Ocean Drilling Program, Scientific Results 104. College Station, TX, pp. 1067–1118.

Thiede, J.R., Winkler, A., Wolf-Welling, T., Eldholm, O., Myhre, A.M., Baumann, K.-H., Henrich, R., Stein, R., 1998. Late Cenozoic history of the polar North Atlantic: Results from Ocean Drilling. Quaternary Science Reviews. 17, 185–208.

Thiede, J., Jessen, C., Knutz, P., Kuijpers, A., Mikkelsen, N., Nørgaard-Pedersen, N., Spielhagen, R., 2011. Millions of Years of Greenland ice sheet history recorded in ocean sediments. Polarforschung. 80, 141–159.

Thierstein, H.R., Geitzenauer, K.R., Molfino, B., Shackleton, N.J., 1977. Global synchroneity of late Quaternary coccolith datum levels: Validation by oxygen isotopes. Geology. 5, 400–404.

Tripati, A.K., Eagle, R.A., Morton, A., Dowdeswell, J.A., Atkinson, K.L., Bahé, Y., Dawber, C.F., Khadun, E., Shaw, R.M.H., Shorttle, O., Thanabalasundaram, L., 2008. Evidence for glaciation in the Northern Hemisphere back to 44 Ma from ice-rafted debris in the Greenland Sea. Earth and Planetary Science Letters. 265, 112–122.

Udeze, C.U., Oboh-Ikuenobe, F.E., 2005. Neogene palaeoceanographic and palaeoclimatic events inferred from palynological data: Cape Basin off South Africa, ODP Leg 175. Palaeogeography, Palaeoclimatology, Palaeoecology. 219, 199–223.

Thierstein, H.R., Geitzenauer, K.R., Molfino, B., Shackleton, N.J., 1977. Global synchroneity of late Quaternary coccolith datum levels: Validation by oxygen isotopes. Geology. 5, 400–404.

Thomson, K., Green, P.F., Whitham, A.G., Price, S.P., Underhill, J.R., 1999. New constraints on the thermal history of North-East Greenland from apatite fisson-track analysis. Geological Scociety of America Bulletin. 111, 1054–1068.

Turco, E., Hilgen, F.J., Lourens, L.J., Shackleton, N.J., Zachariasse, W.J., 2001. Punctuated Evolution of Global Climate Cooling during the Late Middle to Early Late Miocene: High-Resolution Planktonic Foraminiferal and Oxygen Isotope Records from the Mediterranean. Paleoceanography. 16, 405–423.

Van Nieuwenhove, N., Bauch, H.A., Matthiessen, J., 2007. Last interglacial surface water conditions in the eastern Nordic Seas inferred from dinocyst and foraminiferal assemblages. Marine Micropaleontology, 66, 247–263.

Verhoeven, K., Louwye, S., Eirìksson, J., De Schepper, S., 2011. A new age model for the Pliocene–Pleistocene Tjörnes section on Iceland: Its implication for the timing of North Atlantic–Pacific palaeoceanographic pathways. Palaeogeography, Palaeoclimatology, Palaeoecology. 309, 33–52.

Verleye, T.J., Louwye, S., 2010. Recent geographical distribution of organic-walled dinoflagellate cysts in the southeast Pacific (25–53°S) and their relation to the prevailing hydrographical conditions. Palaeogeography, Palaeoclimatology, Palaeoecology. 298, 319–340.

Verleye, T.J. 2011. The late Quaternary palaeoenvironmental changes along the western South-American contiental slope: A reconstruction based on dinoflagellate cysts and TEX_{86}. Unpublished PhD thesis, Ghent University, Belgium. 248 pp.

Verleye, T.J., Mertens, K.N., Young, M.D., Dale, B., McMinn, A., Scott, L., Zonneveld, K.A.F., Louwye, S., 2012. Average process length variation of the marine dinoflagellate cyst Operculodinium centrocarpum in the tropical and Southern Hemisphere Oceans: Assessing its potential as a palaeosalinity proxy. Marine Micropaleontology. 86–87, 45–58.

Versteegh, G. J. M., 1994. Recognition of cyclic and non-cyclic environmental changes in the Mediterranean Pliocene: A palynological approach. Marine Micropaleontology. 23, 147–183.

Versteegh, G.J.M., 1997. The onset of major Northern Hemisphere glaciations and their impact on dinoflagellate cysts and acritarchs from the Singa section, Calabria (southern Italy) and DSDP Holes 607/607A (North Atlantic). Marine Micropaleontology. 30, 319–343.

Versteegh, G.J.M., Zonneveld, K. A. F. 1994. Determination of (palaeo-) ecological preferences of dinoflagellates by applying Detrended and Canonical Correspondence

analysis to Late Pliocene dinoflagellate cyst assemblages of the south Italian Singa section. Review of Palaeobotany and Palynology. 84, 181–199.

Versteegh, G.J.M., Blokker, P., 2004. Resistant macromolecules of extant and fossil microalgae. Phycological Research. 52, 325–339.

Versteegh, G.J.M., Zonneveld, K.A.F., de Lange, G.J., 2010. Selective aerobic and anaerobic degradation of lipids and palynomorphs in the Eastern Mediterranean since the onset of sapropel S1 deposition. Marine Geology. 278, 177–192.

Villanueva, J., Flores, J.A., Grimalt, J.O., 2002. A detailed comparison of the UK'_{37} and coccolith records over the past 290 kyears: implications to the alkenone paleotemperature method. Organic Geochemistry. 33, 897–905.

Vogt, P.R., 1986. Geophysical and geochemical signatures and plate tectonics. In: Hurdle, B.G. (Eds.), The Nordic Seas. Springer Verlag, New York, pp. 413–662.

Vogt, P.R., Perry, R.K., Kovacs, L.C., Johnson, G.L., 1979. Detailed aeromagnetic investigations of the Arctic Basin. Journal of Geophysical Research. 84, 1071–1089.

Vogt, P.R., Johnson, G.L., Kristjansson, L., 1980. Morphology and magnetic anomalies north of Iceland. Journal of Geophysics. 47, 67–80.

Volkman, J.K., Barrerr, S.M., Blackburn, S.I., Sikes, E.L., 1995. Alkenones in *Gephyrocapsa oceanica*: Implications for studies of paleoclimate. Geochimica et Cosmochimica Acta. 59, 513–520.

Wall, D., Dale, B., 1967. The resting cysts of modern marine dinoflagellates and their palaeontological significance. Review of Palaeobotany and Palynology. 2, 349–354.

Wall, D., Dale, B., Harada, K., 1973. Descriptions of new fossil dinoflagellates from the Late Quaternary of the Black Sea. Micropaleontology. 19, 18–31.

Wall, D., Dale, B., Lohmann, G.P., Smith, W.K., 1977. The environmental and climatic distribution of dinoflagellate cysts in modern marine sediments from regions in the North and South Atlantic Oceans and adjacent seas. Marine Micropaleontology. 2, 121–200.

Wan, S., Kürschner, W.M., Clift, P.D., Li, A., Li, T., 2009. Extreme weathering/erosion during the Miocene Climatic Optimum: Evidence from sediment record in the South China Sea. Geophysical Research Letters. 36, L19706.

Wanner, H., Beer, J., Bütikofer, J., Crowley, T.J., Cubasch, U., Flückiger, J., Goosse, H., Grosjean, M., Joos, F., Kaplan, J.O., Küttel, M., Müller, S.A., Prentice, I.C., Solomina, O., Stocker, T.F., Tarasov, P., Wagner, M., Widmann, M., 2008. Mid- to Late Holocene climate change: an overview. Quaternary Science Reviews. 27, 1791–1828.

Warny, S.A., Wrenn, J.H., 2002. Upper Neogene dinoflagellate cyst ecostratigraphy of the Atlantic coast of Morocco. Micropaleontology. 48, 257–272.

Weaver, P.E., Clement, B., 1987. Magnetobiostratigraphy of planktonic foraminiferal datums: Deep Sea Drilling Project Leg 94, North Atlantic. In: Ruddiman, W.F., Kidd, R.B., Thomas, E. et al., Initial Reports DSDP 94. U.S. Government Printing Office, Washington, D.C.,pp. 815–829.

Wei, W., 1998. Calcareous nannofossils from the southeast Greenland margin: biostratigraphy and paleoceanography. In: A.D. Saunders, A.D., H.C. Larsen, H.C., Wise, S.W. (Eds.), Proceedings of the Ocean Drilling Program, Scientific Results 152. College Station, TX, pp. 147–160.

Weller, P., Stein, R. 2008. Paleogene biomarker records from the central Arctic Ocean (Integrated Ocean Drilling Program Expedition 302): Organic carbon sources, anoxia, and sea surface temperature. Paleoceanography. 23, PA1S17.

Westerhold, T., Bickert, T., Röhl, U., 2005. Middle to late Miocene oxygen isotope stratigraphy of ODP site 1085 (SE Atlantic): new constrains on Miocene climate variability and sea-level fluctuations. Palaeogeography, Palaeoclimatology, Palaeoecology. 217, 205-222.

Williams, G.L., 1975. Dinoflagellate and spore stratigraphy of the Mesozoic–Cenozoic offshore Canada. Geological Survey of Canada Paper. 30, 107–163.

Williams, G.L., Bujak, J.P., 1977. Cenozoic palynostratigraphy of offshore eastern Canada. AASP Contributions Series 5A American Association of Stratigraphic Palynologists. 14–47.

Williams, G.L., Bujak, J.P., 1985. Mesozoic and Cenozoic dinoflagellates. In: Bolli, H.M., Saunders, J.B., Perch-Nielsen, K. (Eds.), Plankton Stratigraphy. Cambridge University Press, Cambridge, U.K., pp. 847–964.

Williams, G.L., Manum, S.B., 1999. Oligocene–Early Miocene dinocyst stratigraphy of Hole 985A (Norwegian Sea). In: Raymo, M.E., Jansen, E., Blum, P., Herbert, T.D. (Eds.), Proceedings of the Ocean Drilling Program, Scientific Results 162. College Station, TX, pp. 99–109.

Williams, G.L., Brinkhuis, H., Bujak, J.P., Damassa, S.P., Hochuli, P.A., de Verteuil, L., Zevenboom, D., 1998. Appendix III. In: de Graciansky, P.-C., Hardenbol, J., Jacquin, T., Vail, P.R. (Eds.), Mesozoic and Cenozoic sequence stratigraphy of European basins. Society for Sedimentary Geology, Tusla, Oklahoma.

Williams, G.L., Fensome, R.A., Miller, M.A., Sarjeant, W.A.S., 2000. A glossary of the terminology applied to dinoflagellates, acritarchs and prasinophytes, with emphasis on fossils, third edition. American Association of Stratigraphic Palynologists, Contributions Series 37. 370 pp.

Williams, G.L., Brinkhuis, H., Pearce, M.A., Fensome, R.A., Weegink, J.W., 2004. Southern Ocean and global dinoflagellate cyst events compared: index events for the Late Cretaceous–Neogene. In: Exon, N.F., Kennett, J.P., Malone, M.J. (Eds.), Proceedings of the Ocean Drilling Program, Scientific Results 189. College Station, TX, pp. 1–98.

Winkler, A., Wolf-Welling, T.C.W., Stattegger, K., Thiede, J., 2002. Clay mineral sedimentation in high northern latitudes deep-sea basins since the Middle Miocene (ODP Leg 151, NAAG). International Journal of Earth Sciences. 91, 133–148.

Wold, C.N., 1994. Cenozoic Sediment Accumulation on Drifts in the Northern North Atlantic. Paleoceanography. 9, 917–941.

Wolf, T.C.W. , Thiede, J., 1991. History of terrigenous sedimentation during the past 10 m.y. in the North Atlantic (ODP Legs 104 and 105 and DSDP Leg 81). Marine Geology. 101, 83–102.

Wolf-Welling, T.C.W., Cremer, M., O´Connell, S., Winkler, A., Thiede, J., 1996. Cenozoic Arctic gateway paleoclimate variability: Indications from changes in coarse-fraction compostion. In: Thiede, J., Myhre, A.M., Firth, J.V., Johnson, G.L., Ruddiman, W.F. (Eds.), Proceedings of the Ocean Drilling Program, Scientific Results 151. College Station, TX, pp. 515–567.

Wood, G. D, Gabriel, A. M., Lawson, J. C. 1996. Palynological techniques – processing and microscopy. In: Jansonius, J., McGregor, D. C (Eds.) Palynology: Principles and Applications, Volume 1 Principles. American Association of Stratigraphic Palynologists Foundation, Salt Lake City, 29–50.

Wrenn, J.H., Kokinos, J.P., 1986. Preliminary comments on Miocene through Pleistocene dinoflagellate cysts from De Soto Canyon, Gulf of Mexico. In: Wrenn, J.H., Duffield, S.L., Stein, J.A. (Eds.), Papers from the first symposium on Neogene dinoflagellate cyst biostratigraphy. AASP Contributions Series 17. American Association of Stratigraphic Palynologists Foundation, Dallas, Texas, pp. 169–225.

Wright, J.D., Miller, K.G., 1992. Miocene stable isotope stratigraphy, Site 747, Kerguelen Plateau, in: Wise, S.W.J., Schlich, R. et al., Proceedings of the Ocean Drilling Program, Scientific Results 120. College Station, TX, pp. 855–866.

Wright, J.D., Miller, K.G., 1996. Control of North Atlantic Deep Water Circulation by the Greenland-Scotland Ridge. Paleoceanography. 11, 157–170.

Wright, J.D., Miller, K.G., Fairbanks, R.G., 1992. Early and Middle Miocene Stable Isotopes: Implications for Deepwater Circulation and Climate. Paleoceanography. 7, 357–389.

Zachos, J.C., Dicken, G.R., Zeebe, R.E., 2008. An early Cenozoic perspective on greenhouse warming and carbon-cycle dynamics. Nature. 451, 279–283

Zegarra, M., Helenes, J., 2011. Changes in Miocene through Pleistocene dinoflagellates from the Eastern Equatorial Pacific (ODP Site 1039), in relation to primary productivity. Marine Micropaleontology. 81, 107–121.

Zevenboom, D., 1995. Dinoflagellate cysts from the Mediterranean Late Oligocene and Miocene. PhD thesis, Biology Faculty, Utrecht University, Den Haag, Netherlands. 221 pp.

Zonneveld, K.A.F., Brummer, G.A., 2000. (Palaeo-)ecological significance, transport and preservation of organic-walled dinoflagellate cysts in the Somali Basin, NW Arabian Sea. Deep Sea Research Part II: Topical Studies in Oceanography. 47, 2229–2256.

Zonneveld, K.A.F., Versteegh, G.J.M., de Lange, G.J., 1997. Preservation of organic-walled dinoflagellate cysts in different oxygen regimes: a 10,000 year natural experiment. Marine Micropaleontology. 29, 393–405.

Zonneveld, K.A.F., Meier, K.J., Esper, O., Siggelkow, D., Wendler, I., Willems, H., 2005. The (palaeo)environmental significance of modern calcareous dinoflagellates: a review. Paläontologische Zeitschrift 79, 61–77.

Zonneveld, K.A.F., Bockelmann, F., Holzwarth, U., 2007. Selective preservation of organic-walled dinoflagellate cysts as a tool to quantify past net primary production and bottom water oxygen concentrations. Marine Geology 237, 109–126.

Zonneveld, K.A.F., Versteegh, G., Kodrans-Nsiah, M., 2008. Preservation and organic chemistry of Late Cenozoic organic-walled dinoflagellate cysts: A review. Marine Micropaleontology. 68, 179–197.

Zonneveld, K.A.F., Susek, E. and Fischer, G., 2010a. Seasonal variability of the organic-walled dinoflagellate cyst production in the coastal upwelling region of Cape Blanc (Mauritania): A five-year survey. Journal of Phycology. 46, 202–215.

Zonneveld, K.A.F., Versteegh, G.J.M., Kasten, S., Eglinton, T.I., Emeis, K.-C., Huguet, C., Koch, B.P., de Lange, G.J., de Leeuw, J.W., Middelburg, J.J., Mollenhauer, G., Prahl, F.G., Rethemeyer, J., Wakeham, S.G., 2010b. Selective preservation of organic matter in marine environments; processes and impact on the sedimentary record. Biogeosciences. 7, 483–511.

8. Photo plates

DINOFLAGELLATE CYSTS AND ACRITARCHS

FROM

ODP HOLE 907A
(ICELAND SEA)

PLATES I–V

Plate I

All photomicrographs are in bright field illumination. Various magnifications. Max. dia. = maximum diameter.

1–3 *Cordosphaeridium minimum* sensu Benedek and Sarjeant, 1981. Dorsal? view at upper, middle and lower foci. Note fibrous processes and fibroreticulate central body surface. Max. dia. (including processes), 26 μm. Sample 21H-6, 2–4 cm, slide 1; K44/3.

4–5 *Operculodinium*? *eirikianum* Head et al., 1989 emend. Head, 1997. Antapical view at upper and middle foci. Central body max. dia., 37 μm. Sample 13H-7, 315–325 cm; slide 1; O48/1.

6–7 *Operculodinium*? *piaseckii* Strauss and Lund, 1992 emend. de Verteuil and Norris, 1996. Left lateral view at upper and middle foci. Note finely granulate wall and solid, distally-truncated processes with small vesicles at base of some processes. Central body length, 37 μm. Sample 12H-3, 77–79 cm; slide 1; N52/2.

8–10 *Operculodinium tegillatum* Head, 1997. Dorsal view at upper, middle and lower foci. Central body max. dia., 37 μm. Sample 8H-6, 140–142 cm; slide 1; L46/4.

11–12 *Corrudinium devernaliae* Head and Norris, 2003. Dorsal view at upper and lower foci. Note unornamented margins around archeopyle and vesicles within crest bases. Central body length, 32 μm. Sample 8H-6, 140–142 cm; slide 1; P39/0.

13–15 *Unipontidinium aquaeductus* Wrenn, 1988. Ventral view at upper, middle and lower foci. Central body length, 37 μm. Sample 21-H6, 2–4 cm: slide 1; O41/2.

16–18 *Pyxidinopsis vesiculata* Head and Norris, 2003. Left lateral view at upper, middle and lower foci. Note vesicles within ridge bases. Length (excl. ornament), 35 μm. Sample 8H-6, 140–142 cm; slide 1; O38/4.

19–20 *Habibacysta tectata* Head et al., 1989. Ventral view at middle and lower foci. Max dia., 38 μm. Sample 12H-6, 130–132 cm; slide 1; Q42/3.

Plate I

All photomicrographs are in bright field illumination. Various magnifications. Max. dia. = maximum diameter.

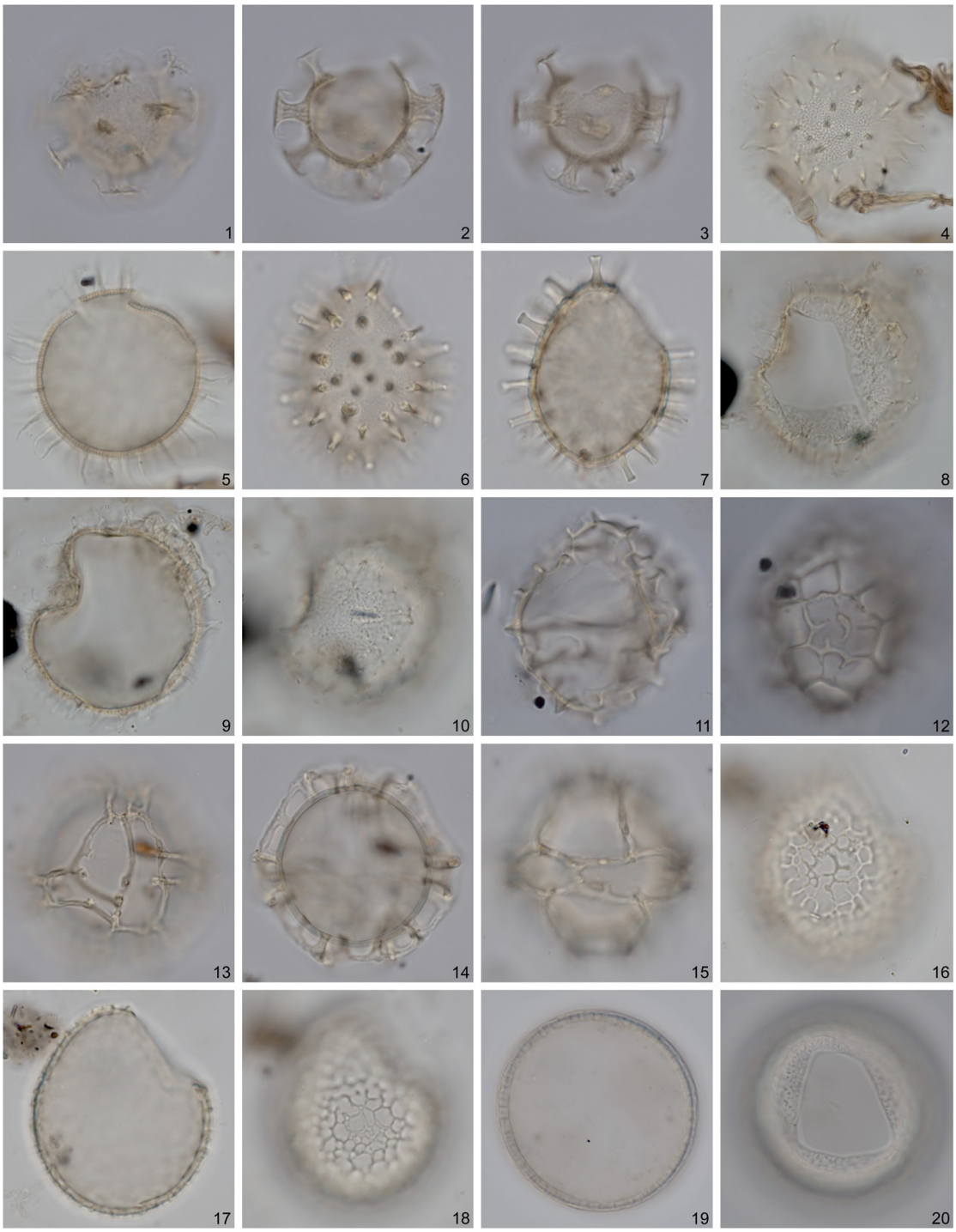

Plate II

All photomicrographs are in bright field illumination. Various magnifications. Max. dia. = maximum diameter.

1–5 *Hystrichosphaeropsis obscura* Habib, 1972.

1–4 Dorsal view at upper through lower foci. Periblast length, 95 μm. Sample 15H-5, 74–76 cm; slide 1; O47/2.

5 Dorsal view at mid-focus. Note rounded opening (hydropyle) in antapical plate. Periblast length, 94 μm. Sample 15H-5, 74–76 cm; slide 1; P48/0.

6–20 *Impagidinium elongatum* sp. nov.

6–10 Holotype in right latero-dorsal view at upper through lower foci. Central body length, 56 μm. Sample 13H-6, 20–22 cm; slide 2; P52/2.

11–16 Left latero-dorsal view at upper through lower foci. Note pronounced apical protuberance. Central body length, 51 μm. Sample 15H-2, 38–40 cm; slide 1; N42/0.

17–18 Ventral view at high and middle focus. Note pronounced fenestrations in crests. Central body length, 54 μm. Sample 15H-1, 74–76 cm; slide 1; S37/2.

19–20 Right latero-dorsal view at upper and middle foci. Note strongly reduced tabulation in equatorial region. Central body length, 57 μm. Sample 13H-2, 142–144 cm; slide 1; J43/0

Plate II

All photomicrographs are in bright field illumination. Various magnifications. Max. dia. = maximum diameter.

Plate III

All photomicrographs are in bright field illumination. Various magnifications. Max. dia. = maximum diameter.

1–3 *Batiacasphaera hirsuta* Stover, 1977. Apical view at upper, slightly lower, and middle focus showing angular apical archeopyle with opercular plates attached. Hairs about 2.0 μm long. Central body max. dia., 27 μm. Sample 17H-5, 138–140 cm; slide 1; J45/4.

4–10 *Batiacasphaera micropapillata* Stover, 1977.

4–5 Vermiculate–rugulate morphotype. Antapical view at middle and lower foci. Central body max. dia., 26 μm. Sample 21H-6, 2–4 cm; slide 1; P38/0. **6–7** Vermiculate–rugulate morphotype. Oblique antapical view at upper and middle foci. Central body max. dia., 30 μm. Sample 14H-4, 10–12 cm; slide 1; N43/2.

8–10 Microreticulate morphotype. Antapical view at upper, middle and lower foci. Note finer microreticulation within a coarser one. Central body max. dia., 27 μm. Sample 15H-5, 74–76 cm; slide 1; M46/0.

11–20 *Cerebrocysta irregulare* sp. nov.

11–14 Holotype in ventral view at upper through lower foci. Note slight apical protuberance. Central body length (including ornament), 39 μm. Sample 17H-5, 138–140 cm; slide 1; P43/4.

15–17 Left lateral view at upper, middle and lower foci. Central body max. dia. (including ornament), 42 μm. Sample 16H-1, 17–19 cm; slide 1; O50/1.

18–20 Dorsal view at upper, middle and lower foci. Central body length (including ornament), 34 μm. Sample 17H-5, 138–140 cm; slide 1; P42/1.

Plate III

All photomicrographs are in bright field illumination. Various magnifications. Max. dia. = maximum diameter.

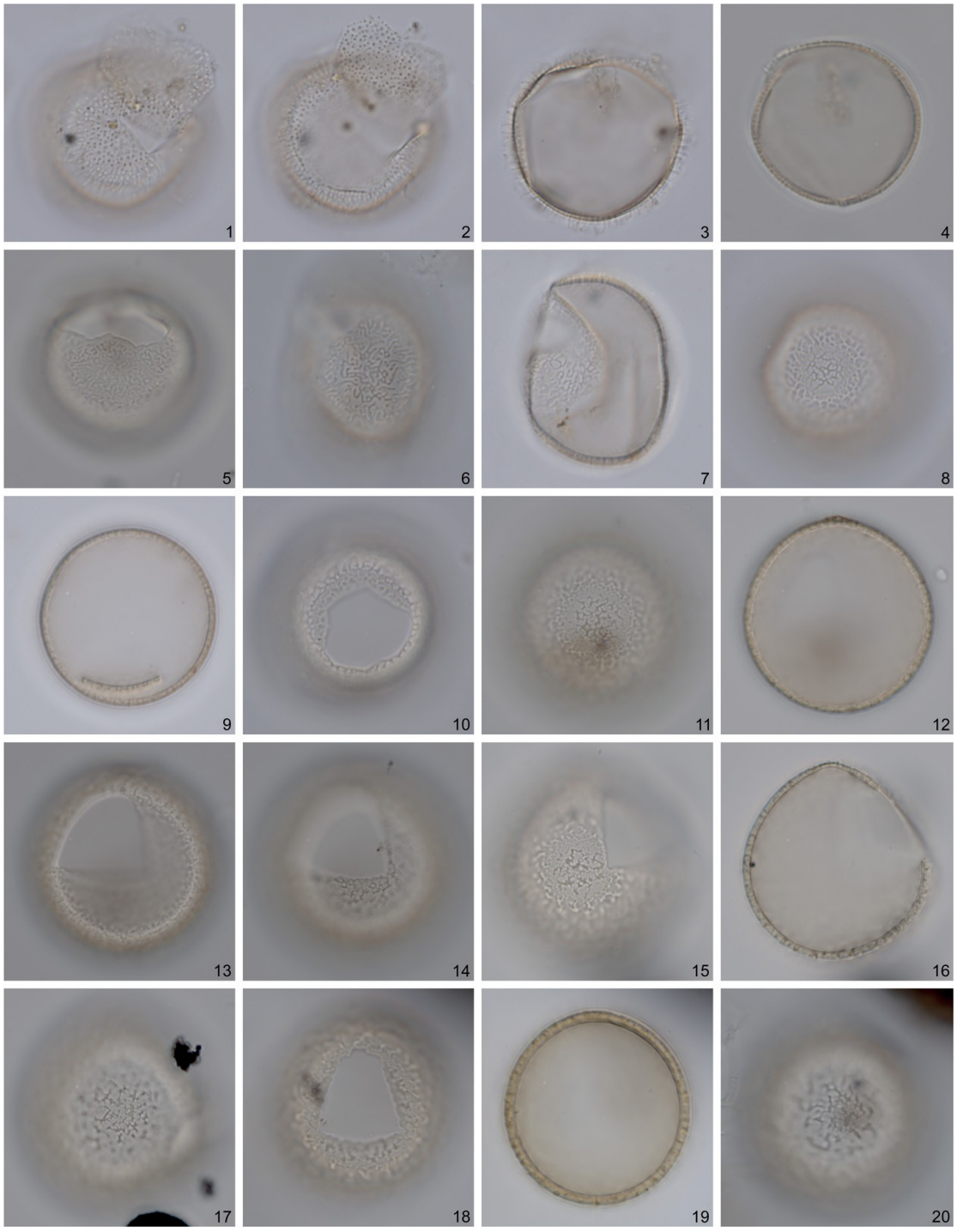

Plate IV

All photomicrographs are in bright field illumination. Various magnifications. Max. dia. = maximum diameter.

1–2 *Cerebrocysta poulsenii* de Verteuil and Norris, 1996. Dorsal view at upper and middle foci. Central body length, 32 μm. Sample 16H-3, 42.5-44.5 cm; slide 1; M49/0.

3–6 *Labyrinthodinium truncatum* Piasecki, 1980 emend. de Verteuil and Norris, 1996.

3–4 Apical view at middle and lower foci. Central body max. dia., 29 μm. Crest height, 6.5–8.5 μm. Sample 16H-1, 17–19 cm; slide 1; O52/0.

5–6 Morphotype with crests showing marked distal expansion. Apical view with upper focus on operculum which is partly collapsed into cyst, and at middle focus. Central body max. dia., 25 μm. Crest height, 5.0–5.5 μm. Sample 17H-4, 60–62 cm; slide 1; K49/3.

7–8 *Reticulatosphaera actinocoronata* Matsuoka, 1983 emend. Bujak and Matsuoka, 1986. View uncertain at upper and middle foci. Central body max. dia., 26 μm. Sample 13H-7, 315–325 cm; slide 1; M38/1.

9 *Dapsilidinium pseudocolligerum* Stover, 1977. Antapical view at mid-focus. Central body surface is granulate, and two pairs of processes (not illustrated) are fused for most of their length. Central body max. dia., 35 μm. Sample 13H-6, 20–22 cm; slide 1; E41/1.

10–12 *Cristadinium cristatoserratum* Head et al., 1989. Ventral view at upper, middle and lower foci. Length, 45μm. Sample 17H-4, 60–62 cm; slide 1; N39/4.

13–15 *Palaeocystodinium* spp.

13–14 Specimen resembling *Palaeocystodinium golzowense*. Left lateral view at upper and lower foci. Total length, 155 μm; central body length, 63 μm. Horns and body unornamented. Sample 13H-2, 142–144 cm; slide 1; L42/4.

15 *Palaeocystodinium* sp. cf. *P. miocaenicum* Strauss in Strauss et al., 2001. Ventral view at upper focus. Surface smooth except for pronounced alignment of granulation on horns, and no indication of tabulation around the archeopyle. Total length, 120 μm; central body length, 47 μm. Sample 23H-6, 97.5–99.5 cm; slide 1; R48/4. Grouped with *Palaeocystodinium* spp. in the range chart.

16–17 *Cleistosphaeridium placacanthum* (Deflandre and Cookson, 1955) Eaton et al., 2001. Antapical view at upper and middle foci. Note ridges demarcating process complexes. Central body max. dia., 73 μm. Sample 23H-6, 97.5–99.5 cm; slide 1; S49/0.

18–19 *Decahedrella martinheadii* Manum, 1997. Overall max. dia. 73 μm. Note thin internal sac. Sample 11H-1, 73–75 cm; slide 1; M50/0.

Plate IV

All photomicrographs are in bright field illumination. Various magnifications. Max. dia. = maximum diameter.

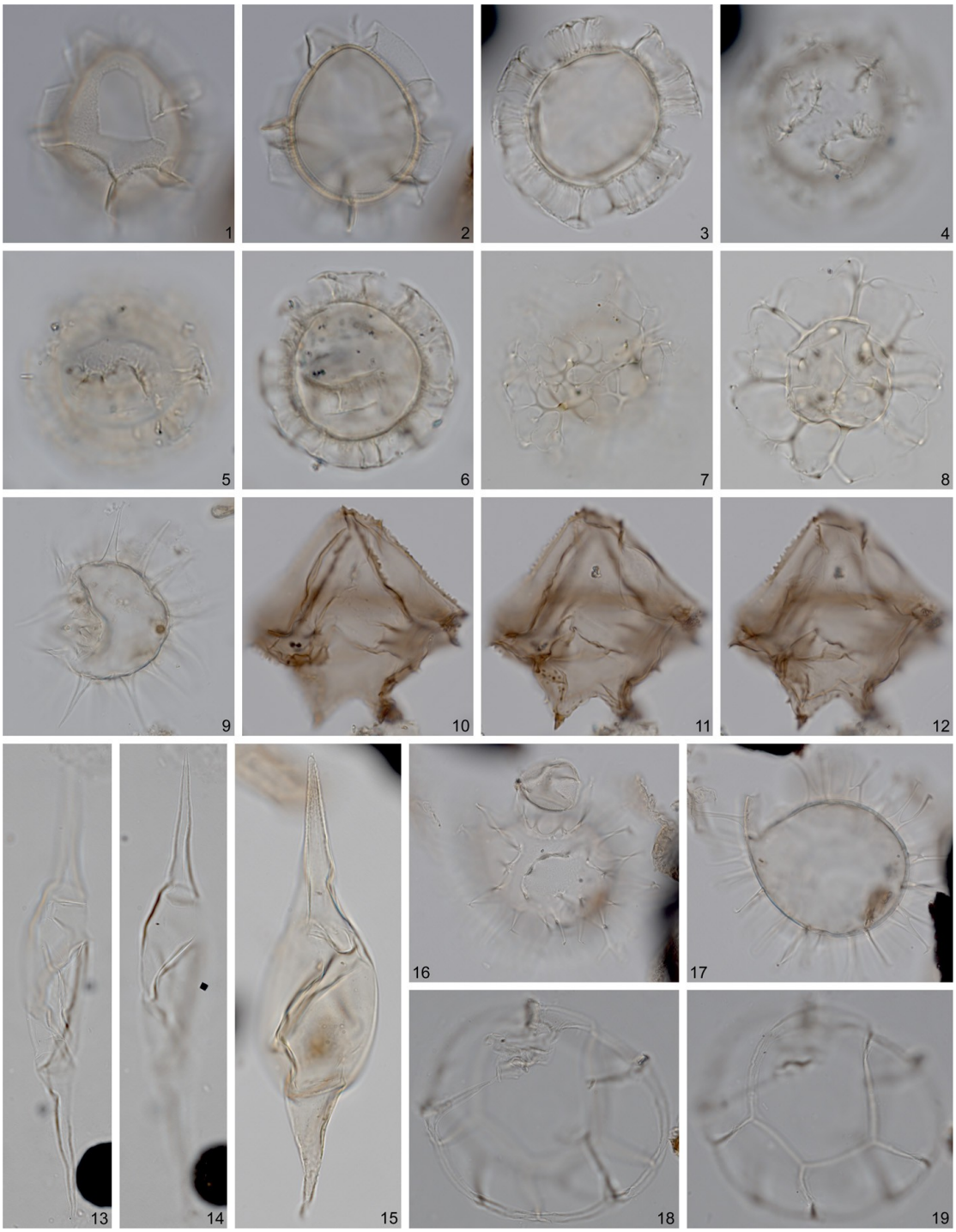

Plate V

All photomicrographs are in bright field illumination. Various magnifications. Max. dia. = maximum diameter.

1–12, 15 *Batiacasphaera micropapillata* Stover, 1977.

1–2 Microreticulate morphotype. Antapical view at upper and lower foci. Note finer microreticulation within a coarser one. Central body max. dia., 27 μm. Sample 907A- 15H-5, 74–76 cm; slide 1; M46/0.

3 Microreticulate morphotype. Apical view at upper foci. Central body max. dia., 32 μm. Sample 907A-14H-4, 10–12 cm; slide 1; P48/3.

4–5 Vermiculate–rugulate morphotype. Oblique apical at upper and lower foci. Central body max. dia., 33 μm. Sample 907A-14H-4, 10–12 cm; slide 1; N43/3.

6, 9 Vermiculate–rugulate morphotype. Oblique antapical view at upper and lower foci. Central body max. dia., 26 μm. Sample 907A-21H-6, 2–4 cm; slide 1; P38/0.

7–8 Vermiculate–microrugulate morphotype. Oblique apical view at upper and slightly lower foci. Central body max. dia., 34 μm. Sample M0002A-32H-3, 68–70 cm; slide 1; M29/0.

10–11 Vermiculate–microrugulate morphotype. Apical view at upper and lower foci. Central body max. dia., 29 μm. Sample M0002A-32H-3, 68–70 cm; slide 1; O28/0.

12, 15 Vermiculate–rugulate morphotype. Oblique antapical view at upper and middle f oci. Central body max. dia., 30 μm. Sample 907A-14H-4, 10–12 cm; slide 1; N43/2.

13–14 *Batiacasphaera sphaerica* Stover, 1977.
Oblique apical view at upper and lower foci showing granulate–punctate surface. Central body max. dia., 27 μm. Sample 907A-21H-6, 2–4 cm; slide 1; M44/2.

Plate V

All photomicrographs are in bright field illumination. Various magnifications. Max. dia. = maximum diameter.

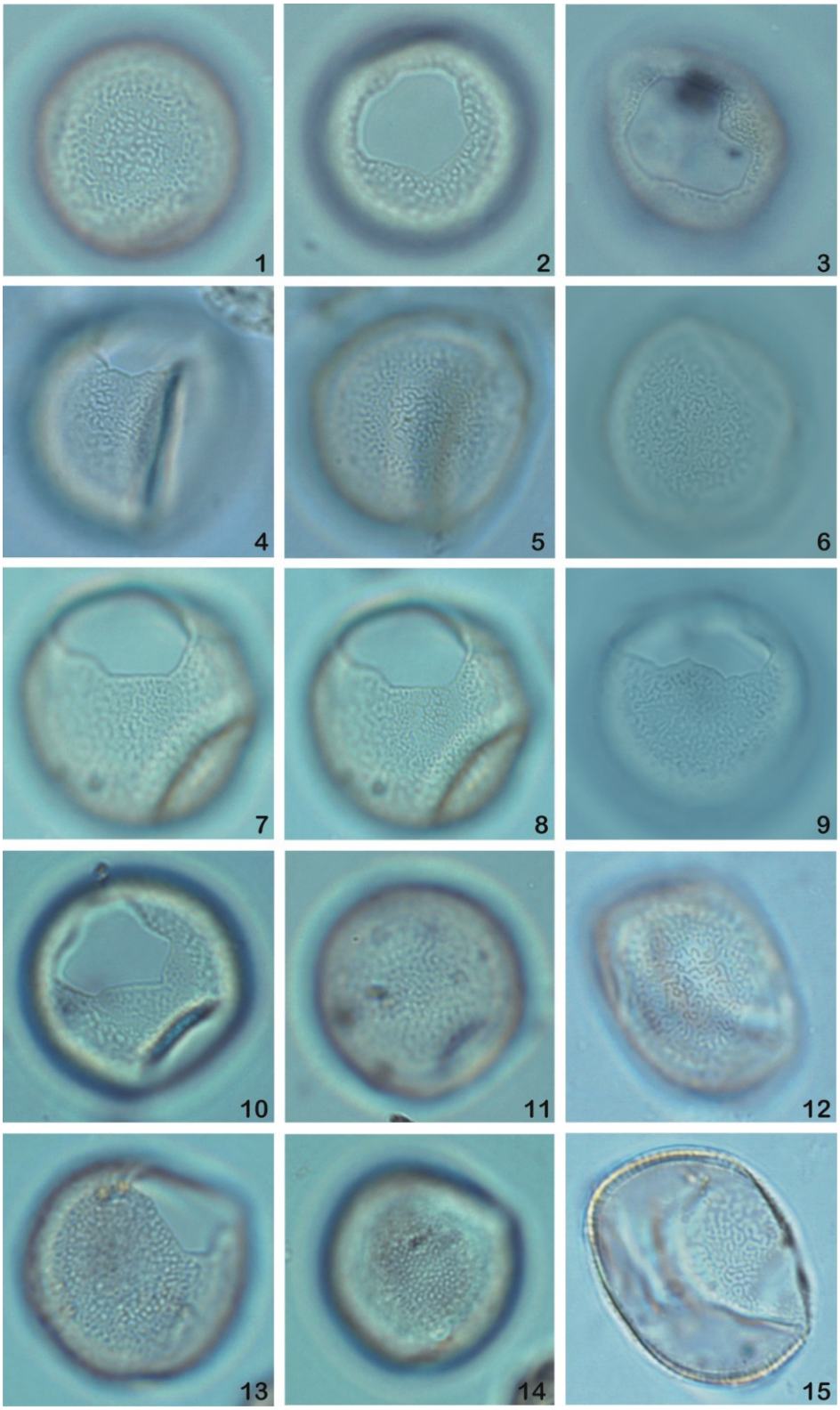

9. Systematic Paleontology

Division DINOFLAGELLATA (Butschli, 1885) Fensome et al., 1993
Subdivision DINOKARYOTA Fensome et al., 1993
Class DINOPHYCEAE Pascher, 1914
Subclass PERIDINIPHYCIDAE Fensome et al., 1993
Order GONYAULACALES Taylor, 1980
Suborder GONYAULACINEAE (Autonym)
Family GONYAULACACEAE Lindemann, 1928
Subfamily GONYAULACOIDEAE (Autonym)

Genus *Achomosphaera* Evitt, 1963
Achomosphaera sp. cf. *A. andalousiensis* Jan du Chêne and Londeix, 1988
Achomoshpaera ramulifera Deflandre, 1937

Genus *Ataxiodinium* Reid, 1974
Ataxiodinium choane Reid, 1974

Genus *Bitectatodinium* Wilson, 1973
Bitectatodinium tepikiense Wilson, 1973
Bitectatodinium ?*arborichiarum* Louwye, 1999

Genus *Corrudinium* Stover and Evitt, 1978
Corrudinium devernaliae Head and Norris, 2003
Corrudinium harlandii Matsuoka, 1983
Corrudinium ?*labradorii* Head et al., 1989

Genus *Hystrichosphaeropsis* (Deflandre, 1935) Sarjeant, 1982
Hystrichosphaeropsis obscura Habib, 1972

Genus *Impagidinium* Stover and Evitt, 1978
Impagidinium aculeatum (Wall, 1967) Lentin and Williams, 1981
Impagidinium aff. *aculeatum* (Wall, 1976) Lentin and Williams, 1981
Impagidinium cf. *antecarcerum* de Verteuil and Norris, 1996
Impagidinium elongatum sp. nov. Schreck et al.
Impagidinium cf. *multiplex* (Wall and Dale, 1968) Lentin and Williams, 1981
Impagidinium cf. *pacificum* Bujak, 1984
Impagidinium pallidum Bujak, 1984
Impagidinium patulum (Wall, 1967) Stover and Evitt, 1978
Impagidinium cf. *sphaericum* (Wall, 1967) Lentin and Williams, 1981
Impagidinium strialatum (Wall, 1967) Stover and Evitt, 1978
Impagidinium velorum Bujak, 1984
Impagidinium sp. A
Impagidinium sp. B
Impagidinium sp. C

Genus *Nematosphaeropsis* (Deflandre and Cookson, 1955) Wrenn, 1988
Nematosphaeropsis labyrinthus (Ostenfeld, 1903) Reid, 1974
Nematosphaeropsis cf. *downiei* Brown, 1986
Nematosphaeropsis cf. *lativittata* Wrenn, 1988
Nematosphaeropsis cf. *rigidia* Wrenn, 1988
Nematosphaeropsis sp. 1

Genus *Spiniferites* (Mantell, 1850) Sarjeant, 1970
Spiniferites elongatus Reid, 1974
Spiniferites ramosus sensu lato (Ehrenberg, 1838) Mantell, 1854
Spiniferites sp. A
Spiniferites sp. B

Genus *Tectatodinium* (Wall, 1967) Head, 1994
Tectatodinium pellitum (Wall, 1967) Head, 1994

Genus *Unipontidinium* Wrenn, 1988
Unipontidinium aquaeductus (Piasecki, 1980) Wrenn, 1988

Subfamily GRIBROPERIDINIODEAE Fensome et al., 1993

Genus *Cordosphaeridium* Eisenhack, 1963
Cordosphaeridium minimum sensu Benedek and Sarjeant, 1981

Genus *Hystrichokolpoma* (Klump, 1953) Zevenboom and Santarelli in Zevenboom, 1995
Hystrichokolpoma rigaudiae Deflandre and Cookson, 1955

Genus *Lingoludinium* (Wall, 1967) Dodge, 1989
Lingoludinium machaerophorum Deflandre and Cookson, 1955
Lingoludinium multivirgatum de Verteuil and Norris, 1996

Genus *Operculodinium* (Wall, 1967) Matsuoka et al., 1997
Operculodinium cf. *borgerholtense* Louwye, 2001
Operculodinium centrocarpum Deflandre and Cookson, 1955
Operculodinium aff. *centrocarpum* sensu Wall and Dale, 1966
Operculodinium? *eirikianum* (Head et al., 1989) Head, 1997
Operculodinium? cf. *eirikianum* (Head et al., 1989) Head, 1997
Operculodinium giganteum sensu Manum et al., 1989
Operculodinium israelianum (Rossignol, 1962) Wall, 1967
Operculodinium cf. *israelianum* (Rossignol, 1962) Wall, 1967
Operculodinium janduchenei Head et al., 1989
Operculodinium piaseckii (Strauss and Lund, 1992) de Verteuil and Norris, 1996
Operculodinium cf. *piaseckii* (Strauss and Lund, 1992) de Verteuil and Norris, 1996
Operculodinium tegillatum Head, 1997
Operculodinium vacuolatum Head et al., 1989
Operculodinium sp. A
Operculodinium sp. B

Subfamily LEPTODINIOIDEAE Fensome et al., 1993

Genus *Lithosphaeridium* (Davey and Williams, 1966) Luca-Clark, 1984
Lithosphaeridium spp.

Family GONYAULACACEAE Lindemann, 1928
Subfamily UNCERTAIN

Genus *Filisphaera* Bujak, 1984
Filisphaera filifera (Bujak, 1984) Head, 1994
Filisphaera microornata (Head et al., 1989) Head, 1994
Filisphaera sp. A
Filisphaera sp. B
Filisphaera sp. C

Filisphaera sp. D

Genus *Habibacysta* Head et al., 1989
Habibacysta tectata Head et al., 1989

Genus *Invertocysta* Edwards, 1984
Invertocysta lacrymosa Edwards, 1984
Invertocysta tabulata Edwards, 1984

Genus *Melitasphaeridium* Harland and Hill, 1979
Melitasphaeridium choanophorum (Deflandre and Cookson, 1955) Harland and Hill, 1979
Melitasphaeridium sp. A

Genus *Pyxidinopsis* Habib, 1976
Pyxidinopsis psilata (Wall and Dale, 1973) Head, 1994
Pyxidinopsis vesiculata Head and Norris, 2003
Pyxidinopsis sp. A
Pyxidinopsis sp. B
Pyxidinopsis sp. C
Pyxidinopsis sp. D

Order GONYAULACALES Taylor, 1980
Suborder UNCERTAIN
Family UNCERTAIN

Genus *Amiculosphaera* Harland, 1979
Amiculosphaera umbraculum Harland, 1979

Genus *Batiacasphaera* Drugg, 1979
Batiacasphaera hirsuta Stover, 1977
Batiacasphaera micropapillata Stover, 1977
Batiacasphaera minuta (Matsuoka, 1983) Matsuoka and Head, 1992 (grouped to *B. micropapillata*)
Batiacasphaera sphaerica Stover, 1977
Batiacasphaera sp. II of Edwards, 1984
Batiacasphaera sp. A

Genus *Cerebrocysta* Bujak, 1980
Cerebrocysta poulsenii de Verteuil and Norris, 1996
Cerebrocysta cf. *lagae* Louwye, 1999
Cerebrocysta irregulare sp. nov. Schreck et al.

Genus *Cleistosphaeridium* Davey et al., 1966
Cleistosphaeridium placacanthum (Deflandre and Cookson, 1955) Eaton et al., 2001
Cleistosphaeridium cf. placacanthum (Deflandre and Cookson, 1955) Eaton et al., 2001

Genus *Dapsilidinium* Bujak et al., 1989
Dapsilidinium pastielsii (Davey and Williams, 1966) Bujak et al., 1980
Dapsilidinium pseudocolligerum (Stover, 1977) Bujak et al., 1980

Genus *Labyrinthodinium* Piasecki, 1980
Labyrinthodinium truncatum (Piasecki, 1980) de Verteuil and Norris, 1996

Genus *Mendicodinium* (Morgenroth, 1970) Bucefalo Palliani et al., 1997
Mendicodinium spp.

Genus *Reticulatosphaera* (Matsuoka, 1983) Bujak and Matsuoka, 1986

Reticulatosphaera actinocoronata (Benedek, 1972) Bujak and Matsuoka, 1986
Reticulatosphaera actinocoronata sensu Manum et al., 1989

Order GONYAULACALES Taylor, 1980
Suborder GONIODOMINEAE Fensome et al., 1993
Family GONIODOMACEAE Lindemann, 1928
Subfamily HELGOLANDINIOIDEAE Fensome et al., 1993

Genus *Tuberculodinium* Wall, 1967
Tuberculodinium vancampoae (Rossignol, 1962) Wall, 1967

Subfamily PYRODINIOIDEAE Fensome et al., 1988

Genus *Hystrichosphaeridium* (Deflandre 1937) Davey and Williams, 1966
Hystrichosphaeridium tubiferum (Ehrenberg, 1838) Deflandre, 1937

Genus *Polysphaeridium* (Davey and Williams, 1966) Bujak et al., 1980
Polysphaeridium spp.

Order PERIDINIALES Haeckel, 1894
Suborder PERIDINIINEAE (Autonym)
Family PERIDINIACEAE Balech, 1988
Subfamily DEFLANDREOIDEAE Bujak and Davis, 1983

Genus *Palaeocystodinium* Alberti, 1961
Palaeocystodinium golzowense Alberti, 1961
Palaeocystodinium minor Strauss et al., 2001

Subfamily OVOIDINIOIDEAE Bujak and Davis, 1983

Genus *Arcticacysta* Sangiorgi et al., 2009
Arcticacysta backmanii Sangiorgi et al., 2009

Family PROTOPERIDINIACEAE Balech, 1988
Subfamily PROTOPERIDINIOIDEAE Balech, 1988

Genus *Barssidinium* Lentin et al., 1994
Barssidinium evangelineae Lentin et al., 1994
Barssidinium graminosum Lentin et al., 1994
Barssidinium pliocenicum (Head, 1993) Head, 1994
Barssidinium wrennii Lentin et al., 1994

Genus *Brigantedinium* Reid, 1977
Brigantedinium cariacoense Wall, 1967 ex Lentin and Williams, 1993
Brigantedinium simplex Wall, 1967 ex Lentin and Williams, 1993

Genus *Cristadinium* Head et al., 1989
Cristadinium diminutivum Head et al., 1989
Cristadinium cristatoserratum Head et al., 1989
Cristadinium cf. *cristatoserratum* Head et al., 1989
Cristadinium sp. A
Cristadinium sp. B

Genus *Lejeunecysta* (Artzner and Dörhöfer, 1978) Bujak, 1980
Lejeunecysta fallax (Morgenroth, 1966), Biffi and Grignani, 1983
Lejeunecysta sp. 1
Lejeunecysta sp. 2
Lejeunecysta sp. 3
Lejeunecysta sp. 4
Lejeunecysta sp. 5
L*ejeunecysta* sp. 6
Lejeunecysta sp. 7
Lejeunecysta sp. 8
Lejeunecysta sp. 9
Lejeunecysta sp. 10

Genus *Selenopemphix* (Benedek, 1972) Head, 1993
Selenopemphix brevispinosa Head et al., 1989
Selenopemphix brevispinosa subsp. *brevispinosa* Head et al., 1989
Selenopemphix brevispinosa subsp. *conspicua* de Verteuil and Norris, 1992
Selenopemphix dionaeacysta Head et al., 1989
Selenopemphix nephroides (Benedek, 1972) Benedek and Sarjeant, 1981
Selenopemphix sp. 3 of Head et al., 1989
Selenopemphix sp. A
Selenopemphix sp. B
Selenopemphix sp. C
Selenopemphix sp. D

Genus *Sumatradinium* (Lentin and Williams, 1976) Lentin et al., 1994
Sumatradinium soucouyantiae de Verteuil and Norris

Genus *Trinovantedinium* (Reid, 1977) de Verteuil and Norris, 1992
Trinovantedinium ferugnomatum de Verteuil and Norris, 1992
Trinovantedinium glorianum (Head et al., 1989) de Verteuil and Norris, 1992
Trinovantedinium harpagonium de Verteuil and Norris, 1992
Trinovantedinium papula de Verteuil and Norris, 1992

Genus *Xandarodinium* Reid, 1977
Xandarodinium xanthum Reid, 1977

DINOFLAGELLATE CYSTS OF UNKNOWN GENERIC AFFINITY

Dinocysts A–O (gonyaulacoid)
Peridinioid cysts A–I (peridiniod)
Protoperidinioid cysts A–C (protoperidinioid)

INCERTAE SEDIS INCLUDING ACRITARCHS

Genus *Cymatiosphaera* (Wetzel, 1983) ex Deflandre, 1954
Cymatiosphaera? *invaginata* Head et al., 1989
Cymatiosphaera spp. (including different morphotypes)

Genus *Decahedrella* Manum, 1997
Decahedrella martinheadii Manum, 1997

Genus *Lavradosphaera* De Schepper and Head, 2008
Lavradosphaera crista De Schepper and Head, 2008
Lavradosphaera lucifer De Schepper and Head, 2008
Lavradosphaera sp. 1

Genus *Micrhystridium* (Deflandre, 1937) Sarjeant, 1963
Micrhystridium sp. 1
Micrhystridium sp. 2
?*Micrhystridium* sp.

Genus *Nannobarbophora* (Habib and Knapp, 1982) Head, 2003
Nannobarbophora gedlii Head, 2003 (possibly including *N. walldalei* Head, 1996)

ACRITARCHS OF UNKNOWN GENERIC AFFINITY

Acritarch sp. 1 (Impagidinium-like)
Acritarch sp. 2
Acritarch sp. 3 (resembling the cyst of *Pentapharssodinium dalei*)

Indeterminate sphaeromorphitic acritarchs (resembling the genera *Leiosphaeridia* and *Halosphaera*)
Indeterminate marine acritarchs (including different morphotypes)

10. Appendix

The appendices A–C provide data that are presented and discussed in this thesis. Further data that were collected within the framework of this thesis will be archived in the PANGAEA database and made available whilst these results are published.

Appendix A *includes data presented in chapter 3*.

Sample information, polarity chrons and nannoplankton zones of the lowest and highest occurrence of species in the north Atlantic DSDP, ODP, and IODP holes, together with the source of dinocyst and stratigraphic data.

Appendix B *includes data presented in chapter 4*.

Sites used for generating the paleo-biogeographic distribution maps. Also given is the author of the dinocyst study. A) Sites with records of the *B. micropapillata* and/or *B. minuta*. B) Sites without records of this species complex.

Appendix C *includes data presented in chapter 5*.

C1: Raw counts and stratigraphic ranges of dinocyst and acritarch genera and species in Hole 907A. Also shown is the result of fluorescence microscopy.

C2: Summary of (paleo)ecological preferences of dinoflagellate cyst species discussed in the text and shown in Figure 3.

C3: TOC content and C/N ratio in ODP Hole 907A

Appendix A

Species	Datum	Leg	Hole	Core, section, interval Bottom	mbsf	Core, section, interval Top	mbsf	mean mbsf	Error in m	Stratigraphy	Source	Source of dinocyst data	identified as
B. hirsuta	HO	104	643A	9-5, 30-32	78.10	8-6, 48-50	70.28	74.19	3.91	C4r.2r	Bleil, 1989	Manum et al., 1989	
B. micropapillata	HO	93	610A	20-4, 16-22	186.49	20-3, 31-36	185.65	186.07	0.42	C2Ar	Clement and Robinson, 1987	de Schepper and Head, 2008	as *Batiacasphaera minuta*
	HPO	105	646B	34-CC	323.40	33-CC	313.80	318.60	4.80	NN16	Knüttel et al., 1989	de Vernal and Mudie, 1989	as *Batiacasphaera sphaerica*
	HO	93	603C	22-2, 84-86	185.96	21H6, 50-52	182.02	183.99	1.97	C2Ar	Canninga et al., 1987	Head (unpubl.)	as *Batiacasphaera micropapillata*
C. irregulare sp. nov.	HO	104	643A	10-5, 31-33	87.61	9-5, 30-32	78.10	82.86	4.76	C4r.2r	Bleil, 1989	Manum et al., 1989	as *Tectatodinium* sp. 4
	LO	104	643A	12-5, 31-33	106.61	12-4, 31-33	105.11	105.86	0.75	-	Goll, 1997 (unpubl.)	Manum et al., 1989	as *Tectatodinium* sp. 4
C. poulsenii	HO	104	643A	11-5, 30-32	97.10	10-5, 31-33	87.61	92.36	4.74	C4Ar	Bleil, 1989	Manum et al., 1989	as Gen. et. sp. indet. Piasecki 1980
	HO	81	555A	21-2, 60-62	226.10	20-1, 50	215.00	220.55	5.55	NN7-8	Backman, 1984	Edwards, 1984	as Gen. et. sp. indet. Piasecki 1980
	HO	150	905A	75-CC	683.80	72-CC	654.90	669.35	14.45	NN7	Shipboard Scientific Party, 1994	de Verteuil, 1996	
C. placacanthum	HO	104	643A	9-5, 30-32	78.10	8-6, 48-50	70.28	74.19	3.91	C4r.2r	Bleil, 1989	Manum et al., 1989	as *Systematophora placacantha*
	HPO	104	643A	12-4, 31-33	105.11	12-1, 31-33	100.61	102.86	2.25	-	Goll, 1997 (unpubl.)	Manum et al., 1989	as *Systematophora placacantha*
	HO	80	548A	11H-1, 8-9	300.58	10H-3, 82-83	293.82	297.20	3.38	NN11	Müller, 1985	Brown and Downie 1985	as *Areoligera senonensis* complex
	HO	81	555A	24-3, 70-72	256.20	22-1, 107-109	234.57	245.39	10.82	NN6	Backman, 1984	Edwards, 1984	as *Systematophora placacantha*
	HPO	307	1318B	11-4, 123-125	96.20	11-4, 23-25	95.20	95.70	0.50	C5An.2n	Louwye et al., 2007	Louwye et al., 2007	
	HO	150	905A	85-CC	780.10	82-CC	751.10	765.60	14.50	NN6	Gartner and Shyu, 1996	de Verteuil, 1996	as *Systematophora placacantha*
C. devernaliae	HPO	105	646B	37-5, 30-35	349.20	37-4, 30-35	347.60	348.40	0.80	NN15	Knüttel et al., 1989	de Vernal and Mudie, 1989	as *Corrudinium* sp. 1
	HO	93	603C	26-2, 50-52	224.02	25-6, 22-24	220.14	222.08	1.94	C3n.1n	Canninga et al., 1987	Head (unpubl.)	
	HO	94	610A	21-1, 24-30	191.67	20-6, 35-40	189.68	190.68	1.00	C2Ar	Clement and Robinson, 1987	de Schepper and Head, 2008	
C. minimum	HO	80	548A	8-1, 75-77	272.75	7-1, 50-52	263.00	267.88	4.88	mid NN11	Müller, 1985	Brown and Downie, 1985	as cf. *Cordosphaeridium minimum*
	HO	150	903C	10-5, 83-88	598.90	9-CC	592.10	595.50	3.40	C5r	Fossen and Urbat, 1996	de Verteuil, 1996	
C. cristatoserratum	HO	105	646B	62-3, 139-141	587.99	62-3, 37-39	586.97	587.48	0.51	mid NN11	Knüttel et al., 1987	Head et al. 1989	
	HO	93	603C	39-6, 14-16	354.46	38-5, 45-47	343.67	349.07	5.39	C3r	Canninga et al., 1987	Head (unpubl.)	
	LO	150	905A	92-CC	847.70	91-CC	838.00	842.85	4.85	NN6	Shipboard Scientific Party, 1994	de Verteuil, 1996	
D. pseudocolligerum	HO	104	643A	8H-6, 48-50	70.28	7CC, 25	62.3	66.29	3.99	C4n.1n	Bleil, 1989	Manum et al., 1989	
	HO	105	646B	69-CC, 5-8	651.75	67-CC,	641.1	646.425	5.325	NN11a	Knüttel et al., 1989	Head et al., 1989	
	HO	81	555A	15H-1, 50-52	167.50	14H-1, 20-22	157.70	162.60	4.90	NN9-10	Backman, 1984	Edwards, 1984	
	HO	150	905A	62-CC	558.50	58-CC	519.90	539.20	19.30	NN11	Gartner and Shyu, 1996	de Verteuil, 1996	
H. tectata	LO	307	1318B	9-7, 29-31	144.60	9-3, 30-32	138.60	141.60	3.00	C5ABn	Louwye et al., 2007	Louwye et al., 2007	
	LO	150	902D	54-CC	497.60	53-CC	487.90	492.75	4.85	mid DN5	de Verteuil and Norris, 1996	de Verteuil, 1996	
H. obscura	HO	104	643A	8-6, 48-50	70.28	7CC, 25	62.25	66.27	4.02	C4n.1n	Bleil, 1989	Manum et al., 1989	
	HO	162	987E	-	-	-	-	-	-	C3Bn	Channell et al. 1999b	Smelror (pers. comm.)	
	HO	81	555A	9-1, 28-30	91.28	8-6, 96-98	70.96	81.12	10.16	NN11	Backman, 1984	Edwards, 1984	as *Hystrichosphaeropsis obscurum*
	HO	150	905A	55-CC	491.30	52-CC	462.30	476.80	14.50	NN11	Gartner and Shyu, 1996	de Verteuil, 1996	
I. elongatum sp. nov.	HO	104	643A	9-5, 30-32	78.10	8H-6, 48-50	70.28	74.19	3.91	C4r.1r	Bleil, 1989	Manum et al., 1989	as *Impagidinium* sp. 3
	HO	104	643A	29-6, 30-32	271.70	28-7, 30-32	263.40	267.55	4.15	-	Goll, 1997 (unpubl.)	Manum et al., 1989	as *Impagidinium* sp. 1

Appendix A

L. truncatum	HO	104	643A	10-5, 31-33	87.61	9H-5, 30-32	78.10	82.86	4.76	C4r.2r	Bleil, 1989	Manum et al., 1989	
	HO	162	987E	-	-	-	-	-	-	C3Bn	Channell et al., 1999b	Channell et al., 1999b	
	HO	105	646B	78-CC, 1-3	747.01	77-4, 64-66	733.04	740.03	6.99	NN10	Knüttel et al., 1989	Head et al., 1989	
	HO	81	555A	14-1, 20-22	157.90	12-2, 40-44	140.40	149.15	8.75	NN9-10	Backman, 1984	Edwards, 1984	
	HO	150	905A	55-CC	491.30	52-CC	462.30	476.80	14.50	NN11	Gartner and Shyu, 1996	de Verteuil, 1996	
O. ? *eirikianum*	HO	104	642C	10-1, 87-89	64.37	uppermost sample, no 642C record by Mudie, 1989				C2An.3n	Bleil, 1989	Manum et al., 1989	as *Operculodinium longispinigerum*
	HO	105	646B	31-2, 27-32	286.70	31-1, 27-32	284.97	285.84	0.87	NN16	Knüttel et al., 1989	de Vernal and Mudie, 1989	as *Operculodinium longispinigerum*
	HO	94	607	12-4, 71-73	103.04	12-1, 11-13	103.30	103.17	0.13	MIS 95	Versteegh, 1997	Versteegh, 1997	
	HO	94	610A	14-3, 124-129	128.47	14-2,64-69	126.37	127.42	1.05	top C2An.1n	Clement and Robinson, 1987	de Schepper and Head, 2008	
	HO	93	603C	15-5, 66-68	123.08	15-2, 85-87	118.77	120.93	2.16	C2An.1r	Canninga et al., 1987	Head (unpubl.)	
	HPO	93	603C	20-6, 85-87	172.77	20-1, 83-85	165.25	169.01	3.76	C2An.3n	Canninga et al., 1987	Head (unpubl.)	
	LO	307	1318	17-6,33-35	155.60	17-3, 21-23	150.90	153.25	2.35	C5ACn	Louwye et al., 2007	Louwye et al., 2007	
O. piaseckii	HO	104	643A	8-6, 48-50	70.28	7CC, 25	62.25	66.27	4.02	C4n.1n	Bleil, 1989	Manum et al., 1989	as *Operculodinium* sp. of Piasecki 1980
	HO	105	646B	76-CC	727.70	74-CC	708.60	718.15	9.55	NN10	Knüttel et al., 1989	Head et al., 1989	as cf. *Operculodinium* sp. of Piasecki 1980
	HO	81	555A	9-1, 28-30	91.28	8-6, 96-98	70.96	81.12	10.16	NN11	Backman, 1984	Edwards, 1984	as *Operculodinium* sp. of Piasecki 1980
	HO	150	905A	55-CC	491.30	52-CC	462.30	476.80	14.50	NN11	Gartner and Shyu, 1996	de Verteuil, 1996	
O. tegillatum	HO	94	610A	19-4, 62-67	177.35	19-3, 111-116	176.43	176.89	0.46	C2Ar	Clement and Robinson, 1987	de Schepper and Head, 2008	
	HO	93	603C	20-6, 85-87	172.77	20-1, 83-85	165.25	169.01	3.76	lower C2An.3n	Canninga et al., 1987	Head (unpubl.)	
	HPO	93	603C	24-2, 50-52	204.82	23-3, 100-102	197.22	201.02	3.80	mid C2Ar	Canninga et al., 1987	Head (unpubl.)	
	HPO	105	646B	35-2, 22-28	325.12	35-1, 22-28	323.62	324.37	0.75	NN16	Knüttel et al., 1989	de Vernal and Mudie, 1989	as *Operculodinium crassum*
?*Palaeocystodinium* spp	HO	104	643A	12-1, 31-33	100.61	11-5, 30-32	97.10	98.86	1.76	-	Goll, 1997 (unpubl.)	Manum et al., 1989	as *Palaeocystodinium golzowense*
	HO	162	987E	-	-	-	-	-	-	C3Br	Channell et al., 1999b	Smelror (pers. comm.)	as *Palaeocystodinium golzowense*
	HO	81	555A	10-5, 70-72	107.20	9-1, 28-30	91.28	99.24	7.96	NN11	Backman, 1984	Edwards, 1984	as *Palaeocystodinium golzowense* s.l.
	HO	48	400A	30-1, 22-25	350.22	29-1, 80-84	341.30	345.76	4.46	NN7	Müller, 1979	Harland, 1979	as *Palaeocystodinium golzowense*
	HO	80	548A	8-1, 75-77	272.75	7-1, 50-52	263.00	267.88	4.88	NN11	Müller, 1985	Brown and Downie, 1985	as *Palaeocystodinium golzowense*
	HPO	80	548A	11-5, 8-9	306.58	11-3, 8-9	303.58	305.08	1.50	NN6	Müller, 1985	Brown and Downie, 1985	as *Palaeocystodinium golzowense*
	HO	150	905A	62-CC	558.50	58-CC	519.90	539.20	19.30	NN11	Gartner and Shyu, 1996	de Verteuil, 1996	as *Palaeocystodinium golzowense*
P. vesiculata	HO	94	610A	21-2, 35-40	193.28	21-1, 24-30	191.67	192.48	0.81	C2Ar	Clement and Robinson, 1987	de Schepper and Head, 2008	
	HO	93	603C	28-6, 35-37	249.07	28-2, 15-17	242.60	245.84	3.23	C3n.2n	Canninga et al., 1987	Head (unpubl.)	
R. actinocoronata	HO	104	642C	11-1, 108-109	74.08	11-1, 38-39	73.38	73.73	0.35	C2Ar/C3n.2r	Bleil, 1989	Mudie, 1989	
	HO	162	987E	-	-	-	-	-	-	C3n.3n	Channell et al., 1999b	Channell et al., 1999b	
	HO	105	646B	40-4, 27-31	376.47	40-3, 27-31	374.94	375.71	0.77	lower NN15	Knüttel et al., 1989	de Vernal and Mudie, 1989	as *Impletosphaeridium* sp. 1
	HO	94	607A	23-6, 50	215.60	23-2, 50	209.60	212.60	3.00	top Chron C3n.4n	Baldauf et al., 1987	Mudie, 1987	as ?*Cannosphaeropsis* sp. 1
	HO	94	611C	27-4, 50	238.19	26-2, 50	225.59	231.89	6.30	C3n.2n	Baldauf et al., 1987	Mudie, 1987	as ?*Cannosphaeropsis* sp. 1
	HO	80	548A	2-2, 10-12	216.50	uppermost sample				top NN11	Müller, 1985	Brown and Downie, 1985	as *Impletosphaeridium* sp. 1 of Manum
	HO	81	555A	5-6, 45-47	41.95	4-6, 57-59	32.57	37.26	4.69	upper NN11	Backman, 1984	Edwards, 1984	as ?*Cannosphaeropsis* sp. B of Shimakura
	HO	93	603C	24-4, 84-86	208.16	24-2, 50-52	204.82	206.49	1.67	C2Ar	Canninga et al., 1987	Head (unpubl.)	
	HCO	93	603C	28-6, 35-37	249.07	28-2, 15-17	242.87	245.97	3.10	C3n.2n	Canninga et al., 1987	Head (unpubl.)	
U. aquaeductus	HO	104	643A	12-4, 31-33	105.11	12-1,31-33	100.61	102.86	2.25	-	Goll, 1997 (unpubl.)	Manum et al., 1989	as *Impagidinium aquaeductus*
	HO	48	406	20-3, 61-65	521.61	16-2, 70-72	482.30	501.96	19.66	NN5	Müller, 1979	Costa and Downie, 1979	as *Leptodinium* sp. V
	HO	150	905A	85-CC	780.10	82-CC	751.10	765.60	14.50	NN6	Gartner and Shyu, 1996	de Verteuil, 1996	
	HO	307	1318B	11-4, 123-125	96.20	11-4, 23-25	95.20	95.70	0.50	C5An.2n	Louwye et al., 2007	Louwye et al., 2007	

Appendix B

A) Site	Author	identified species	illustration
DSDP 400/408	Engel 1992	*B. micropapillata, B. minuta*	Pl. 1, 1–2
DSDP 603	M.J.H. unpubl. data	*B. micropapillata (microreticulate)*	–
DSDP 610	De Schepper & Head 2008, 2009	*B. minuta*	Pl. 1, 6–8
ODP 643	Manum et al. 1989	*B. micropapillata*	Pl. 1, 10; Pl. 4, 1–4; Pl. 2, 16
ODP 645	Head et al. 1989a	*Batiacasphaera/Cerebrocysta? group A*	Pl. 1, 1–6, 9–12, 17, 18, 23, 24
ODP 646	Head et al. 1989b; de Vernal & Mudie 1989	*B. micropapillata "complex"*	Pl. 9, 6–7, 11–13; Pl. 3, 17–19
ODP 765	McMinn 1992	*B. micropapillata*	Pl. 3, 14–15, 16
ODP 900	McCarthy & Mudie 1996	*B. micropapillata*	Pl. 1, 7
ODP 907	this study, Schreck et al., subm.	*B. micropapillata, B. minuta*	Pl. 1, 1–6, 9, 12–15
ODP 985	Williams & Manum 1999	*B. micropapillata*	–
ODP 1151	Kurita & Obuse 2003	*B. minuta*	–
IODP U1318	Louwye et al. 2008	*B. micropapillata, B. minuta*	–
IODP M0002	this study	*B. micropapillata, B. minuta*	Pl. 1, 7–8, 10–11
Davis Strait	Piasecki 2003	*B. minuta*	–
Iceland	Verhoeven et al. 2011	*B. minuta*	Pl. 1, N
Bering Sea	Matsuoka & Bujak 1988	*B. minuta*	Pl. 18, 10
Belgium	De Schepper et al. 2008; Louwye & De Schepper 2010 Louwye & Laga 1998, 2008; Louwye 2002 Louwye et al. 2000, 2004, 2007, 2010	*B. micropapillata, B. minuta*	Pl. 2, 6; in Louwye 2002 Fig. 6, c; in Louwye & Laga 1998 Fig. 7, l; in Louwye & Laga 2008
England	Head 1997, 1998	*B. minuta*	Fig. 6, 21–23; Fig. 7, 1–2
Germany	Köthe 2003; Rusbült & Strauss 1992	*B. minuta*	Abb. 4, 1–2
Netherlands	Kuhlmann et al. 2006	*B. minuta*	–
central Europe	Jimenez-Moreno et al. 2006	*B. micropapillata (vermiculoreticulate)*	Pl. 1, 4–6
Japan	Matsuoka 1983; Matsuoka et al. 1987	*B. minuta*	Pl. 5, 6; Pl. 6, 7a-7b
Argentina	Guerstein and Junciel 2001	*B. micropapillata*	Fig. 4A, J
Argentina	Guler and Guerstein 2003	*B. micropapillata, B. minuta*	Fig. 12, a–h

B) Site	Author	identified species	illustration
DSDP 183–192	Bujak 1984	–	–
DSDP 400	Harland 1979	–	–
DSDP 406	Costa & Downie 1979	–	–
DSDP 548	Brown & Downie 1984	–	–
DSDP 552–555	Edwards 1984	*B. sphaerica*	Pl. 1, 1
DSDP 572–575	Jarvis & Tocher 1985	–	–
DSDP 607/611	Mudie 1987	–	–
ODP 815	McMinn 1993	*Batiacasphaera* spp.	Pl. 2, 15
ODP 902–906	de Vertuil 1996	*B. sphaerica*	–
ODP 1039	Zegarra and Helenes 2011	*Batiacasphaera* spp.	–
ODP 1085–1087	Udeze & Oboh-Ikuenobe 2005	*B. sphaerica* sensu lato	Fig. 2, H
ODP 1095–1096	Pudsey & Harland 2001	–	–
ODP 1165	Mcphail & Truswell 2004; Hannah 2006	Batiacasphaera sp. A–C	Pl. 4, 5–8, 11–12 in Mcphail & Truswell 2004
ODP 1168	Brinkhuis et al. 2003	*Batiacasphaera* spp.	
northern North Sea	Piasecki et al. 2002	*B. sphaerica*	–
Netherlands	Munstermann & Brinkhuis 2004	*Batiacasphaera* spp.	–
France	Londeix 1998	*B. sphaerica*	–
North Italy	Powell 1986; Zevenboom 1995	*B. sphaerica*	–
Sicily	Londeix 2007	–	–
Crete	Santarelli et al. 1998	–	–
Salisbury Embayment	de Verteuil & Noris 1996	*B. sphaerica*	Pl. 1, 1–3; Pl. 11, 4–5, 7–8
South Carolina	Edwards 1986	–	–
Gulf of Mexico	Wrenn & Kokinos 1986	*Batiacasphaera* spp.	–
Great Bahama Bank	Head & Westphal 1999	–	–
off Morocco	Warny & Wrenn 2002	–	–
Gulf of Suez	Soliman et al. 2012	*B. sphaerica*	Pl. 6, 6
Gulf of Suez	Mahmoud 1993	*Batiacasphaera* spp.	–
Argentina	Quattroccio et al. 1986	*Batiacasphaera* spp.	Pl. 1, 2
McMurdo Sound	Hannah et al. 1998	–	–

Depth (mbsf)	49.1	51.1	53.0	55.1	56.6	58.0	60.3	62.2	63.2	64.2	65.2	66.2	67.2	68.2	69.2	70.2	71.2	72.1	73.2	74.2	75.2	76.2	77.2	78.2	79.2	80.2	81.2	82.2	83.2	84.2	85.2	86.2
calibrated age (Ma)	2.59	2.69	2.78	2.89	2.97	3.04	3.16	3.27	3.34	3.42	3.48	3.55	3.66	3.82	3.98	4.14	4.26	4.34	4.45	4.55	4.64	4.74	4.84	4.94	5.04	5.13	5.23	5.32	5.42	5.52	5.62	5.71
Sample (core, section, interval in cm)	6H3 82-84	6H4 130-132	6H6 16.5 -18.5	7H1 30-32	7H2 31-33	7H3 17-19	7H4 102-104	7H5 137.5-139.5	7H6 87-89	7H7 41-43	8H1 90-92	8H2 40-42	8H2 140-142	8H3 90-92	8H4 43-45	8H4 140-142	8H5 90-92	8H6 32-34	8H6 140-142	9H1 40-42	9H1 140-142	9H2 90-92	9H3 41-43	9H3 140-142	9H4 93-95	9H5 40-42	9H5 140-142	9H6 90-92	9H7 40-42	10H1 88-90	10H2 40-42	10H2 140-142
Lycopodium clavatum tablets	**2**	**2**	**2**	**2**	**2**	**2**	**2**	**2**	**2**	**2**	**2**	**2**	**2**	**2**	**2**	**2**	**2**	**2**	**2**	**2**	**2**	**2**	**2**	**2**	**2**	**2**	**2**	**2**	**2**	**2**	**2**	**2**
total in-situ dinocyst counted	**4**	**3**	**7**	**7**	**2**	**2**	**2**	**9**	**403**	**407**	**2**	**0**	**196**	**10**	**0**	**0**	**137**	**53**	**367**	**414**	**362**	**355**	**393**	**379**	**28**	**89**	**134**	**173**	**351**	**72**	**459**	**377**
total Lycopodium spores counted	**58**	**157**	**176**	**200**	**216**	**339**	**196**	**832**	**92**	**45**	**272**	**220**	**2090**	**456**	**177**	**458**	**222**	**153**	**259**	**129**	**75**	**55**	**47**	**90**	**440**	**392**	**326**	**215**	**488**	**291**	**141**	**324**
Achomosphaera cf. andalousiensis																																
Achomosphaera cf. ramulifera																																
Achomosphaera spp.																			1	*					1							
Amiculosphaera umbraculum																																
Arcticacysta backmanii																			9	55												
Ataxodinium choane																						*						2	1	3		
Barssidinium evangelineae																																
Barssidinium graminosum																				2												
Barssidinium pliocenicum																																
Barssidinium wrenni																																
Batiacaspahera/Pyxidinopsis group								9																								
Batiacasphaera hirsuta																							*						1			
Batiacasphaera cf. hirsuta																				2										1		
Batiacasphaera micropapillata complex										4	1		3				2		2	63		167	16	9	11	6		2			1	5
Batiacasphaera sphaerica																				4	32									1		
Batiacasphaera sp. II of Edwards 1984																																
Batiacasphaera sp. A																							9									
Bitectatodinium? arborichiarum																																
Bitectatodinium tepikiense																							9									
Brigantedinium caiacoense																																
Brigantedinium simplex																																
Brigantedinium spp.														1						29	13				1					2		
Cerebrocysta cf. lagae																														1		
Cerebrocysta poulsenii																																
Cerebrocytsa irregulare																																
Cleistosphaeridium cf. placacantum																																
Cleistosphaeridium placacanthum																														1		
Cordosphaeridium minimum sensu B.S.																																
Corrudinium devernaliae																			36													
Corrudinium labradorii																				41			1						1			
Corrudinium sp. cf. labradorii																																
Corrudinium? harlandii																	2	1	1													
Cristadinium cristatoserratum																														3		
Cristadinium cf. cristatoserratum																																
Cristadinium diminutivum																																
Cristadinium sp. A																																
Cristadinium sp. B																																
?Cyclopsiella spiculosa																																
Dapsilidinium pastielsii																																
Dapsilidinium pseudocolligerum																																
Dinocyst A																								278		1						
Dinocyst B																																
Dinocyst C																																
Dinocyst D																																
Dinocyst E																																
Dinocyst F																																
Dinocyst G																																
Dinocyst H																																
Dinocyst H																																
Dinocyst I																																
Dinocyst J																																
Dinocyst K																																
Dinocyst L																																
Dinocyst M																																
Dinocyst N																																
Filisphaera filifera							1													2												
Filisphaera cf. filifera																																
Filisphaera microornata																																
Filisphaera sp. A																																
Filisphaera sp. B																																
Filisphaera sp. C																																
Filisphaera sp. D																																
Habibacysta tectata			3			1																	*	1		4	2			1		
Hystrichokolpoma rigaudiae																																
Hystrichosphaeridium ?tubiferum																																
Hystrichosphaeropsis obscura																																
Impagidinium aculeatum													1				1		1	*		1	1									
Impagidinium aff. aculeatum																																
Impagidinium cf. antecarcerem																																
Impagidinium elongatum																																
Impagidinium multiplexum																																
Impagidinium pallidum													12				4	4	10	7	1	2			8			1		1		
Impagidinium patulum																																
Impagidinium cf. pacificum		2	1						1				33				2	9		18	27			2			2	2	3	9		

Depth (mbsf)	49.1	51.1	53.0	55.1	56.6	58.0	60.3	62.2	63.2	64.2	65.2	66.2	67.2	68.2	69.2	70.2	71.2	72.1	73.2	74.2	75.2	76.2	77.2	78.2	79.2	80.2	81.2	82.2	83.2	84.2	85.2	86.2
calibrated age (Ma)	2.59	2.69	2.78	2.89	2.97	3.04	3.16	3.27	3.34	3.42	3.48	3.55	3.66	3.82	3.98	4.14	4.26	4.34	4.45	4.55	4.64	4.74	4.84	4.94	5.04	5.13	5.23	5.32	5.42	5.52	5.62	5.71
Sample (core, section, interval in cm)	6H3 82-84	6H4 130-132	6H6 16.5 -18.5	7H1 30-32	7H2 31-33	7H3 17-19	7H4 102-104	7H5 137.5 -139.5	7H6 87-89	7H7 41-43	8H1 90-92	8H2 40-42	8H2 140-142	8H3 90-92	8H4 43-45	8H4 140-142	8H5 90-92	8H6 32-34	8H6 140-142	9H1 40-42	9H1 140-142	9H2 90-92	9H3 41-43	9H3 140-142	9H4 93-95	9H5 40-42	9H5 140-142	9H6 90-92	9H7 40-42	10H1 88-90	10H2 40-42	10H2 140-142
Lycopodium clavatum tablets	**2**	**2**	**2**	**2**	**2**	**2**	**2**	**2**	**2**	**2**	**2**	**2**	**2**	**2**	**2**	**2**	**2**	**2**	**2**	**2**	**2**	**2**	**2**	**2**	**2**	**2**	**2**	**2**	**2**	**2**	**2**	**2**
total in-situ dinocyst counted	**4**	**3**	**7**	**7**	**2**	**2**	**2**	**9**	**403**	**407**	**2**	**0**	**196**	**10**	**0**	**0**	**137**	**53**	**367**	**414**	**362**	**355**	**393**	**379**	**28**	**89**	**134**	**173**	**351**	**72**	**459**	**377**
total Lycopodium spores counted	**58**	**157**	**176**	**200**	**216**	**339**	**196**	**832**	**92**	**45**	**272**	**220**	**2090**	**456**	**177**	**458**	**222**	**153**	**259**	**129**	**75**	**55**	**47**	**90**	**440**	**392**	**326**	**215**	**488**	**291**	**141**	**324**
Impagidinium cf. sphaericum										1															1							
Impagidinium strialatum																																
Impagidinium cf. velorum				2													1														1	
Impagidinium sp. A																																
Impagidinium sp. B																																
Impagidinium sp. C																																
Impagidinium sp. indet													4				1	1														2
Invertocysta lacrymosa																			3	*	1		*									
Invertocysta paratabulata																																
Labyrinthodinium truncatum																																
Lejeunecysta fallax																				2												
Lejeunecysta sp. 1																														6		
Lejeunecysta sp.3																																
Lejeunecysta sp. 2																																
Lejeunecysta sp. 4																																
Lejeunecysta sp. 5																																
Lejeunecysta sp. 6																																
Lejeunecysta sp. 7																																
Lejeunecysta sp. 8																																
Lejeunecysta sp. 9																																
Lejeunecysta sp. 10																																
Lejeunecysta sp. indet																								1								
Lingoludinium machaerophorum																																
Lingoludinium multivirgatum																																
Litosphaeridium spp.																																
Melitasphaeridium choanophorum																			2				1									
Melitasphaeridium sp. A																																
Mendicodinium sp. indet																					2											
Nematosphaeropsis labyrinthus				5									3	1			73	20		137	30	41	17		1	64	99	140	284	18	285	145
Nematosphaeropsis labyrinthus "scrumbled"													3				19	5	5	34	18	25	4		1	9	6	12	20	3	171	95
Nematosphaeropsis labyrinthus (robust)																			273		188	5										
Nematosphaeropsis cf. downiei																																
Nematosphaeropsis cf. lativattus										1																						
Nematosphaeropsis cf. rigidius																		6														
Nematosphaeropsis sp. 1																																
Nematosphaeropsis sp. indet					1												24	3				23					22	14	31			
Operculodinium? borgerholtense																																
Operculodinium centrocarpum s.s.																																
O. aff. centrocarpum Wall and Dall 1966													4						*													
Operculodinium? eirikianum																			3	2		*	5		1		1				1	2
Operculodinium cf. eirikianum																																
Operculodinium israelianum						1			1	1							5		2	2	2	2	1			2			6	3		
Operculodinium cf. israelianum													2																			
Operculodinium piaseckii																													1			
Operculodinium cf. piaseckii																			1													
Operculodinium cf. vaculata																																
Operculodinium giganteum																																
Operculodinium janduchenei																																
Operculodinium tegillatum																			4	2	1	20	20	12		2						
Operculodinium sp. A																																
Operculodinium sp. B																																
Palaeocystodinium golzowense s.l.																																
Palaeocystodinium minor																																
Peridinioid cyst A																																
Peridinioid cyst B																																
Peridinioid cyst C																																
Peridinioid cyst E																																
Peridinioid cyst F																																
Peridinioid cyst G																																
Peridinioid cyst H																																
Peridinioid cyst I																																
Polysphaeridium spp.																																
Protoperidiniod cyst A																						2								1		
Protoperidinioid cyst B																														3		
Protoperidinioid cyst C																																
Pyxidinopsis psilata																																
Pyxidinopsis vesiculata																			10										1			
Pyxidinopsis sp. A																																
Pyxidinopsis sp. B																																
Pyxidinopsis sp. C																																
Pyxidinopsis sp. D																																
Pyxidinopsis spp.																											2					
Reticulatosphaera actinocoronata																			1	5		1	6	2		1				7		
R. actinocoronata sensu Manum et al. 1989																																
Round brown cysts																		1				4	57	66						6		6

Depth (mbsf)	49.1	51.1	53.0	55.1	56.6	58.0	60.3	62.2	63.2	64.2	65.2	66.2	67.2	68.2	69.2	70.2	71.2	72.1	73.2	74.2	75.2	76.2	77.2	78.2	79.2	80.2	81.2	82.2	83.2	84.2	85.2	86.2
calibrated age (Ma)	2.59	2.69	2.78	2.89	2.97	3.04	3.16	3.27	3.34	3.42	3.48	3.55	3.66	3.82	3.98	4.14	4.26	4.34	4.45	4.55	4.64	4.74	4.84	4.94	5.04	5.13	5.23	5.32	5.42	5.52	5.62	5.71
Sample (core, section, interval in cm)	6H3 82-84	6H4 130-132	6H6 16.5 -18.5	7H1 30-32	7H2 31-33	7H3 17-19	7H4 102-104	7H5 137.5-139.5	7H6 87-89	7H7 41-43	8H1 90-92	8H2 40-42	8H2 140-142	8H3 90-92	8H4 43-45	8H4 140-142	8H5 90-92	8H6 32-34	8H6 140-142	9H1 40-42	9H1 140-142	9H2 90-92	9H3 41-43	9H3 140-142	9H4 93-95	9H5 40-42	9H5 140-142	9H6 90-92	9H7 40-42	10H1 88-90	10H2 40-42	10H2 140-142
Lycopodium clavatum tablets	**2**	**2**	**2**	**2**	**2**	**2**	**2**	**2**	**2**	**2**	**2**	**2**	**2**	**2**	**2**	**2**	**2**	**2**	**2**	**2**	**2**	**2**	**2**	**2**	**2**	**2**	**2**	**2**	**2**	**2**	**2**	**2**
total in-situ dinocyst counted	**4**	**3**	**7**	**7**	**2**	**2**	**2**	**9**	**403**	**407**	**2**	**0**	**196**	**10**	**0**	**0**	**137**	**53**	**367**	**414**	**362**	**355**	**393**	**379**	**28**	**89**	**134**	**173**	**351**	**72**	**459**	**377**
total Lycopodium spores counted	**58**	**157**	**176**	**200**	**216**	**339**	**196**	**832**	**92**	**45**	**272**	**220**	**2090**	**456**	**177**	**458**	**222**	**153**	**259**	**129**	**75**	**55**	**47**	**90**	**440**	**392**	**326**	**215**	**488**	**291**	**141**	**324**
Selenopemphix brevispinosa																														1		
S. brevispinosa subsp. brevispinosa																								2								
S. brevispinosa subsp. conspicua																																
Selenopemphix dinoaecysta																																
Selenopemphix nephroides																				*			1									
Selenopemphix sp. 3 of Head et al. 1989																																
Selenopemphix sp. A																																
Selenopemphix sp. B																																
Selenopemphix sp. C																																
Selenopemphix sp. D																																
Selenopemphix sp. indet																																
Spiniferites elongatus			1														3	1		6	13	37	196	5	2							
Spiniferites ramosus "group"																			1													
Spiniferites sp. A																			1													
Spiniferites sp. B																																
Spiniferites spp.																			1	6	34	24	49	1						1		122
Sumatradinium soucouyantae																																
Tectatodinium pellitum																									1				1			
Trinovantedinium ferugnomatum																																
Trinovantedinium glorianum																																
Trinovantedinium harponium																																
Trinovantedinium papulum																						1										
Tuberculodinium vancampoae																																
Unipontedinium aquaeductus																																
Xandarodinium ?xanthum																																
Dinoflagellate cyts spp. indet.	4	1	2		1		1		1				1																1			
Dinoflagellate cyts spp. indet. (scan)																																
Reworked dinoflagellate cysts	63	3			1	1											1		1								1					
Acritarchs																																
acritarchs total counted	**1**	**2**	**4**		**2**				**1**	**1**						**1**	**2**	**5**	**290**	**114**	**351**	**392**	**35**	**80**	**199**	**4**		**49**	**67**	**3**	**3**	**16**
Acritarch sp. 1 (Impagidinium-like)																																
Acritarch sp. 2																		1	3													
Acitarch sp. 3 (resembling cyst of P. dalei)																			1	13		11								3		
Cymatiosphaera? invaginata		1	2	4		1											1	1		130	39	255	186	24		1	4		2	60	3	3
Cymatiosphaera spp.																																
D. martinheadii																																
?Impletosphaeridium sp.																																
Lavradosphaera crista																				52	25	17	3	2								
Lavradosphaera lucifer																														4		
?Lavradosphaera sp. 1																																
?Micrhystridium sp. 1																																
?Micrhystridium sp. 2																																
?Micrhystridium sp.																																
?Nannobarbophora gedlii (possibly including N. walldalei)										1											1											
Sphaeromorphitic acritarchs						1														60	49	68	201	9	80	198			47			
Undifferentiated acritarchs											1								1	35			2									

Depth (mbsf)	87.2	88.0	89.2	90.4	91.7	92.3	92.9	93.5	94.4	95.5	96.4	97.0	97.4	98.0	98.5	99.0	99.6	100.0	100.5	101.1	101.4	101.9	102.5	103.1	103.6	104.0	104.5	105.1	105.5	106.1	106.6
calibrated age (Ma)	5.81	5.88	6.00	6.10	6.21	6.26	6.37	6.46	6.54	6.65	6.73	6.85	6.95	7.07	7.18	7.28	7.40	7.50	7.60	7.72	7.79	7.89	8.02	8.14	8.25	8.34	8.44	8.56	8.66	8.78	8.88
Sample (core, section, interval in cm)	10H3 90-92	10H4 17.5-19.5	10H4 140-142	10H5 110-112	10H6 87-89	10H7 1-3	11H1 11-13	11H1 73-75	11H2 11-13	11H2 121-123	11H3 60-62	11H3 117.5-119.5	11H4 12-14	11H4 69.5-71.5	11H4 121-123	11H5 18-20	11H5 77-79	11H5 122-124	11H6 20-22	11H6 77-79	11H6 111-113	11H7 7-9	12H1 20-22	12H1 77-79	12H1 127-129	12H2 22-24	12H2 68-70	12H2 127-129	12H3 20-22	12H3 77-79	12H3 127-129
Lycopodium clavatum tablets	**2**	**2**	**2**	**2**	**2**	**2**	**2**	**2**	**2**	**2**	**2**	**2**	**2**	**2**	**2**	**2**	**2**	**2**	**2**	**2**	**2**	**2**	**2**	**2**	**2**	**2**	**2**	**2**	**2**	**2**	**2**
total in-situ dinocyst counted	**392**	**33**	**30**	**51**	**363**	**37**	**0**	**28**	**64**	**227**	**251**	**363**	**13**	**401**	**365**	**318**	**1**	**3**	**1**	**0**	**0**	**0**	**1**	**14**	**75**	**360**	**365**	**397**	**355**	**392**	**288**
total Lycopodium spores counted	**253**	**246**	**137**	**410**	**223**	**1013**	**636**	**155**	**74**	**41**	**312**	**10**	**359**	**40**	**46**	**653**	**814**	**766**	**1534**	**1796**	**382**	**554**	**195**	**265**	**-**	**167**	**84**	**34**	**23**	**159**	**235**
Achomosphaera cf. andalousiensis																															
Achomosphaera cf. ramulifera													1		12															*	1
Achomosphaera spp.									*							4															*
Amiculosphaera umbraculum											10				*																*
Arcticacysta backmanii																										2					
Ataxodinium choane	10	3			7					24	2	*		54	30	7										8	4				
Barssidinium evangelineae																															
Barssidinium graminosum															*												1				
Barssidinium pliocenicum																															
Barssidinium wrenni																															
Batiacasphaera/Pyxidinopsis group			1	1				*	3																	2	6				3
Batiacasphaera hirsuta																											3			1	
Batiacasphaera cf. hirsuta																													1		
Batiacasphaera micropapillata complex	4				2					23	22			171	78	1									13	223	129	50	304	180	155
Batiacasphaera sphaerica																												2			
Batiacasphaera sp. II of Edwards 1984																															
Batiacasphaera sp. A																															
Bitectatodinium? arborichiarum																															
Bitectatodinium tepikiense														3	5																
Brigantedinium caiacoense																															
Brigantedinium simplex		2																										*			
Brigantedinium spp.															7										1		17	20			
Cerebrocysta cf. lagae																1															
Cerebrocysta poulsenii																															
Cerebrocytsa irregulare																															
Cleistosphaeridium cf. placacantum																															
Cleistosphaeridium placacanthum																															
Cordosphaeridium minimum sensu B.S.																															
Corrudinium devernaliae																															
Corrudinium labradorii														8	4											1					
Corrudinium sp. cf. labradorii														6																	
Corrudinium? harlandii																															
Cristadinium cristatoserratum	2														*										22	9	28	1	23		1
Cristadinium cf. cristatoserratum																															
Cristadinium diminutivum	1																														
Cristadinium sp. A																															
Cristadinium sp. B																															
?Cyclopsiella spiculosa																															
Dapsilidinium pastielsii																															
Dapsilidinium pseudocolligerum																															
Dinocyst A																															
Dinocyst B					43																										
Dinocyst C																									1	1					
Dinocyst D																															
Dinocyst E																															
Dinocyst F																															
Dinocyst G																															
Dinocyst H																															
Dinocyst H																															
Dinocyst I																															
Dinocyst J																															
Dinocyst K																															
Dinocyst L																															
Dinocyst M																															
Dinocyst N																															
Filisphaera filifera																															
Filisphaera cf. filifera				11																											
Filisphaera microornata					1							*																			
Filisphaera sp. A																															
Filisphaera sp. B																															
Filisphaera sp. C																															
Filisphaera sp. D																															
Habibacysta tectata	*	1			16	5		2	17		1	5		13	17	13									2	11	10		1	43	24
Hystrichokolpoma rigaudiae																															
Hystrichosphaeridium ?tubiferum																															
Hystrichosphaeropsis obscura																														*	
Impagidinium aculeatum																3													*		
Impagidinium aff. aculeatum																															
Impagidinium cf. antecarcerem																															
Impagidinium elongatum																															
Impagidinium multiplexum																															
Impagidinium pallidum				2	5	1		21	1	11	2	1		13	1										3	12	16		3		4
Impagidinium patulum									3			2																			
Impagidinium cf. pacificum	2			2							1			1	1										4		4	3	10	4	5

Depth (mbsf)	87.2	88.0	89.2	90.4	91.7	92.3	92.9	93.5	94.4	95.5	96.4	97.0	97.4	98.0	98.5	99.0	99.6	100.0	100.5	101.1	101.4	101.9	102.5	103.1	103.6	104.0	104.5	105.1	105.5	106.1	106.6
calibrated age (Ma)	5.81	5.88	6.00	6.10	6.21	6.26	6.37	6.46	6.54	6.65	6.73	6.85	6.95	7.07	7.18	7.28	7.40	7.50	7.60	7.72	7.79	7.89	8.02	8.14	8.25	8.34	8.44	8.56	8.66	8.78	8.88
Sample (core, section, interval in cm)	10H3 90-92	10H4 17.5-19.5	10H4 140-142	10H5 110-112	10H6 87-89	10H7 1-3	11H1 11-13	11H1 73-75	11H2 11-13	11H2 121-123	11H3 60-62	11H3 117.5-119.5	11H4 12-14	11H4 69.5-71.5	11H4 121-123	11H5 18-20	11H5 77-79	11H5 122-124	11H6 20-22	11H6 77-79	11H6 111-113	11H7 7-9	12H1 20-22	12H1 77-79	12H1 127-129	12H2 22-24	12H2 68-70	12H2 127-129	12H3 20-22	12H3 77-79	12H3 127-129
Lycopodium clavatum tablets	**2**	**2**	**2**	**2**	**2**	**2**	**2**	**2**	**2**	**2**	**2**	**2**	**2**	**2**	**2**	**2**	**2**	**2**	**2**	**2**	**2**	**2**	**2**	**2**	**2**	**2**	**2**	**2**	**2**	**2**	**2**
total in-situ dinocyst counted	**392**	**33**	**30**	**51**	**363**	**37**	**0**	**28**	**64**	**227**	**251**	**363**	**13**	**401**	**365**	**318**	**1**	**3**	**1**	**0**	**0**	**0**	**1**	**14**	**75**	**360**	**365**	**397**	**355**	**392**	**288**
total Lycopodium spores counted	**253**	**246**	**137**	**410**	**223**	**1013**	**636**	**155**	**74**	**41**	**312**	**10**	**359**	**40**	**46**	**653**	**814**	**766**	**1534**	**1796**	**382**	**554**	**195**	**265**	**-**	**167**	**84**	**34**	**23**	**159**	**235**
Impagidinium cf. sphaericum																											1				
Impagidinium strialatum						1																									
Impagidinium cf. velorum																													*		
Impagidinium sp. A																															
Impagidinium sp. B																															
Impagidinium sp. C																															
Impagidinium sp. indet	1															1										7					
Invertocysta lacrymosa						4																								1	
Invertocysta paratabulata												*			*																
Labyrinthodinium truncatum																											5		*	3	1
Lejeunecysta fallax															7																
Lejeunecysta sp. 1	2																														
Lejeunecysta sp.3																															
Lejeunecysta sp. 2																												1			
Lejeunecysta sp. 4																															
Lejeunecysta sp. 5																															
Lejeunecysta sp. 6																															
Lejeunecysta sp. 7																															
Lejeunecysta sp. 8															11																
Lejeunecysta sp. 9															2																
Lejeunecysta sp. 10																															
Lejeunecysta spp.																															
Lingoludinium machaerophorum								*				*													2	1	1			*	*
Lingoludinium multivirgatum																															
cf. Litosphaeridium spp.																															
Melitasphaeridium choanophorum					*							*															6		*	1	
Melitasphaeridium sp. A																															
Mendicodinium sp.											212			3													1				
Nematosphaeropsis labyrinthus	179	1	13	28	195			3	15	29		339	10	70	23	242	1	2					1	12	22	37	51	10	4	149	75
Nematosphaeropsis labyrinthus "scrumbled"	163	1	16	2	7			1	2	5		13		10	12	35		1						1		11	13	28	1	4	8
Nematosphaeropsis labyrinthus (robust)		17			9	19			21					3														251			
Nematosphaeropsis cf. downiei																															
Nematosphaeropsis cf. lativitattus												*																			
Nematosphaeropsis cf. rigidius																															
Nematosphaeropsis sp. 1																															
Nematosphaeropsis sp. indet	9																														
Operculudinium? borgerholtense																															
Operculodinium centrocarpum s.s.									*																						
O. aff. centrocarpum Wall and Dall 1966																															
Operculodinium? eirikianum				1							1			1	1											5	2				1
Operculodinium cf. eirikianum																													1		*
Operculodinium israelianum		1			2	4		1	1			*			1	1											*				
Operculodinium cf. israelianum																								1							
Operculodinium piaseckii																											2	*	1	1	2
Operculodinium cf. piaseckii																															
Operculodinium cf. vaculata															1																
Operculodinium giganteum																															
Operculodinium janduchenei																															*
Operculodinium tegillatum													1																*		1
Operculodinium sp. A																															
Operculodinium sp. B																															
Palaeocystodinium golzowense s.l.																															1
Palaeocystodinium minor																															
Peridinioid cyst A		1																								1					
Peridinioid cyst B																											1	4			*
Peridinioid cyst C																															
Peridinioid cyst E																															
Peridinioid cyst F																															
Peridinioid cyst G																															
Peridinioid cyst H																															
Peridinioid cyst I																															
?Polysphaeridium spp.																															
Protoperidiniod cyst A	2														1												*	2			*
Protoperidinioid cyst B																															
Protoperidinioid cyst C																															
Pyxidinopsis psilata																														*	
Pyxidinopsis vesiculata		1																													
Pyxidinopsis sp. A										135						1															
Pyxidinopsis sp. B	4	1										1		6	15	1															
Pyxidinopsis sp. C																															
Pyxidinopsis sp. D																															
Pyxidinopsis spp.									*							1										10			3		
Reticulatosphaera actinocoronata	1	1									*	2		21	87	2			1						1	9	15		*		
R. actinocoronata sensu Manum et al. 1989																															
Round brown cysts	12	3													12											10	45	25	2		4

Depth (mbsf)	87.2	88.0	89.2	90.4	91.7	92.3	92.9	93.5	94.4	95.5	96.4	97.0	97.4	98.0	98.5	99.0	99.6	100.0	100.5	101.1	101.4	101.9	102.5	103.1	103.6	104.0	104.5	105.1	105.5	106.1	106.6
calibrated age (Ma)	5.81	5.88	6.00	6.10	6.21	6.26	6.37	6.46	6.54	6.65	6.73	6.85	6.95	7.07	7.18	7.28	7.40	7.50	7.60	7.72	7.79	7.89	8.02	8.14	8.25	8.34	8.44	8.56	8.66	8.78	8.88
Sample (core, section, interval in cm)	10H3 90-92	10H4 17.5-19.5	10H4 140-142	10H5 110-112	10H6 87-89	10H7 1-3	11H1 11-13	11H1 73-75	11H2 11-13	11H2 121-123	11H3 60-62	11H3 117.5-119.5	11H4 12-14	11H4 69.5-71.5	11H4 121-123	11H5 18-20	11H5 77-79	11H5 122-124	11H6 20-22	11H6 77-79	11H6 111-113	11H7 7-9	12H1 20-22	12H1 77-79	12H1 127-129	12H2 22-24	12H2 68-70	12H2 127-129	12H3 20-22	12H3 77-79	12H3 127-129
Lycopodium clavatum tablets	**2**	**2**	**2**	**2**	**2**	**2**	**2**	**2**	**2**	**2**	**2**	**2**	**2**	**2**	**2**	**2**	**2**	**2**	**2**	**2**	**2**	**2**	**2**	**2**	**2**	**2**	**2**	**2**	**2**	**2**	**2**
total in-situ dinocyst counted	**392**	**33**	**30**	**51**	**363**	**37**	**0**	**28**	**64**	**227**	**251**	**363**	**13**	**401**	**365**	**318**	**1**	**3**	**1**	**0**	**0**	**0**	**1**	**14**	**75**	**360**	**365**	**397**	**355**	**392**	**288**
total Lycopodium spores counted	**253**	**246**	**137**	**410**	**223**	**1013**	**636**	**155**	**74**	**41**	**312**	**10**	**359**	**40**	**46**	**653**	**814**	**766**	**1534**	**1796**	**382**	**554**	**195**	**265**	**-**	**167**	**84**	**34**	**23**	**159**	**235**
Selenopemphix brevispinosa																															
S. brevispinosa subsp. brevispinosa																															
S. brevispinosa subsp. conspicua																											1				
Selenopemphix dinoaecysta																															
Selenopemphix nephroides															3													*			
Selenopemphix sp. 3 of Head et al. 1989																															
Selenopemphix sp. A																															
Selenopemphix sp. B																															
Selenopemphix sp. C																															
Selenopemphix sp. D																															
Selenopemphix sp. indet																															
Spiniferites elongatus													1																		
Spiniferites ramosus "group"					70				*		*			12	25	5											2		*	2	
Spiniferites sp. A																														2	
Spiniferites sp. B																															
Spiniferites spp.				4	6	1								3	3										4		1		1		2
Sumatradinium soucouyantae																															
Tectatodinium pellitum														3																	
Trinovantedinium ferugnomatum																															
Trinovantedinium glorianum															4																
Trinovantedinium harponium																															
Trinovantedinium papulum																															
Tuberculodinium vancampoae																															
Unipontedinium aquaeductus																															
Xandarodinium ?xanthum																															
Dinoflagellate cyts spp. indet.									1						2																
Dinoflagellate cyts spp. indet. (scan)																													1		
Reworked dinoflagellate cysts														1		1							1								
Acritarchs																															
acritarchs total counted			**1**	**32**	**5**		**364**	**356**	**189**	**128**	**18**	**2**	**61**	**66**	**68**		**1**			**1**	**1**		**2**	**7**	**38**	**48**	**9**	**14**	**11**	**100**	**67**
Acritarch sp. 1 (Impagidinium-like)																															
Acritarch sp. 2																										10	4	3	1	1	
Acitarch sp. 3 (resembling cyst of P. dalei)				1	2							*		25	11											3	26	1		5	
Cymatiosphaera? invaginata	15				30	1				*	3	1	2	1				1				1		1			1				
Cymatiosphaera spp.																															
D. martinheadii						2		363	355	185	125	12		6	31	60								1	7	21	7	5	8	5	97
?Impletosphaeridium sp.																															
Lavradosphaera crista														4																	
Lavradosphaera lucifer																															
?Lavradosphaera sp. 1																															
?Micrhystridium sp. 1																															
?Micrhystridium sp. 2																															
?Micrhystridium sp.																															
?Nannobarbophora gedlii (possibly including N. walldalei)	1																														
Sphaeromorphitic acritarchs						2						5		3	12	7											2		1		
Undifferentiated acritarchs								1	1	4				22	12	1					1					4	8		4		3

Depth (mbsf)	107.0	107.6	107.9	108.5	109.1	109.5	109.9	110.5	111.1	111.5	113.1	114.7	116.4	117.9	119.5	121.1	122.7	124.3	125.9	127.5	129.1	130.3	131.5	132.7	133.8	135.0	136.3	137.5	138.7	139.3	140.5	141.7
calibrated age (Ma)	8.97	9.09	9.17	9.29	9.42	9.51	9.59	9.71	9.84	9.92	10.06	10.16	10.26	10.35	10.44	10.53	10.63	10.72	10.82	10.91	11.00	11.09	11.19	11.28	11.37	11.47	11.57	11.67	11.76	11.81	11.90	12.00
Sample (core, section, interval in cm)	12H4 18-20	12H4 77-79	12H4 111.5-113.5	12H5 19-21	12H5 82.5-84.5	12H5 123-125	12H6 12-14	12H6 69-71	12H6 130-132	12H7 16.5-18.5	13H1 130-132	13H2 142-144	13H4 8-10	13H5 12-14	13H6 20-22	13H7 31.5-33.5	14H1 141.5-143.5	14H3 4-6	14H4 10-12	14H5 20-22	14H6 30-32	14H7 1-3	15H1 74-76	15H2 38-40	15H3 4-6	15H3 123-125	15H4 100-102	15H5 74-76	15H6 37-39	15H6 92-94	16H1 17-19	16H1 140-142
Lycopodium clavatum tablets	**2**	**2**	**2**	**2**	**2**	**2**	**2**	**2**	**2**	**2**	**2**	**2**	**2**	**2**	**2**	**2**	**2**	**2**	**2**	**2**	**2**	**2**	**2**	**2**	**2**	**2**	**2**	**2**	**2**	**2**	**2**	**2**
total in-situ dinocyst counted	**316**	**239**	**289**	**291**	**336**	**265**	**263**	**363**	**355**	**327**	**372**	**386**	**301**	**369**	**374**	**339**	**352**	**369**	**355**	**359**	**354**	**372**	**368**	**367**	**362**	**375**	**383**	**352**	**358**	**359**	**376**	**356**
total Lycopodium spores counted	**131**	**72**	**67**	**119**	**51**	**213**	**244**	**134**	**73**	**19**	**40**	**64**	**176**	**27**	**15**	**163**	**175**	**30**	**20**	**38**	**52**	**27**	**60**	**94**	**46**	**81**	**39**	**69**	**20**	**122**	**150**	**303**
Achomosphaera cf. andalousiensis											*			*											*							
Achomosphaera cf. ramulifera							1	1	*	1								*	1			*		*	*							
Achomosphaera spp.										*			1	2	*	1		1	2				1	5	2	*		7				
Amiculosphaera umbraculum																										*		*			*	
Arcticacysta backmanii										1	3	5																				
Ataxodinium choane						2	4						2													8	3	2		*		
Barssidinium evangelineae																								*								
Barssidinium graminosum	2		*	1						*	1		1	4	1	6		*			*										
Barssidinium pliocenicum									*									*														
Barssidinium wrenni	1			*										*																		
Batiacasphaera/Pyxidinopsis group	4	1	1	4	4		32						2	4	139		29	27	7	9	7	5	23		9	39	31	31		32		
Batiacasphaera hirsuta	1			1					1									3	6	1				2		*	6			3		7
Batiacasphaera cf. hirsuta																												*				
Batiacasphaera micropapillata complex	143	115	126	69	15	27	122	95	92	120	100	142	47	76	131	22	17	134	148	238	155	97	124	64	214	246	95	91	298	30		112
Batiacasphaera sphaerica		5	3			1	2	3	2	10	11	22	6	13		5	5	8	6	2	8	4	3	7	7	25	24	30	7			3
Batiacasphaera sp. II of Edwards 1984																																
Batiacasphaera sp. A																									6							
Bitectatodinium? arborichiarum																																
Bitectatodinium tepikiense							4															2				2				5		
Brigantedinium caiacoense																		*														
Brigantedinium simplex																																
Brigantedinium spp.				2				9		5								26							*							
Cerebrocysta cf. lagae																																
Cerebrocysta poulsenii																												*				
Cerebrocytsa irregulare														4	2	10	12	3	6	1	3	11	*	20	8	5	5	3	*	17	3	8
Cleistosphaeridium cf. placacantum																							1									
Cleistosphaeridium placacanthum																	1	*	1	1	1	2				*						1
Cordosphaeridium minimum sensu B.S.														8		3	*	1	2	4	4				1							6
Corrudinium devernaliae																																
Corrudinium labradorii												1																				
Corrudinium sp. cf. labradorii																																
Corrudinium? harlandii																																
Cristadinium cristatoserratum		*	26	34	2		1	6	2	3		1		1	1	1			3	5	3		5	*	4			*				6
Cristadinium cf. cristatoserratum																		4			4	1	7	6	*	*	*	5	*			
Cristadinium diminutivum		*																									*					
Cristadinium sp. A																																
Cristadinium sp. B																																
?Cyclopsiella spiculosa														1																		
Dapsilidinium pastielsii									*																							
Dapsilidinium pseudocolligerum		*		1	2	3	2			*			*	2	1		2							*		*			1	3	1
Dinocyst A																																
Dinocyst B																																
Dinocyst C																																
Dinocyst D		1	*	1																												
Dinocyst E											*													1								
Dinocyst F			*											1																		
Dinocyst G											*				*			*														
Dinocyst H																1	1															
Dinocyst H																																
Dinocyst I																																
Dinocyst J																																
Dinocyst K																																
Dinocyst L																																
Dinocyst M																																
Dinocyst N																			1		1	8								1		
Filisphaera filifera																															5	
Filisphaera cf. filifera																																
Filisphaera microornata																																
Filisphaera sp. A																										*		29				
Filisphaera sp. B																						3										
Filisphaera sp. C																								29								
Filisphaera sp. D																																
Habibacysta tectata	15	8	6	6	4	12	8	162	171	98	50	8		34	25	34	70	20	33	42	90	20	75	64	17	15	74	16	36	69	26	19
Hystrichokolpoma rigaudiae																										*						
Hystrichosphaeridium ?tubiferum																																
Hystrichosphaeropsis obscura				*											*		9	*			2			1	*			5				2
Impagidinium aculeatum																																
Impagidinium aff. aculeatum						*						1		*	1	5	*	*	2		1	*	*	*		1		1			3	
Impagidinium cf. antecarcerem																																
Impagidinium elongatum			*									3	10	0	3	16	24	4	9	4	6	10	10	8	6	*	4		1	15	3	
Impagidinium multiplexum																																
Impagidinium pallidum	1	2	2			3	9	2	1	2	2	1	4			*	1		2	2	1	5	2	8	6	*	3	4	*	5	11	17
Impagidinium patulum																																
Impagidinium cf. pacificum	3	6	7	7	7	4	6		1	2			3				16	4		1	*		1	7	3	6	28	1		38	8	

Depth (mbsf)	107.0	107.6	107.9	108.5	109.1	109.5	109.9	110.5	111.1	111.5	113.1	114.7	116.4	117.9	119.5	121.1	122.7	124.3	125.9	127.5	129.1	130.3	131.5	132.7	133.8	135.0	136.3	137.5	138.7	139.3	140.5	141.7
calibrated age (Ma)	8.97	9.09	9.17	9.29	9.42	9.51	9.59	9.71	9.84	9.92	10.06	10.16	10.26	10.35	10.44	10.53	10.63	10.72	10.82	10.91	11.00	11.09	11.19	11.28	11.37	11.47	11.57	11.67	11.76	11.81	11.90	12.00
Sample (core, section, interval in cm)	12H4 18-20	12H4 77-79	12H4 111.5-113.5	12H5 19-21	12H5 82.5-84.5	12H5 123-125	12H6 12-14	12H6 69-71	12H6 130-132	12H7 16.5-18.5	13H1 130-132	13H2 142-144	13H4 8-10	13H5 12-14	13H6 20-22	13H7 31.5-33.5	14H1 141.5-143.5	14H3 4-6	14H4 10-12	14H5 20-22	14H6 30-32	14H7 1-3	15H1 74-76	15H2 38-40	15H3 4-6	15H3 123-125	15H4 100-102	15H5 74-76	15H6 37-39	15H6 92-94	16H1 17-19	16H1 140-142
Lycopodium clavatum tablets	**2**	**2**	**2**	**2**	**2**	**2**	**2**	**2**	**2**	**2**	**2**	**2**	**2**	**2**	**2**	**2**	**2**	**2**	**2**	**2**	**2**	**2**	**2**	**2**	**2**	**2**	**2**	**2**	**2**	**2**	**2**	**2**
total in-situ dinocyst counted	**316**	**239**	**289**	**291**	**336**	**265**	**263**	**363**	**355**	**327**	**372**	**386**	**301**	**369**	**374**	**339**	**352**	**369**	**355**	**359**	**354**	**372**	**368**	**367**	**362**	**375**	**383**	**352**	**358**	**359**	**376**	**356**
total Lycopodium spores counted	**131**	**72**	**67**	**119**	**51**	**213**	**244**	**134**	**73**	**19**	**40**	**64**	**176**	**27**	**15**	**163**	**175**	**30**	**20**	**38**	**52**	**27**	**60**	**94**	**46**	**81**	**39**	**69**	**20**	**122**	**150**	**303**
Impagidinium cf. sphaericum																																
Impagidinium strialatum																																
Impagidinium cf. velorum																														*		
Impagidinium sp. A											*				1	16	20															
Impagidinium sp. B						1	4																									
Impagidinium sp. C								9																								
Impagidinium sp. indet															1		1							*		1						
Invertocysta lacrymosa						*	1				*							1									2					
Invertocysta paratabulata																																
Labyrinthodinium truncatum	27	18	10	18	33	19	10	8	11	14	8	47	11	99	5	25	19	17	25	12	4	2	2	4	6	1	2	3		1	5	3
Lejeunecysta fallax			1							1	*																					
Lejeunecysta sp. 1																																
Lejeunecysta sp.3				1				*			*																		*			
Lejeunecysta sp. 2																																
Lejeunecysta sp. 4																																
Lejeunecysta sp. 5																																
Lejeunecysta sp. 6																																
Lejeunecysta sp. 7											*																					
Lejeunecysta sp. 8																																
Lejeunecysta sp. 9																																
Lejeunecysta sp. 10				1																	*	*										
Lejeunecysta spp.				1							1							*	1	1	2						1					1
Lingoludinium machaerophorum	*					1			1	1		25	22	8	1	1	2	1	9		*			1	2			8				
Lingoludinium multivirgatum																																
cf. Litosphaeridium spp.																1												1				
Melitasphaeridium choanophorum	1	*	*		*	*			*		*		1			2			1				*	*				1				
Melitasphaeridium sp. A																																
Mendicodinium sp.																																
Nematosphaeropsis labyrinthus	52	47	25	85	218	93	22	3	14	30	9	10	30	18		19	31	22	12	6	9	34	41	53	17	18	34	75	3	112	232	62
Nematosphaeropsis labyrinthus "scrumbled"		10	2	10	17	8	4		6			4	3	7	6	7	3		2			2	15	7						9		
Nematosphaeropsis labyrinthus (robust)																																
Nematosphaeropsis cf. downiei																																
Nematosphaeropsis cf. lativattus																																
Nematosphaeropsis cf. rigidius																																
Nematosphaeropsis sp. 1					1	3																*	*									
Nematosphaeropsis sp. indet																																
Operculodinium? borgerholtense																																
Operculodinium centrocarpum s.s.														*								*	*	18	3		38	6		1	3	2
O. aff. centrocarpum Wall and Dall 1966																																
Operculodinium? eirikianum	1	*		*		1		2	*		1	*	7	4	1	1	2	4	1	2				4	2	*	1	3		1	*	3
Operculodinium cf. eirikianum				*		1									*																	
Operculodinium israelianum	3		1			*		*	*	1	*	1		*		*			1		*			*								
Operculodinium cf. israelianum						1	*									1	1	*														
Operculodinium piaseckii		*		*	*		*				1	*								1	*											
Operculodinium cf. piaseckii		1																														
Operculodinium cf. vaculata																																
Operculodinium giganteum															*		4	*				117										
Operculodinium janduchenei										*															*							
Operculodinium tegillatum																																
Operculodinium sp. A							1						5	1											*							
Operculodinium sp. B																																
Palaeocystodinium golzowense s.l.	2		*			*						1		1				1	1	1									*			1
Palaeocystodinium minor																																
Peridinioid cyst A									1			1																				
Peridinioid cyst B													*																			
Peridinioid cyst C								1														4									1	2
Peridinioid cyst E																								*								
Peridinioid cyst F																																
Peridinioid cyst G																																
Peridinioid cyst H																																
Peridinioid cyst I							*				1					9	14															1
?Polysphaeridium spp.																																
Protoperidiniod cyst A		*	1	2		1		1	1	*					*	1		2														
Protoperidinioid cyst B																																
Protoperidinioid cyst C											4			9	23																	
Pyxidinopsis psilata																							8	16			6				*	
Pyxidinopsis vesiculata																																
Pyxidinopsis sp. A																																
Pyxidinopsis sp. B		2																2														
Pyxidinopsis sp. C											79																					
Pyxidinopsis sp. D							2					*																				
Pyxidinopsis spp.						13	6									1							7									
Reticulatosphaera actinocoronata	2	4	3	2	4	4	4	1	5	*	29	2	3	24	7	7	13	3	8	5	11	22	3	7	11	*		1	*	3	1	1
R. actinocoronata sensu Manum et al. 1989																							*	*								
Round brown cysts	36	15	62	37	6	19	2	23	12	14	25	18	2	19	16	13		45	46	14	22	10	33	4	6	3		1	10			17

Depth (mbsf)	107.0	107.6	107.9	108.5	109.1	109.5	109.9	110.5	111.1	111.5	113.1	114.7	116.4	117.9	119.5	121.1	122.7	124.3	125.9	127.5	129.1	130.3	131.5	132.7	133.8	135.0	136.3	137.5	138.7	139.3	140.5	141.7
calibrated age (Ma)	8.97	9.09	9.17	9.29	9.42	9.51	9.59	9.71	9.84	9.92	10.06	10.16	10.26	10.35	10.44	10.53	10.63	10.72	10.82	10.91	11.00	11.09	11.19	11.28	11.37	11.47	11.57	11.67	11.76	11.81	11.90	12.00
Sample (core, section, interval in cm)	12H4 18-20	12H4 77-79	12H4 111.5-113.5	12H5 19-21	12H5 82.5-84.5	12H5 123-125	12H6 12-14	12H6 69-71	12H6 130-132	12H7 16.5-18.5	13H1 130-132	13H2 142-144	13H4 8-10	13H5 12-14	13H6 20-22	13H7 31.5-33.5	14H1 141.5-143.5	14H3 4-6	14H4 10-12	14H5 20-22	14H6 30-32	14H7 1-3	15H1 74-76	15H2 38-40	15H3 4-6	15H3 123-125	15H4 100-102	15H5 74-76	15H6 37-39	15H6 92-94	16H1 17-19	16H1 140-142
Lycopodium clavatum tablets	**2**	**2**	**2**	**2**	**2**	**2**	**2**	**2**	**2**	**2**	**2**	**2**	**2**	**2**	**2**	**2**	**2**	**2**	**2**	**2**	**2**	**2**	**2**	**2**	**2**	**2**	**2**	**2**	**2**	**2**	**2**	**2**
total in-situ dinocyst counted	**316**	**239**	**289**	**291**	**336**	**265**	**263**	**363**	**355**	**327**	**372**	**386**	**301**	**369**	**374**	**339**	**352**	**369**	**355**	**359**	**354**	**372**	**368**	**367**	**362**	**375**	**383**	**352**	**358**	**359**	**376**	**356**
total Lycopodium spores counted	**131**	**72**	**67**	**119**	**51**	**213**	**244**	**134**	**73**	**19**	**40**	**64**	**176**	**27**	**15**	**163**	**175**	**30**	**20**	**38**	**52**	**27**	**60**	**94**	**46**	**81**	**39**	**69**	**20**	**122**	**150**	**303**
Selenopemphix brevispinosa											*			2				*	1													
S. brevispinosa subsp. brevispinosa															*						*	*										
S. brevispinosa subsp. conspicua														1																		
Selenopemphix dinoaecysta								2						*																		
Selenopemphix nephroides		*	*	*	*						*				*			1			*			*								
Selenopemphix sp. 3 of Head et al. 1989														1																		
Selenopemphix sp. A								1		*																						
Selenopemphix sp. B																1																
Selenopemphix sp. C																																
Selenopemphix sp. D																																
Selenopemphix sp. indet																1		*														
Spiniferites elongatus													1																			
Spiniferites ramosus "group"			3	3	8	33	2	14	32	10	2	68	91	15		76	12	2	8		2	7	1	13	8	*		10		12	45	14
Spiniferites sp. A		1	1	*	3	3					44			1	7		28	26	1	1	8	6	5	4	4	3	24	12	*		4	64
Spiniferites sp. B																5	*				1	*		3	6	1					1	
Spiniferites spp.	20	3	8		12	11	14	20	2	13	0	30	48	8	2	48		5	4	6	9		1	10	7	1	4	4		4	22	3
Sumatradinium soucouyantae																																
Tectatodinium pellitum													1												6							
Trinovantedinium ferugnomatum											1																					
Trinovantedinium glorianum																		*	*		*											
Trinovantedinium harponium																		*	5													
Trinovantedinium papulum	1																															
Tuberculodinium vancampoae											*				*			*													
Unipontedinium aquaeductus																																
Xandarodinium ?xanthum			1	*				*		*				1	*				*		*							*			
Dinoflagellate cyts spp. indet.	1					1				1				1				2							1							
Dinoflagellate cyts spp. indet. (scan)														1				5			2	3			1							
Reworked dinoflagellate cysts	1																	1							1			1		1		3
Acritarchs																																
acritarchs total counted	**142**	**106**	**77**	**55**	**146**	**126**	**50**	**32**	**49**	**136**	**76**	**557**	**88**	**52**	**71**	**223**	**42**	**761**	**757**	**237**	**76**	**181**	**26**	**12**	**60**	**117**	**37**	**6**	**24**	**156**	**757**	**1033**
Acritarch sp. 1 (Impagidinium-like)											132		478		32	49	4	10	601	551		1	18			15	91	1			1	
Acritarch sp. 2		1			2	3	*			1		7		32				15														
Acitarch sp. 3 (resembling cyst of P. dalei)	*					2	4		3		1	13	10	38	6	13	27	12			11	35	1	5	3	3	5	14	1			
Cymatiosphaera? invaginata		2	1	2	2								1		6				3	12	9	7	*	2	2	1	10					1
Cymatiosphaera spp.																				24	1											
D. martinheadii	46	135	101	72	39	110	116	49	27	40	3	1	47			8																
?Impletosphaeridium sp.																																
Lavradosphaera crista																																
Lavradosphaera lucifer																																
?Lavradosphaera sp. 1																														9		
?Micrhystridium sp. 1																				75	124	13	145	14	3	1					92	
?Micrhystridium sp. 2														1	3		3					3										702
?Micrhystridium sp.																																
?Nannobarbophora gedlii (possibly including N. walldalei)												3	2	9					157	95		3	17	4		1		15			63	48
Sphaeromorphitic acritarchs					9	22						1	5	1		1		1							1	34	6	2	4	7		
Undifferentiated acritarchs	21	4	4	3	3	9	6	1	2	8		51	14	7	5		189	4			92	14		1	3	5	5	5	1	8		6

Depth (mbsf)	142.7	143.7	144.7	145.7	148.0	150.3	152.6	154.9	157.2	159.5	163.0	166.5	167.8	169.1	174.7	180.3	185.3	190.3	195.3	200.3	205.3	210.3	215.3	216.3	216.5
calibrated age (Ma)	12.11	12.21	12.32	12.42	12.52	12.62	12.71	12.81	12.91	13.01	13.11	13.26	13.35	13.39	13.49	13.59	13.68	13.83	13.94	14.03	14.13	14.23	14.33	14.43	14.53
Sample (core, section, interval in cm)	16H2 91.5-93.5	16H3 42.5-44.5	16H3 141-143	16H4 92-94	16H6 20-22	17H1 51.5-53.5	17H2 130-132	17H4 60-62	17H5 138-140	18H1 20-22	18H3 65-67	18H5 121-123	18H6 97-99	19H1 34-36	19H4 138-140	20H2 46-48	20H5 98-100	21H2 97.5-99.5	21H6 2-4	22H2 147-149	22H6 51-53	23H3 51.5-53.5	23H6 97.5-99.5	23H7 48-50	23CC 10-12
Lycopodium clavatum tablets	**2**	**2**	**2**	**2**	**2**	**2**	**2**	**2**	**2**	**2**	**2**	**2**	**2**	**2**	**2**	**2**	**2**	**2**	**2**	**2**	**2**	**2**	**2**	**2**	**2**
total in-situ dinocyst counted	**362**	**363**	**361**	**372**	**368**	**368**	**370**	**367**	**365**	**363**	**362**	**360**	**370**	**363**	**364**	**355**	**383**	**382**	**360**	**360**	**385**	**356**	**379**	**373**	**347**
total Lycopodium spores counted	**167**	**84**	**63**	**110**	**44**	**144**	**33**	**74**	**38**	**109**	**110**	**36**	**41**	**5**	**10**	**43**	**20**	**21**	**26**	**25**	**12**	**19**	**11**	**12**	**14**
Achomosphaera cf. andalousiensis						2			1																
Achomosphaera cf. ramulifera		*												*											
Achomosphaera spp.	1	4	*	34	11	33		1	*									1			4			1	
Amiculosphaera umbraculum	*																								
Arcticacysta backmanii																									
Ataxodinium choane																									
Barssidinium evangelineae																									
Barssidinium graminosum												52	39	*		1		1							
Barssidinium pliocenicum																									
Barssidinium wrenni						*			1																
Batiacaspahera/Pyxidinopsis group			58	1	13	2	5														12	36		18	9
Batiacasphaera hirsuta		2	7		13	8	5	11	22	2	17	7	6	3	5	1		4	8	2	36	25	4		
Batiacasphaera cf. hirsuta																									
Batiacasphaera micropapillata complex	48	73	188	100	152	88	205	137	135	8	232	159	192	124	286	274	333	176	308	33	6	162	45	37	29
Batiacasphaera sphaerica	1		5	2	28	18	30	34	6	4	38	54	37	36	40	29	9	9	2	8	21	81	50	67	116
Batiacasphaera sp. II of Edwards 1984																									1
Batiacasphaera sp. A																									
Bitectatodinium? arborichiarum	1																								
Bitectatodinium tepikiense																									
Brigantedinium caiacoense																									
Brigantedinium simplex																									
Brigantedinium spp.	*							6	2		5	1			6	4				4	1				
Cerebrocysta cf. lagae																									
Cerebrocysta poulsenii	2	*	1	*	5	1			*	1					*			*	*	2	1				
Cerebrocytsa irregulare		5	*	*	21	*	*	3	4	34	4	3	3	2	1	2	2	1							
Cleistosphaeridium cf. placacantum										1															
Cleistosphaeridium placacanthum	*	*		2	1	*		1														*	3		
Cordosphaeridium minimum sensu B.S.			1		3				1			1			1	1	2	8	*	2	3	3	5	13	1
Corrudinium devernaliae																									
Corrudinium labradorii																									
Corrudinium sp. cf. labradorii																									
Corrudinium? harlandii																									
Cristadinium cristatoserratum			3		*	1	*	8	*		*	1	*			1				1			*		
Cristadinium cf. cristatoserratum			*			2					2		*												
Cristadinium diminutivum																									
Cristadinium sp. A						*	*		1		1	1	1	1	1	1	5		1	1					
Cristadinium sp. B									3		1												*		
?Cyclopsiella spiculosa																									
Dapsilidinium pastielsii										*															
Dapsilidinium pseudocolligerum		*	*		*					1	*	*	*	*				*			3			3	
Dinocyst A																									
Dinocyst B																									
Dinocyst C																									
Dinocyst D																									
Dinocyst E																									
Dinocyst F			*								1														
Dinocyst G																									
Dinocyst H																									
Dinocyst H		*								*	*	*	*	*		*		2	*						
Dinocyst I														1											
Dinocyst J																					177				
Dinocyst K																								4	8
Dinocyst L																*			*						
Dinocyst M						*	*				*	*		*											
Dinocyst N																					30				
Filisphaera filifera															4				*						
Filisphaera cf. filifera																1			*						
Filisphaera microornata																									
Filisphaera sp. A			*											172	1	1	1								
Filisphaera sp. B																									
Filisphaera sp. C																									
Filisphaera sp. D																		136	*		1				
Habibacysta tectata	31	50	17	29	21	48	2	46	26	28	20	9		7	9	3		3	2	8	1	17			
Hystrichokolpoma rigaudiae															*					*					
Hystrichosphaeridium ?tubiferum																							70		
Hystrichosphaeropsis obscura		*			*											*									
Impagidinium aculeatum																									
Impagidinium aff. aculeatum		2	2	1	2				1	*															
Impagidinium cf. antecarcerem														*											
Impagidinium elongatum	1	2	3	7	1	3			2	9			3					*	13	10	8				
Impagidinium multiplexum														*		*	1	*				1	1		3
Impagidinium pallidum	3		1	15	3	4	3		5	24			2			*	2								
Impagidinium patulum																									
Impagidinium cf. pacificum	10	2	5	46	1	8	2	13	3	36	4	3	2	1	*	2	3		1	2	2				

Depth (mbsf)	142.7	143.7	144.7	145.7	148.0	150.3	152.6	154.9	157.2	159.5	163.0	166.5	167.8	169.1	174.7	180.3	185.3	190.3	195.3	200.3	205.3	210.3	215.3	216.3	216.5
calibrated age (Ma)	12.11	12.21	12.32	12.42	12.52	12.62	12.71	12.81	12.91	13.01	13.11	13.26	13.35	13.39	13.49	13.59	13.68	13.83	13.94	14.03	14.13	14.23	14.33	14.43	14.53
Sample (core, section, interval in cm)	16H2 91.5-93.5	16H3 42.5-44.5	16H3 141-143	16H4 92-94	16H6 20-22	17H1 51.5-53.5	17H2 130-132	17H4 60-62	17H5 138-140	18H1 20-22	18H3 65-67	18H5 121-123	18H6 97-99	19H1 34-36	19H4 138-140	20H2 46-48	20H5 98-100	21H2 97.5-99.5	21H6 2-4	22H2 147-149	22H6 51-53	23H3 51.5-53.5	23H6 97.5-99.5	23H7 48-50	23CC 10-12
Lycopodium clavatum tablets	**2**	**2**	**2**	**2**	**2**	**2**	**2**	**2**	**2**	**2**	**2**	**2**	**2**	**2**	**2**	**2**	**2**	**2**	**2**	**2**	**2**	**2**	**2**	**2**	**2**
total in-situ dinocyst counted	**362**	**363**	**361**	**372**	**368**	**368**	**370**	**367**	**365**	**363**	**362**	**360**	**370**	**363**	**364**	**355**	**383**	**382**	**360**	**360**	**385**	**356**	**379**	**373**	**347**
total Lycopodium spores counted	**167**	**84**	**63**	**110**	**44**	**144**	**33**	**74**	**38**	**109**	**110**	**36**	**41**	**5**	**10**	**43**	**20**	**21**	**26**	**25**	**12**	**19**	**11**	**12**	**14**
Impagidinium cf. sphaericum																									
Impagidinium strialatum																									
Impagidinium cf. velorum							*	*																	
Impagidinium sp. A																									
Impagidinium sp. B																									
Impagidinium sp. C																									
Impagidinium sp. indet																		*							
Invertocysta lacrymosa	*																								
Invertocysta paratabulata																									
Labyrinthodinium truncatum	*	155	1	30	12	4	*	5	6	2	8			*	*	1		10	8	212	6		107	104	71
Lejeunecysta fallax			*				*							*											
Lejeunecysta sp. 1																									
Lejeunecysta sp.3			3																						
Lejeunecysta sp. 2																									
Lejeunecysta sp. 4			*	*	*				1								*								
Lejeunecysta sp. 5												1	1		*		1								
Lejeunecysta sp. 6												*	*	1	*										
Lejeunecysta sp. 7																									
Lejeunecysta sp. 8																									
Lejeunecysta sp. 9																									
Lejeunecysta sp. 10		1															*								
Lejeunecysta spp.			*		1					1							1	*					*		
Lingoludinium machaerophorum	2	1		1	*	1	*		1	*	*	2		*	*			*	*		1	1	5		
Lingoludinium multivirgatum																				4					
cf. Litosphaeridium spp.																									
Melitasphaeridium choanophorum		1																					*		
Melitasphaeridium sp. A																				1			*		
Mendicodinium sp.																									
Nematosphaeropsis labyrinthus	162	20	28	32	32	59	104	67	128	182	4	36	41	8	2	8	1	12	6	9	11	4	10	10	14
Nematosphaeropsis labyrinthus "scrumbled"					4																				
Nematosphaeropsis labyrinthus (robust)																									
Nematosphaeropsis cf. downiei																							1		
Nematosphaeropsis cf. lativattus																									
Nematosphaeropsis cf. rigidius																									
Nematosphaeropsis sp. 1																									
Nematosphaeropsis sp. indet																									
Operculodinium? borgerholtense																				2					
Operculodinium centrocarpum s.s.		10	*	*	*	3			2	1	1	2	*			1		*	*	6	8	5	2	5	5
O. aff. centrocarpum Wall and Dall 1966		*								*															
Operculodinium? eirikianum	1	5	1	*	4	3		*		*															
Operculodinium cf. eirikianum																									
Operculodinium israelianum	1	*				*			1						*	1	*				3		1		1
Operculodinium cf. israelianum										*												*	1		9
Operculodinium piaseckii																					1				
Operculodinium cf. piaseckii																									
Operculodinium cf. vaculata																									
Operculodinium giganteum																					1				
Operculodinium janduchenei		1																*							
Operculodinium tegillatum																									
Operculodinium sp. A				*																			1		
Operculodinium sp. B		*	*																						
Palaeocystodinium golzowense s.l.					*			7	1		3			2		6	11	*		*	4	4	25	26	25
Palaeocystodinium minor							*																		
Peridinioid cyst A																									
Peridinioid cyst B																							1		
Peridinioid cyst C																									
Peridinioid cyst E							*																		
Peridinioid cyst F								*								1									
Peridinioid cyst G										*								1							
Peridinioid cyst H																							1	1	
Peridinioid cyst I	*				2							*					*		*	1		1			
?Polysphaeridium spp.								1			*												*		
Protoperidiniod cyst A																									
Protoperidinioid cyst B																									
Protoperidinioid cyst C																									
Pyxidinopsis psilata		*																							
Pyxidinopsis vesiculata																									
Pyxidinopsis sp. A																									
Pyxidinopsis sp. B																									
Pyxidinopsis sp. C																									
Pyxidinopsis sp. D																									
Pyxidinopsis spp.																									
Reticulatosphaera actinocoronata	2	6	7	13	10	8	1	1	4	7	2	11	22	1	1	2		9	6	10	8	8	17	8	10
R. actinocoronata sensu Manum et al. 1989																									
Round brown cysts	1		14	3	2		10	15			1	1	8	3	5		6		1						

Depth (mbsf)	142.7	143.7	144.7	145.7	148.0	150.3	152.6	154.9	157.2	159.5	163.0	166.5	167.8	169.1	174.7	180.3	185.3	190.3	195.3	200.3	205.3	210.3	215.3	216.3	216.5
calibrated age (Ma)	12.11	12.21	12.32	12.42	12.52	12.62	12.71	12.81	12.91	13.01	13.11	13.26	13.35	13.39	13.49	13.59	13.68	13.83	13.94	14.03	14.13	14.23	14.33	14.43	14.53
Sample (core, section, interval in cm)	16H2 91.5-93.5	16H3 42.5-44.5	16H3 141-143	16H4 92-94	16H6 20-22	17H1 51.5-53.5	17H2 130-132	17H4 60-62	17H5 138-140	18H1 20-22	18H3 65-67	18H5 121-123	18H6 97-99	19H1 34-36	19H4 138-140	20H2 46-48	20H5 98-100	21H2 97.5-99.5	21H6 2-4	22H2 147-149	22H6 51-53	23H3 51.5-53.5	23H6 97.5-99.5	23H7 48-50	23CC 10-12
Lycopodium clavatum tablets	**2**	**2**	**2**	**2**	**2**	**2**	**2**	**2**	**2**	**2**	**2**	**2**	**2**	**2**	**2**	**2**	**2**	**2**	**2**	**2**	**2**	**2**	**2**	**2**	**2**
total in-situ dinocyst counted	**362**	**363**	**361**	**372**	**368**	**368**	**370**	**367**	**365**	**363**	**362**	**360**	**370**	**363**	**364**	**355**	**383**	**382**	**360**	**360**	**385**	**356**	**379**	**373**	**347**
total Lycopodium spores counted	**167**	**84**	**63**	**110**	**44**	**144**	**33**	**74**	**38**	**109**	**110**	**36**	**41**	**5**	**10**	**43**	**20**	**21**	**26**	**25**	**12**	**19**	**11**	**12**	**14**
Selenopemphix brevispinosa							*							1											
S. brevispinosa subsp. brevispinosa																									
S. brevispinosa subsp. conspicua																									
Selenopemphix dinoaecysta			*																						
Selenopemphix nephroides								1	*				*				2								
Selenopemphix sp. 3 of Head et al. 1989																									
Selenopemphix sp. A																									
Selenopemphix sp. B			1																						
Selenopemphix sp. C											1														
Selenopemphix sp. D											*									1					
Selenopemphix sp. indet				*																	1				
Spiniferites elongatus																									
Spiniferites ramosus "group"	58	12		8	12				3	1	2				1	5								18	
Spiniferites sp. A	37	8	12	42	9	28	1	7	*	19	9	10	5		1	6	1	2	*	10					
Spiniferites sp. B	*	1																							
Spiniferites spp.		2	3	5	5	44	0	3		2	5	1	3	0	0	0	2	5		23	30	7	20	50	45
Sumatradinium soucouyantae																			*		1		1		
Tectatodinium pellitum		*										3	5		*	3		2	*	*			1	1	
Trinovantedinium ferugnomatum																									
Trinovantedinium glorianum																									
Trinovantedinium harponium																									
Trinovantedinium papulum																									
Tuberculodinium vancampoae																									
Unipontedinium aquaeductus																			*	8	2		6		*
Xandarodinium ?xanthum								*																	
Dinoflagellate cyts spp. indet.											1	4							1		2	1	1	7	
Dinoflagellate cyts spp. indet. (scan)		3		1			2				1				2	2			2	1			2		
Reworked dinoflagellate cysts	2		1	1	1	1	1	6	5	4	4	2			2	1			1	1			2	4	
Acritarchs																									
acritarchs total counted	**153**	**745**	**104**	**1092**	**204**	**116**	**118**	**81**	**392**	**71**	**161**	**111**	**185**	**6**	**72**	**20**	**67**	**68**	**373**	**76**	**122**	**300**	**76**	**122**	
Acritarch sp. 1 (Impagidinium-like)				3	1070	23	1	4				30	3	16	1	22	11	2	1						
Acritarch sp. 2																									
Acitarch sp. 3 (resembling cyst of P. dalei)		3																							
Cymatiosphaera? invaginata									2	1			*	*		1		1		1	1			4	7
Cymatiosphaera spp.					3	28	24		1	40	4	81	29												
D. martinheadii																									
?Impletosphaeridium sp.																		1	17		15	44	187		5
Lavradosphaera crista																									
Lavradosphaera lucifer																									
?Lavradosphaera sp. 1	3		10		9	1		17	29	1			18	3				11	21		4	39	87	14	13
?Micrhystridium sp. 1	23			62	4	2	3							1				20		3					
?Micrhystridium sp. 2	972	129	707	25		127	81	73	48	291	17	41	37	149	5	48	6	13	7	330	56				
?Micrhystridium sp.																								11	12
?Nannobarbophora gedlii (possibly including N. walldalei)	35		18	13		21	5	11					7	15			3			32			21	43	82
Sphaeromorphitic acritarchs								1		56	38	3	4							7					
Undifferentiated acritarchs		21	10	1	6	2	2	12	1	3	12	6	13	1		1		19	22			39	5	4	3

Appendix C2

species	recent cyst	Pliocene data base of De Schepper et al., 2011	temperature	neritic/ocenanic	trophic stage	reference
Ataxodinium choane	x		cold-temperate to temperate	inner to outer neritic	-	Edwards and Andrle, 1992; Rochon et al., 1999
Barssidinium graminosum			-	-	-	
Batiacasphaera micropapillata complex			cool to warm temperate	outer neritic to oceanic	-	Schreck and Matthiessen (chapter 4)
Batiacasphaera hirsuta			-	-	-	
Batiacasphaera sphaerica			-	-	-	
Cleistosphaeridium placacanthum			-	-	-	
Cerebrocysta irregulare			-	-	-	
Corrudinium harlandii		x	no clear affinity	-	-	Versteegh and Zonneveld, 1994; De Schepper et al., 2011
Corrudinium devernaliae				-	-	
Corrudinium labradorii		x	no clear affinity	-	-	Versteegh and Zonneveld, 1994; De Schepper et al., 2011
Corrudinium cristatoserratum			-	-	-	
Dapsilidinium pseudocolligerum			tropical to warm-temperate	-	-	Head and Westphal, 1999
Habibacysta tectata		x	cold/cool tolerant	-	-	Versteegh, 1997; Head, 1994; De Schepper et al., 2011
Hystrichosphaeropsis obscura			warm-water	-	-	Head et al., 1989
Impagidinium elongatum			-	-	-	
Impagidinium cf. *pacificum*			-	-	-	
Impagidinium pallidum	x	x	cold	oceanic	meso-eutrophic	Marret and Zonneveld, 2003; Rochon et al., 1999
Impagidinium aculeatum	x	x	temperate-subtropical/tropical	oceanic	-	Marret and Zonneveld, 2003; Rochon et al., 1999
Impagidinium aff. *aculeatum*			-	-	-	
Impagidinium lacrymosa		x	warm	outer neritic-oceanic	-	Wrenn and Kokins, 1986; Versteegh and Zonneveld, 1994
Labyrinthodinium truncatum			-	-	-	
Lingoludinium machaerophorum	x	x	temperate-tropical	coastel	eutrophic	Marret and Zonneveld, 2003
Melitasphaeridium choanophorum			thermophilic	-	-	Head et al., 1989
Nematosphaeropsis labyrinthus	x	x	temperate-supolar	oceanic	-	Rochon et al., 1999
Operculodinium centrocarpum s.s.			-	-	-	
Operuclodinium ? eirikanum		x	cold sensitive	-	-	Head, 1993
Operculodinium israelianum	x	x	temperate/subtropical-tropical	-	-	Marret and Zonneveld, 2003
Operculodinium tegillatum			-	-	-	
Palaeocystodinium golzowense s.l.			-	-	-	
Protoperidinium spp.			-	-	-	
Reticulatosphaera actinocoronata			-	-	-	
Spiniferites elongatus	x		cool temperate - subarctic	inner neritic-oceanic	-	Harland, 1983; Rochon et al., 1999
Spiniferites ramosus s.l.	x		temperate to sub-arctic (latitudinally restricted to south of 70°N)			Rochon et al., 1999
Spiniferites spp.			-	-	-	
Tectatodinium pellitum	x	x	subtropical-tropical	coastal	oligotrophic-eutrophic	Marret and Zonneveld, 2003

Appendix C3

Depth mbsf	TOC %	C/N ratio
49.1	0.44	6.31
51.1	0.31	4.98
53.0	0.27	4.52
55.1	0.26	3.93
56.6	0.25	3.43
58.0	0.21	3.75
60.3	0.21	4.00
62.2	0.24	4.15
63.2	0.27	6.25
64.2	0.22	4.13
65.2	0.19	3.08
66.2	0.26	3.18
67.2	0.28	4.34
68.2	0.17	3.86
69.2	0.11	3.75
70.2	0.19	4.43
71.2	0.21	3.60
72.1	0.27	3.94
73.2	0.25	4.40
74.2	0.47	6.88
75.2	0.51	6.09
76.2	0.36	4.65
77.2	0.47	5.48
78.2	0.37	5.25
79.2	0.21	3.78
80.2	0.19	3.72
81.2	0.30	4.53
82.2	0.27	5.32
83.2	0.29	3.95
84.2	0.39	5.00
85.2	0.25	7.06
86.2	0.25	4.72
87.2	0.36	4.41
88.0	0.32	4.54
89.2	0.26	4.08
90.4	0.23	3.23
91.7	0.24	3.41
92.3	0.25	4.00
92.9	0.18	5.06
93.5	0.26	2.54
94.4	0.18	3.10
95.5	0.23	3.64
96.4	0.12	4.01
97.0	0.22	3.74
97.4	0.19	3.25
98.0	0.43	4.84
98.5	0.45	10.98
99.0	0.25	3.75
99.6	0.18	3.60
100.0	0.15	3.69
100.5	0.16	7.62
101.1	0.14	3.48
101.4	0.12	2.80
101.9	0.15	3.85
102.5	0.25	4.83
103.1	0.23	2.35
103.6	0.24	3.96
104.0	0.39	5.09
104.5	0.57	6.20
105.1	0.60	6.10
105.5	0.57	4.65
106.1	0.29	5.31
106.6	0.28	3.62
107.0	0.38	5.24
107.6	0.48	5.29
107.9	0.57	6.84
108.5	0.55	6.11
109.1	0.45	5.55
109.5	0.35	4.34
109.9	0.28	4.11
110.5	0.32	4.68
111.1	0.40	4.74
111.5	0.54	6.08
113.1	0.44	5.80
114.7	0.31	4.82
116.4	0.29	3.93
117.9	0.37	6.07
119.5	0.40	9.24
121.1	0.17	3.18
122.7	0.21	3.50
124.3	0.49	5.39
125.9	0.51	7.09
127.5	0.57	6.47
129.1	0.54	5.79
130.3	0.38	5.56
131.5	0.34	4.85
132.7	0.26	3.96
133.8	0.42	4.37
135.0	0.22	3.45
136.3	0.26	3.69
137.5	0.33	4.57
138.7	0.18	3.63
139.3	0.20	3.03
140.5	0.62	6.48
141.7	0.16	4.94
142.7	0.51	4.98
143.7	0.19	3.28
144.7	0.35	3.87
145.7	0.29	3.55
148.0	0.30	3.07
150.3	0.20	3.79
152.6	0.53	5.49
154.9	0.50	6.43
157.2	0.32	5.34
159.5	0.18	3.58
163.0	0.46	6.69
166.5	0.49	9.72
167.8	0.34	5.77
169.1	0.35	5.50
174.7	0.68	7.96
180.3	0.47	9.22
185.3	0.56	7.86
190.3	0.53	7.07
195.3	0.88	9.19
200.3	0.48	7.79
205.3	0.52	8.39
210.3	0.64	9.64
215.3	0.55	15.12
216.3	0.29	3.98
216.5	0.37	9.62